COMBUSTION AND HEAT TRANSFER STUDIES UTILIZING ADVANCED DIAGNOSTICS: FUELS RESEARCH

D. R. Ballal, R. J. Byrd, S. P. Heneghan, C. R. Martel, T. F. Williams, and S. Zabarnick
University of Dayton
Dayton, OH 45469-0001

November 1992

FINAL REPORT FOR THE PERIOD FEBRUARY 27, 1991 TO SEPTEMBER 30, 1992

Approved for Public Release; Distribution is Unlimited

AERO PROPULSION AND POWER DIRECTORATE
WRIGHT LABORATORY
AIR FORCE MATERIEL COMMAND
WRIGHT-PATTERSON AIR FORCE BASE, OH 45433-6563

NOTICE

When Government drawings, specifications, or other data are used for any purpose other than in connection with a definitely Government-related procurement operation, the United States Government incurs no responsibility nor any obligation whatsoever. The fact that the Government may have formulated, furnished, or in any other way supplied the said drawings, specifications, or other data, is not to be regarded by implication or otherwise in any manner construed, as licensing the holder or any other person or corporation, or as conveying any rights or permission to manufacture, use or sell any patented invention that may in any way be related thereto.

This report is releasable to the National Technical Information Service (NTIS). At NTIS, it will be available to the general public, including foreign nations.

This technical report has been reviewed and is approved for publication.

W. M. Roquemore
Government Monitor
W. MELVYN ROQUEMORE
Fuels Branch
Fuels & Lubrication Division

Royce P. Bradley
Supervisor
ROYCE P. BRADLEY
Section Chief, Fuels Branch
Fuels & Lubrication Division
Aero Propulsion & Power Directorate

Leo S. Harootyan Jr
Division Chief
LEO S. HAROOTYAN, JR.
Chief, Fuels & Lubrication Division
Aero Propulsion & Power Directorate

If your address has changed, if you wish to be removed from our mailing list, or if the addressee is no longer employed by your organization, please notify WL/POSF, Wright-Patterson AFB, OH 45433-7103 to help us maintain a current mailing list.

Copies of this report should not be returned unless return is required by security considerations, contractual obligations, or notice of a specific document.

DISCLAIMER NOTICE

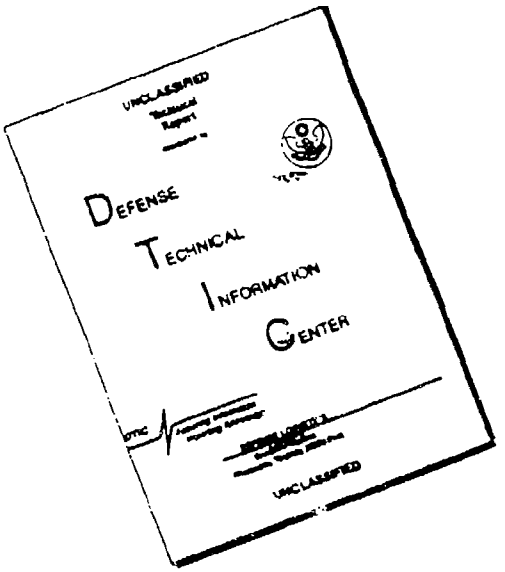

THIS DOCUMENT IS BEST QUALITY AVAILABLE. THE COPY FURNISHED TO DTIC CONTAINED A SIGNIFICANT NUMBER OF PAGES WHICH DO NOT REPRODUCE LEGIBLY.

REPORT DOCUMENTATION PAGE

Form Approved
OMB No 0704-0188

1. AGENCY USE ONLY (Leave blank)	2. REPORT DATE	3. REPORT TYPE AND DATES COVERED
	November 1992	Final 2/27/91 - 9/30/92

4. TITLE AND SUBTITLE Combustion & Heat Transfer Utilizing Advanced Diagnostics : Fuels Research

5. FUNDING NUMBERS
C-F33615-87-C-2767
PE-62203
PR-3048
TA-05
WU-60

6. AUTHOR(S) D. R. Ballal, R. J. Byrd, S. P. Heneghan, C. R. Martel, T. F. Williams, and S. Zabarnick

7. PERFORMING ORGANIZATION NAME(S) AND ADDRESS(ES)
University of Dayton
300 College Park
Dayton, OH 45469-0001

8. PERFORMING ORGANIZATION REPORT NUMBER

9. SPONSORING/MONITORING AGENCY NAME(S) AND ADDRESS(ES)
Aero Propulsion & Power Directorate
Wright Laboratory (WL/POSF)
Air Force Materiel Command
Wright-Patterson Air Force Base, OH 45433-6563
W. Melvin Roquemore, 513-255-6813

10 SPONSORING MONITORING AGENCY REPORT NUMBER
WL-TR-92-2112

11. SUPPLEMENTARY NOTES

12a DISTRIBUTION AVAILABILITY STATEMENT
Approved for public release; distribution is unlimited.

12b. DISTRIBUTION CODE

13. ABSTRACT

As the Air Force continues to advance engine technology, aviation fuel heat loading has steadily increased. Therefore, a thermally stable JP-8 fuel is required that can operate at higher temperatures than current fuels. This research program had two objectives: (1) to identify fundamental conditions of fuel thermal decomposition, and (2) to provide the data needed to develop and evaluate global chemistry and heat transfer models for predicting jet fuel thermal decomposition and deposition rate.

We successfully designed and performed numerous static and flowing experiments on a variety of JP fuels. These experiments illuminated the role of antioxidants, peroxides, ketones, and hetero-atom sulfur molecules in the oxidation of surrogate JP-8 and other jet fuels. We developed an autoxidation theory which distinguishes oxidative stability from thermal stability and accounts for the observed oxygen consumption and methane production. Also, we examined several additives and found a select few which produce the least deposits. Finally, our data led to the evaluation and refinement of global chemistry and heat transfer models for predicting jet fuel deposition rates.

14. SUBJECT TERMS	15. NUMBER OF PAGES
Fuel Decomposition, Fuel Stability, Fuel Deposition, JP-8 Stability	197
	16. PRICE CODE

17. SECURITY CLASSIFICATION OF REPORT	18. SECURITY CLASSIFICATION OF THIS PAGE	19. SECURITY CLASSIFICATION OF ABSTRACT	20. LIMITATION OF ABSTRACT
Unclassified	Unclassified	Unclassified	UL

TABLE OF CONTENTS

TABLES

FIGURES

APPENDICES

PREFACE

This final report was submitted by the University of Dayton Research Institute (UDRI) under Contract No. F33615-87-C-2767, sponsored by the U.S. Air Force Wright Laboratory, Aero Propulsion and Power Directorate, Wright-Patterson Air Force Base OH. Dr. W. M. Roquemore of WL/POSF was the Air Force Technical Monitor; Dr. D. R. Ballal of the Applied Physics Division, UDRI, was the Principal Investigator; and Dr. E. H. Gerber, Head of the Applied Physics Division, UDRI, was the Project Supervisor. This report covers work performed during the period February 27, 1991 through September 30, 1992.

The Principal Investigator wishes to express his gratitude and appreciation to Dr. W. M. Roquemore for his encouragement and support; to Ms. Ruth Rodak, UDRI, for technical editing; and to Ms. W. Barnes, UDRI, for report preparation.

SUMMARY

As the Air Force has continued to advance engine technology through its Integrated High Performance Turbine Engine Technologies (IHPTET) initiative, aviation fuel heat loading has increased. Thus, aircraft development in the near future will suffer performance penalties as tremendous quantities of ram air or excess fuel will be required to meet the heat sink requirements. To address this problem, the Air Force Wright Laboratory, Aero Propulsion and Power Directorate (WL/PO) modified, on February 27, 1991, the University of Dayton Research Institute (UDRI) Contract No. F33615-87-C-2767. This research program had two objectives: (1) to identify conditions of aviation jet fuel thermal decomposition, and (2) to provide the data needed to develop and evaluate global chemistry and heat transfer models which include mechanisms of jet fuel thermal decomposition and deposition.

To address these program objectives, we formulated tests designed to thermally stress several baseline and blended jet fuel samples in a flask or an MCRT apparatus (static tests) and in a single-pass heat exchanger "Phoenix Rig" (flowing tests). The deposited residue samples which comprise gums, insolubles, and carbon residue were examined by using a variety of sophisticated chemical analysis instrumentation. In these tests, a hydrotreated Jet A-1 (POSF-2747) fuel served as a baseline, a thermally stable JPTS (POSF-2799) fuel served as a calibration standard, and a nonhydrotreated fuel (POSF-2827) was also acquired for analysis. New blends were made to test various additives. For example, POSF-2747 + blend = POSF-2814, Jet A-1 + blend = JP-8, POSF-2827 + JFA-5 (12 mg/l) = POSF 2827A, and POSF-2827 + JFA-5 (50 mg/l) = POSF 2827B. Also, a surrogate JP-8 (JP-8S) fuel comprising a mixture of selected hydrocarbons, was used in static tests.

Our tests revealed that jet fuel oxidation results in the buildup of peroxides, ketones, aldehydes, alcohols, and acids from the autoxidation cycle; sulfates, sulfones, and nitrous compounds from the inhibitors originally present; and alkenes from the decomposition of radicals. Many of these oxidized compounds can, if present in sufficient quantity, inhibit fuel oxidation and, hence, form deposits. However, if sufficient quantities of the easily oxidized compound are available, the compound will help stimulate oxidation and again affect deposit production.

Work on the chemistry of surrogate fuels, by our subcontractor, Eastern Kentucky University, showed that many fuels (surrogate JP-8, JP-7, JP-TS, and POSF-2747) produce increasing amounts of insoluble material with an increasing concentration of oxidized species, whereas fuels such as POSF-2827 produce large amounts of insolubles (phenolic compounds) with essentially no detectable concentration of oxidation products. Further, deposits from JP-8S and POSF-2747 were varnish-like polar species. In contrast, fuels such as POSF-2827 produce deposits strongly bonded (hemiketal type R'OH + RCOR → R-O-CH(OR')R bond) into a solid phase.

We found that previous deposit formation results were inadequate in predicting the observed dependence of oxygen consumption and methane production on deposit formation. Our tests with both oxygen-saturated and oxygen-depleted fuels showed that the amount of deposit is linearly related to the total quantity of dissolved oxygen passed, and that oxygen consumption is pseudo-zero-order in the early stages, decaying to pseudo-first-order when the oxygen nears depletion. As for methane production, we found that it results from hydrogen abstraction by methyl radicals.

These important experimental observations led us to formulate a comprehensive free-radical autooxidation theory of deposit formation. In this theory, a clear distinction is made between the fuel thermal stability (based on the deposit forming tendency) and oxidative stability (based on the ability to oxidize and form peroxides, ketones, alcohols, and acids). This leads to the seemingly anomalous statement: "Fuels that oxidize easily are likely to be thermally stable, while fuels that are not thermally stable are not easily oxidized." This statement was found to hold in experimental tests.

Of the several additives supplied by Mobil Corporation, our MCRT tests demonstrated that only MCP-922 exhibited a measurable tendency toward solids inhibition. In the modified Phoenix rig, antioxidant in Jet-A reduced the hot-section deposits, metal deactivator reduced both hot- and cold-section deposits, and JFA-5 produced the least amount of deposits in the heated section.

Our subcontractor, Purdue University, examined the effect of fuel composition for five different fuels in the recirculation test mode. It was found that the JPTS fuel (POSF-2799) yielded exceptionally low deposits, whereas the Jet A fuel (POSF-2827) had the poorest thermal stability. Likewise, the deposition rates in the fuel tubes with surface treatment were higher. This negative result was attributed to too severe a surface pretreatment that increases surface roughness and promotes the collection of precursors.

The research work described above has led to 8 archival journal publications, 10 presentations at national and international meetings, and 2 internal reports. It is due to appear in the American Institute of Aeronautics and Astronautics (AIAA)--1992 National Aerospace Highlights.

This report describes the experimental work, theoretical results, and conclusions. The fuels data sets for all the work performed on the fuels research task are presented in Report No. WL-TR-92-2113.

1. INTRODUCTION

1.1 Program Objectives

As the Air Force has continued to advance engine technology through its Integrated High Performance Turbine Engine Technologies (IHPTET) initiative, aviation fuel heat loading has increased. In a recent report by Harrison [1], an Aircraft Thermal Management Working Group of Wright Research and Development Center, Wright-Patterson Air Force Base (W-PAFB), Ohio, concluded that, *"aircraft development in the near future will suffer performance penalties as tremendous quantities of ram air or excess fuel will be required to meet the heat sink requirements."* To resolve this problem, the working group recommended the development of thermally stable fuels that can operate at higher temperatures than current fuels. Subsequently, an add-on contract was awarded to the University of Dayton Research Institute (UDRI) on February 27, 1991. This research program had two objectives: (1) to identify conditions of fuel thermal decomposition, and (2) to provide the data needed to develop and evaluate global chemistry and heat transfer models which include mechanisms of jet fuel thermal decomposition and deposition.

1.2 Fuels Research

In an aircraft, fuel is used as a heat sink to cool the engine lubricant, hydraulic controls, environmental system, and avionics. A further rise in fuel temperature occurs as it flows through the burner feed arm. Combined, these various heat inputs stimulate oxidation reactions which deposit gums, insoluble compounds, and carbon in fuel lines, heat exchanger surfaces, and fuel injectors, thus leading to blockage. Deposition within fuel nozzle or afterburner spraybars is especially harmful because it can distort the fuel spray pattern causing combustor and turbine blade overheating and burnout. The present work was undertaken to understand jet fuel thermal stability at a fundamental level and to provide data sets for refining global chemistry and heat transfer models. Accordingly, we formulated three technical tasks:

(1) Thermal Stability Studies (Static Tests),
(2) Thermal Stability Studies (Flowing Tests), and
(3) Analysis of Deposit Formation.

Recognizing the technical complexity of the thermal stability problem and the importance of its resolution to the Air Force, we sought the expertise of two subcontractors: (1) Professor W. D. Schulz, Department of Chemistry, Eastern Kentucky University, Richmond KY, who investigated the chemistry of oxidation deposits and fuel additives; and (2) Professor A. H. Lefebvre of The School of Mechanical Engineering and Professor L. F. Albright of The School of Chemical Engineering, both of Purdue University, West Lafayette IN, who examined the influence of fuel composition, additives, and surface composition on deposition rates. Final reports from both these subcontractors are attached as Appendices E and F.

2. TEST APPARATUS AND INSTRUMENTATION

All static fuels tests were performed in the Chemistry Laboratory in Building 490, Rooms 208 and 236 of the Fuels and Lubrication Division (WL/POSF); all flowing fuels tests were conducted in the Fuels Laboratory in Building 490, Room 152 of WL/POSF. To accomplish these tasks required static flask tests, Micro Carbon Residue Tests (MCRT), and the design, fabrication, and instrumentation of a fuel nozzle feed arm apparatus known as the "Phoenix" rig. These test devices are described below.

2.1 Flask Apparatus

A flask test represents a simple static test. A fuel sample (30 ml) is heated in a flask at a temperature near 180C. Oxygen may be flowed into this thermally stressed fuel because this provides a gravimetrically measurable degradation of the fuel in approximately 4 hours; also, maintaining oxygen saturation removes the dissolved oxygen content as a variable. Deposits are collected either (1) by cooling the entire fuel sample and decanting it through the filter; or (2) filtering, washing, drying, and weighing a 10-ml fuel sample. The deposits are then ready for measurements.

2.2 MCRT Apparatus

We developed a modified version of the ASTM D4530-5 static test for JP fuels using the MCRT as sketched in Figure 1. This modification was necessary because the standard method measures coking under strictly pyrolytic conditions and was developed for lubricants. In the MCRT apparatus, instead of the 12- mm-o.d.-x -55-mm vials, 21-mm-o.d.-x-70-mm vials are used to provide greater surface area for reactions. One milliliter of sample fuel is weighed into *six* pre-weighed vials and lowered into the test chamber. The oven is heated to 250 C at the rate of 8.3 C/min and held for 3 hours while air is purged through the chamber at the rate of 150 mL/min. At the conclusion of the test, the vials are cooled and weighed; the difference in weight is reported as a percentage of the original fuel weight. The degraded fuel, which has been condensed in the trap, is analyzed along with the insoluble gums.

2.3 Phoenix Rig

As shown in Figure 2, this is a flowing single-pass fuel heat exchanger. The fuel supply tank has gas sparging (two Brooks 5850E mass flow controllers and a 5876A controller) and a capacity of 189-liters. An American Lewa Model EK-1 variable stroke, positive displacement pump with surge suppression provides fuel flow in the 1 to 100 ml/min range at 3.45 MPa. A Hewlett Packard (HP 5641A) gas chromatograph is used to measure fuel oxygen and methane concentrations.

The fuel tube has a 2.15-mm i.d. and is 560 mm long. It is heated by a copper block heater (460 mm × 75 mm dia.) to a predetermined temperature (544K, 573K, or 608K) so that the wall temperature profile remains constant. The fuel flow rate is 16 ml/min for 6, 12, or 24 hours. At

the conclusion of the test, the fuel tube is removed, drained, cut into 25-mm or 50-mm lengths, rinsed in hexane, dried in a vacuum oven, and analyzed for carbon deposits on a Leco RC-412 carbon analyzer. This method measures carbon deposits but does not measure other deposit constituents such as oxygen, hydrogen, sulphur, or trace metals.

2.4 Fuels Tested

Various baseline and blended fuels were tested. Table 1 lists the properties of these fuels. A hydrotreated Jet A-1 (POSF-2747) fuel served as a baseline. A thermally stable JPTS (POSF-2799) fuel served as a calibration standard, thereby establishing a goal that the fuel additives program would like to achieve. Finally, a nonhydrotreated fuel (POSF-2827) was also acquired for analysis.

New blends were made to test various additives. For example, POSF-2747 + blend = POSF-2814, Jet A-1 + blend = JP-8, POSF-2827 + JFA-5 (12 mg/l) = POSF 2827A, and POSF-2827 + JFA-5 (50 mg/l) = POSF 2827B. Also, a surrogate JP-8 (JP-8S) was used in static tests. As listed in Table 1, the surrogate fuel comprises a mixture of selected hydrocarbons.

2.5 Instrumentation

We purchased and made operational several new and sophisticated instruments to perform chemical analysis. These instruments are described in the following paragraphs.

The LECO RC-412 multicarbon determinator is designed strictly to measure carbon, regardless of the phase of the material. In particular, we use the RC-412 to determine the amount of carbon attached to metal surfaces. The metal surfaces can be tubes through which fuel has flowed, metal or glass disks which have been submersed in static heated fuel, or filters through which fuel either from flowing or static tests has been subsequently passed. The RC-412 has a stated capability of measuring percentage of carbon in 0.02 mg to 0.5 g samples with a 3 percent accuracy. The operating range for carbon detection is from 40 µgms to 100 mgms.

The LECO CHNS-932 is a multi elemental analyzer. It is capable of measuring the absolute quantities of carbon, hydrogen, oxygen, nitrogen, and sulfur from microgram-size solid samples. It is used to analyze the deposit material formed in fuel static tests. All analyzed material must be transferred to tin cups for measurement. The CHNS-932 is capable of measuring relative quantities of carbon from 0.001 to 100 percent; and hydrogen, nitrogen, oxygen, and sulfur from 0.01 to 100 percent. The stated accuracy is 0.1 percent for carbon, 1 percent for hydrogen and nitrogen, and 2 percent for sulfur and oxygen.

The Hewlett Packard Gas Chromatograph Atomic Emission Detection (GCAED) is an ordinary gas chromatograph (Hewlett Packard HP-5890) which allows fuels to be separated into individual components based on boiling point or polarity. The detector, however, is capable of analyzing the eluted compounds for the presence of almost any element. Several elements (e.g.,

carbon, hydrogen, and sulfur) can be analyzed simultaneously. The atomic ratios, together with the retention index from the chromatograph, allow the unique molecular formula to be determined. The GCAED detection levels of the various atoms are from 1 pg/sec for sulfur to 100 pg/sec for nitrogen.

The Hewlett Packard ultraviolet (UV) visible (VIS) spectrophotometer is a simple qualitative/quantitative diagnostic for the static analysis of fuels. The instrument measures the absorption of light in the 200 to 900 nm range. With only one moving part (the spectrometer slit) the instrument is well-suited to laboratory settings. We have used the UV-VIS to study the output of the Phoenix rig, static flask tests, and the MCRT. The UV-VIS measures absorbance (the negative log of transmittance ratio) in the 0.1 to 3 range, with useful signals in the neighborhood of 1 and noise of about 0.5 percent. The dynamic range increases slightly for 0.1 percent noise. The resolution of the instrument is about 2 nm.

3 THERMAL STABILITY STUDIES

Objective. The objectives of the static and flowing tests were: (1) to subject the jet fuel and fuel surrogate samples to the temperature/time history of the aircraft fuel system; (2) to analyze the resulting deposits of soluble gum, insoluble products, and carbon; and (3) to gain insight into the chemical and physical processes important to deposit formation.

3.1 Flask (Static) Tests

3.1.1 Results. In the flask test, the Fourier Transform Infrared Technique (FTIR) was used to quantify the amount of alcohol and ketone species in surrogate fuels. The HP-5890 GCAED instrument was used to follow the production and consumption of oxygen and sulfur- containing molecules, and the High Pressure Liquid Chromatography (HPLC) instrument was used to measure the dielectric constant of the stressed fuel thereby providing information on the unsaturated fuel content. Finally, a multi-elemental analysis was used to find the elemental makeup of the deposits.

The FTIR analysis of POSF-2747 (hydrocreated fuel) showed that the amount of insoluble material was directly related to the amount of oxygenated product in the fuel. However, JPTS fuel did not produce any deposits. The GCAED traces verified the FTIR observations that some fuels (e.g., POSF-2827) do not form soluble oxidative products, but rather the sulfur atoms produce insoluble products. The elemental analysis of POSF-2747 deposits showed that sulfur atoms tend to concentrate in the deposits. Finaliy, the HPLC traces of fuel POSF-2747 are consistent with a large increase in oxygen- containing molecules, but POSF-2827 does not show an increase in the dielectric constant of the unsaturated fraction. Appendix A describes these and other results in detail.

3.1.2 Highlights and Conclusions. These tests provided several conclusions.

(a) The level of oxidation in more thermally stable fuel (as determined by JFTOT breakpoint and other flowing tests) is significantly higher than in less stable fuel.

(b) FTIR oxidation measurements confirmed that there is an inverse relationship between thermal stability as measured by solid deposits vs. that measured by oxidation. Further, the static tests we performed yielded results in broad agreement with our flowing tests.

(c) To adequately assess fuel stability, the availability of oxygen must be both limited and controlled. Arbitrarily increasing oxygen availability may yield results which are not applicable to oxygen-starved stressing processes. Finally, there is not a direct relation between the amount of oxidized products dissolved in a stressed fuel and the amount of insoluble solids formed.

3.2 MCRT (Static) Tests

3.2.1 Results. We used the MCRT method for studying the chemistry of deposit formation as well as for screening additives. This method is described in Appendix B. MCRT fuel samples were analyzed using a variety of diverse procedures such as Thermal Gravimetric Analysis (TGA), X-ray Photoelectron Spectroscopy (XPS), Fourier Transform Infrared Spectroscopy (FTIR), and Gel Permeation Chromatography (GPC).

Several fuels were evaluated using the MCRT in addition to the reference fuel (POSF-2827) and the thermally stable fuel (JPTS, POSF-2799). We found that the deposition tendency in the MCRT was primarily dependent on the fuel molecular weight. We performed cycling tests to study the deposit morphology and found that JPTS fuel gave a smooth layer even after completion of the tenth cycle. In contrast, the POSF-2827 fuel produced a flaky, wrinkled deposit along with the smooth layer after the fourth cycle. Scanning Electron Microscope (SEM) photographs revealed that the flakes are sheets or thin films which are crinkled rather than porous particles. We quantified insoluble gums produced in the MCRT. Such tests illustrate the effectiveness of antioxidants in reducing gum formation. Our test results showed that the rate of gum formation was not significantly higher for POSF-2827 fuel.

The TGA provides a quantitative measurement of weight change associated with thermally induced transitions. TGA of solid deposits from the MCRT cycling test of POSF-2827 and JPTS fuels revealed somewhat similar behavior under inert conditions (nitrogen); however, different profiles were observed in an oxidative atmosphere (air). The JPTS fuel exhibited a sharp trar si-tion at 432C. This indicates volatilization of a relatively simple material. The XPS technique can detect all the elements except H and He within 4 nm of a sample surface. We discovered that the sample containing an antioxidant (2761) is the most highly oxidized, followed by JPTS and hexadecane with DPDS, while POSF-2827 fuel showed the least oxidation. FTIR is a powerful tool in detecting the oxidation of fuel, and GPC separates molecules according to their effective size in solution. Preliminary data showed differences between gum deposits from the POSF-2827 and JPTS fuel formulations.

Table 2 is a summary of additive candidates evaluated using the MCRT and the relative ranking of those formulations. In Table 2, the insoluble gum values are given in absolute gum weight. The relationship between the gum polar fraction and MCRT solid residue is illustrated in Figure 3 for five different fuels. This result exemplifies the need for fuel characterization in terms of both criteria: oxidative stability (which is manifested in gum formation) and deposition tendency (which is manifested in solid formation). Thus, fuels which fall near the inflection point of this type of curve would be most thermally stable due to minimization of both the insoluble gums and the solids.

We evaluated additives supplied by Mobil Corporation with respect to their capability to hinder fuel degradation under oxidative conditions. Antioxidants were blended into jet fuel

POSF-2827 at a concentration of 25 mg/l and detergents were added at a level of 1000 mg/l. The formulated fuels were then subjected to the MCRT and the Isothermal Corrosion-Oxidation Test (ICOT). Table 3 summarizes the results. In the MCRT tests, only MCP-922 exhibited a measurable tendency toward solids inhibition. With respect to decreased carbon burn-off value, the HLPS test conducted by Pratt and Whitney showed that MCP-922 is the best antioxidant candidate submitted by Mobil Corporation to date.

3.2.2 Highlights and Conclusions. We completed this study of fuel deposits and additive effects using MCRT and reached the following conclusions.

(a) The MCRT test data correlated well with results from a variety of other techniques such as MTPT and Phoenix rig.

(b) Fuel molecular weight governed the deposition tendency in the MCRT tests.

(c) MCRT cycling tests showed marked differences in deposit morphology; JPTS fuel produced a smooth layer but POSF-2827 fuel gave a flaky, wrinkled deposit.

(d) The relationship between MCRT solid residue and gum polar fraction suggests a need for fuel characterization in terms of both criteria: oxidative stability (which is manifested in gum formation) and deposition tendency (which is manifested in solid formation). Thus, fuels which fall near the inflection point of this type of curve would be most thermally stable due to minimization of both the insoluble gums and the solids.

(e) Evaluation of additive samples supplied by Mobil Corporation showed that MCP-922 was the best antioxidant candidate.

3.3 Phoenix Rig (Flowing) Tests

3.3.1 Results. We performed extensive measurements in a Phoenix rig; the results of these measurements are presented in Appendix C.

These experiments revealed that the deposit thickness increases along the length of the test section until a maximum is reached, then it decreases. Also, tests with all the blended fuel samples showed a noticeable improvement in fuel thermal stability. The effects of block temperature on carbon deposition was also studied. As expected, carbon deposition increases with block temperature. Test duration also proved to be important; we found that carbon deposits increased by factors of 2.2 to 5.8 when the test duration was doubled to 12 hours. The most striking result was that at low bulk fuel temperatures, the oxygen and methane concentrations remain constant (oxygen at saturation level and methane at 0 ppm); however, as the temperature is increased, the oxygen concentration drops suddenly. Two fuels (POSF-2747 and POSF-2799) exhibited a drop of over 90 percent in the concentration of dissolved oxygen within a range of

about 40K change in the bulk fuel temperature. The third fuel (POSF-2827) showed a slow but measurable decrease in oxygen level over a wider temperature range. The onset of methane production occurs at a temperature that is very close to the bulk temperature at which there is a significant decrease in oxygen content.

The Phoenix rig was modified as shown in Figure 4 to include not just the heated single tube, but also a cooled test section and both hot and cold filters. Figure 5 compares the deposits measured in the hot section, on the hot filter, in the cold section, and on the cold filter for the Jet-A, Jet-A+25 mg/l AO-2, and Jet-A+6 mg/l MDA for a 12-hour 573K block temperature, 16-ml/min test. The extra test length (12 vs. 6 hours) resulted in a significant buildup of deposits at F3, where essentially none was visible after 6 hours for the baseline Jet-A. The antioxidant did not substantially affect the hot deposits, but significantly reduced the cold deposits while the metal deactivator reduced both the hot and cold section deposits. A noticeable reduction in the cold section deposits occurred even though the pressure drop across the cold filter had risen dramatically for all the additives.

Finally, the results of the oxygen depletion test are shown in Figure 6. This figure shows dissolved oxygen fraction as a function of the output bulk fuel temperature. The output fuel temperature is varied by increasing the block temperature while maintaining a constant flow rate. Two separate initial conditions are shown, each represented by the percentage of oxygen in the sparge gas.

3.3.2 Highlights and Conclusions. We reached the following conclusions from our study of the carbon deposition, oxygen depletion, and methane production in a single-pass flowing heat exchanger (Phoenix rig).

(a) Both block temperature and test duration increased the total carbon deposits in a nonlinear fashion. Tests with all the blended fuel samples showed a noticeable improvement in fuel thermal stability.

(b) Above a threshold bulk temperature of 450K, the fuel- dissolved oxygen concentration dropped suddenly and the onset of methane production was triggered. The consumption of oxygen had a complicated behavior; it was different in the early and later stages. With nitrogen sparging, methane production was greatly reduced.

(c) Tests with both oxygen-saturated and oxygen-depleted fuels show that the solubility of oxygen is linearly related to the fraction of oxygen in a sparge gas, and the amount of deposit is linearly related to the total quantity of dissolved oxygen passed.

(d) Antioxidants were effective in reducing the deposits on the hot test section, but caused increased plugging of cool downstream filters. The use of antioxidants in nonhydrotreated fuels

was of little use in preventing total deposits. Metal deactivators show limited promise; however, there is significant promise from the use of packages such as JFA-5.

3.4 Analysis of Deposit Formation

3.4.1 Results. It has long been known [2] that oxygen consumption is an important first step in the formation of deposits in jet fuels. Also, there is general agreement that peroxides, alcohols, ketones, and acids are precursors to solid formation and that fuels oxidize to form gums which, in turn, polymerize and condense to form solids. Hazlett [3] has described three key criteria any proposed mechanism must meet: (1) dissolved oxygen must initiate the deposition process, (2) hetero-atom-containing molecules should play an important role, and (3) only a small amount of the fuel should be involved in the deposit formation process.

Our analysis of deposit formation is presented in Appendix D. In this analysis, stability measurements are divided into two parts: (1) those based on deposit formation (referred to as thermal stability) and (2) those based on the ability to oxidize (referred to as oxidative stability).

From our measurements, we have observed that the relative thermal stability of the base fuels, in order from most to least stable, is POSF-2799, POSF-2747, and POSF-2827. This conclusion is based on the heteroatom concentration, boiling range, past experience with hydrotreated fuels, and the fact that F-2799 is a special, thermally stable fuel that includes a thermal stability additive package (JFA-5). Note that less deposit indicates greater thermal stability, as does a higher breakpoint temperature. Now, in contrast to past observations [2-4], the Phoenix rig experiments showed an inverse order of oxidation temperature (oxidative stability) versus thermal stability. This lends strong support to a free-radical autooxidation theory that proposes the following ideas.

(a) Oxygen Consumption. Deposit formation does not follow oxidation. Rather, the presence of some heteroatoms is responsible for increased deposit formation and their removal increases both the thermal stability and susceptibility to oxidation of jet fuels. As early as 1963, it was recognized [5] that hydrotreating removed some of the natural antioxidants from jet fuels, and naturally occurring antioxidant molecules inhibit the oxidation of fuel and deposit forming precursors. Consequently, antioxidant additives have been specified in UK and USA military specifications DERD-2494 (1963) and MIL-T-5624 (modified 1976) for addition to hydrotreated fuels.

(b) Methane Production. The free-radical nature of the chemical reactions is supported by the appearance of methane in the Phoenix rig at temperatures near 500K, and only when the oxygen is largely removed. It is reasonable to expect that methane is the result of methyl-radical production arising from the unimolecular fission of larger alkyl radicals to form methyl and alkenes. Our analysis shows that the appearance of methane only after significant depletion of the oxygen

concentration is consistent with a free-radical mechanism. Calculations indicate that the global activation energy of 10.6 kcal/mole is very reasonable for this type of reaction mechanism.

(c) ***Thermal versus Oxidative Stability.*** Jet fuel oxidation results in the buildup of peroxides, ketones, aldehydes, alcohols, and acids from the autoxidation cycle; sulfates, sulfones and nitrous compounds from the inhibitors originally present; and alkenes from the decomposition of radicals. Many of these oxidized compounds can, if present in sufficient quantity, inhibit fuel oxidation. However, the inability to oxidize is closely linked to the tendency to form deposits.

A qualitative picture of the behavior of both oxidizability and deposit formation is shown in Figure 7 for increasing amounts of easily oxidized material in the fuel. Ease of oxidation decreases as concentration increases; however, it must eventually increase, causing a minimum in the oxidation curve. Deposit formation rate should steadily increase with increasing concentration. Note that the region for jet fuels is shown where these two measures of stability move inverse to each other. Identification of this region is empirical.

The above discussion implies that there is an optimum amount of antioxidant that should be present in a jet fuel. Less than the optimum amount does not prevent oxidation, while too much can induce deposit formation. The formulation of antioxidants for addition to fuels should be based not only on their ability to act as antioxidants, but also on their ability to ensure that the termination products of the antioxidant radical are soluble rather than insoluble.

3.4.2 Highlights and Conclusions. We have tested several fuels in a variety of different test apparatuses to determine their relative stability. A comprehensive analysis of these results and those of previous researchers has produced the following conclusions.

(a) Dividing fuel stability into thermal stability (based on the deposit forming tendency) and oxidative stability (based on the ability to oxidize and form peroxides, ketones, alcohols, and acids) leads to the seemingly anomalous statement: "Fuels that oxidize easily are likely to be thermally stable, while fuels that are not thermally stable are not easily oxidized." This statement was found to hold, independent of the fact that oxygen reaction with fuel is a necessary first step for the production of solid deposits.

(b) A theoretical analysis of the autoxidation mechanism of hydrocarbons can account for the observed oxygen dependencies as well as all the other needed criteria for the deposit mechanism, if the peroxy radical of the antioxidant molecules are the precursors to the deposit formation.

(c) Analysis of the free-radical chemical reactions accounts for the appearance of methane in the Phoenix rig and also other past observations [4-6].

4. HIGHLIGHTS AND CONCLUSIONS

In this section, we analyze our entire effort from the viewpoint of program objectives, how we met those objectives, what new knowledge about the chemistry of deposit formation emerged, and how this can be used to develop advanced thermally stable jet fuels for aircraft of the future.

To address the program objectives, we formulated tests designed to thermally stress several baseline and blended jet fuel samples in a flask or an MCRT apparatus (static tests) and in a single-pass heat exchanger "Phoenix Rig" (flowing tests). The deposited residue samples which comprise gums, insolubles, and carbon residue were examined by using a variety of sophisticated chemical analysis instrumentation. The following highlights and conclusions emerged.

4.1 Highlights

4.1.1 Role of Sulfur and Oxygen Species in Deposit Formation. Jet fuel oxidation results in the buildup of peroxides, ketones, aldehydes, alcohols, and acids from the autoxidation cycle; sulfates, sulfones, and nitrous compounds from the inhibitors originally present; and alkenes from the decomposition of radicals. Many of these oxidized compounds can, if present in sufficient quantity, inhibit fuel oxidation and, hence, form deposits. However, if sufficient quantities of the easily oxidized compound are available, the compound will help stimulate oxidation and again affect deposit production.

We established MCRT as an important static test technique and used it to determine the extent of oxidation occurring in POSF-2827 jet fuel. We found that the POSF 2827 fuel showed very little total acid number (TAN) increase but did exhibit a relatively strong carbonyl peak, indicating the presence of ketones, aldehydes, and possibly esters. Further, our study revealed that the oxidation of the fuel, and consequently its acidity, were strongly temperature-dependent. These important experimental observations led us to formulate a comprehensive theory of deposit formation.

4.1.2 Chemistry of Surrogate and Other JP Fuels. Our subcontractor, Eastern Kentucky University (Principal Investigator: Professor W. D. Schulz, Department of Chemistry) completed the chemical investigation of oxidation deposits and the effects of additives on deposits. The final report for this effort is attached as Appendix E.

This work showed that many fuels (surrogate JP-8, JP-7, JP-TS, and POSF-2747) produce increasing amounts of insoluble material with an increasing concentration of oxidized species, whereas fuels such as POSF-2827 produce large amounts of insolubles (phenolic compounds) with essentially no detectable concentration of oxidation products. In the early stages of the oxidation of JP-8S, the main products resulted from the reaction of cyclooctane and hydrogen alpha to an aromatic ring (xylene, butylbenzene, tetramethylbenzene, tetralin, and

methylnapthalene). As the oxidation progresses, the concentration of secondary alkylalcohols and ketones as well as substituted furanones increase, presumably due to alkane oxidation.

From the GC-MS analysis of soluble oxidation products, it was found that deposits from JP-8S and POSF-2747 were varnish-like polar species with some peroxide-linking that can be alleviated by using a proper detergent. In contrast, fuels such as POSF-2827 produce deposits strongly bonded (hemiketal type R'OH + RCOR → R-O-CH(OR')R bond) into a solid phase. Phenols interacting with carbonyls from aldehydes, ketones, or furanones form a real, reversible, covalent bond that increases molecular weight and polarity to produce deposit components.

4.1.3 Oxygen Consumption/Methane Production. In previous literature [2], oxygen consumption was believed to lead to deposit formation. Our static and flowing tests have questioned this time-honored process. We found that previous deposit formation models are inadequate in that they do not predict both observed oxygen dependencies. We have shown that our theory can account for the observed oxygen dependencies in not only the recent work but also many previous efforts. Finally, tests with both oxygen-saturated and oxygen-depleted fuels show that the amount of deposit is linearly related to the total quantity of dissolved oxygen passed, and that oxygen consumption is pseudo-zero-order in the early stages, decaying to pseudo-first-order when the oxygen nears depletion [7,8].

As for methane production, we found that the production of methane in the Phoenix rig experiments results from hydrogen abstraction by methyl radicals. This process is in competition with the reaction of methyl with oxygen.

$$CH_3 + O_2 + M \rightarrow CH_3O_2 + M \qquad (1)$$

$$CH_3 + RH \rightarrow CH_4 + R \qquad (2)$$

Thus, methane formation begins to occur at temperatures near 500K at which the oxygen is completely removed. An activation energy for the hydrogen abstraction reaction can be calculated and was found to be 10.6 kcal/mole. This value agrees well with the activation energies of similar processes such as the reaction of ethane: $CH_3 + C_2H_6 \rightarrow CH_4 + C_2H_5$ (E = 10.8 kcal/mole).

4.1.4 Theory of Deposit Formation. We developed a general theory of hydrocarbon oxidation (Appendix D) and its implication to the formation of jet fuel deposits. This theory embodies a free-radical, autooxidation chain mechanism and proposes that the presence of naturally occurring antioxidant molecules plays an important role in both inhibiting the oxidation of fuel and forming deposit precursors. Thus, an optimum amount of antioxidant should be present in a jet fuel; less than the optimum amount does not prevent oxidation, and too much can induce deposit formation.

In this theory, a clear distinction is made between the fuel thermal stability (based on the deposit forming-tendency) and oxidative stability (based on the ability to oxidize and form peroxides, ketones, alcohols, and acids). This leads to the seemingly anomalous statement: "Fuels that oxidize easily are likely to be thermally stable, while fuels that are not thermally stable are not easily oxidized." This statement was found to hold, independent of the fact that oxygen reaction with fuel is a necessary first step for the production of solid deposits. Also, if the peroxy radicals of the antioxidant molecules are the precursors to deposit formation, then the theory accounts for the observed effects of oxygen consumption and methane production on deposit formation, the observed first-order rate dependence of oxygen uptake in doped-hydrocarbon systems [4], and the fact that adding of small amounts of easily oxidized compounds to alkanes causes a decrease in the oxidation rate rather than an increase [5,6].

4.1.5 Effects of Additives. We evaluated several additives supplied by Mobil Corporation (Table 3) with respect to their capability to hinder fuel degradation under oxidative conditions. We found that in the MCRT tests, only MCP-922 exhibited a measurable tendency toward solids inhibition. With respect to decreased carbon burn-off value, the HLPS test conducted by Pratt and Whitney showed that MCP-922 is the best antioxidant candidate submitted by Mobil Corporation to date.

In the modified Phoenix rig (Figure 4), the addition of antioxidant to Jet-A had limited success in reducing the hot-section deposits and adding a phenol-based antioxidant caused a serious deposition problem. The metal deactivator reduced both hot- and cold-section deposits. Finally, the JFA-5 additive package (believed to contain a combination of antioxidant and metal deactivator) produced the least amount of deposit in the heated section.

4.1.6 Deposit Formation Studies. Our subcontractor, Purdue University (Principal Investigators: Professor A. H. Lefebvre, School of Mechanical Engineering, and Professor L. F. Albright, School of Chemical Engineering), examined the influence of fuel composition, additives, surface composition, and flow conditions on deposit formation. Their final report is attached as Appendix F.

The effect of fuel composition was examined for five different fuels in the recirculation test mode. It was found that the JPTS fuel (POSF-2789) yielded exceptionally low deposits, whereas the Jet A fuel (POSF-2827) had the poorest thermal stability. Using a single-pass experimental technique, it was found that fuel additives in POSF-2827 failed to decrease total deposits. Likewise, the deposition rates in the fuel tubes with surface treatment were higher. This negative result was attributed to too severe a surface pretreatment that increases surface roughness and promotes the collection of precursors. Finally, it was found that a reduction in fuel tube diameter will initially increase deposit thickness. However, a continual decrease in tube diameter increases the scrubbing action of the fuel along the tube wall, thus decreasing deposit thickness.

4.2 Conclusions

The conclusions of our research may be summarized as follows.

(a) The presence of small quantities of certain antioxidant compounds (peroxides, ketones, alcohols, etc.), naturally occurring or produced during fuel oxidation, inhibits oxidation. In large quantities, these compounds stimulate oxidation and, therefore, deposit formation.

(b) Deposit formation does not follow oxidation. Rather, the presence of hetero-atoms increases deposit formation, and their absence increases both thermal stability and susceptibility to jet fuel oxidation.

(c) A free-radical autooxidation theory of deposit formation has been developed. In this theory, a clear distinction is made between the fuel thermal stability (based on the deposit forming tendency) and oxidative stability (based on the ability to oxidize and form peroxides, ketones, alcohols, and acids). This leads to the seemingly anomalous statement: "Fuels that oxidize easily are likely to be thermally stable, while fuels that are not thermally stable are not easily oxidized." This statement was found to hold in experimental tests.

(d) Of the several additives supplied by Mobil Corporation, our MCRT tests demonstrated that only MCP-922 exhibited a measurable tendency toward solids inhibition. In the modified Phoenix rig, antioxidant in Jet-A reduced the hot-section deposits, metal deactivator reduced both hot- and cold-section deposits, and JFA-5 produced the least amount of deposits in the heated section.

REFERENCES

1. Harrison, W. E., III, "Aircraft Thermal Management: Report of the Joint WL/ASD Aircraft Thermal Management Working Group," Report No. TR-90-2021, Wright-Patterson Air Force Base OH, 1990.

2. Baker, C. E., Bittker, D. A., Cohen, S. M., and Seng, G. T., "Research on Aviation Fuel Instability," NASA Tech. Memo 83420, 1983.

3. Hazlett, R. N., "Frontiers of Free Radical Chemistry," Academic Press, New York NY, 1980, p. 195.

4. Beaver, B. D., and Gilmore, C., "Oxidation Degradation of Petroleum Products via a Non-Peroxyl Radical Chain Pathway: Electron Transfer Initiated Oxidation (ETIO) Revisited," Fuel Sci. and Tech., Vol. 9, 1991, p. 811.

5. Mayo, F. R., and Lan, B. Y., "Gum and Deposit Formation from Jet Turbine and Diesel Fuels at 130C," Ind. Eng. Chem. Prod. Res. Dev., Vol. 25, 1986, p. 333.

6. Reddy, K. T., Cernansky, N. P., and Cohen, R. S., "Degradation Mechanism of n-Dodecane with Sulfur and Nitrogen Dopants During Thermal Stressing," J. Propulsion and Power, Vol. 5, 1989, p. 6.

7. Heneghan, S. P., Martel, C. R., Williams, T. F., and Ballal, D. R., "Effects of Oxygen and Additives on the Thermal Stability of Jet Fuels," to be presented at the 38th ASME (Int.) Gas Turbine and Aeroengine Conference, Cincinnati OH May, 1993.

8. Jones, E. G., Balster, W. J., and Post, M. E., "Degradation of a Jet-A Fuel in a Single-Pass Heat Exchanger," to be presented at the 38th ASME (Int.) Gas Turbine and Aeroengine Conference, Cincinnati OH, May, 1993.

Table 1. Properties of Baseline, Blended, and Surrogate Fuels

Baseline Fuels

	ASTM Method	POSF-2747	POSF-2799	POSF-2827
Source		Sun Oil	Exxon	Shell
JFTOT	D3241	605	672	539
Breakpoint(K)				
Sulfur wt. %*	D3227	0	0	0.1
Aromatics Vol %	D1319	19	9	19
Existent Gum mg/ml	D381	0	0.4	0
Flash Point (K)	D93	395	393	413

Blended Fuels

Fuel Identification	JFTOT (K)	Base Fuel	Additives
POSF-2814	590	POSF-2747	Fuel system icing inhibitor Static Dissipator Corrosion Inhibitor
POSF-2827A	530	POSF-2827	JFA-5-12 mg/l
POSF-2827B		POSF-2827	JFA-5 - 50 mg/l

Surrogate JP-8S Fuel

Compound	mass %
methylcyclohexane	5
m-xylene	5
cyclooctane	5
decane	15
butylbenzene	5
tetramethylbenzene	5
tetralin	5
dodecane	20
methylnapthalene	5
tetradecane	15
hexadecane	10
isooctane	5

Table 2. Summary of Fuel Additives Evaluation Using MCRT Test

Additive Evaluation Using MCRT Test at 250 C, Air Atmosphere 3 Hour Test Time				
Sample	**Percent Residue**	**Standard Deviation**	**Gums (mg/g)**	**TAN**
Base Fuels				
2747	0.10	0.03	6.7	9.18
2799	0.11	0.02	ND	ND
2828	0.21	0.03	ND	ND
2857	0.31	0.05	18.1	11.73
2827	0.46	0.09	25.8	17.16
Fuels + Additive				
2827/OU-23	0.35	0.11	11	11.77
2827/TBHQ-100	0.35	0.11	10.9	13.58
2827/2753	0.37	0.08	13.3	14.32
2827/2774	0.37	0.09	ND	ND
2827/2778	0.37	0.09	ND	ND
2827/TBHQ-200	0.39	0.06	9.7	11.62
2827/2748	0.40	0.09	ND	ND
2827/2761	0.40	0.06	ND	ND
2827/TBHQ/D1/JFA-5	.40	0.09	20.6	12.09
2827/TBHQ/JFA-5	0.40	0.09	17.8	12.00
2827/2786	0.42	0.08	21.1	13.77
2827/PANA/DODPA	0.42	0.07	13.8	11.58
2827/TBHQ/BHA	0.43	0.09	18.4	13.21
2827/2744	0.46	0.07	ND	ND
2827/2726	0.48	0.09	ND	ND
2827/2850	0.48	0.09	22.1	14.70
2827/2736	0.51	0.08	12.9	12.90
ND = Not Determined				

Table 3. Results on Best Additives Blended with POSF-2827 Fuel

% Improvement

	MCP-922 (AO-N)	MCP-1020 (Det.)	MCP-1025 (Det.)
ICOT @180°C (Bulk, Surface Deposits)	ND	100	100
MCRT @250°C			
TAN	16	21	32
Gums	64	68	29
Solids	28	10	10
HLPS@335°C P&W Data Carbon	76	30	ND

ND = Not Determined

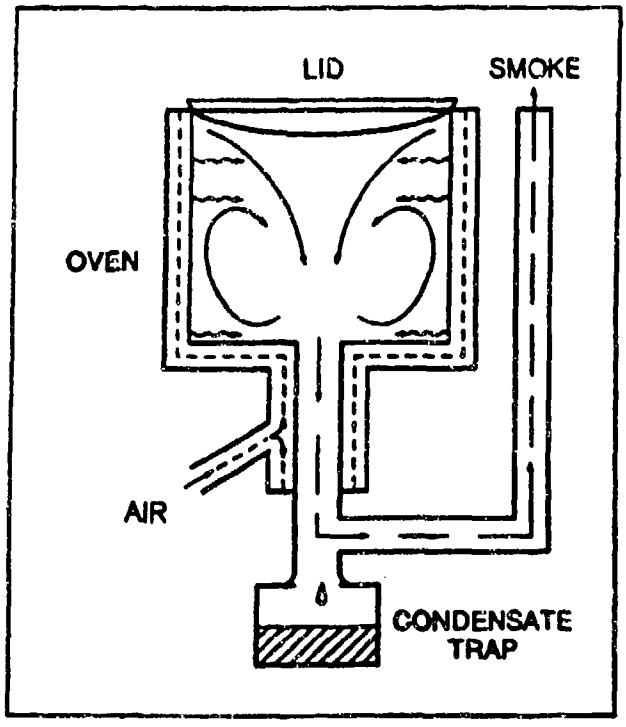

Figure 1. Schematic diagram of the MCRT test apparatus

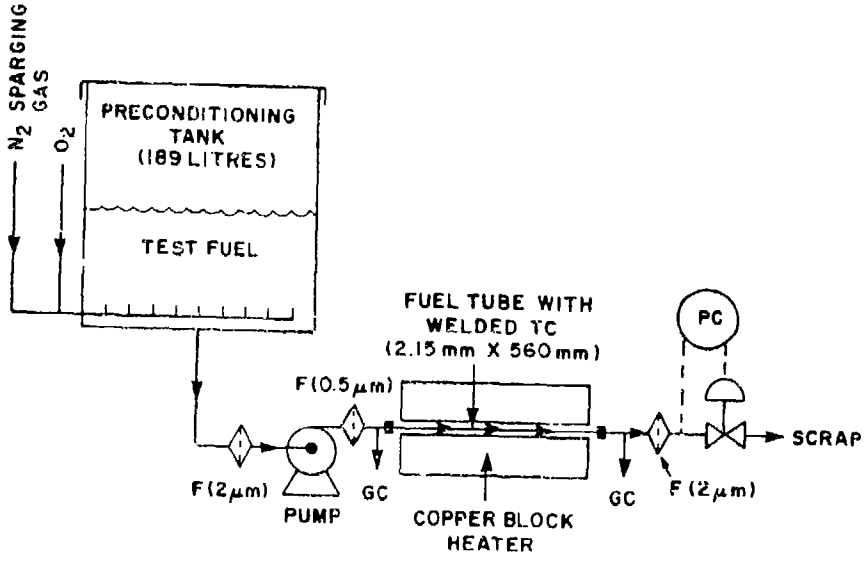

Figure 2. Schematic of the Phoenix rig showing the fuel preconditioning tank, pump, filters (F), copper block heater, and gas chromatograph (GC) sampling locations.

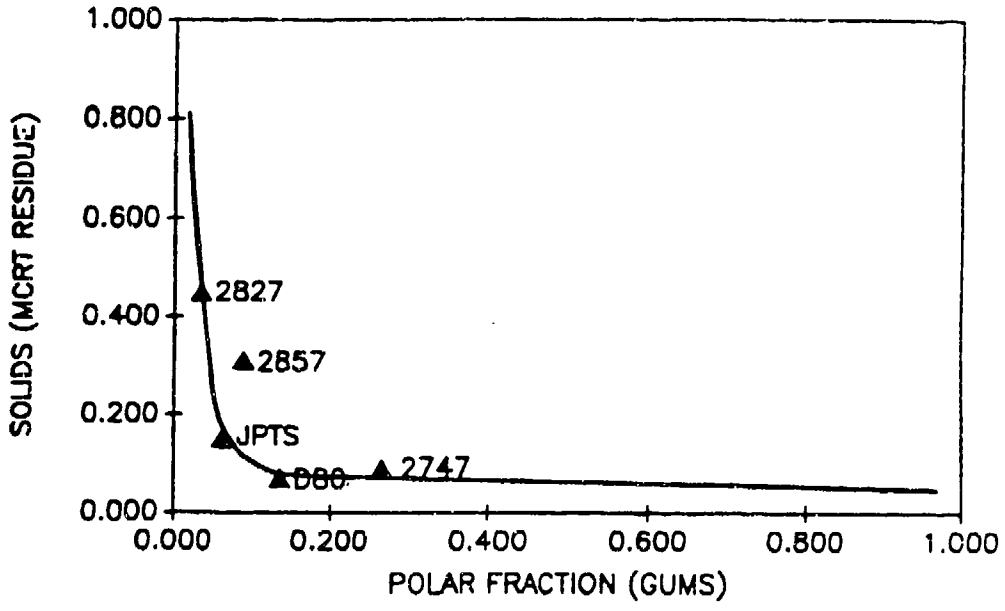

Figure 3. MCRT solid residue vs. gum polar fraction relationship

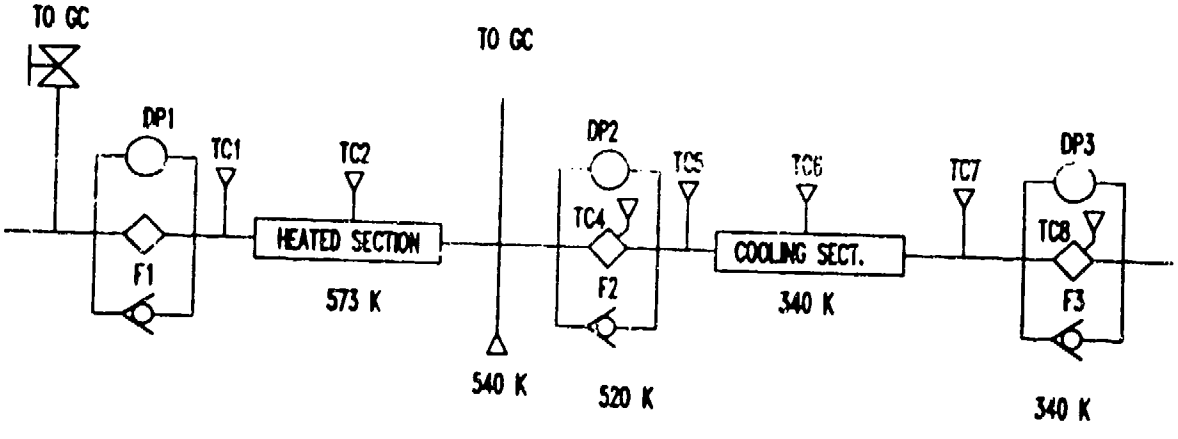

Figure 4. Flow diagram of the modified Phoenix rig showing the relative location of thermocouples (TC), differential pressure gauges (DP), filters (F), and gas chromatograph sampler (GC). Listed temperatures are typical for 16 ml/min flow and 300C (573K) block temperature.

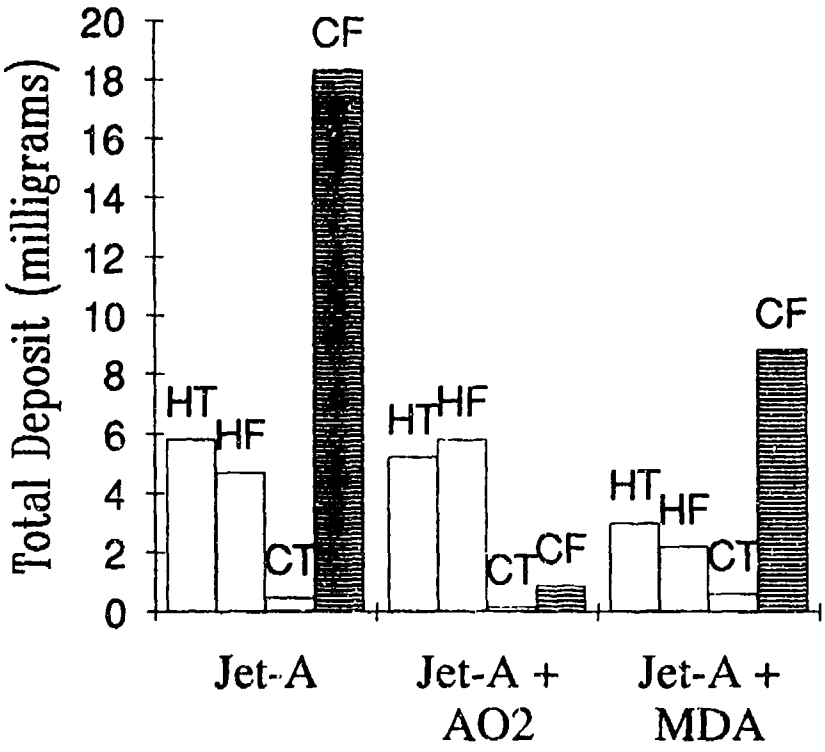

Figure 5. Effectiveness of antioxidant (AO) and metal deactivator (MDA) additives on deposit from Jet-A fuel; (HT-Hot Tube, HF-Hot Filter, CT-Cold Tube, CF-Cold Filter)

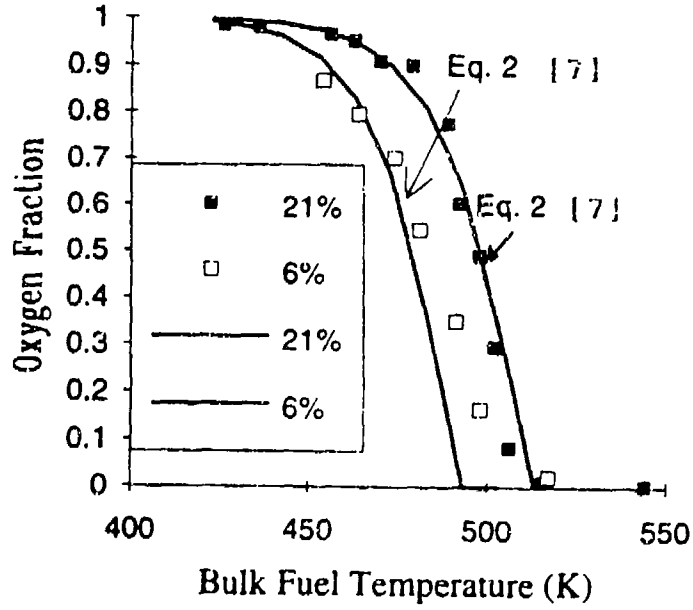

Figure 6. Variation of oxygen consumption with bulk fuel temperature for two initial oxygen sparge conditions

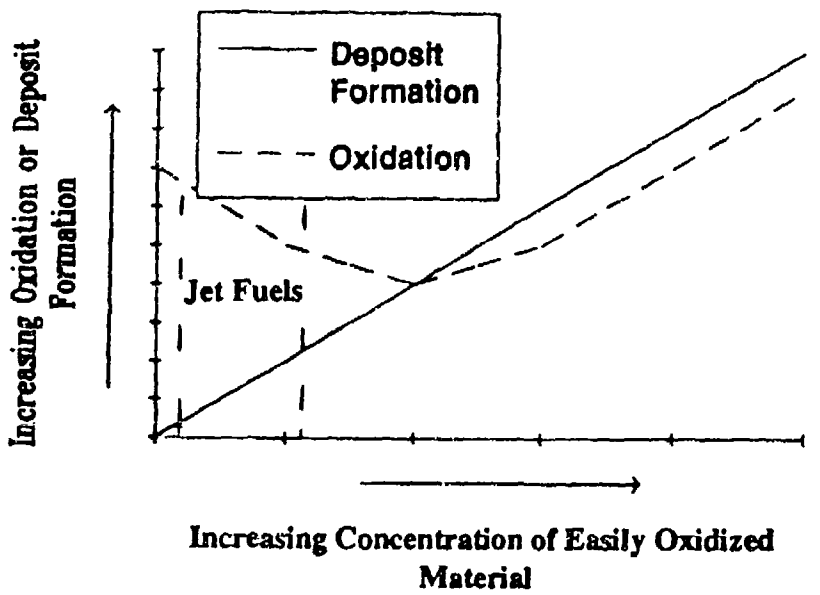

Figure 7. Qualitative behavior of fuel oxidative and thermal stability with increasing concentration of easily oxidized species

APPENDIX A

STATIC TESTS FOR THE EVALUATION OF FUEL ADDITIVES

by

Shawn P. Heneghan
University of Dayton, Dayton, Ohio

Stacy L. Locklear, David L. Geiger, and Steven D. Anderson
Wright Laboratories, Wright Patterson Air Force Base, Ohio

and

William D. Schultz
Eastern Kentucky University, Richmond, Kentucky

Published as AIAA Paper No. 92-0686. To Appear in AIAA Journal of Propulsion.

STATIC TESTS FOR THE EVALUATION OF FUEL ADDITIVES

Shawn P. Heneghan
University of Dayton
Dayton, OH 45469
Stacy L. Locklear, David L. Geiger, and Steven D. Anderson
Wright Laboratories
Wright Patterson Air Force Base, OH 45433
and
William D. Schultz
Eastern Kentucky University
Richmond, KY 40475

Abstract

Jet fuels and jet fuel surrogates have been thermally stressed to simulate the time/temperature history of aircraft fuel handling systems. The resulting fuels, soluble products, and insoluble products have been analyzed. Quantitative and qualitative measurements of the deposits and the fuels are presented. These yield insights into the chemical and physical processes important to the formation of deposits.

Surrogate fuels have been used to develop quantitative Fourier transform infrared (FTIR) techniques for detecting the formation of oxidation products. Gravimetric analysis is used to quantify the amount of deposit materials formed in thermal stressing. FTIR gives qualitative details of the chemical structure of the deposits and soluble oxidized products. Gas chromatography with atom sensitive atomic emission detection is used to detail some of the molecules involved in the chemistry of deposit formation.

In general, the static tests described here indicate that there is good agreement between static and flowing tests concerning the quality of a fuel. However, to adequately assess fuel stability, the availability of oxygen must be both limited and controlled. Arbitrarily increasing the oxygen availability is likely to yield results which are not applicable to oxygen starved stressing processes. Further, there is not a direct relation between the amount of oxidized products dissolved in a stressed fuel, and the amount of insoluble solids formed.

Abbreviations

ASTM - American Society for Testing and Materials
FTIR - Fourier Transform InfraRed
GCAED - Gas Chromatography with Atomic Emission Detection
HPLC - High Pressure Liquid Chromatography
IR - Infrared
JFTOT - Jet Fuel Thermal Oxidative Tester
JP - Jet Propellant (fuel)
JPTS - Jet Propellant Thermally Stable
POSF - Propulsion Directorate - Fuels Branch

Introduction

The Air Force JP-8 + 100 is a systematic program to investigate the performance of various fuel additives, with a goal of substantively increasing the cooling capacity of jet fuel. Fuel additives have been supplied to Wright Laboratories by a variety of manufacturers, and have been blended and shipped to several researchers to evaluate additive performance.

The fuel was subjected to a variety of tests, each of which simulated some portion of the thermal history of the real fuel as it encounters different thermal environments in a jet fuel handling system. Stagnant heated flask tests, as described here, were used to replicate on-board fuel storage systems, and to study the chemistry associated with the thermal degradation of fuel through the auto-oxidation process.

Among the goals of this study are the evaluation of jet fuel stability and the products of jet fuel breakdown by spectroscopic techniques, the chemical evaluation of the actual deposits formed, and the development of sufficient kinetics understanding to compare flowing tests, independent of operating conditions with non-flowing tests. In particular, Fourier transform infrared (FTIR) techniques are developed to quantify the amount of alcohol and ketone species in surrogate fuels. Gas chromatography with atomic emission detection (GCAED) is used to follow the production/consumption of oxygen/sulfur containing molecules. Multi-elemental analysis is used to study the elemental makeup of the deposits.

This paper describes the fuels used in the various experiments, the experiments used to stress the fuels, and the results of both qualitative and quantitative analysis techniques used to analyze the deposits and the fuels. In particular, the importance of the auto-oxidation process to the formation of deposit material is discussed.

Experimental Work

Fuels Description

To assist in the development of analytic/ spectroscopic tests, two systems (one consisting of the reference jet fuels, and one consisting of a surrogate jet fuel) were used. The reference fuels and some of their properties are listed in Table 1. Propulsion Directorate - Fuels Branch (POSF)-2747 is a highly hydro-treated Jet A-1 fuel, while POSF-2799 is an Air Force specification fuel, jet propellant thermally stable (JPTS), which has good thermal stability characteristics. The goal of the Air Force JP 8+100 program is to develop a fuel which exhibits the thermal stability characteristics of JPTS through the addition of additives to typical JP-8. Fuel POSF-2827 is a non-hydro-treated Jet A, with a broader boiling range, and increased hetero-atom concentration. It is expected that this fuel will exhibit lower thermal stability than POSF-2747. In addition, POSF-2814 is a JP-8 made by adding icing inhibitor, static dissipator, and corrosion inhibitor to POSF-2747. Finally, a JP-7 and two other JP-8 fuels were also tested.

JPTS has a Jet Fuel Thermal Oxidative Tester (JFTOT) breakpoint of 399C - indicative of its excellent thermal stability. POSF-2747 has a breakpoint of 332C while POSF-2827 has a breakpoint of 266C. These fuels all pass ASTM D3241 and the breakpoints indicate the anticipated ordering of the stability. Further, the relative thermal stability of these three fuels has been established recently in several flowing systems, and it is in agreement with the JFTOT breakpoint analysis.

Surrogate fuels comprise a mixture of selected hydrocarbons. The selection and mixture ratio of the hydrocarbons is designed to yield a solution which can mimic many of the properties of a real fuel, yet still have the simplicity of a pure hydrocarbon mixture. The great value of surrogate fuels is their simplicity which allows for the observation of intermediate product formation. This formation is often obscured by the complexity of real fuels. The makeup of the surrogate fuel is listed in Table 2. This mixture exhibits a boiling range of 92C to 286C, contains 22% aromatics, 0% alkenes, and a density of 0.8 g/ml.

Flask test

Fuels were heated in round-bottom flasks under 0C reflux at a temperature of 180C. Oxygen was flowed into the heated fuel for two reasons. First, it was found that bubbling oxygen at 180C was necessary to achieve significant (gravimetrically measurable) degradation in time periods approaching four hours. Second we hoped that maintaining oxygen saturation would remove the dissolved oxygen content as a variable in the system.

Deposits were collected by two separate methods. In one set of experiments, the entire 30 ml sample of fuel was cooled, and decanted though a filter. Deposits were collected either in the filter or in an acetone wash. Deposits were then dried and weighed. In the second set of experiments 10 ml of a 100 ml sample were extracted filtered, washed, dried, and weighed. These filterable deposits were collected from the same samples used in the quantitative FTIR measurements.

FTIR

Surrogate fuel was used to show that the amount of oxidized product in the fuel could be measured quantitatively. Various quantities of alcohol (octanol), and ketone (2-octanone) were added to the fuel, and the integrated response of FTIR was determined. The spectrometer used for these tests was a Mattson Galaxy Series 4020. The surrogate fuel was described in Table 2 and all chemicals are 99% purity from Aldrich. A Nicolet model 740 FTIR was used for qualitative analysis of the fuels and the deposits.

Other Tests

Fuels (stressed and unstressed) and deposits were studied by following the total acid number of the fuel (ASTM D3242). The fuels were further analyzed by GCAED (Hewlett Packard HP5962a), and high pressure liquid chromatography (HPLC). Elemental composition of the deposits was measured on a Leco CHN-932 elemental analyzer.

Results

Flask Tests

Table 3 shows the development of insolubles at constant time (5hrs.) and temperature (180C), while allowing the flow rate of oxygen to vary for fuel POSF-2747. Table 3 also lists values of total acid number of the fuel and the integrated FTIR absorption near 1700 cm^{-1}.

Under similar conditions of stressing, JPTS produces essentially no insoluble materials, despite having an elevated acid number, and showing absorption in the 1722 cm^{-1} region. Similarly, POSF-2827 produces only 3-7 mg of insoluble product independent of the oxygen flow. It shows no other signs of being strongly oxidized.

Qualitative IR

The infra-red spectra of products from POSF-2747 show a similar qualitative behavior (Figure 1). The absorption pattern is typical of an organic acid, with

absorptions in the region of 1700 cm^{-1} from the carbonyl group and the broad absorptions near 3000 cm^{-1} from the OH moiety. Again, JPTS stressed fuel shows similar features, while the stressed fuel from POSF-2827 shows almost no absorption in the 1700 cm^{-1} or 3100 cm^{-1} region.

Quantitative IR

A surrogate fuel was used to establish the ability of FTIR to quantitatively measure the amount of oxidized product in fuel. After determining the integrated response factors for ketones and alcohols in surrogate fuels, seven different fuels were stressed under oxygen rich conditions for two hours at 175C. The amount of alcohol and ketone was determined, and the amount of filterable solid deposits formed (in 10 ml) was determined. Table 4 lists the results of the concentration of alcohol, ketone, the sum of oxidation products, and the amount of filterable solids.

Other tests

The HPLC of stressed and unstressed POSF-2747 shows that there has been a significant change in the unsaturated fraction of the fuel. Figure 2. shows the dielectric constant detection of fuel POSF-2747 before and after stressing at 180C with bubbling oxygen for 4 hours. The negative response of the second (the unsaturated fraction) peak after stressing indicates that the dielectric constant of that fraction has increased significantly. As a result, changes in the amount of unsaturates cannot be determined. The HPLC of POSF-2827 does not show the same type of major change in the dielectric constant of the stressed fuel.

A GCAED analysis of two fuels, the hydrotreated POSF-2747 and the non hydro-treated POSF-2827, provide additional data on the oxidation of fuels. POSF-2827 shows the presence of sulfur (Figure 3), while POSF-2747 does not. In the stressed fuels (Figure 4), POSF-2827 shows that the sulfur has been intimately involved in the reactions, yet the oxygen level is barely visible. POSF-2747 shows significant oxidation

Finally, the deposits formed in stressed POSF-2747 have been analyzed for elemental composition. The deposits are greater than 20% oxygen by mass and nearly .2% sulfur. As yet the elemental composition of the deposits for POSF-2827 has not been measured.

Discussion

Table 3 indicates that the amount of insoluble material was directly related to the amount of oxygenated product in the fuel. However, this is true for only one fuel (POSF-2747 -- the highly hydrotreated fuel). JPTS also forms oxygenated fuel soluble products (according to the IR spectra), but produces almost no deposits. POSF-2827 produces very little insoluble product, and the total insoluble solids formed are not a strong function of the amount of oxygen available.

The GCAED traces (Figures 3 and 4) verify the FTIR observations that some fuels do not form soluble oxidative products. POSF-2827 has sulfur atoms present, and these compounds are significantly involved in the chemical reactions which take place under stressing. This fuel however does not form significant amounts of soluble oxidation products. POSF-2747 contains no detectable sulfur. This fuel consumes oxygen, forming a large number of detectable oxygen containing compounds (Figure 4).

The HPLC traces of POSF-2747 (Figure 2) are consistent with a large increase in oxygen containing molecules. POSF-2827 does not show a similar increase in the dielectric constant of the unsaturated fraction. This is consistent with the GCAED observations that fewer oxygen containing species are present in stressed POSF-2827 relative to POSF-2747 as highly oxygenated species are likely to be more polar, and exhibit a greater dielectric constant than non-polar compounds.

The sulfur atoms which are involved in reactions in the stressed POSF-2827 probably show up in the insoluble products. The number of sulfur atoms in the fuel has decreased by more than a factor of 2 (note the change of scale in Figure 4). Sulfur atoms tend to concentrate in the deposits as shown by the elemental analysis of POSF-2747 deposits. The deposits formed by POSF-2747 contain nearly .2% sulfur, despite having less than 50 ppm sulfur in the fuel. The large amount of oxygen in the solids is also consistent with an easily oxidized fuel.

Figure 5 is a plot of the oxygenated fuel-dissolved products versus the filterable solid materials formed (Table 4). There is good agreement between the observed amount of ketone and alcohol produced. Interestingly, some fuels produce deposits, while not forming any oxygen containing products at all. In fact, if JPTS and surrogate jet fuel (JP-8S) are not considered, the general conclusion is that fuels which oxidize easily will, in general, not form large amounts of insoluble solids. JPTS seems to not oxidize sufficiently to follow this trend, but it has an added anti-oxidant which may account for the low level of oxidative products. JP-8S oxidizes too much given the large amount of solids formed. However, JP-8S is not really a fuel; thus its comparison here may not be appropriate

The general behavior of ease of oxidation being inverse to ease of solid formation has been observed in the past by Hardy[1] His conclusion was based on the observation of 13 jet fuels. He measured the ability to oxidize by measuring the resulting peroxide number after an accelerated storage test under oxygen overpressure at 100C for 48 hours, and the deposits in a flowing gravimetric JFTOT test. His conclusions are identical to ours in that fuels which oxidize easily are invariably stable when measured by filterable deposits. Conversely, Hardy noted that fuels which do not oxidize easily exhibit a wide range of thermal stability as measured by deposits.

Using the same three reference fuels (POSF-2747, 2827, and 2799) Heneghan[2] et. al showed that the amount of solid formed on the walls of a single pass heat exchanger was inversely related to the temperature that the fuel consumed oxygen. Since the "ease of oxidation" is inversely related to the temperature at which the fuel consumes oxygen, this is a repeat of the general behavior observed here and by Hardy.

Finally, Biddle[3] showed that the amount of deposit formed in a hot liquid process simulator was inversely related to the onset of oxidation exotherm in differential scanning calorimetry. Biddle used the same three fuels as Heneghan, so the result is not surprising.

As indicated above, it was originally hoped that use of the FTIR to monitor oxygenated compounds would help monitor the initial buildup of precursors to deposit formation. The data of figure 5, as well as the observation that JPTS and the hydrotreated POSF-2747 consume oxygen more easily than POSF-2827 suggests that the relation between the formation of oxygen containing products in the fuel may be related to the production of solids in a much more complicated manner than previously believed. The additional evidence presented by Heneghan, Hardy, and Biddle are consistent with a more complicated relation.

Interestingly, the amount of deposit which is formed by POSF-2747 relative to POSF 2827 is strongly dependent on the amount of oxygen available. The deposits formed by POSF-2747 increase linearly with the bubbling rate of oxygen, while the deposits formed by POSF 2827 are essentially independent of the availability of oxygen. At zero oxygen flow or under a nitrogen purge, the hydro-treated fuel POSF-2747 appears to be the better fuel, that is produces less insoluble product, - an expected result based on JFTOT breakpoint, and other flowing tests under limited oxygen availability conditions. However under strong oxygen flow, the stock feed 2827 appears to be the better fuel, when both insoluble gums and solids are considered.

The oxygen was originally bubbled into the fuels to maintain a saturated oxygen level and thus remove it as a variable. However, the results indicate that only POSF-2827 has been maintained in the saturated oxygen condition. The increase of deposits with the increase of oxygen flow in POSF-2747 indicates that the fuel has not reached and maintained a saturated oxygen level despite the oxygen flow rate reaching 3 cm^3/min of oxygen per milliliter of fuel. The unsaturated condition of POSF-2747 is probably caused by the rapid consumption of oxygen.

Trying to correlate the results of our flask test to other tests designed to measure the thermal stability (JFTOT, single tube flowing heat exchangers) showed that the correlation depended upon either the amount of oxygen flowing or how the solids were collected. The fuels exhibit the expected order of stability if the oxygen is limited, or as in the FTIR experiments, the filterable solids are collected. Since the condition of bubbling oxygen into heated fuel is not indicative of any real system, the milder oxygen conditions are deemed more useful in predicting fuel thermal stability.

Conclusion

FTIR, HPLC, GCAED, and elemental analysis, tests of fuels and deposits for a hydro-treated and a non hydrotreated fuel have shown that the level oxidation in the more thermally stable fuel (as determined by JFTOT breakpoint and other flowing tests) is significantly higher than in the less stable fuel.

An extension of the FTIR oxidation measurements to 7 different fuels confirm that there is an inverse relation between the thermal stability as measured by solid deposits and the stability as measured by oxidation. The relationship of these two values has now been shown by at least 4 research groups using a total of 20 different fuels.

FTIR can be a useful tool in following the onset of oxidation products and is quantitatively useful in following the buildup of acids, aldehydes, and ketones in real fuel samples. The evaluation of fuels and additives in a static flask test will yield results which are strongly dependent on the availability of oxygen.

Acknowledgment

This work was supported by the U. S. Air Force Wright Laboratories, Wright Patterson Air Force Base, Ohio, under Contract No. F33615-87-C-2767 with W. M. Roquemore serving as Technical Monitor and D. R. Ballal serving as Principal Investigator

References

1. Hardy, D. R., Beal, E. J., and Burnett, J. C., "The Effect of Temperature on Jet Fuel Thermal Stability using a Flow Device which Employs Direct Gravimetric Analysis of Both Surface and Fuel Insoluble Deposits," 4th International Conference on Stability and Handling of Liquid Fuels, page 20, Orlando FL, Nov 19-22, 1991

2. Heneghan, S. P., Williams, T. F., Martel, C. R., and Ballal, D. R., "Studies of Jet Fuel Thermal Stability in a Flowing System," ASME International Gas Turbine Institute, Cologne Germany, June 22-23, 1992

3. Biddle, T. B., Hamilton, E. H., and Edwards, W. H., United Technologies Corporation R&D Status Report No.13 to WL/POSF, Wright Patterson Air Force Base, Ohio, 1991

Table 1. Properties of Baseline Jet Fuels

		Fuel Identification Number		
	ASTM Method	POSF-2747	POSF-2799	POSF-2827
Sulfur mass %	D4294	0	0	0.1
Aromatics Vol %	D1319	19	9	19
Gum mg/ml	D381	0	0.4	0
Flash Point (C)	D93	122	120	140
JFTOT Breakpoint (C)	D3241	332	399	266

Table 2. Composition of Surrogate Jet Fuel-8S

Compound	mass %
methylcyclohexane	5
m-xylene	5
cyclooctane	5
decane	15
butylbenzene	5
tetramethylbenzene	5
tetralin	5
dodecane	20
methylnapthalene	5
tetradecane	15
hexadecane	10
isooctane	5

Table 3. Comparison of Acid Number, Insolubles , and FTIR in Fuel POSF-2747

Sample oxygen flow cc/min	Acid Number mg KOH/g of fuel	Deposit mg/30 ml of fuel	FTIR 1722 cm^{-1} peak area
0	x	0	x
15	8.03	62	x
30	10.6	154	11.9
60	14.0	200	14.2
90	16.4	321	16.0

x = not measured

Table 4 Analysis of the Oxidation Products of Various Fuels

Fuel	ID #	Insoluble mg	Alcohol moles/l	Ketone moles/l	sum moles/l
JPTS	POSF-2799	0.1	0.312	0.278	0.59
JP-7	POSF-2818	10.0	1.853	0.588	2.441
JP-8	POSF-2814	12.5	1.142	0.875	2.017
Jet A	POSF-2747	13.7	1.140	0.636	1.776
JP-8	POSF-2813	18.0	0.022	0.013	0.035
JP-8		34.8	0.029	0.020	0.049
JP-8S	Surrogate	38.3	0.352	0.253	0.605

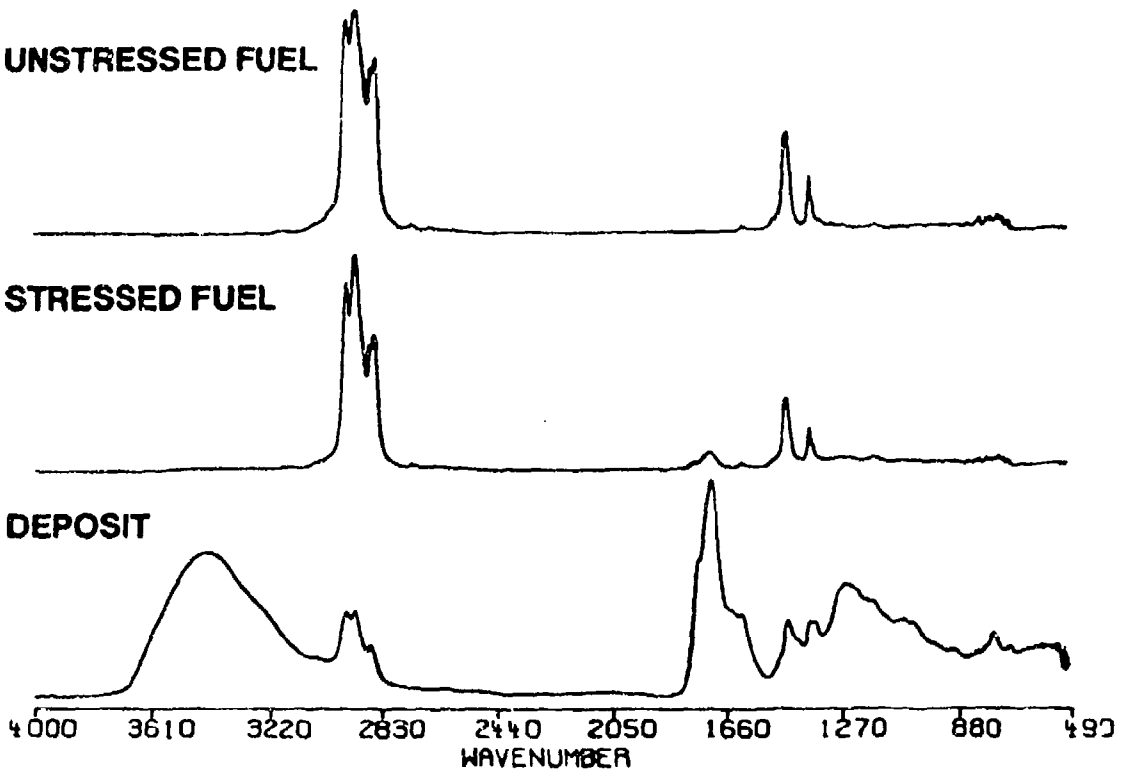

Figure 1. Infrared spectra of POSF-2747 before and after stressing and the insoluble products.

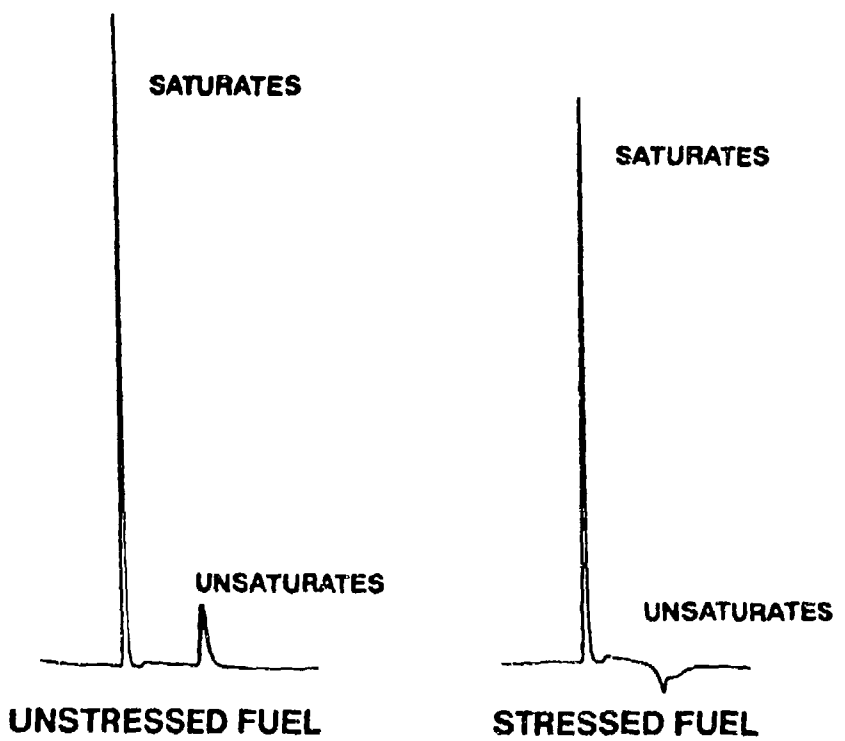

Figure 2. Dielelctric constant detection of HPLC of POSF-2747 before and after stressing.

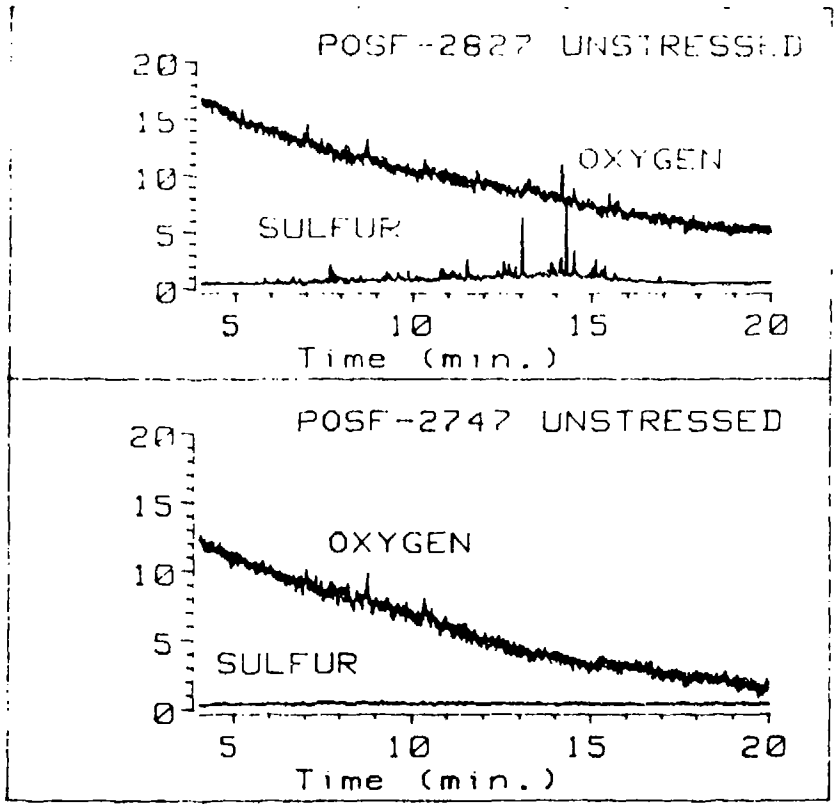

Figure 3. GCAED sulfur and oxygen analysis of POSF-2747 and POSF-2827.

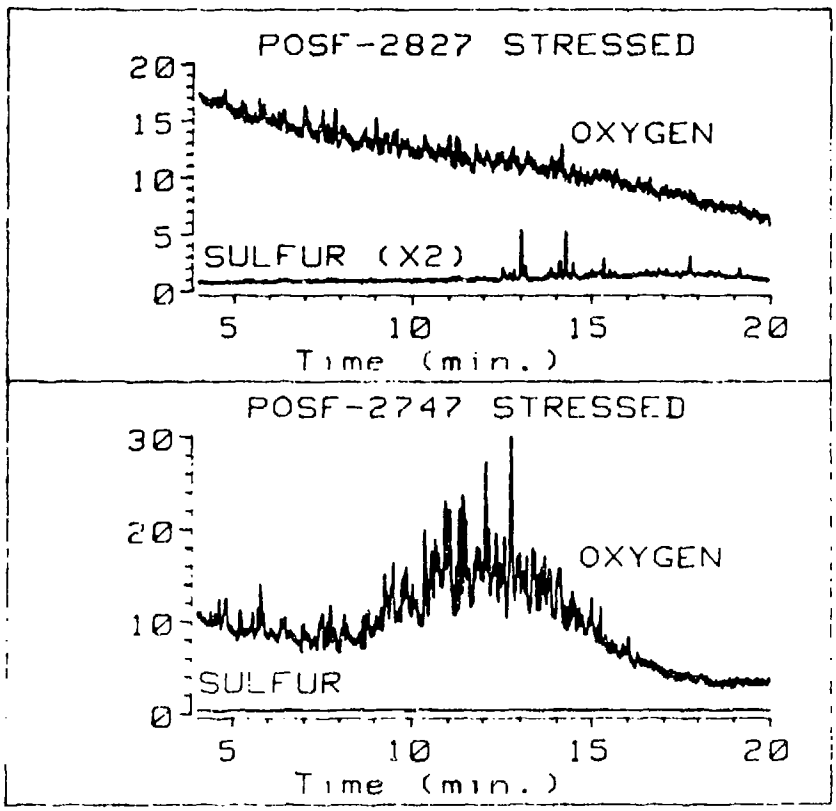

Figure 4. GCAED sulfur and oxygen analysis of stressed POSF-2747 and POSF-2827.

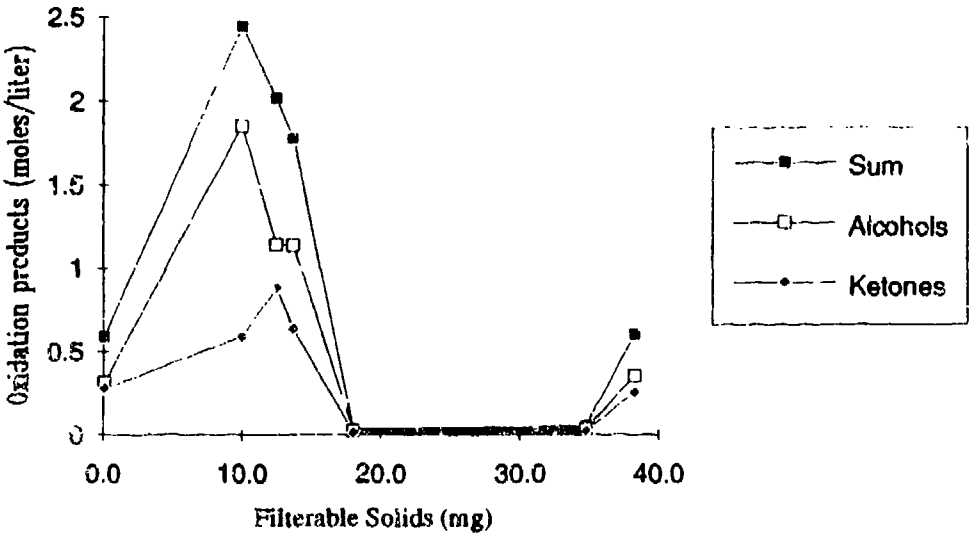

Figure 5. Comparison of the oxidation products concentration and the filterable solids from seven different fuels

APPENDIX B

MICRO CARBON RESIDUE TESTS (MCRT) AND ANALYSIS

by

Rita J. Byrd, University of Dayton, Dayton, Ohio

MICROCARBON RESIDUE TESTS (MCRT) AND ANALYSIS

1. Introduction

We developed a modified version of ASTM D4530-5 test for JP fuels using the MCRT sketched in Figure 1. This modification was necessary because the standard method measures coking under strictly pyrolytic conditions and was developed for lubricants. Instead of the 12 mm o.d. x 55 mm vials, 21 mm o.d. x 70 mm vials were used to provide greater surface area for reactions. One milliliter of sample was weighed, to the nearest 0.01 gram, into *six* pre-weighed vials and lowered into the test chamber. The oven was heated to 250 C at the rate of 8.3 C/min and held for *three* hours while air is purged through the chamber at the rate of 150 mL/min. At the conclusion of the test, the vials are cooled and weighed, and the difference in weight is reported as a percentage of the original fuel weight. The degraded fuel which has been condensed in the trap is analyzed along with the insoluble gums.

The potential of the MCRT method as a valuable device for studying the chemistry of deposit formation as well as for screening additives was demonstrated in several ways: (i) a correlation with the Micro Thermal Precipitation Test (MTPT) used by Pratt and Whitney, West Palm Beach, FL was demonstrated, (ii) the thermal stability performance of POSF-2827 reference fuel was evaluated with several new anti-oxidants and additional base fuels were tested, and (iii) POSF-2827 fuel and a thermally stable jet fuel (JPTS) were subjected to a cycling test to produce multiple layers of deposits and quantify the level of gum formation in the oxidized fuel. Finally, development of new test methods continued using a variety of diverse procedures such as Thermal Gravimetric Analysis (TGA), X-ray Photoelectron Spectroscopy (XPS), Fourier Transform Infrared Spectroscopy (FTIR), and Gel Permeation Chromatography (GPC).

2. Correlation with Micro Thermal Precipitation (MTPT) Test Data

Figure 2 shows the correlation between the MCRT and MTPT tests, indicating excellent agreement for the POSF-2827 fuel containing additives. However, when the data for the reference fuel without additives is included, the correlation is somewhat diminished. This may be due to the fuel's unusual behavior in flask type tests (which has been attributed to its diverse molecular structure) which lends it *natural* antioxidant qualities in oxygen rich environments.

To further understand the deposition characteristics of these fuels, a test was developed to analyze the carbon content of the MCRT deposits. In this test, the bottoms of MCRT vials were cut off, weighed, and analyzed in the LECO Carbon Analyzer. Since MCRT results are measured as a total deposit whereas MTPT data are measured as carbon deposits, we converted the MCRT values to carbon values, and re-evaluated the correlation. Figure 3

depicts the carbon as a percentage of the total residue and reveals striking differences which could be due to the varying extents of oxidation among the fuels. Figure 4 shows correlation in terms of carbon versus carbon. This result indicates less correlation than that presented in Figure 2. Currently, reasons for these differences are being investigated.

3. Correlation with Phoenix Rig Test Data

It has not been established whether static tests such as the flask test, MCRT, and MTPT produce data which compare favorably with data from dynamic, flowing systems, nor has the effect of pressure and oxygen availability been exhaustively studied in experiments todate. To this end, Figure 5 illustrates an initial comparison of the performance of four fuels in the MCRT and Phoenix Rig. These results compare the two extremes. Therefore, the good correlation exhibited here needs further verification by choosing a fuel of intermediate stability such as POSF-2857.

4. Evaluation of New Fuels and Additives

Several fuels have been evaluated in addition to the reference fuel (POSF-2827) and the thermally stable fuel (JPTS, POSF-2799). Figure 6 illustrates the differences between these two fuels and EXXSOL D-80, a solvent resembling JP-7, POSF-2747, the hydrotreated JET-A1, POSF-2828 and POSF-2857, intermediate stability fuels, POSX-0174, a JP-8 fuel and Hexadecane with and without Diphenyl disulfide (DPDS). These results suggest that the deposition tendency in the MCRT is strongly dependent on fuel volatility and hence the molecular weight. However, since the MCRT measurments agree with data from other (closed system) test methods in which volatility is restricted, the molecular weight of the fuel and that of degradation products is a primary factor in deposition despite test configurations. Experiments to be performed during next quarter will hopefully substantiate this premise.

During this quarter, we primarily performed antioxidant testing. Mr. Bob Kauffman of UDRI performed cyclic voltammetry experiments using his Remaining Useful Life Evaluation Rig (RULER) device to explore the oxidation inhibiting capabilities of various additives. He found that the prevention of oxidation does not necessarily reduce deposit formation to a great degree as shown by Figure 7. Although the RULER ranked the antioxidants as effective oxidation inhibitors, there was only approximately 25% reduction in deposits with the 100 ppm TBHQ (tertiary butylhydroxyquinone) in the MCRT tests. The deposit level is still substantially above that of the thermally stable or hydrotreated fuels, in agreement with Pratt and Whitney's Differential Scanning Calorimetry (DSC) study.

5. Cycling Tests

We performed the cycling tests to accomplish four objectives; (i) to provide sufficient quantities of solids and gums for subsequent analyses, (ii) to study the rate of formation of deposit layers, (iii) to magnify differences between the fuel formulations, and (iv) to characterize deposits according to morphology.

MCRT vials were filled with fresh fuel after being removed from the oven chamber and re-run through the MCRT cycle. This procedure was repeated for a total of ten cycles, thus producing multiple layers of deposit. As seen in Figure 8, the formation rate was linear. As expected, the POSF-2827 fuel showed a much steeper slope than the JPTS fuel. Tests such as this one greatly magnify the differences between fuels with respect to deposit formation and should be applied whenever a candidate additive appears to significantly improve fuel performance. This can ensure that the formulation is truly effective in an environment where a surface layer of deposit has already been laid down. Another important area where the cycling test is very useful is in determining deposit morphology. Here, the JPTS gave a smooth layer even after completion of the tenth cycle. In contrast, the POSF-2827 fuel produced a flaky, wrinkled deposit along with the smooth layer after the fourth cycle. Future cycling tests will include an application of a stable fuel over an unstable fuel to determine whether the potentially harmful flakes which can clog low tolerance valves and plug filters can be minimized by the application of a smooth layer from a thermally stable fuel. In the present tests, a Scanning Electron Microscope (SEM) was used to examine the characteristics of the flaky deposit from POSF-2827 fuel and the micrographs are shown in Figure 9. These photographs reveal that the flakes are sheets or thin films which are crinkled rather than porous particles, and this is consistent with the relatively low test temperature of 250 C. At higher temperatures a more coke-like carbonaceous deposit would be formed.

6. Gum Formation

Insoluble gums are formed in flask tests and the MCRT for certain fuels at varying levels. We developed a procedure for quantifying insoluble gums produced in the MCRT. The condensed fuel which is collected in the trap is decanted thus isolating the gum which adheres to the bottom of the jar. The gum is rinsed with hexane to remove fuel, and a stream of nitrogen is passed over the gum, spreading it into a thin layer and presenting a high surface area for the second hexane extraction. After the second hexane rinse, the gum is dried under nitrogen to a stable weight. The weight of gum in milligrams is divided by the total fuel weight and reported as mg gum per gram of fuel. These test results are presented in Figure 10. They illustrate the effectiveness of antioxidants in reducing gum formation. Unfortunately, this reduction does not always translate into lower solids. Figure 11 shows the gum formation during cycling. It reveals that the rate of gum formation was not

significantly higher for POSF-2827 fuel; the initial amount produced was higher but the slope remained lower than anticipated.

7. Instrumental Analysis

(a) Thermal Analysis: Thermo Gravimetric Analysis (TGA) provides a quantitative measurement of weight change associated with thermally induced transitions by recording weight loss as a function of temperature. Transitions involving dehydration or decomposition are of interest because they are characteristic of a given compound and occur in unique sequences. Rates of weight change are often a function of molecular structure, resulting from chemical bonds forming and breaking at elevated temperatures. The identity of the volatile products can provide valuable insight into the composition of a sample. Analyses of the purge gas exiting from the TGA can be accomplished by coupling to a mass spectrometer (TG-MS) which is often used in studies of volatile organic pyrolysis of oil shales.

Another complementary technique which makes TGA a more valuable tool is Differential Scanning Calorimetry (DSC) which measures energy changes or heat flow. A clear distinction can be made between physical and chemical changes, since nearly all weight change processes absorb or release energy, but not all energy-change processes are accompanied by a weight change.

TG analysis of solid deposits from the MCRT cycling test of POSF-2827 and JPTS fuels revealed somewhat similar behavior under inert conditions (nitrogen), but different profiles were observed in an oxidative atmosphere (air). As shown by Figure 12, the JPTS fuel exhibits a sharp transition at 432 C. This result indicates volatilization of a relatively simple material, becoming 17% unevaporated material. However Figure 13 shows that the POSF-2827 fuel goes through transitions beginning at 361 C, 482 C, and 521 C, all of these at slower rates than the JPTS fuel deposit. This behavior is expected only for a more complex mixture. Since the deposits were formed under identical test conditions, the TG analysis shows a definite difference in the end deposition products. The POSF-2827 fuel deposit was also analyzed by ambient DSC but showed no transitions. If any subsequent reactions are taking place, they are in competition with vaporization. Since the reactions could be exothermic as is vaporization, two processes will overlap in the scan, resulting in unresolved transitions. High pressure DSC could allow observations of the separate transitions by causing vaporization to occur at a higher temperature.

(b) XPS Analysis: Four fuel deposits from the MCRT were sent to Mr. Tom Wittberg of UDRI Nonmetallic Materials Division for X-ray Photoelectron Spectroscopy (XPS). This technique can detect all the elements except H and He within 4 nm of a sample surface. From a careful analysis of shifts in photoelectron binding energies, differences in chemical bonding can be detected.

Table 1 shows the measured percent composition of the samples which show differences in the oxidation levels among them. Interestingly, the sample containing an antioxidant (2761) is the most highly oxidized, followed by JPTS, hexadecane with DPDS, while POSF-2827 fuel showed the least oxidation. This may be the strongest evidence yet to support the notion that the role of oxygen in solid formation is not the primary cause of increased deposit formation.

(c) Fourier Transform Infrared Spectroscopy (FTIR) Analysis: FTIR is a powerful tool in detecting the oxidation of fuel by a linear relationship between the carbonyl (C = 0) peak area at 1710 cm^{-1} and the cc/min of oxygen flow in a flask test at 185 C. A similar relationship was also found between C = 0 peak area and the Total Acid Number (TAN) of the oxidized fuel. In the MCRT, the relationship between carbonyl absorbence and acid production is not simple. This is due to the effect of additives in hindering oxidation, and then driving products to ketones, alcohols, and aldehydes. Although the alcohols and aldehydes may further react to form acids, the ketones will not react further but will still contribute to the carbonyl absorbtion. The higher test temperature of 250 C also contributes to the difference in the oxidation products between a flask test and the MCRT.

Emphasis has been given to the analysis of solids. The characterization of solids is accomplished as follows: A KBL pellet can be made if sufficient sample (0.5 mg) is available to grind into the salt. Scraping the glass vials is time consuming and messy and often yields less than the required quantity; therefore a sonic disrupter using hot (90 C) distilled water is used to effectively remove solids. The dislodged deposit is hot filtered through a 1.2 μm silver membrane and dried briefly in a vacuum oven. Thus far most deposits have easily been removed within several hours; however, future samples from higher temperature tests may not lend themselves to this procedure.

The extent of oxidation of solids can be studied by the oxidation ratio method. Tests on four fuel formulations of varying thermal stability as measured by the amount of solids produced in the MCRT, indicated that the ratio remains fairly constant. Also, there is a consistent pattern in the composition of the deposits regardless of the presence of additives. Since the additives did not significantly reduce the fuel's deposition tendency, it follows that all went to essentially the same product, even if oxidation was hindered during stressing. Eventually, deposit reducing additives will be necessary that do more than simply inhibit oxidation.

(d) GPC Analysis: GPC separates molecules according to their effective size in solution. A column packing with pores of a particular average size allows molecules that are too large to enter the pores to pass directly through the column, appearing first in the chromatogram. The small molecules permeate the pores, moving slowly through the column and eluting according to retention time, which is dependent on their relative size.

Deposition or precipitation of solids and gums out of solution is intimately related to the molecular weight of the products formed, as well as their polarity. Determination of the molecular weight distribution of the fuels and subsequent thermal and oxidative degradation products is an important area. This is because the high molecular weight compounds such as dimers and polymers do not remain soluble in the fuel but rather "plate out" under certain conditions related to temperatures, time, and flow. Unfortunately, only the molecular weight of the stressed fuels and insoluble gums is measurable as the solids cannot be put into solution. Data from the fuels and gums can provide information about the ability of additives to interfere with reactions such as condensation polymerization, in which alcohols react with carboxylic acid to produce esters and liberate water. A typical condensation reaction is shown below.

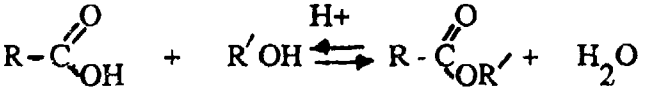

Carboxylic Acid Alcohol Ester Water

Preliminary data shows differences between gum deposits from the POSF-2827 and JPTS fuel formulations. These will be further quantified as soon as results for actual molecular weight determination by vapor pressure osmometry are received.

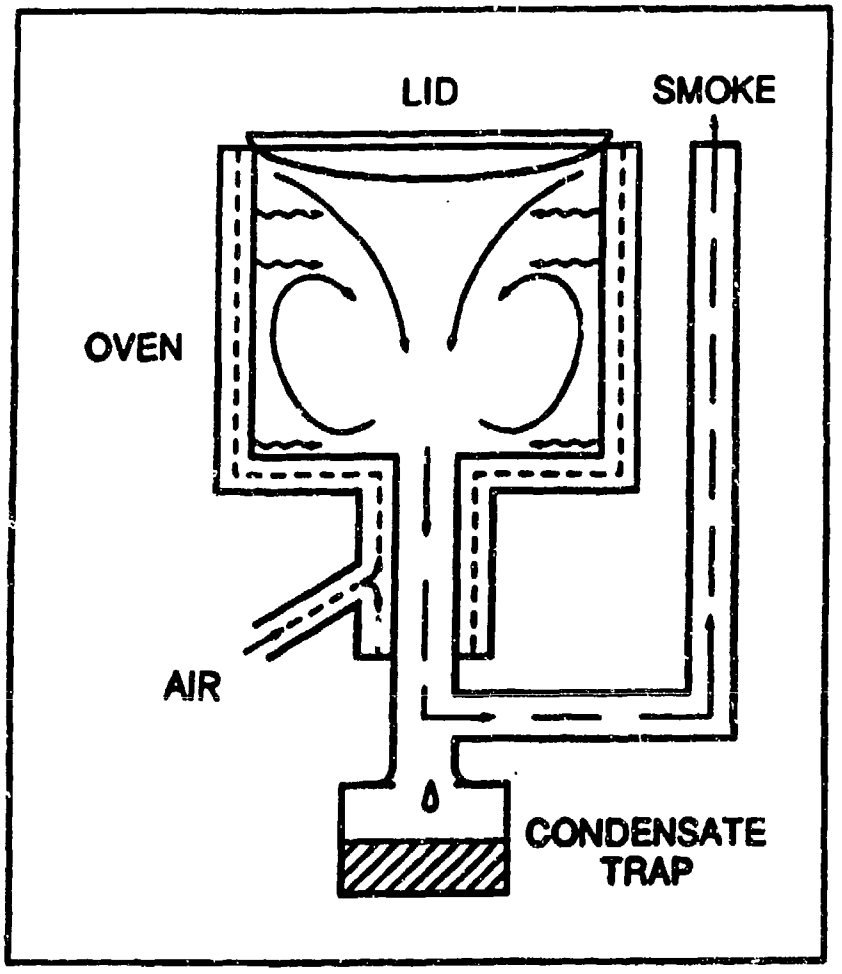

Figure 1: A simplified schematic diagram of the Micro Carbon Residue Tester (MCRT)

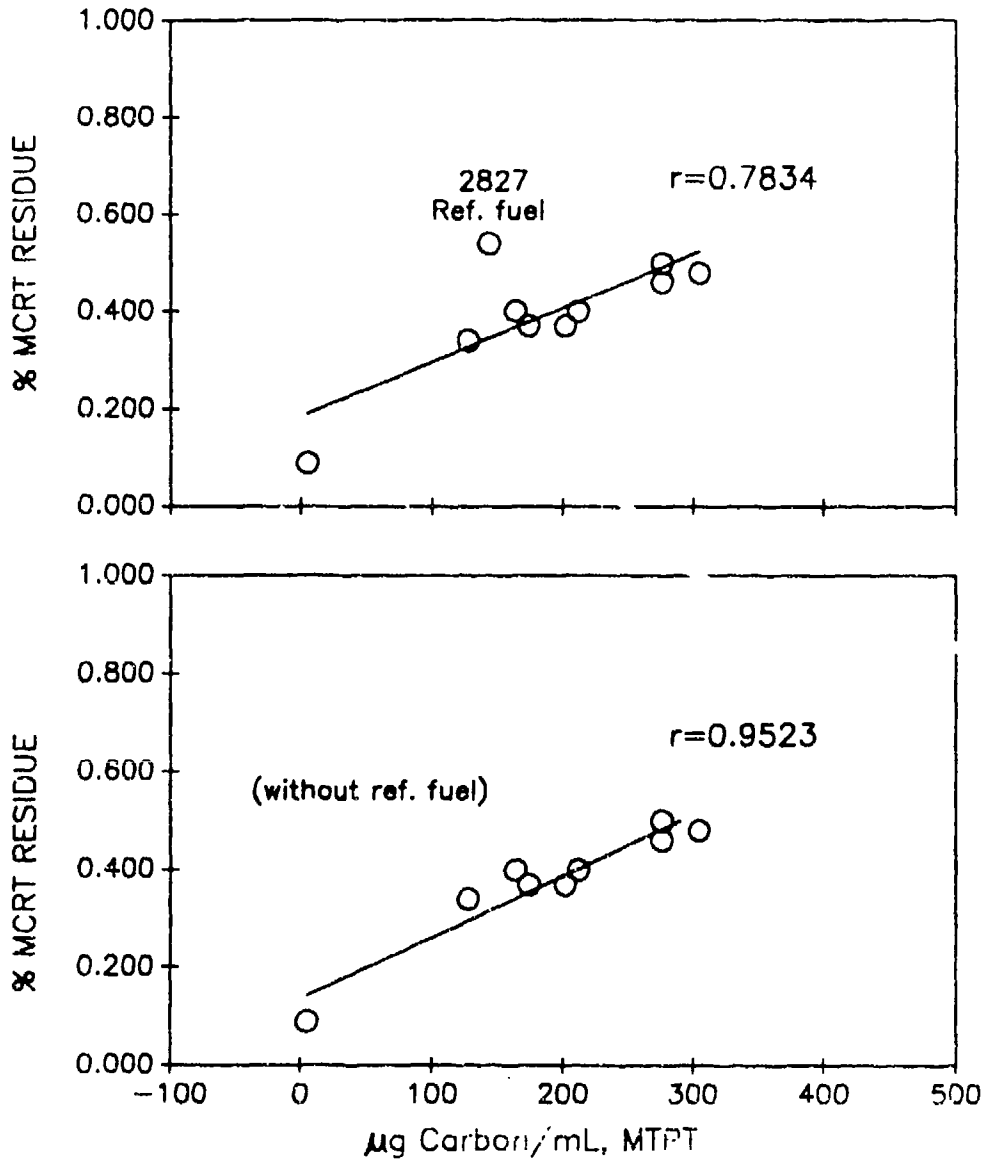

Figure 2: Correlation of MCRT with MTPT results for the POSF-2827 reference fuel with and without additives.

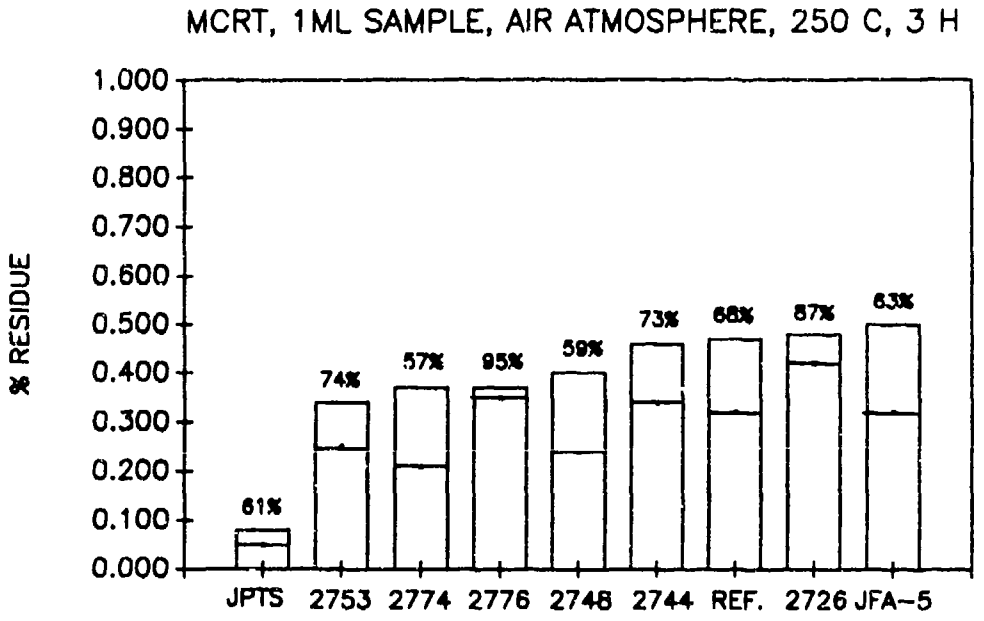

Figure 3: Carbon deposition as a percentage of total residue in the MCRT sample of various JP fuels.

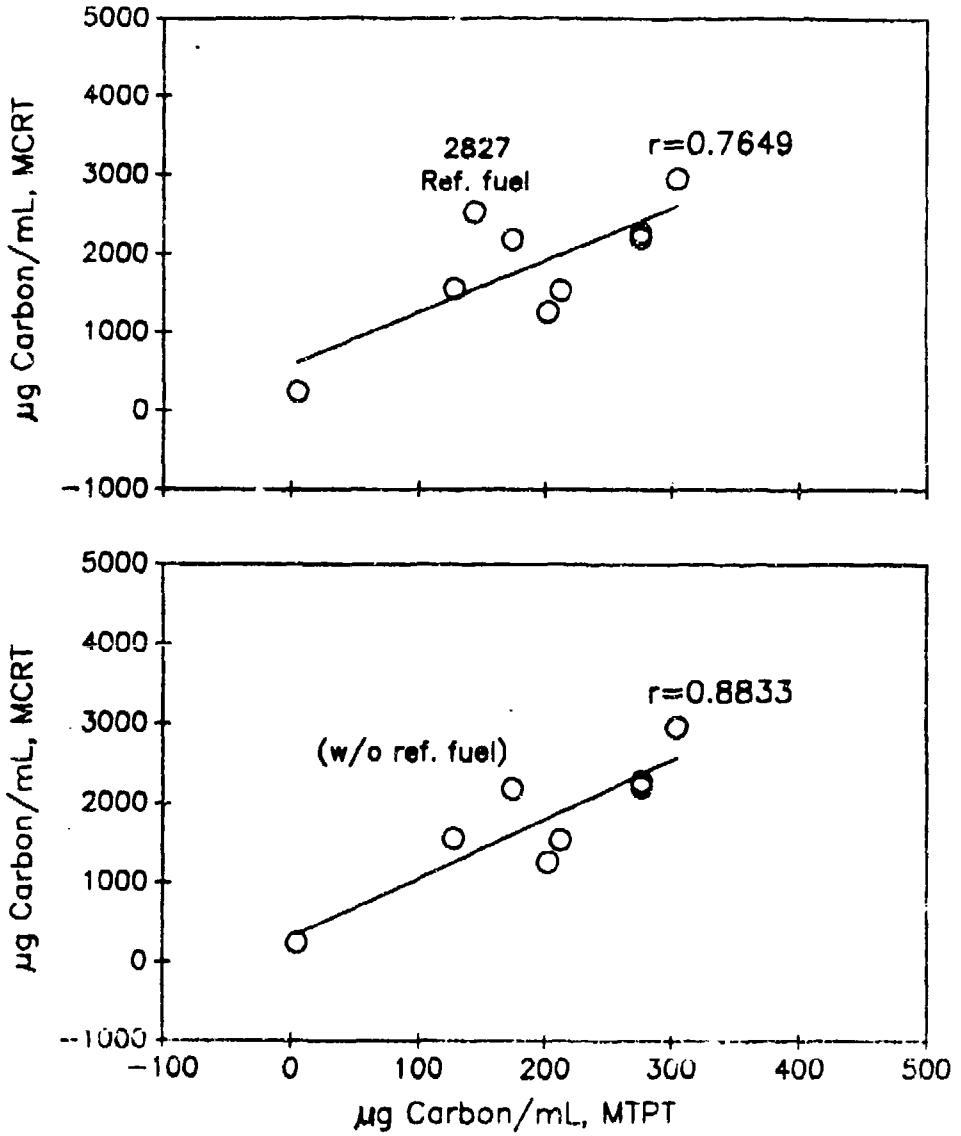

Figure 4: Correlation of carbon deposition measured in MCRT and MTPT tests.

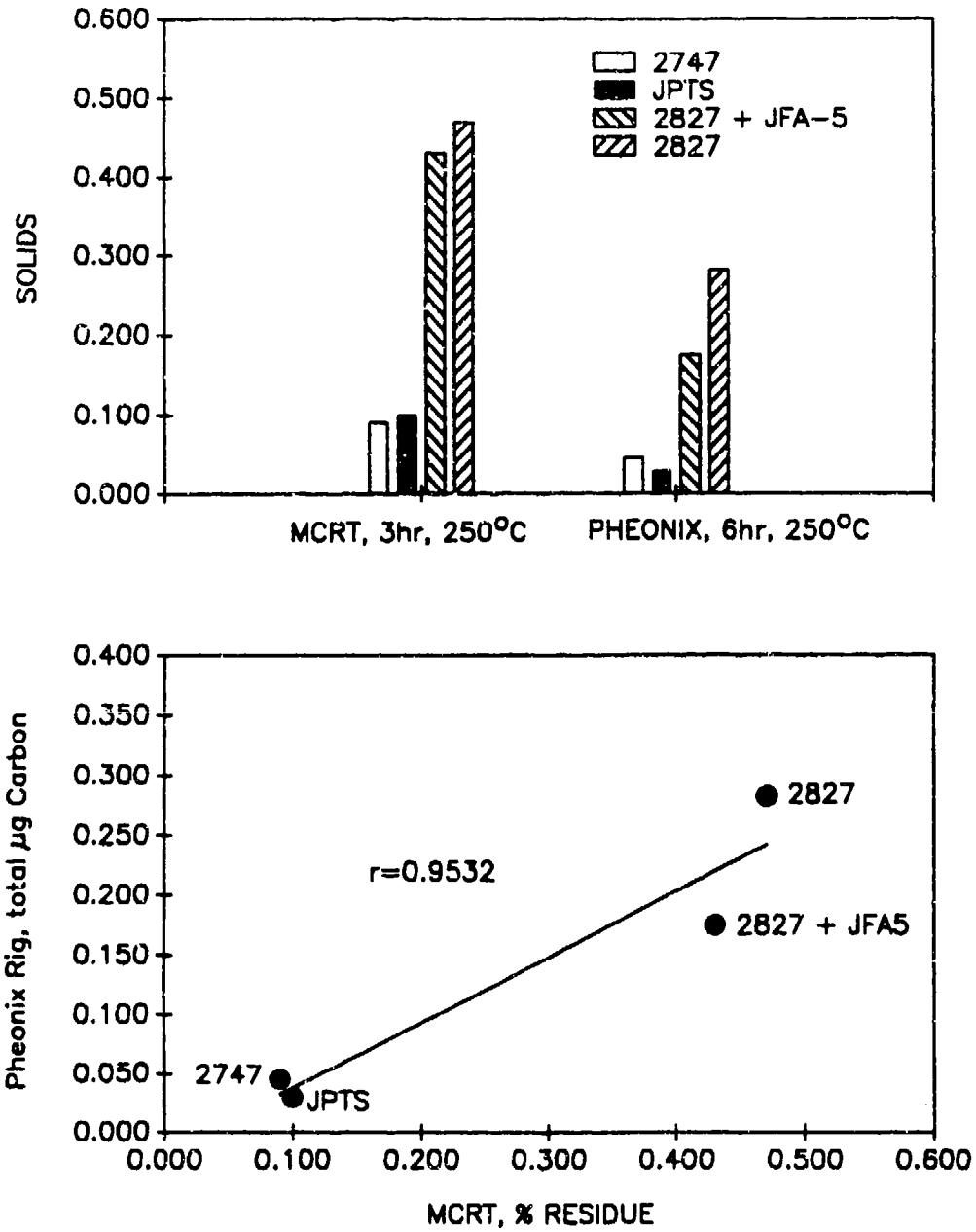

Figure 5: A comparison of the thermal stability performance of four JP fuels in the (static) MCRT and (flowing) Phoenix rig tests.

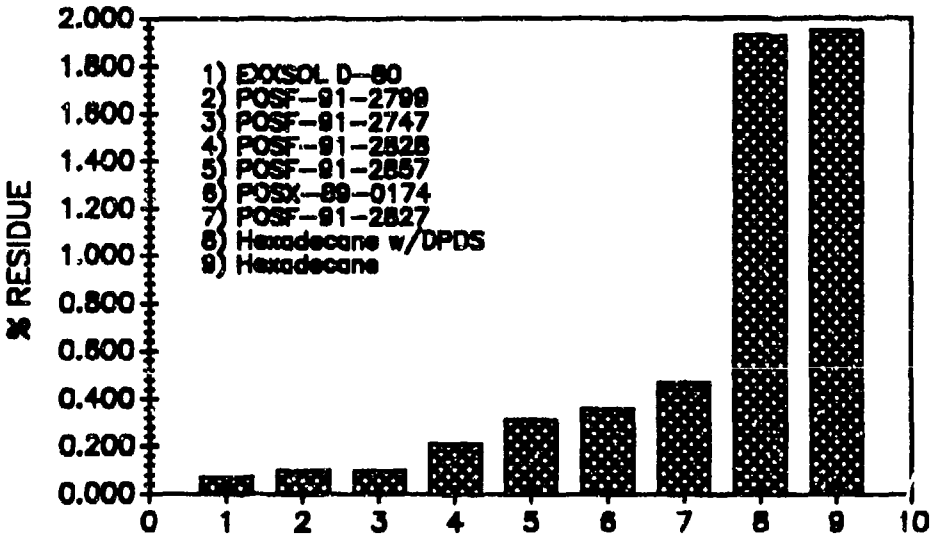

Figure 6: Deposit forming tendencies of various JP fuels in the MCRT.

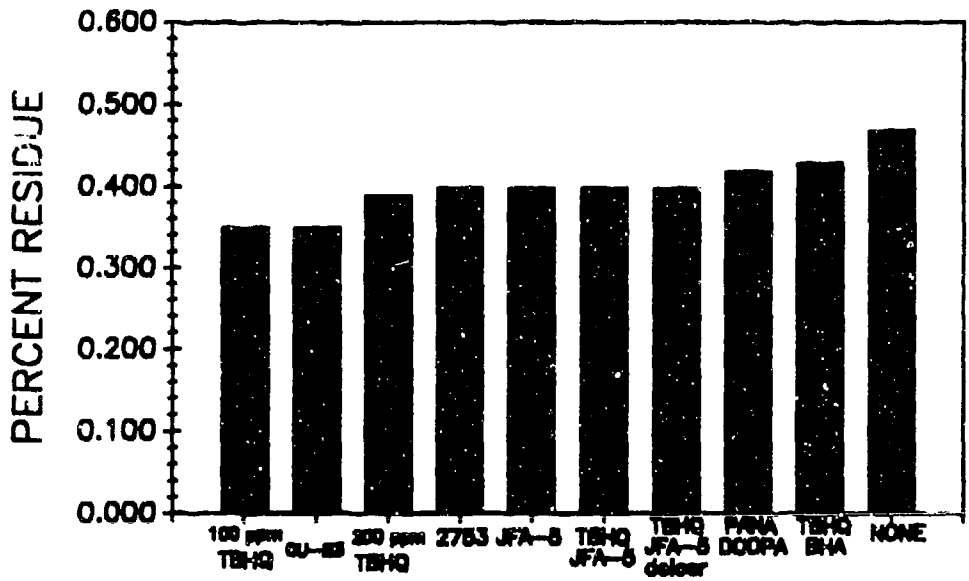

Figure 7: Effectiveness of various antioxidants in POSF-2827 fuel. These measurements were performed in the Cyclic Voltammetry experiments using the RULER device.

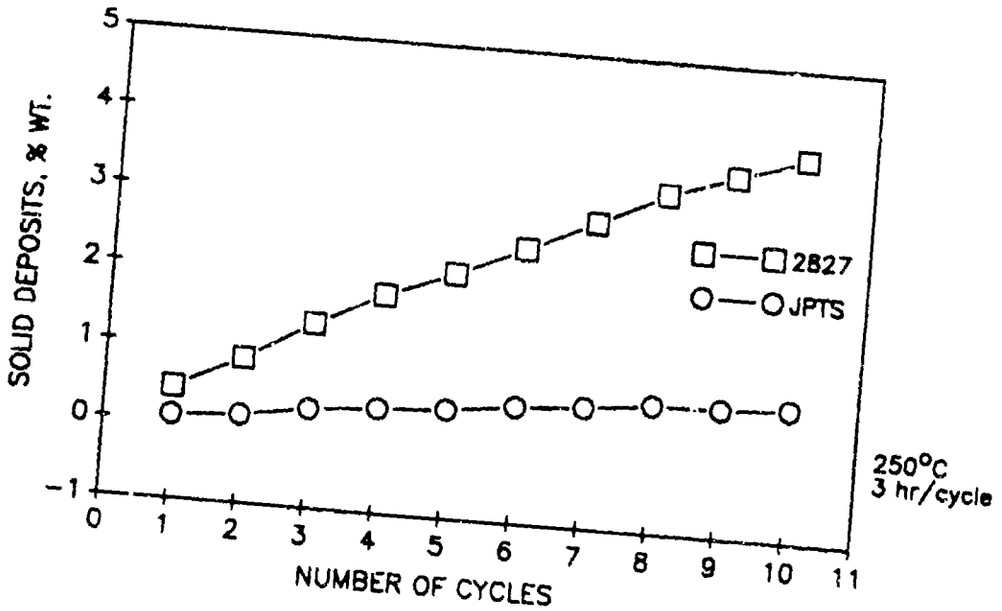

Figure 8. Formation of solid deposits during cycling at 250 C and 3-hr test duration/cycle for POSF-2827 and JPTS fuel samples.

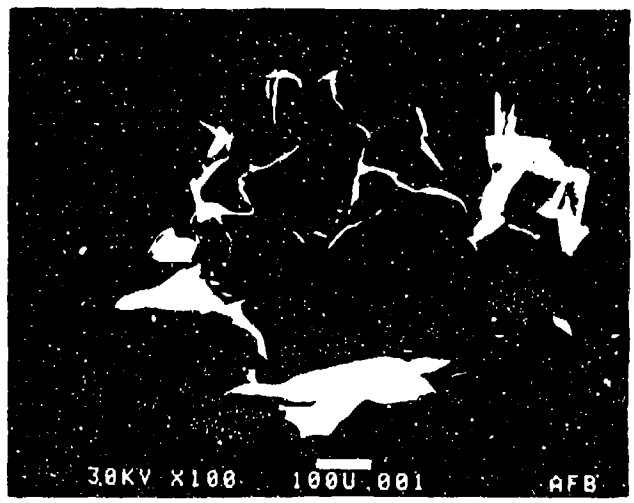

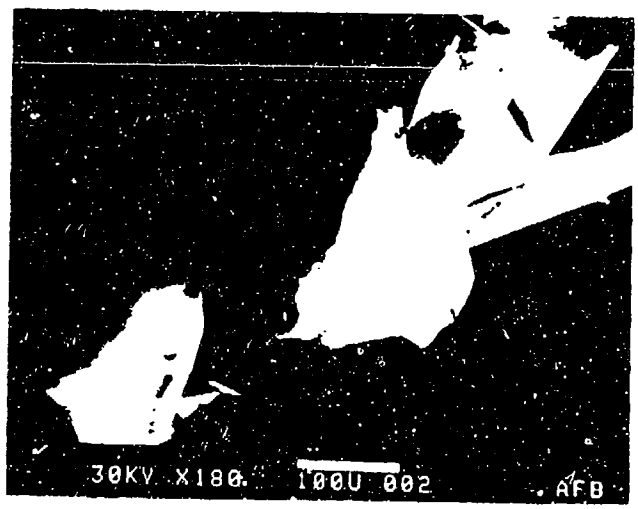

Figure 9: Scanning Electron Microscope (SEM) photographs of the flaky deposits from the POSF-2827 fuel.

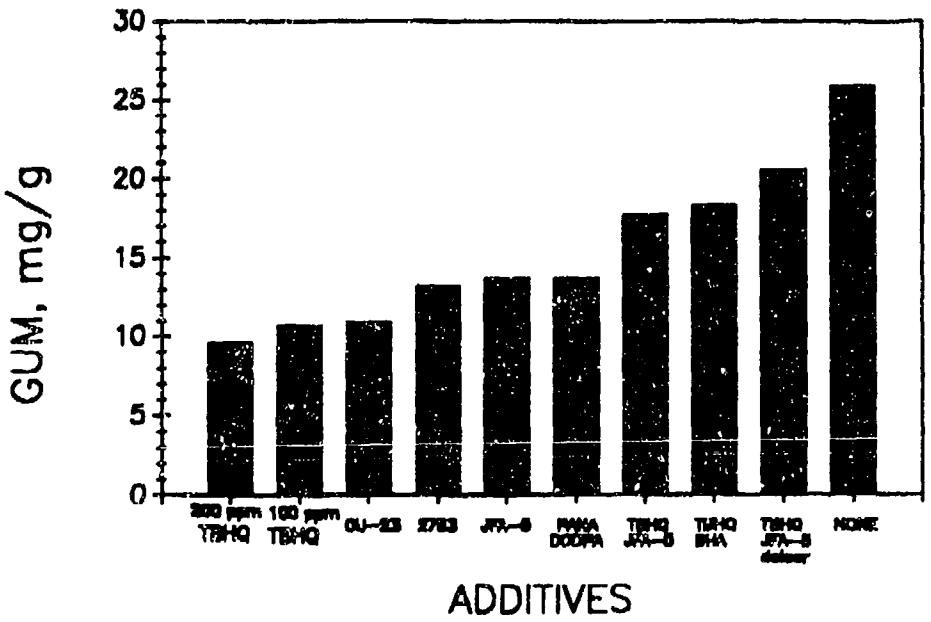

Figure 10: Insoluble gum deposits produced in the MCRT for the POSF-2827 fuels blended with different additives.

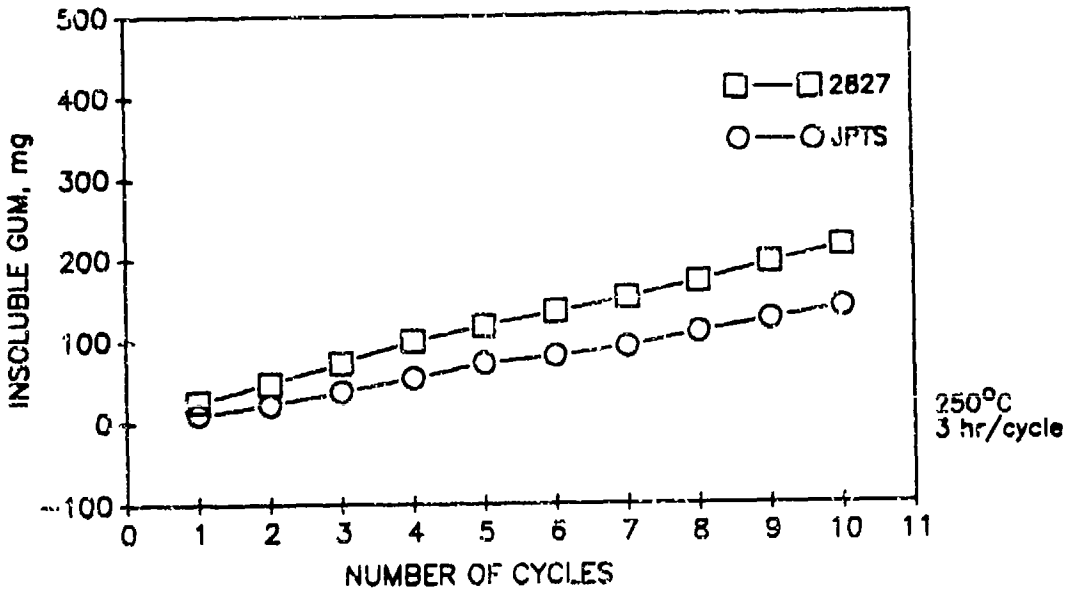

Figure 11: Insoluble gum formation in POSF-2827 and JPTS fuels in the MCRT during cycling.

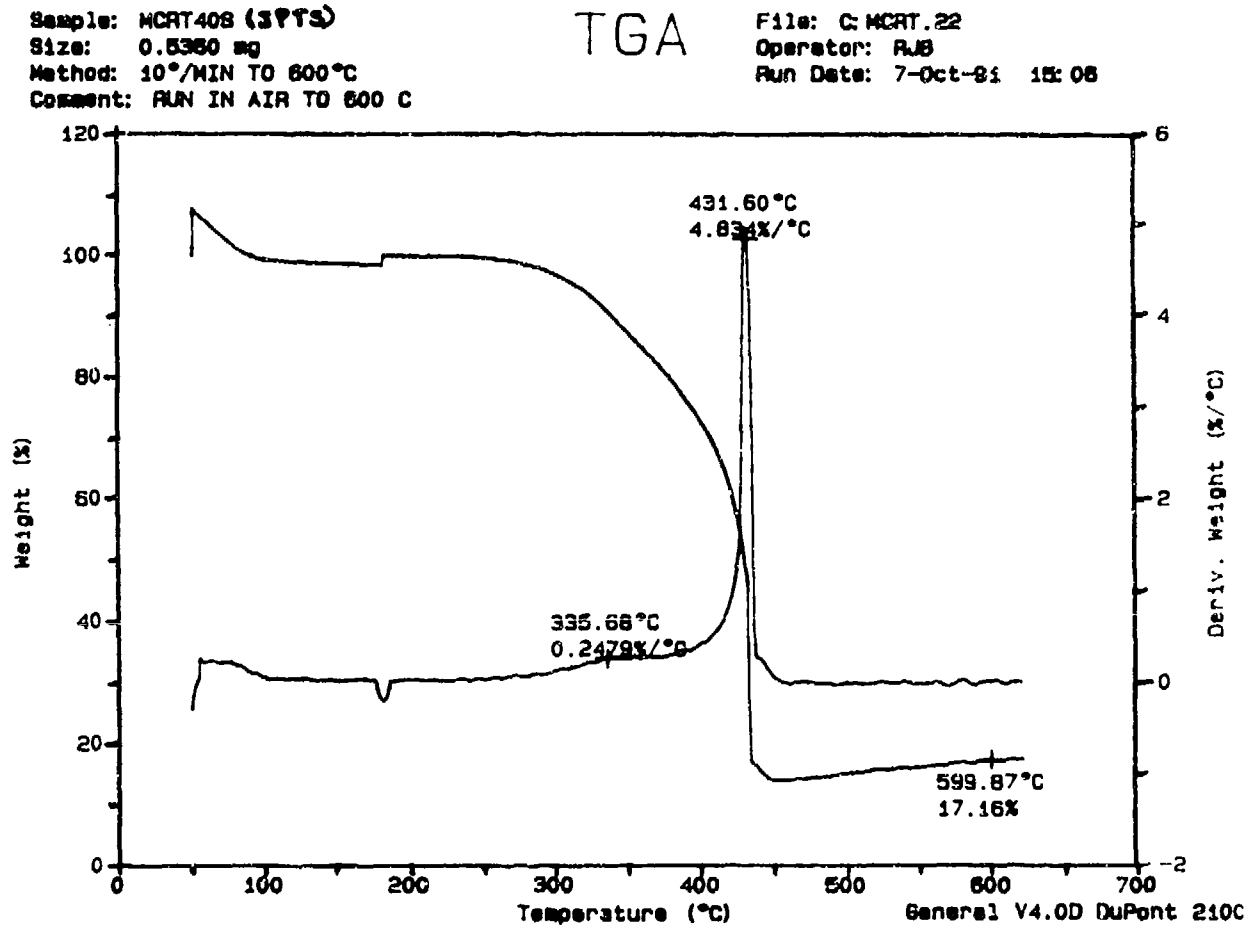

Figure 12: Thermo Gravimetric Analysis (TGA) of solid deposits from the MCRT cycling test of JPTS fuel samples.

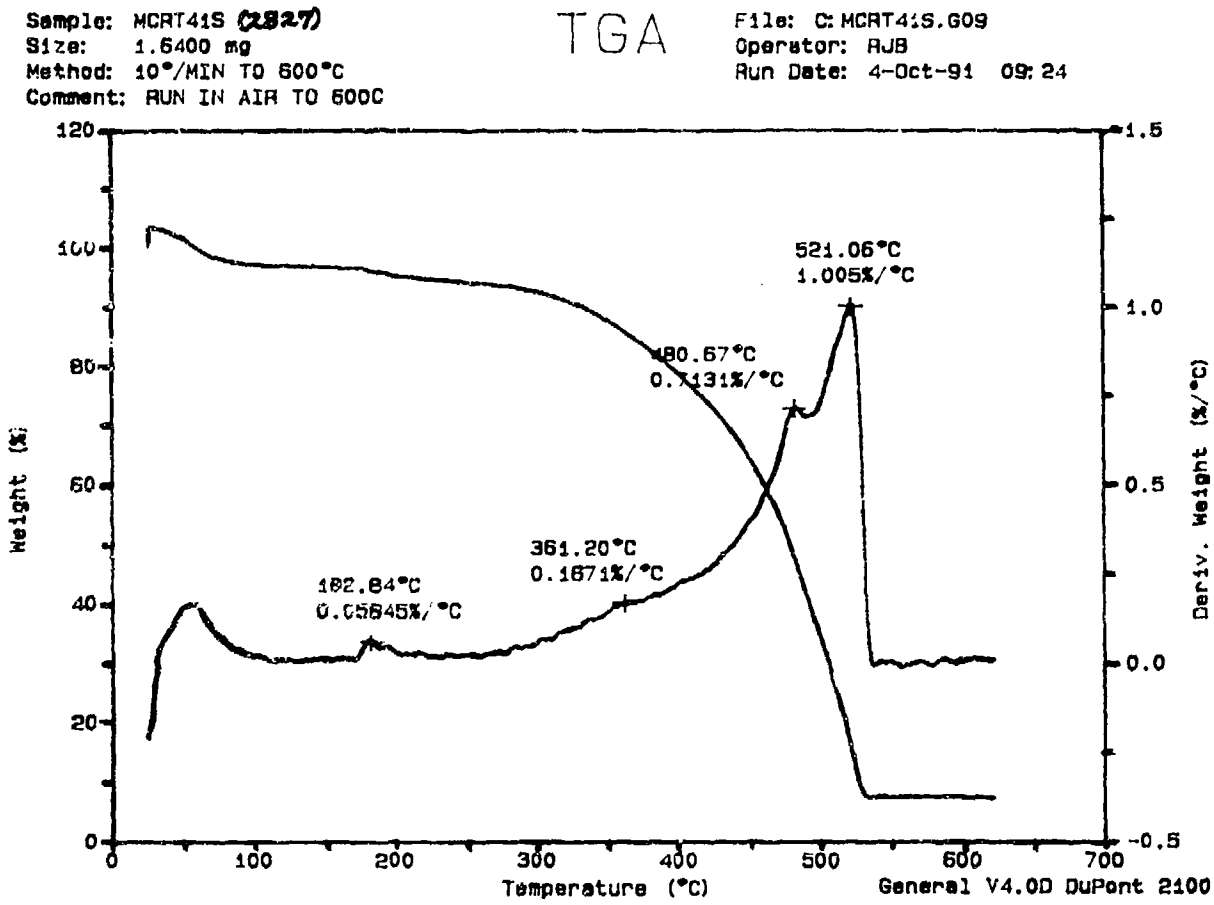

Figure 13: Thermo Gravimetric Analysis (TGA) of solid deposits from the MCRT cycling test of POSF-2827 fuel samples.

Table 1: Percentage composition of the MCRT samples measured by X-ray Photoelectron Spectroscopy. These measurements illustrate the differences in the oxidation levels.

Sample #	C					O	N	Si
	Chemical Shift in eV							
	289.3 O-C=O	288.2 C=O	286.8 C-O	285.9 C-C=O, C-N	285 CHn, C			
Hexadecane + DPDS	4.1	6.1	16.4	8.3	38.1	25.4	1.3	
POSF - 2627 + 2761	2.4	6.2	21.5	5.6	31.2	29.4	1.2	2.3
POSF - 2827	5.5	5.3	7.3	8.1	48.8	21.7	1.5	1.5
JPTS	5.9	6.2	10.9	9.9	35.2	28.3	1.2	2.3

APPENDIX C

STUDIES OF JET FUEL THERMAL STABILITY IN A FLOWING SYSTEM

by

S. P. Heneghan, C. R. Martel, T. F. Williams, and D. R. Ballal
University of Dayton, Dayton, Ohio

Published as ASME Paper No. 92-GT-106, To Appear in Transactions of ASME, Journal of Engineering for Gas Turbines & Power.

345 E. 47 St., New York, N.Y. 10017

Studies of Jet Thermal Stability in a Flowing System

S. P. HENEGHAN, C. R. MARTEL, T. F. WILLIAMS, and D. R. BALLAL
University of Dayton
Dayton, Ohio

Abstract

A flowing, single-pass heat exchanger test rig, with a fuel capacity of 189 litres, has been developed to evaluate jet fuel thermal stability. This so called, "Phoenix Rig" is capable of supplying jet fuel to a 2.15 mm I.D. tube at a pressure up to 3.45 MPa, fuel temperature up to 900K, and a fuel-tube Reynolds number in the range 300-11,000. Using this test rig, fuel thermal stability (carbon deposition rate), dissolved oxygen consumption, and methane production were measured for three baseline jet fuels and three fuels blended with additives. Such measurement were performed under oxygen-saturation or oxygen-starved conditions.

Tests with all of the blended fuel samples showed a noticeable improvement in fuel thermal stability. Both block temperature and test duration increased the total carbon deposits in a nonlinear fashion. Interestingly, those fuels that need a higher threshold temperature to force the consumption of oxygen exhibited greater carbon deposits than those that consume oxygen at a lower temperature. These observations suggested a complicated relationship between the formation of carbon deposits and the temperature-driven consumption of oxygen. A simple analysis, based on a bi-molecular reaction rate, correctly accounted for the shape of the oxygen consumption curve for various fuels. This analysis yielded estimates of global bulk parameters of oxygen consumption. The test rig yielded quantitative results which will be very useful in evaluating fuel additives, understanding the chemistry of deposit formation, and eventually developing a global chemistry model.

Nomenclature

A	= pre-exponential factor
E	= activation energy
[F]	= fuel concentration
f,g	= functions
k,k'	= reaction rate constants
$[O_2]$	= oxygen concentration
R	= universal gas constant
T	= temperature
t	= time
τ	= fuel residence time

Abbreviations

ASTM	= American Society of Testing Materials
GC	= Gas Chromatograph
JFA	= Jet Fuel Additive
JFTOT	= Jet Fuel Thermal Oxidative Tester
JP	= Jet Propellant (Fuel)
JPTS	= Jet Propellant Thermally Stable
MIL	= Military Specifications
POSF	= Propulsion Directorate-Fuels Branch

Introduction

Commercial and military jet aircraft use jet fuel as a heat sink or working fluid for heat management. After absorbing heat only a fraction of the fuel is consumed by the engines and the rest is recycled to the storage tanks. Some aircraft require ram air heat exchangers to cool the recirculated fuel to acceptable fuel tank temperatures because when jet fuel is heated above 420K, dissolved oxygen reacts with fuel components to form gums and insoluble precipitates. These gums and precipitates can foul heat exchangers, burner feed arms, and fuel injectors.

In the future, the thermal management problems of advanced aircraft, including the thermal oxidative instability problems associated with heated fuels, will become increasingly severe for the following reasons.

(1) Continuing demands for decreased fuel consumption will result in less fuel available for heat management.

Presented at the International Gas Co[illegible]n
This paper has been accepted
Discussion of it will be accepted

d Aeroengine Congress and Exposition
une 1-4, 1992
on in the Transactions of the ASME
eadquarters until September 30, 1992

(2) Increased engine efficiency will be accomplished by higher operating temperatures, further increasing the heat load on the available fuel.

(3) Future aircraft will probably use powerful heat-generating hydraulic systems to increase maneuverability and/or decrease drag.

(4) The development of supersonic cruise capability will result in higher airframe temperatures.

(5) Ram air coolers will be dispensed with because they are both heavy and contrary to the development of efficient subsonic aircraft and also become ineffective at supersonic speeds.

(6) The heat rejection rate of the avionics subsystems of military aircraft has doubled every 10 to 20 years, and can be expected to continue to increase.

In response to these problems and following the recommendations of the U.S. Air Force Thermal Management Working Group (see Harrison, 1990), the Aero Propulsion and Power Directorate of Wright Laboratories, Wright-Patterson Air Force Base, Ohio, initiated a research program aimed at increasing the thermal stability (and thus the heat sink capacity) of jet fuels. A primary objective of this program is to develop an additive package that will increase the thermal stability of JP-8 by 60K. A secondary, and a long-range goal, is to develop modelling techniques using global parameters to evaluate the deposition of solids in fuel system components (see Reddy and Roquemore, 1990).

This paper discusses the development of a single-pass heat exchanger system to evaluate jet fuel additives and presents numerous results on carbon deposition, oxygen consumption, and methane production that are used for global modelling studies.

Experimental Work

1 Test Rig. The experimental apparatus (known as the Phoenix rig) is a single-pass fuel-flow system that heats the fuel in a stainless steel tube. Figure 1 is a flow schematic diagram of the Phoenix rig. A 189-litre preconditioning tank is equipped with a gas sparging system. The sparging system consists of two Brooks Model Number 5850E mass flow gas controllers and a Model 5876A indicator controller. This setup bubbles nitrogen/oxygen mixtures through the test fuel to control the dissolved oxygen content and to remove the dissolved argon.

An American Lewa Model EK-1 variable stroke, positive displacement diaphragm pump with a surge suppressor provides fuel flow in the range 1 to 100 ml/min at a pressure of 3.45MPa. To monitor the fuel flow rate independently, a Max Machinery Model 213-310 positive displacement flowmeter is employed. A manually set metering valve is located downstream of this flowmeter. This valve provides a 965kPa pressure differential to isolate the surge suppressor from the pressure fluctuations produced by the downstream control valve.

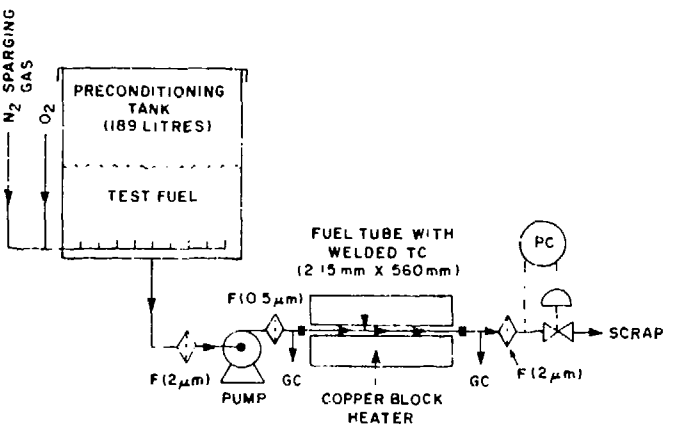

Fig. 1: Schematic diagram of the Phoenix Rig: (F-Filter, GC-Gas Chromatograph, TC-Thermocouple, and PC-Pressure Controller)

2 Test Section. The test section through which the fuel flows is constructed of type 316 stainless steel tubing (560 mm long, 3.18 mm O.D., and 2.15 mm I.D.) heated by a copper block heater. The copper block heater is 460 mm long with a 76-mm diameter. It is capable of heating the test section to 770K in such a way that the tube wall temperature profile remains constant during the experiment. This type of heater produces an axial fuel temperature gradient in the test section. It should be noted that the fuel heater used by Marteney and Spadaccini (1986) not only produces a temperature gradient in the test section, but also a test section wall temperature which increases with the time duration of the experiment. A Sensotech type TJE differential pressure transducer measures the pressure drop across the test section. The fuel tubes used in our tests have an interior surface finish of 0.380 to 0.635 μm (rms value) and are tested for hydrocarbon and particulate deposits. The tubes are cut to size, cleaned using a Blue Gold alkaline metal cleaning solution in an ultrasonic bath and then rinsed with deionized water.

Upstream of the fuel test section, a 0.5 μm sintered stainless steel filter with a bypass valve and a second Sensotech type TJE differential pressure transducer are installed. To maintain system pressure at 2.48 MPa a Jordan MK708 6.35-mm pneumatic control valve is used. The control valve is actuated by a Micristar controller acting through a Fisher Model 546 I/P converter. A Sensotech Type TJE pressure transducer provides the pressure signal to the Micristar controller. Data are recorded using a Fluke model 2400B computer with a Model 1722A controller.

3 Gas Analyzer. We perform oxygen and methane analyses using a Hewlett Packard (HP) 5641A gas chromatograph. It is equipped with a three-member tandem separation column, a thermal conductivity detector for oxygen, and a flame ionization detector for methane. This combination is capable of detecting oxygen concentrations as low as 150 parts per billion corresponding to 7,500 counts. The sensitivity of this instrument to methane has not been fully determined, but it is estimated to be significantly more sensitive to methane than to oxygen. The in-line detection

system is capable of sampling the fuel at the entrance to the heated test section, and at the exit of the heated section. Full details concerning the installation, construction, and calibration of the oxygen analyzer form the subject of a forthcoming paper by Rubey et al. (1992).

4 Carbon Deposition Test Procedure. The test fuel passes through the tubular test section at a flow rate of 16 ml/min for 6, 12, or 24 hours. The test section is heated by the copper block heater, which is maintained at a predetermined temperature (544K, 573K, or 608K). At the conclusion of the test, the test section is removed, drained, cut into 25-mm or 50-mm length segments, rinsed with hexane, dried in a vacuum oven, and analyzed for carbon deposits on a Leco RC-412 multiphase carbon analyzer. This method measures the amount of surface carbon deposit in the tube, but does not measure other deposit constituents, such as oxygen, hydrogen, sulfur, or trace metals. The amount of carbon deposit is then compared to baseline test results.

5 Temperature Measurements. A test section with welded thermocouples is used to obtain the wall temperature profile. Figure 2 shows typical measured tube wall temperatures. In this figure the bulk fuel temperature profile was calculated using a model developed by Reddy and Roquemore (1990). This model uses inlet and outlet fuel temperatures, tube wall temperature profile, fuel flow rate, and bulk fuel properties for calculations. To obtain reasonable agreement between the calculated and the measured bulk fuel discharge temperature, the model assumes turbulent pipe flow conditions, even through the Reynolds number of the fuel entering the test section was less than 100. The model also predicts high radial temperature profiles. It is possible that buoyancy effects caused by the high radial temperature gradient may produce secondary flow patterns that cause turbulent flow conditions. The measured output bulk temperature indicates that the flow is in the laminar-to-turbulent transition state.

6 Oxygen Consumption/Methane Production. The fuel flow rate is established at 16 ml/min and the copper block heater temperature is increased incrementally. The dissolved oxygen content, methane content, and temperature of the fuel are measured at the entrance to and the exit from the test section. The dissolved oxygen and methane contents of the heated fuel are then plotted vs. the measured output bulk temperature and compared to baseline results. This test was performed to yield insights into the way fuel additives work, and was used to calculate global chemistry parameters for the oxygen consumption.

7 Fuels Tested. Various baseline and blended jet fuels were tested. The properties of these fuels are identified in Tables 1 and 2 respectively. The initial baseline fuel (POSF-2747) was a Jet A-1 fuel procured from the Sun Oil Co. This hydrotreated product is also marketed as Super K-1 Kerosene. In our laboratory, it fails ASTM D3241 (or JFTOT) tests at a temperature of 605K. This result was indicative of its excellent thermal oxidative stability. Fuel POSF-2799 (JPTS), an Air Force Spec. fuel (MIL-F-25524), was tested. JPTS is a known thermally stable fuel which hopefully will serve as a calibration standard and thereby establish a goal that the fuel additive program would like to achieve. Finally, a non-hydrotreated fuel (POSF-2327) was acquired for analysis. Together, these three fuels represent the baseline fuels.

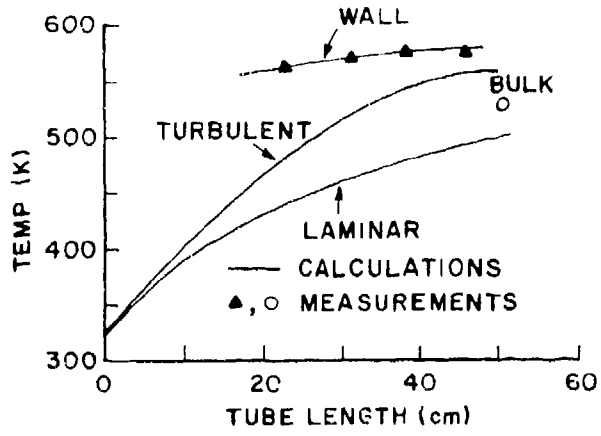

Fig. 2: Measured and calculated wall and bulk temperatures along the tube length for laminar and turbulent flow conditions.

Table 1: Properties of Baseline Jet Fuels.

Source	ASTM Method	POSF-2747 Sun Oil	POSF-2799 Exxon	POSF-2827 Shell
JFTOT Break-point, K	D3241	605	672	539
Sulfur wt.(%)	D3227	0	0	0.1
Aromatics (Vol %)	D1319	19	9	19
Existent Gum (mg/ml)	D381	0	0.4	0
Flash Point, K	D93	395	395	413

Table 2: Properties of Blended Jet Fuels.

Fuel Identification	JFTOT (K)	Base Fuel	Additives
POSF-2814	590	POSF-2747	DuPont DCI-4A Corrosion Inhibitor Static Dissipator Corrosion Inhibitor
POSF-2827A	530	POSF-2827	JFA-5-12 mg/l
POSF-2827B		POSF-2827	JFA-5-50 mg/l

New blends were made to test various additives using the baseline fuels. POSF-2814, was developed by mixing POSF-2747 with 22.5 ppm DuPont DCI-4A corrosion inhibitor, 1.0 ppm ASA-3 static dissipator, and 0.15 percent by volume diethylene glycol monomethyl ether. These additives, when blended with Jet A-1, produce JP-8. JFA-5 (the only currently accepted thermal stability additive package) was added to POSF-2827 in the concentration of 12 mg/l (POSF-2827A) and 50 mg/l (POSF-2827B).

Test Results

The carbon deposition test described above was used to measure the deposition characteristics of the fuels. Figure 3 shows a plot of the surface concentration of the deposit vs. the axial length of the test section for various JP fuels using a copper block temperature of 573K and test durations of 6 hours. Note that the deposits increase along the length of the test section until a maximum is reached, and then decrease. It should also be noted that while our JFTOT tests indicated a decrease in the fuel thermal stability with the blending of additives to POSF-2747 (i.e., fuel POSF-2814), the flowing test here indicates that POSF-2814 has increased thermal stability. As a matter of fact, tests with all the blended fuel samples showed a noticeable improvement in fuel thermal stability.

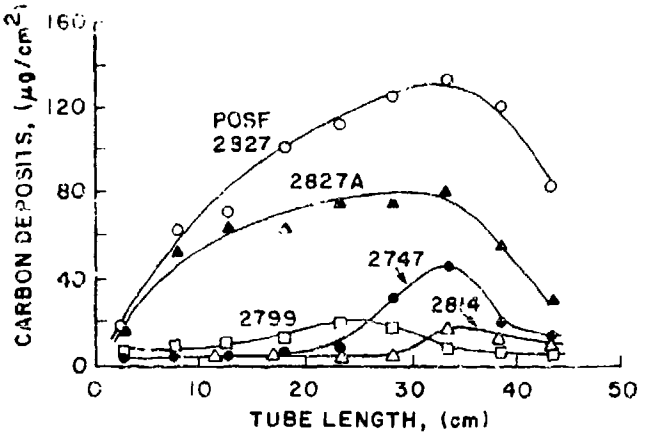

Fig. 3: Surface concentration of carbon deposits along the test section (block temperature = 573K) for jet fuels during a six-hour test.

The effects of block temperature on carbon deposition are shown in Figure 4. The total deposit weight measured in the test section are plotted vs. copper block heater temperature. As expected carbon deposition increases with block temperature. Test duration also proved to be important. As shown in Figure 5, carbon deposits increased by factors of 2.2 to 5.8 when the test duration was doubled to 12 hours. Further the deposits increased by a factor between 22 and 37 when the test duration was quadrupled to 24 hours.

The oxygen consumption and methane production curves for the three baseline fuels are shown in Figure 6. The oxygen and methane concentrations were measured by the number of counts at the detector. The gas concentrations (corresponding to relative areas) presented in Figures 6-8 and 10 were all normalized to the saturated oxygen level of 50 ppm (estimated) corresponding to $3x10^5$ counts. Methane detection is significantly more sensitive than oxygen detection, and it is estimated to be less than 25 ppm at all times. The results of Figure 6 suggest that at low bulk fuel temperatures, the oxygen and methane concentrations remain constant (oxygen at saturation level and methane at 0 ppm). As the temperature is increased the oxygen concentration drops suddenly. Two fuels (POSF-2747 and POSF-2799) exhibited a drop of over

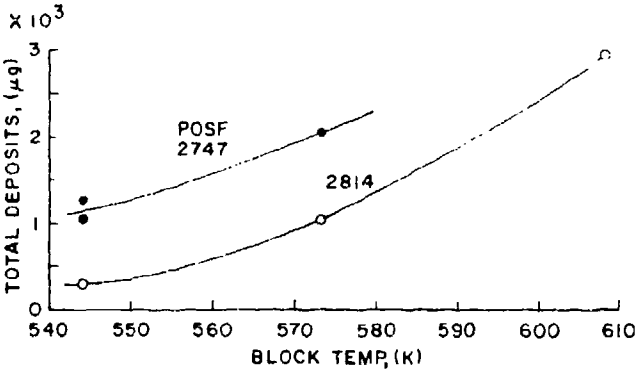

Fig. 4: Surface concentration of total carbon deposits for different block temperatures during a 12-hour test.

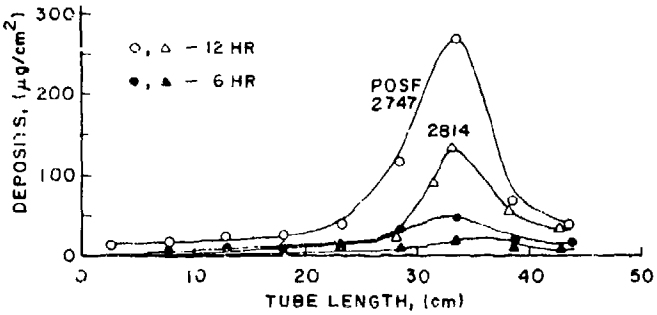

Fig. 5: Effect of test duration on the formation of carbon deposits in two representative jet fuels.

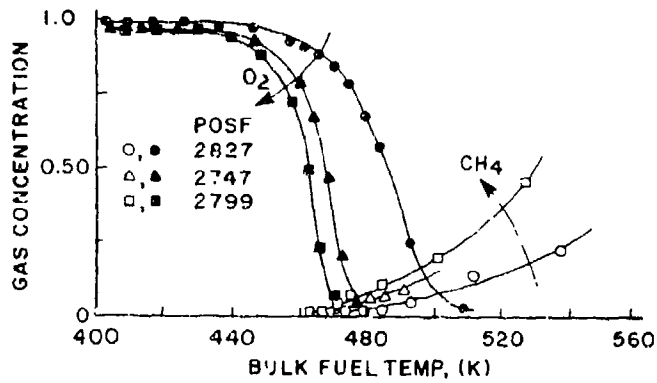

Fig. 6: Oxygen concentration and methane production vs. bulk fuel temperature for baseline jet fuels.

90 percent in the concentration of dissolved oxygen within a range of about 40K change in the bulk fuel temperature. The third fuel (POSF-2827) showed a slow but measurable decrease in oxygen level over a wider temperature range. To preserve clarity in Figure 6, results for the fuel POSF-2814 are not shown. However, it was found that presence of the additives had a minimal effect on the oxygen consumption trends. The onset of methane production occurs at a temperature that is very close to the bulk temperature at which there is a significant decrease of oxygen content. Tests of the fuels with nitrogen sparging showed a strong correlation between the initial oxygen concentration and the production of methane at 573K block temperature.

As shown in Figure 7, at this temperature, the available oxygen is consumed to below the detectable limit of the HP 5641A GC and the methane production rate decreases with a decrease in the initial oxygen concentration.

Additives were tested in the Phoenix rig by measuring the oxygen consumption/methane production trends, and also by measuring the carbon deposition for 6- and 12-hour tests. Figures 8 and 9 show the results of these tests. While JFA-5 acted to decrease the deposits in the test section, a 2-μm sintered metal filter located downstream (see Figure 1) exhibited significantly increased plugging as measured by the pressure drop across the filter. This observation was made at a temperature of 400K at the filter. Currently, testing continues to evaluate additives of four major varieties; anti-oxidants, dispersants, detergents, and metal deactivators.

Discussion

The carbon deposition trends observed for the four fuels (Figure 3) were not surprising. The best thermally stable fuel in the JFTOT tests was JPTS, while it was POSF-2814 in the Phoenix rig. The worst fuel thermal stability in either test was exhibited by POSF-2827. Fuel POSF-2827 contains 1000 ppm hetero-atoms (namely sulfur) and these atoms are known to form deposits when the fuel is oxidized. Fuel POSF-2747 was expected to exhibit *good* thermal stability because it is a strongly hydrotreated fuel. It has a narrow boiling range and less than 50 ppm hetero-atoms (ASTM D3227 sensitivity). Therefore, it is not surprising that it exhibited a JFTOT breakpoint temperature higher than POSF-2827.

In Figure 5, a decrease in deposition for fuel POSF-2814 versus fuel POSF-2747 was observed. It is hard to account for this improvement in thermal stability upon the addition of the static dissipator, anti-icing additive, and corrosion inhibitor. In fact, several other systems including the JFTOT test, microcarbon residue test, microthermal precipitation test, hot liquid process simulator test (see Pearce et al. 1992), and a multipass heat exchanger (see Lefebvre et al. 1992) indicated the contrary. Thus, the most significant conclusion is that several different tests which may yield conflicting results, are needed to evaluate the effects of given additives on the thermal stability of a fuel.

Our other observations on the baseline fuels appear to be consistent with the observations of previous researchers. For example, the increase in carbon deposits with increasing block temperature, the decrease in deposits with decreasing oxygen, and the nonlinear increase in carbon deposit with test duration are consistent with the results obtained by Giovanetti and Szetela (1986). In general, these observations indicate that carbon deposit formation is stimulated by the temperature-driven absorption of oxygen, and catalyzed by itself.

As illustrated in Figure 9, JFA-5 also exhibited a significant ability to decrease deposits. JFA-5 is an additive that includes an amine-type antioxidant, a dispersant, and a metal deactivator.

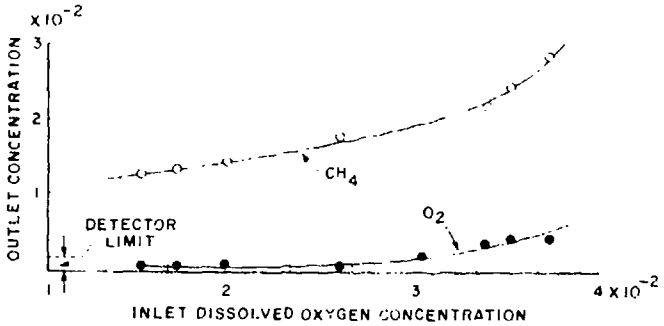

Fig. 7: Influence of inlet dissolved oxygen on the concentration of oxygen and methane at the outlet (block temperature = 573K).

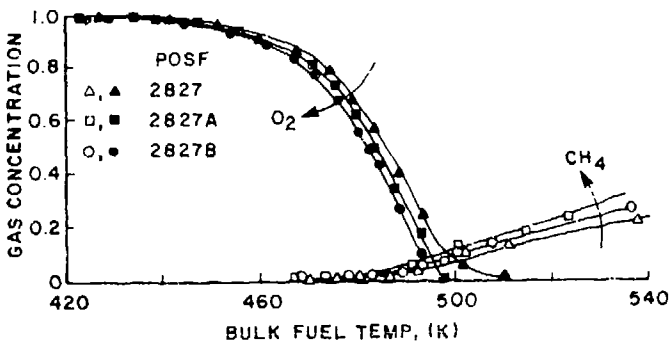

Fig. 8: Effect of fuel additives on the oxygen consumption and methane production.

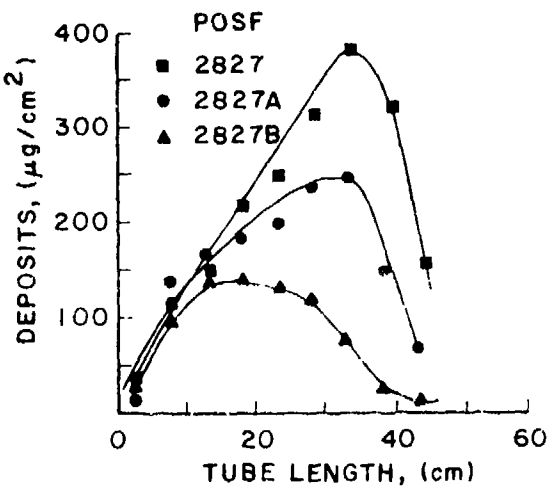

Fig. 9: Effect of fuel additives on the carbon deposition along the tube length.

The decrease in carbon deposit for fuel POSF-2827A was nearly by a factor of two. Fuel POSF-2827B showed a significant decrease again, indicating that JFA-5 can be effective at concentrations above that specified in MIL. T-25524. However, the causes and implications of the increased plugging of the downstream filter are currently under investigation.

Figure 10 shows the depletion of oxygen vs. temperature for fuels POSF-2747 and POSF-2827. In these oxygen depletion measurements, several interesting observations can be made. These observations are best explained by a simple analysis based on the following assumptions:

(a) For a turbulent flow, the radial fuel temperature profile is flat.

(b) The fuel temperature increases linearly along the tube length. This assumption is an approximation of the calculated heating curve in Figure 2.

(c) The consumption of oxygen in the fuel is treated as a bimolecular reaction, i.e.:

$$d[O_2]/dt = - k'[O_2][F].$$

(d) $[F] >> [O_2]$ so that $k'[F]$ can be approximated by the pseudo first-order rate constant $k = k'[F]$.

(e) The rate constant for the consumption of oxygen can be treated as an Arrhenius-type reaction rate constant.

$$k = A \exp(-E/RT)$$

(f) The chemistry pathway is independent of the temperature.

Based on these assumptions, we can evaluate the rate of oxygen disappearance, or the concentration of oxygen with time as follows:

If $O_2 + F \rightarrow$ product (1)

then $d[O_2]/dt = k'[O_2][F]$ and

$d[O_2]/dt = k[O_2]$ where $k = k'[F]$

or $d[O_2]/[O_2] = -k\,dt$ (2)

Since $k = f(T)$ and $T = g(t)$, Equation (2) cannot be integrated easily. Hence we assume that

$$T = 300 + (T_{final} - 300)t/\tau \quad \text{or} \quad dT = (T_{final} - 300)dt/\tau$$

Then, Equation (2) integrates to a form

$$\ln([O_2]_t/[O_2]_0) = (T_{final} - 300)(t/\tau) \int_{300}^{T_{final}} A \exp(-E/RT)dT. \quad (3)$$

There is no closed form solution to Equation (3) and therefore, a MathCad program (developed by Mathsoft Inc.) was used for integration. As shown in Figure 10, we can predict, fairly accurately, the oxygen depletion from fuels POSF-2747 and POSF-2827 using pre-exponential values of 10^{27} sec^{-1} and 10^{16} sec^{-1}, and activation energies of 57 kcal/mole and 35.5 kcal/mole in Equation (3), respectively.

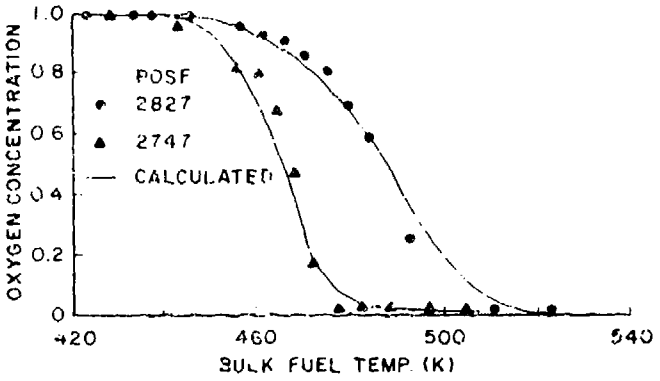

Fig. 10: A comparison of measured and calculated values for the oxygen consumption in the POSF-2747 and POSF-2827 fuels.

These measured pre-exponential factors are significantly higher than those expected from theory. A liquid-phase diffusion-limited bimolecular pre-exponential is normally about $10^{9.5}$ l/m-sec or less. The measured pre-exponential should therefore be less than the product of $10^{9.5}$ l/mole-sec and the fuel concentration of about 3 moles/l. However, jet fuel is not constituted of only one compound, and moreover we have measured the global oxygen consumption Arrhenius parameters. It remains to be seen if these measured global parameters can be somehow incorporated into the global models of fuel behavior.

Another interesting observations is that the fuel POSF-2827 which exhibits the highest temperature for oxygen consumption also produces the largest amount of carbon deposit. This observation implies that forming carbon deposits and inhibiting some types of molecules are responsible for oxygen consumption in a jet fuel. Most probably these molecules are the hetero-atom (sulfur) compounds. Fuel POSF-2827, which is not hydrotreated, should have more of these compounds than the fuel POSF-2747. Finally, there is a difference between the present results and the data of Giovanetti and Szetela (1986). Our results show that the oxygen is nearly completely consumed at a temperature of 500K; while Giovanetti and Szetela (1986) report that approximately 40 percent of the original oxygen remains at fuel temperatures as high as 585K. As yet, our attempts to account for this discrepancy have not been successful.

In Figure 8, we observe that the thermally stable fuels produce more methane than the unstable fuel. Zabarnick (1992) has shown that this production of methane gives additional clues to the chemical mechanisms occuring in the heated tube section. Methane production almost certainly arises from the presence of methyl radicals in the system. Methyl radicals initially appear at or near the temperature at which methane first appears because these radicals react extremely quickly with oxygen to produce methyl peroxide radicals. Only after the oxygen depletion can the abstraction reaction to form methane be observed. The abstraction reaction is slower than the recombination reaction with oxygen despite the fact that methane formation is an exothermic reaction.

This is because, even at 473K, the activation energy associated with H-abstraction by methyl of about 6 kcal/mole, slows the reaction down by almost three orders of magnitude. This analysis indicates that the stable fuels produce methyl radicals at lower temperatures, and that these radicals are important in the subsequent consumption of oxygen

In the future, it will be interesting to study the oxygen and methane behavior for fuel additives to determine if the observed trends of oxygen, methane, and deposits continue. So far, these trends clearly suggest that the consumption of oxygen at lower temperature and the more rapid production of methane indicate fewer deposits on the test section walls.

Conclusions

A single-pass flowing heat exchanger facility (Phoenix rig) was designed to test the carbon deposit forming tendencies of jet fuels in flowing systems. Three samples each of baseline JP fuels and JP fuels blended with the additives package were tested. The results, some of which were in qualitative agreement with those of other researchers, proved the design and usefulness of the Phoenix rig. Accordingly, measurements of carbon deposits, oxygen depletion, and methane production were performed for a variety of test conditions and the following conclusions emerged.

(1) Tests with all the blended fuel samples showed a noticeable improvement in fuel thermal stability.

(2) Both block temperature and test duration increased the total carbon deposits in a nonlinear fashion.

(3) Above a threshold bulk temperature of 450K, the fuel-dissolved oxygen concentration dropped suddenly and the onset of methane production was triggered. With nitrogen sparging, the methane production was greatly reduced. These observations suggest a complicated relationship between the formation of carbon deposits and the temperature-driven consumption of oxygen.

(4) A simple analysis, based on a bi-molecular reaction rate, correctly accounted for the fuel dissolved oxygen consumption rate. Such an approach proves the feasibility of developing a more rigorous model based on global kinetic parameters.

Acknowledgement

This research was supported by the U.S. Air Force Wright Laboratory, Aero Propulsion and Power Directorate, Wright-Patterson Air Force Base, Ohio, under Contract F33615-87-C-2767 with Dr. W. M. Roquemore serving as Technical Monitor

References

Giovanetti, A. J. and Szetela, E. J., 1986, "Long Term Deposit Formation in Aviation Turbine Fuels at Elevated Temperature," *AIAA Paper 86-0525*, 24th Aerospace Sciences Meeting, Reno, NV.

Harrison III, W. E., 1990, "Aircraft Thermal Management: Report of the Joint WRDC/ASD Aircraft Thermal Management Working Group," *Report No. TR-90-2021*, Wright-Patterson Air Force Base, OH.

Lefebvre, A. H., Chin, J., and Sun, F., 1992, "Experimental Techniques for the Assessment of Fuel Thermal Stability," *AIAA Paper 92-0685*, 30th Aerospace Sciences Meeting, Reno, NV.

Marteney, P. J. and Spadaccini, L. J., 1986, "Thermal Decomposition of Aircraft Fuel," *Journal of Engineering for Gas Turbine and Power* Vol. 108, pp. 648-654.

Pearce, J. A., Harrison III, W. E., Anderson, S. D., Edwards, J. T., Byrd, R. J., Heneghan, S. P., Martel C. R., Williams, T. F., Biddle, T. B., and Edwards, W. H., 1992, "Advanced Thermally Stable Jet Fuels Development," To be published in *Aviation Fuels: Thermal Stability Requirements*, ASTM STP-1138, (Edts: Perry W. Kirklin and Peter David) American Society of Testing and Materials, Philadelphia, PA.

Reddy, K. V. and Roquemore, W. M., 1990, "A Time Dependent Model with Global Chemistry for Decomposition and Deposition of Aircraft Fuels," *Paper 90-14, Symposium on the Stability and Oxidation Chemistry of The Middle Distillate Fuels*, August, American Chemical Society, Washington, D.C.

Rubey, W. A., Tissandier, M. D., Striebich, R. C., and Tirey, D. A., 1992, "In-Line Gas Chromatographic Measurement of Trace Oxygen and Other Dissolved Gases in Flowing High Pressure Thermally Stressed Jet Fuel," Paper to be presented at the *Symposium on Structure of Jet Fuels*, American Chemical Society, April, San Francisco, CA.

Zabarnick, S., 1992, " A Possible Mechanism for the Production of Methane in Thermally Stressed Fuels," To be published.

APPENDIX D

OXIDATION OF JET FUELS AND THE FORMATION OF DEPOSITS

by

Shawn P. Heneghan and Steven Zabarnick
University of Dayton, Dayton, Ohio

A Paper Submitted to Fuels, May 1992.

Abstract

Jet fuels and jet fuel surrogate have been thermally stressed to simulate the time/temperature history of aircraft fuel-handling systems. The resulting fuels, soluble products, and insoluble products have been analyzed. The results of these tests are shown to be incompatible with previous mechanisms concerning the source of deposit precursors.

In general, two important dependencies on oxygen have been found. First, in agreement with previous research, the amount of deposit formed decreases significantly if oxygen is removed from the fuel prior to heat stressing. Second, fuels which oxidize easily are likely to be more stable (as measured by deposits). We also present new evidence to support the free-radical mechanisms of oxidation and deposit formation in contrast to proposed ionic mechanisms of oxidation.

A general theory of oxidation of hydrocarbons has been incorporated to account for the observed oxygen dependencies. This theory is a free-radical, autoxidation, chain mechanism. The presence of naturally occurring antioxidant molecules is proposed to play an important role in both inhibiting the oxidation of the fuel and forming deposit precursors. Some properties (concentration, reactivity) of these antioxidant molecules are discussed and the implications of the theory are presented.

Abbreviations

ASTM	American Society for Testing and Materials
BDE	Bond Dissociation Energy
DCD	Dielectric Constant Detection
DMP	Dimethylpyrrole
DSC	Differential Scanning Calorimetry
ETIO	Electron Transfer Initiated Oxidation
FTIR	Fourier Transform Infrared
GCAED	Gas Chromatography with Atomic Emission Detection
HPLC	High Pressure Liquid Chromatography
JFTOT	Jet Fuel Thermal Oxidation Tester
JFA-5	Thermal stability additive package
JP	Jet Propellant (fuel)
JP-8S	Surrogate JP-8 Fuel
JPTS	Jet Propellant Thermally Stable
O-FID	Oxygen - Flame Ionization Detection

Introduction

It has long been known that oxygen consumption is an important first step in the formation of deposits in jet fuels.[1-7] Many mechanisms have been proposed to account for deposit formation. Most of the mechanisms start with the autoxidation chain cycle, and assume the products of the oxidation initiate the formation of deposits.

Bol'shakov[1] stated that condensation reactions of peroxides and other oxidized products are responsible for solid formation. Clark and Smith[2] define the initial stage of deposit formation as oxidation via a free-radical chain mechanism and the second stage as the reaction of trace compounds with the oxidation products. Hazlett[3] proposes that hydroperoxides are precursors to deposits. He attributes the cause of deposits to the alkoxy free radical that forms from the decomposition of hydroperoxides.

The general consensus of what was known about the chemistry and physics of jet-fuel thermal-oxidative stability was summarized by Baker et al.[4] based on the results of a NASA workshop held in 1978[8]. The six key points are:

1. The initial process is a reaction involving both oxygen and fuel.

2. The chemistry involved is primarily free-radical.

3. Deposit formation is dependent on temperature, fuel flow, dissolved metals, and dissolved oxygen.

4. Deposits form in liquid and vapor phases. Simultaneous occurrence of both phases enhances deposit formation.

5. Metals can have a significant effect on the deposit formation.

6. The amount of dissolved oxygen is important; removal of oxygen generally reduces the amount of deposit formed significantly.

Since all of the reported research has demonstrated the importance of oxygen to the deposition process, there is a general agreement that peroxides, alcohols, ketones, and acids are precursors to solid formation and that fuels oxidize to form gums which, in turn polymerize and condense to form solids. Although several researchers[5] have noted that there is not a direct correlation between the oxidation of fuels and the formation of deposits, many groups have followed the deposition process by monitoring the appearance of oxidation products[9-15].

Recent reports on deposit formation in jet fuels (in both flowing and static tests), combined with oxidation measurements[9-12,16-21], have questioned the above time-honored mechanisms. In this paper, we review the current research. The review is divided into two sections. The first discusses stability measurements based on deposit formation (referred to as thermal stability) while the second uses a measure of the ability to oxidize (referred to as oxidative stability). A theoretical analysis employing standard chain reactions for autoxidation and radical trapping is then developed and the relation between reactivity and concentration of antioxidant molecules is calculated. The discussion section is divided also into two parts; the mechanism for deposit formation and the mechanism for oxidation. Concerning deposit formation, we show that previous models of the deposit formation are inadequate in that they do not predict the observed oxygen dependence of both the thermal and oxidative stability. In the oxygen consumption discussion we show how the antioxidant mechanism presented here can account for the observed oxygen dependencies in not only the recent work but also many previous results. Then, with one assumption concerning the source of the deposit molecules, we show how this mechanism can be used to account for the formation of deposits. The implications of the analysis are then presented. A summary of the antioxidant mechanism can be found at the end of the article.

Review of Recent Experiments

Many different apparatuses[9-12,17,18,21] have been used to evaluate the thermal stability* of jet fuels. and several techniques have been used to measure their oxidative

* In this article, thermal stability will be used to refer to the stability of fuel as measured by the tendency to form deposits. This is distinct from the oxidative stability which is measured by the ability to oxidize and form peroxides, ketones, alcohols, and acids.

stability[9-12,19,20]. The experimental details and actual results of the individual measurements are detailed elsewhere; therefore, only a brief compilation of the important results is presented here.

Most of these recent results were obtained using three distinct fuels. The fuels and some of their properties are listed in Table 1. F-2747 is a highly hydrotreated Jet A-1 fuel, while F-2799 is an Air Force specification fuel, jet propellant thermally stable (JPTS), which has good thermal stability characteristics. Fuel F-2827 is a nonhydrotreated Jet A fuel, with a broader boiling range and increased heteroatom concentration. It is expected that this fuel will exhibit lower thermal stability than F-2747 and F-2799.

In addition to the large number of experiments that used the three fuels in Table 1, two sets of experiments were conducted to study more diverse sets of fuels. Heneghan et al.[11] studied the base fuels plus three JP-8 fuels, a JP-7 fuel, and a surrogate JP-8 fuel (JP-8S). Using a Fourier transform infrared (FTIR) spectroscopic probe, they measured the concentration of alcohols and ketones to estimate the amount of oxidation, and also made a gravimetric determination of the amount of filterable solids. Hardy et al. studied F-2747, F-2827[22], and 13 additional JP-5 fuels[9]. They measured the amount of deposit by weighing a metal strip from a flowing system, and used a separate measurement to determine the "peroxide potential." The "peroxide potential" is the sum of the peroxide numbers determined by titration after 24, 48, 72, and 96 hours.

Thermal Stability of Base Fuels

The expected relative thermal stability of the base fuels, in order from most to least stable, is F-2799, F-2747,and F-2827. This expectation is based on the heteroatom concentration, boiling range, past experience with hydrotreated fuels, and the fact that F-2799 is a special, thermally stable fuel that includes a thermal stability additive package (JFA-5). The ordering of thermal stability was verified by the JFTOT breakpoint (Table 1). JFTOT breakpoint values were verified by Biddle[12]. The relative thermal stability of these three fuels has also been established in several flowing systems including single-pass heat exchangers[10], multipass heat exchangers[17], the hot liquid process simulators[12], a microthermal precipitation test[12], a gravimetric determination in a flowing system[9], and a vaporization deposition test at high temperatures[21]. Static tests, such as a microcarbon residue tester[23] and flask tests[11,18], have also been used to study the relative thermal stability of the three fuels. The flowing and static tests agree well with the JFTOT breakpoint in indicating that the thermal stability of the baseline fuels decreases in the expected order (F-2799>F-2747>F-2827). A summary of these measurements is given in Table 2. Note that the appearance of less deposit indicates greater thermal stability, as does a higher breakpoint temperature.

Oxidative Stability of Base Fuels

Originally, we believed[13] the more thermally stable fuels would oxidize less easily. The first indication that this supposition was not accurate came from the Phoenix Rig[10]. Using a dissolved-oxygen analyzer[19] a plot of the bulk-fuel temperature versus dissolved-oxygen concentration showed an inverse order of oxidation temperature versus thermal stability (Figure 1). The shape of the curves was accounted for by assuming a first-order oxygen dependence, Arrhenius behavior of the rate constant, and a linear heating rate of the fuel through the test section. The appearance of methane is also shown in Figure 1. Methane appears at approximately the same temperature as oxygen disappears. As will be shown later, it lends strong support to the theory that free radicals

are involved in the deposition/oxygen-consumption process. A lower temperature for the disappearance of dissolved oxygen indicates a more easily oxidized fuel.

The observation that the more thermally stable fuels (F-2799 and F-2747) were more easily oxidized was verified in flask tests at 180C with bubbling oxygen. The relative amounts of oxidative products were measured using FTIR, gas chromatography using atomic emission detection and oxygen-flame ionization detection, high pressure liquid chromatography using dielectric constant detection and gravimetric techniques.[11,13] The availability of oxygen was found to significantly increase the amount of deposit from F-2747. However, most (>98%) of these deposits were soluble in acetone or methanol. If only those deposits which are insoluble in hexane and acetone or methanol were considered, then the relative ranking of thermal stability is independent of oxygen availability. These additional deposit materials also proved to be rich in oxygen, while those deposits made in F-2827 showed almost no absorption in the carbonyl stretch region of the infra-red[13]. This was taken as further evidence that the thermally stable fuels reacted easily with oxygen.

The amount of oxidation was also studied in three additional, separate static tests. First, in a flask test, the fuels were heated (175C) in a flask under bubbling oxygen for two hours. The three test fuels were studied by FTIR[11] to determine the concentration of ketones, alcohols, and acids. Second, two of the baseline fuels were studied in an accelerated storage stability test at 100C and oxygen-over-pressure of 3.4 atm.[9] In this test the peroxide potential of the fuel is measured. Third, the total acid number[23] was determined after the fuels were heated under bubbling air at 180C for five hours. Since these techniques measure the appearance of oxidized products, larger numbers indicate more oxidation.

Differential scanning calorimetry (DSC)[12] was used to determine the onset temperature for the oxidation exotherm. The Phoenix rig also measures the temperature at which these fuels consume oxygen. The oxygen consumption curve for the Phoenix rig is shown in Figure 1. These two tests heat the fuels at different rates; therefore the temperatures are not expected to be the same for the two tests. However, the trend for the baseline fuels should be the same. The DSC technique and the Phoenix rig should give lower temperatures for fuels which are more easily oxidized.

Finally, a cyclic voltammetry technique[20] was used to evaluate the appearance of oxidation products in flask tests. These tests all showed that the hydrotreated fuels oxidized at lower temperatures or to a greater extent than the nonhydrotreated fuel (F-2827). Some discrepancies in the oxidation of F-2799 may be due to the relative effectiveness of antioxidants in JPTS, and the hydrotreated F-2747. The results, to the extent they are quantitative and can be tabulated, are summarized in Table 3.

These recent experiments clearly show that the thermal stability order of the three baseline fuels (in decreasing order of stability) is F-2799, F-2747, F-2827. This ordering has been established by seven quantitative techniques. The two technique which deviate from this ordering show F-2747 only slightly better than F-2799. All of the techniques agree that F-2827 is the least thermally stable. Conversely, these same fuels show an inverse order to oxidative stability. The oxidative-stability order has been demonstrated by four quantitative techniques. Again, one measurement has F-2747 more easily oxidized than F-2799. All five techniques show that F-2827 is the most oxidatively stable.

Just as clearly as the three baseline fuels show an inverse relation between oxidative and thermal stability, three fuels do not represent the entire range of fuels.

Hardy[9] measured the peroxide potential and the gravimetric JFTOT deposits for '3 JP-5 fuels as well as two of the baseline fuels[22]. The results for this set of 15 fuels are shown in Figure 2. Heneghan et al.[11] studied seven fuels (including a JP-7, two JP-8's, and JP-8S); their results are shown in Figure 3. Two fuels seem to digress from the inverse relation: F-2799 (the fuel which gave the least deposit) and JP-8S (the fuel which gave the most deposit). However, as noted previously the discrepancies may be due to the relative effectiveness of antioxidants added to JPTS, JP-7 and F-2747, or the dispersant and metal deactivator which are part of the thermal stability additive package (JFA-5) in JPTS. Also, JP-8S is not really a fuel; therefore, its comparison here may not be totally appropriate.

Despite some small discrepancies, the data show a clear trend. As expected, the hydrotreated fuels (F-2799 and F-2747) are significantly more thermally stable than F-2827 when the deposition tendency of the fuels is considered the stability criterion. However, the trend is strong and unexpectedly reversed when measuring oxidative stability. As shown in Figures 2 and 3, the inverse relationship between the oxidative and thermal stability holds for a large number of fuels.

Theoretical Discussion

A detailed look at the mechanism of chain-breaking antioxidants can provide an interesting view of the structure of jet fuels. It also accounts for the apparent anomaly in the above set of experimental data:

> An inverted relation exists between the stability as measured by oxidation and by deposit formation.

A review of the theory of oxidation and antioxidants will help explain some previous kinetic data and present a new idea concerning the source of the deposit. The individual reactions are listed here in the theoretical discussion, and summarized again after the conclusion. The mechanism for oxidation has been kept as simple as possible in order to convey the concept of how some molecules could act as antioxidants. The actual mechanism for autoxidation, including possible intitiation sources and back reactions, is significantly more complicated.

Consider how a chain-breaking mechanism works, starting with the basic chemistry for the autoxidation chain reaction.[24] First, consider a single compound, RH.

initiation	Formation of $R\cdot$	(1)
propagation	$R\cdot + O_2 \rightarrow RO_2\cdot$	(2)
	$RO_2\cdot + RH \rightarrow RO_2H + R\cdot$	(3)
termination	$RO_2\cdot + RO_2\cdot \rightarrow$ products	(4)

Reaction (4), termination, has been written as the recombination of $RO_2\cdot$ rather than $R\cdot$ because Reaction (2) proceeds with no activation energy, while Reaction (3) has a significant activation energy[25]. Therefore, Reaction (3) is the slow step and $RO_2\cdot$ is the major radical species. A hydrocarbon is easily oxidized if Reaction (3) proceeds with a small activation energy. This requires a weak carbon-hydrogen bond.[25]

The concentration of radicals can then be calculated (Eqs. 1 and 2) by assuming the rate of initiation (R_i) equals the rate of termination (R_t). This is known as the Quasi Steady State Hypothesis[26].

$$R_i = 2k_4[RO_2\cdot]^2 = R_t \qquad \text{Eq. 1}$$

$$[RO_2\cdot] = [R_i/(2k_4)]^{.5} \qquad \text{Eq. 2}$$

Using the concentration of $RO_2\cdot$ from Equation 2, the rate of oxygen consumption(or RH consumption), can be written from Reaction (3), assuming that Reaction (4) contributes negligibly to the overall consumption process.

$$-d(O_2)/dt = -d(RH)/dt = k_3[RO_2\cdot][RH]=k_3[R_i/(2k_4)]^{.5}[RH] \qquad \text{Eq. 3}$$

Therefore the peroxidation of hydrocarbons by the chain mechanism proceeds without any dependence on the oxygen concentration. This, of course, can only be true for situations in which sufficient oxygen is available. In flowing tests, the amount of oxygen available is limited to that which is dissolved in the fuel at the beginning of the transit past the heated section (≈50 ppm by weight[27]). Consequently, it should not be surprising to find an oxygen dependence in these cases. Further, as the oxygen is removed, $RO_2\cdot$ can no longer be the major radical. As we shall see later, the buildup of R· radicals is responsible for the appearance of methane in the Phoenix rig at the same time/temperature that the oxygen is consumed.

Now we can add a chain-breaking antioxidant, AH, to this chain mechanism. The antioxidant operates by the transfer Reaction (3t), thus removing the chain-carrying radical, $RO_2\cdot$, from the autoxidation process.

$$RO_2\cdot + AH \rightarrow RO_2H + A\cdot \qquad (3t)$$

To be effective, the new radical formed in (3t), A·, must not propagate the chain. This is easily accomplished if Reaction (3t) is significantly exothermic, implying that the AH bond strength is weak as compared to RH. This prevents A· from regenerating the R·radical and continuing the chain. however, It is also possible that some of the A· radicals could combine with oxygen producing $AO_2\cdot$ peroxy radical as in Reaction (2'). In this case, Reaction (3t') must progres very slowly so that the chain-propagation (Reactions (2) and (3)) is effectively terminated by (3t).

$$A\cdot + O_2 \rightarrow AO_2\cdot \qquad (2')$$

$$AO_2\cdot + RH \rightarrow AO_2H + R\cdot \qquad (3t')$$

It is generally argued that the activation energy for hydrogen atom abstraction by peroxy radicals (as in Reaction (3t')) is dependent on the Carbon-Hydrogen bond strength in RH, and not on the stability of the underlying radical of the peroxy radical, A·. This would seem to indicate that the activation energy of Reaction (3t') is not significantly different than Reaction (3), and therefore the radical formed in Reaction (2') would then be capable of regenerating the original chain.

There are three possible causes for reaction (3t') to be significanly slower than Reation (2). The first is through steric hinderance which would lower the A-factor for the reaction. The second, as postulate here is that there is stabilization accross the O-O bond

for some radicals, and that the activation energy is increased, and the third is that there may be a unimolecualr rearrangement of the $AO_2\cdot$ radical after formation.

The radicals formed in Reactions (2') or (3t) are then consumed in the major termination Reaction (4').

$$AO_2\cdot + AO_2\cdot \rightarrow \text{products}$$

or (4')

$$A\cdot + A\cdot \rightarrow \text{products}$$

It is Reaction (4'), and in particular the $AO_2\cdot$ termination product that we propose is the major oxidative pathway to the formation of insoluble products. The rational for the selection of this reaction, and its implications will be discussed later in this article.

For Reaction (3t) to effectively terminate the chain reaction, it must compete with Reaction (3) such that the rate of (3t) is approximately equal to or faster than (3). That is,

$$k_3[RH][RO_2\cdot] < k_{3t}[AH][RO_2\cdot]. \quad \text{Eq. 4}$$

To maintain the inequality of Equation 4, k_{3t}/k_3 must exceed the ratio of [RH]/[AH]. Assuming Arrhenius behavior of the rate constants and ignoring possible differences in the preexponential, the concentration of AH required to act as an antioxidant for the compound RH can be determined from the difference in the activation energies for (3) and (3t) (Equation 5). For example, if the difference in E_a is about 5.6 kcal/mole at room temperature, AH must be added at about 100 ppm (at room temperature). Obviously, if the hydrogen atom in AH is more easily abstracted in (3t), an even smaller concentration of AH can be effective.

$$10^{(Ea_{3t}-Ea_3)/\Theta} < \frac{[AH]}{[RH]} \quad \text{where } \Theta = 2.3RT \quad \text{Eq. 5}$$

One additional consideration is that AH can oxidize in its own chain to consume oxygen as shown in Reactions (2') and (3').

propagation $A\cdot + O_2 \rightarrow AO_2\cdot$ (2')

$$AO_2\cdot + AH \rightarrow AO_2H + A\cdot \quad (3')$$

However, analogous to Equation 3, Equation 6 shows that the rate of oxygen consumption will decrease for ever-decreasing concentrations of AH.

$$-d(O_2)/dt = -d(AH)/dt = k_{3'}[AO_2\cdot][AH] = k_{3'}[R_i/(2k_{4'})]^{.5}[AH] \quad \text{Eq. 6}$$

Further, in a fully quenched system (one in which Reaction (3t) dominates (3)), the disappearance of RH is equal to the initiation rate. The initiation rate in the preliminary stages is dependent on both oxygen and hydrocarbon[28] (equation 7).

$$-d(RH)/dt = R_i = k_i[O_2][RH] \quad \text{Eq. 7}$$

This analysis shows that the addition of a small amount of an easily oxidized material can interfere with the major chain autoxidation mechanism, transferring the radical to a chain which may have faster rate constants, but significantly less concentration. The result is that the rate of oxidation is decreased, despite the addition of easily oxidized compounds.

We can conclude from this analysis that if our assumptions concerning the rate of Reaction (3') are true then any molecule with a labile (easily removed) hydrogen can act like an antioxidant, providing it has sufficient concentration so that (3t) competes with (3), and yet has a sufficiently small concentration so that the autoxidation rate from Equation 6 is less than the autoxidation rate from Equation 3. Interestingly, molecules with labile hydrogens typically have less activation energy for Reaction (3) or (3'); thus, they are more easily oxidized. This leads to the conclusion that adding a small amount of easily oxidized material to alkanes will decrease the rate of oxygen consumption, not increase it.

It is also important to note that the oxidation of a hydrocarbon system can proceed through a free-radical mechanism and yield a rate law which has either zero- or first-order dependence on the oxygen concentration. Other proposed radical mechanisms show fractional-order dependences[29]. It is unwise to try to infer mechanisms from rate laws; however, rate laws can be derived from mechanisms, and an oxygen/hydrocarbon system with a good antioxidant could easily exhibit first-order dependence on the concentration of oxygen molecules for the formation of peroxides.

Discussion

Mechanism of Deposit Formation

Our observations have not disagreed with any previous observations, but rather add to them. Hazlett[5] described three key criteria for deposit formation any proposed mechanism must meet:

1. Dissolved oxygen initiates the process.

2. Heteroatom-containing molecules should play an important role.

3. Only a small amount of the fuel is involved in the deposit formation process.

The proposed mechanism meets these criteria. As a result of our recent experiments, we have added a fourth criterion:

4. The mechanism must account for the inverted relation between the ease of oxidation and the formation of deposits.

Clark and Smith[2] proposed a simplified two-step model. The first step is the production of peroxides and other oxidized intermediate materials. In the second step, these products react with sulfur- and nitrogen-containing compounds to form deposit materials. Taylor[6] has proposed a mechanism in which the first step is the reaction of a sulfur- and nitrogen- containing compound with dissolved oxygen. These reaction products then oxidize further to form insoluble materials.

These two schemes differ only in that Taylor[6] proposes oxidation in both steps. The Clark and Smith[2] mechanism implies that fuels which form more oxidized product

in the first step would form more deposit material in the second step. This clearly differs with our observations (Criterion 4). This is not necessarily the case in the Taylor mechanism, since he does not rule out other oxidation pathways. However, the inverted behavior of oxidation to deposit formation does not necessarily follow from his mechanism.

Oxygen Consumption

The conclusion concerning the behavior of easily oxidized materials added to alkanes can be used to explain many previous observations. In particular, it can be used to explain the rate-law behavior of n-dodecane oxidations, the apparent antioxidant capability of dimethylpyrrole (DMP)[30], and several other previously measured oxidation rates for binary mixtures[14,15,30].

While studying DMP in n-dodecane, Beaver[30] noted that the deposit formed appeared to be oxidized DMP, while the rate law was first order in oxygen. He proposed an electron transfer initiated oxidation (ETIO) mechanism to account for the observations. The ETIO mechanism proposes that DMP reacts with oxygen molecules. The antioxidant capability observed by Reddy[15] is explained by assuming the DMP is in competition with n-dodecane for the limited amount of oxygen available in the flowing JFTOT. Since the DMP is easily oxidized, it would preferentially acquire the oxygen, leave solution, and not be analyzed (only soluble oxidation products were analyzed)[15]. If this were the case, the addition of DMP to n-dodecane would (a) increase the rate of oxygen consumption, and (b) lower the temperature at which the oxygen reacted in the JFTOT test section.

Neither of the last two statements has been studied, but several similar cases would indicate that neither is true. Hazlett[4] used a modified JFTOT to find the tube temperature at which half the dissolved oxygen would react. None of the compounds he added to n-dodecane caused the oxygen to be consumed at a decreased tube temperature, while several (e.g., fluorene, indene, triphenylmethane) increased the consumption temperature by 30 C or more. Mayo and Lan[14] measured the amount of oxygen consumed versus time in n-dodecane oxidation. The addition of N-methylpyrrole resulted in a decrease in the amount of oxidation, not an increase. The test method employed by Mayo would not be deceived by oxidative deposit formation, since he measured the disappearance of oxygen rather than the appearance of soluble oxidation products.

The free-radical mechanism can account for the appearance of oxidized DMP, the antioxidant characteristic of DMP, and the apparent first-order dependence on oxygen molecules. There seems to be little evidence that the mechanisms are not free radical in nature. Further evidence that the oxidation reactions are free radical will be presented later in the description of methane production.

The addition of a more easily oxidized compound to a less easily oxidized compound decreases the oxidation rate. This was seen by Russel in a cumene/tetralin system[31], Mayo and Lan in an indene/n-dodecane system and N-methylpyrrole/n-dodecane[14], and Reddy, Cernansky, and Cohen in a DMP/n-dodecane.[15] Further, Mayo and Lan[14] noted that the continuing increase in concentration of the easily oxidized compounds resulted in steadily increasing oxidation rates until they finally surpassed that of the original alkane. The theory of autoxidation presented here can account for each of these observations.

A look at which compounds might be available in a fuel reveals something about the origin of deposit materials. Table 4 shows possible molecules and the bond strength of the weakest bonds. The bond strength of a normal alkane is also shown for comparison. Recall that the ease of oxidation of a compound moves inverse to the bond strength of the most weakly bound hydrogen. Following the proposed oxidation scheme, each type of molecule listed could act as an antioxidant if present in the correct quantity. Each type of molecule is present in fuels--in only small quantities--and interestingly, each has been implicated in the formation of deposits. If we consider that the precursor to deposits is the $AO_2\cdot$ radical, this mechanism explains our observation that easily oxidized materials are inherently stable, while unstable materials are difficult to oxidize. Further, the list is also rich in heteroatoms; this indicates that deposit material should be rich in heteroatoms. Finally, the removal of oxygen would limit the formation of $AO_2\cdot$, and thus limit the amount of deposit formed.

We propose that naturally occurring molecules in fuels which have weakly bound hydrogens are responsible for the formation of deposits. However, while they are oxidizing to form deposits, they are acting as chain breaking antioxidants, thus slowing down the overall rate of oxygen consumption. This dual action of these antioxidant compounds is what yields the seemingly conflicting result that while oxygen is necessary for the formation of deposits, the more difficult it is to oxidize a fuel the more stable it is likely to be.

The proposed mechanism accounts for each of the three key facts put forth by Hazlett:

1. If oxygen is removed from the system, Reaction (2') cannot proceed and the precursors ($AO_2\cdot$) to the formation of deposits are eliminated.

2. Since $A\cdot$ is formed from a molecule with a labile hydrogen (see table 4) it is likely to be rich in heteroatoms as will the $AO_2\cdot$ radical and the resulting insoluble products.

3. Only a small fraction of the total fuel molecules are oxidized, and only a small fraction of those oxidized are terminated by reactions leading to insoluble products.

This proposed mechanism, together with an understanding of the makeup of fuels accounts for the observed fourth key fact.

4. The observed inverted behavior of oxidation versus deposit formation should be expected, if not required.

Deposit formation does not follow oxidation; this has been observed and commented on previously[5,7] and, in fact, several of the concepts described herein have been known. It has been noted that the presence of some heteroatoms is responsible for increased deposit formation and their removal increases both the thermal stability[6] and susceptibility to oxidation[5,33] of jet fuels. As early as 1963, it was recognized that hydrotreating removed some of the natural antioxidants from jet fuels. Consequently, antioxidant additives have been specified in UK and USA military specifications DERD-2494 (1963) and MIL-T-5624 (modified 1976) for addition to hydrotreated fuels.

Mechanism for the Production of Methane

The free-radical nature of the chemical reactions is supported further by the appearance of methane in the Phoenix rig. Methane is produced in the Phoenix rig at temperatures near 500K (see Figure 1), and only when the oxygen is largely removed. It is reasonable to expect that methane is the result of methyl-radical production arising from the unimolecular fission of larger alkyl radicals to form methyl and alkenes (Reaction (5)).

$$R\cdot \rightarrow R'{=}CH_2 + CH_3\cdot \qquad (5)$$

where $R'{=}CH_2$ is the resulting alkene, containing one less carbon than the original R· radical.

This process is normally associated with short hydrocarbons. While there is a dearth of these compounds in jet fuels, there is usually a significant quantity of compounds with short active hydrocarbons. The simplest source would be ethyl or propyl benzene.

The appearance of methane only after significant diminishment of the oxygen concentration is consistent with a free-radical mechanism as shown by the competing reactions (Reactions (6) and (7)) and their respective rate equations (Eqs. 8 and 9). Reaction (6) has the advantage of no activation energy and high preexponential. However, it suffers from a small and decreasing concentration of oxygen. As the concentration of oxygen decreases, Reaction (7) will dominate and methane will appear.

$$CH_3\cdot + O_2 \rightarrow CH_3O_2\cdot \qquad (6)$$

$$R_6 = -d[CH_3\cdot]/dt = A_6\,[CH_3\cdot][O_2] \qquad \text{Eq. 8}$$

$$CH_3\cdot + RH \rightarrow CH_4 + R\cdot \qquad (7)$$

$$R_7 = -d[CH_3\cdot]/dt = A_7 \exp(-E_7/RT)\,[CH_3\cdot][RH] \qquad \text{Eq. 9}$$

If we assume the preexponential values (A_6 and A_7) are nearly equal, and Reaction (6) competes evenly with (7) (i.e., $R_6 = R_7$) at an oxygen concentration of 25 ppm and temperature of 500K, we can evaluate Eq. 10 for E_8.

$$E_7 = -RT \ln([O_2]/[RH]) = 10.6 \text{ kcal/mole} \qquad \text{Eq. 10}$$

This global activation energy is very reasonable for this type of reaction. For comparison, if RH is ethane, the activation energy is expected to be 10.8 kcal/mole[32] and larger alkanes would not be expected to show a significant change in activation energy. This does not prove that methane is the result of free-radical reactions; however, it shows that the assumption of a free-radical mechanism is a reasonable and self-consistent explanation which yields expected kinetic parameters.

Implications

Jet fuel oxidation results in the build up of peroxides, ketones, aldehydes, alcohols, and acids from the autoxidation cycle; sulfates, sulfones and nitrous compounds from the inhibitors originally present; and alkenes from the decomposition of radicals. Many of these oxidized compounds can, if present in sufficient quantity, inhibit fuel oxidation. That is, fuels will exhibit a self-inhibition towards oxidation over time.

However, the inability to oxidize is closely linked to the tendency to form deposits. Therefore, evaluation of jet fuel performance under accelerated conditions with excess oxygen may yield results which are not indicative of fuel quality.

The oxidative stability of a fuel is related to the availability of easily oxidized compounds. Interestingly, the addition of a small amount of easily oxidized compound will have an inhibiting effect on the overall oxidation rate. However, if sufficient quantities of the easily oxidized compound are available, the compound will help stimulate oxidation. The production of solids is strongly and positively affected by the presence of easily oxidized materials. A qualitative picture of the behavior of both oxidizability and deposit formation is shown in Figure 4 for increasing amounts of easily oxidized material in the fuel. Ease of oxidation decreases as concentration increases; however, it must eventually increase, causing a minimum in the oxidation curve. Deposit formation rate should steadily increase with increasing concentration. Note that the region for jet fuels is shown where these two measures of stability move inverse to each other. Identification of this region is empirical. Other types of fuel may not behave in this manner because they may be in a different region of the graph (Figure 4). Also, we may yet test a jet fuel which does not fall in the indicated region.

The above implies that there is an ideal amount of antioxidant that should be present in a jet fuel. Less than the ideal amount does not prevent oxidation, while too much can induce deposit formation. The formulation of antioxidants for addition to fuels should be based not only on their ability to act as antioxidants, but to ensure that the termination products of the antioxidant radical are soluble rather than insoluble.

A fuel is not one compound, but rather it comprises a large variety of compounds and chemical structures. It is the variety of chemical structures, and the resulting range of hydrogen BDEs, not the range of boiling points, which are of interest, because different structures will have H-atoms which are more or less accessible to the metathesis reactions (Reactions (3) and (3t)) important in the autoxidation chain propagation. In general, regardless of the initiation step, the chain oxidation of RH will be terminated by Reaction (3t) if there are molecules with H-atoms that can be easily abstracted in sufficient quantity (based on Eq. 4). However, the AH chain oxidation will continue unless the AH concentration is insufficient to maintain a separate autoxidation cycle.

Conclusion

Several fuels have been tested in a variety of different test apparatuses to determine their relative stability. Dividing fuel stability into thermal stability (based on the deposit forming tendency) and oxidative stability (based on the ability to oxidize and form peroxides, ketones, alcohols, and acids) leads to the seemingly anomalous statement: "Fuels that oxidize easily are likely to be thermally stable, while fuels that are not thermally stable are not easily oxidized." This statement was found to hold, independent of the fact that oxygen reaction with fuel is a necessary first step for the production of solid deposits.

A theoretical analysis of the autoxidation mechanism of hydrocarbons can account for the observed oxygen dependencies as well as all the other needed criteria for the deposit mechanism[5], if the peroxy radical of the antioxidant molecules are the precursors to the deposit formation. Analysis of the reactions also accounts for the appearance of methane in the Phoenix rig[10], the previously surprising results of additions of small amounts of easily oxidized compounds to alkanes causing a decrease in the oxidation rate rather than an increase[14,15,30], and the observed first-order rate

dependence of oxygen uptake in doped-hydrocarbon systems[30]. All the data are consistent with a free radical-inhibited-autoxidation mechanism.

We believe the number of key facts, as described by Hazlett[5], for which a deposit formation mechanism must account should be increased from three to four-- to include the inverse relation between oxidative stability and thermal stability.

Summary of Autoxidation Mechanism

Autoxidation Chain Mechanism of Alkanes

initiation	Formation of R· -	(1)
propagation	$R\cdot + O_2 \rightarrow RO_2\cdot$	(2)
	$RO_2\cdot + RH \rightarrow RO_2H + R\cdot$	(3)
termination	$RO_2\cdot + RO_2\cdot \rightarrow$ products	(4)
	Chain Transfer Reactions	
	$RO_2\cdot + AH \rightarrow RO_2H + A\cdot$	(3t)
	$AO_2\cdot + RH \rightarrow AO_2H + R\cdot$	(3t')
	Autoxidation of AntiOxidants	
propagation	$A\cdot + O_2 \rightarrow AO_2\cdot$	(2')
	$AO_2\cdot + AH \rightarrow AO_2H + A\cdot$	(3')
termination	$AO_2\cdot + AO_2\cdot \rightarrow$ products	(4')

We propose that Reaction (4') is the major production pathway of solid formation.

Acknowledgment

This work was supported by the U.S. Air Force Wright Laboratories, Wright-Patterson Air Force Base, Ohio, under Contract No. F33615-87-C-2767 with W. M. Roquemore serving as technical monitor.

References

1. Bol'shakov, G. F. 'The Physico-Chemical Principles of the Formation of Deposits in Jet Fuels' USSR, Translated by U.S. Air Force FTD-MT-24-416-74, 1970

2. Clark, R. H. and Smith, L. Proceedings of the 3rd International Conference on the Stability and Handling of Liquid Fuels, 1988, Institute of Petroleum, London, Eng., p. 268

3. Hazlett, R. N. 'Frontiers of Free Radical Chemistry' (Ed. W. Pryor), Academic Press, New York, 1980, p. 195

4. Baker, C. E., Bittker, D. A., Cohen, S. M. and Seng, G. T. NASA Tech Memorandum 83420, 1983

5. Hazlett, R. N. 'Thermal Oxidation Stability of Aviation Turbine Fuels', ASTM, Philadelphia, PA, 1991

6. Taylor, W. F. and Frankenfeld, J. W. Proceedings of the 2nd International Conference on Long-Term Storage Stabilities of Liquid Fuels, Southwest Research Institute Institute, San Antonio, TX, 1986, p. 496

7. Hazlett, R. N. 'Fouling of Heat Transfer Equipment' (Eds. E. F. C. Somerseald and J. G. Knudsen), Hemisphere Pub. Corp., Washington D. C., 1981

8. Taylor, W. F. 'Jet Fuel Thermal Stability', NASA TM-79231, 1979

9. Hardy, D. R., Beal, E. J. and Burnett, J. C. Proceedings of the 4th International Conference on Stability and Handling of Liquid Fuels, U. S. Department of Energy Washington D. C., 1991, p. 260

10. Heneghan, S. P., Williams, T. F., Martel, C. R., and Ballal, D. R. *Journal of Engineering for Gas Turbines and Power*, Accepted for Publication 1992, see also International Gas Turbine Institute, Cologne, Germany, June 1992, Paper No. 92-GT-106

11. Heneghan, S. P., Lockiear, S. L., Geiger, D. E., Anderson, S. D. and Schulz, W. D. *AIAA Journal of Propulsion and Power*, 1992, Accepted for Publication, see also 30th Aerospace Sciences Meeting, Paper No. AIAA 92-0686, Jan 1992, Reno, NV

12. Biddle, T. B., Hamilton, E. H. and Edwards, W. H. United Technologies Corporation R&D Status Report No.13 to WL/POSF, Wright Patterson Air Force Base, Ohio, 1991

13. Anderson, S. D., Edwards, J. T., Byrd, R. J., Biddle, T. B., Edwards, W. H., Martel, C. R., Williams, T. F., Pearce, J. A., Harrison, W. E. and Heneghan, S. P. 'Aviation Fuel: Thermal Stability Requirements', ASTM STP 1138 (Eds. P. W. Kirklin and P. David), ASTM, Philadelphia, PA, in press

14. Mayo, F. R. and Lan, B. Y. *Ind. Eng. Chem. Prod. Res. Dev.* 1986, **25**, 333

15. Reddy, K. T., Cernansky, N. P. and Cohen, K. S. *J. Propulsion* 1989, **5**, 6

16. Heneghan, S. P. and Harrison, W. E. ACS Symposium. Structure of Jet Fuels III, 1992, PETR 404, San Francisco, CA

17. Lefebvre, A. H., Chin, J., and Sun, F. 30th Aerospace Sciences Meeting, Paper No. AIAA 92-0685, Jan. 1992,

18. Jones, E. G. and Balster, W. J., Paper No. 92-GT-122, International Gas Turbine Institute, Cologne, Germany, June, 1992

19. Rubey, W. A., Striebich, R. C., Anderson, S. A., Tissandier, M. D. and Tirey, D. A. ACS Symposium: Structure of Jet Fuels III, 1992, PETR 371, San Francisco CA

20. Kauffman, R. E. and Tirey, D. A. ACS Symposium: Structure of Jet Fuels III, 1992, PETR 412, San Francisco CA

21. Edwards, J. T. 30th Aerospace Sciences Meeting, Paper No. AIAA 92-0687, Reno, NV, 1992

22. Hardy, D. L. Private communication, 1992

23. University of Dayton Quarterly Progress Report No. 18 to WL/POSF, Wright-Patterson Air Force Base, OH, 1992

24. Nixon A. C. 'Autoxidation and Antioxidants' (Ed. W. O. Lundberg), Wiley, New York,1962

25. Benson, S. W. and Nangia, P. S. *Accounts of Chemical Research*, 1979, **12**, 223

26. Benson, S. W. 'The Foundation of Chemical Kinetics', McGraw-Hill, New York, 1960

27. CRC Report No. 530, Coordinating Research Council, 1983, Atlanta GA

28. Emanuel, N. M. 'The Oxidation of Hydrocarbons in the Liquid Phase', Pergamon, Oxford, England 1965

29. Baird, J. K. ACS Symposium: Structure of Jet Fuels III, 1992, PETR 420, San Francisco, CA

30. Beaver, B. D. and Gilmore, C. *Fuel Sci and Tech.* 1991, **9**, 811

31. Russel, G. A. JACS, 1956, **78**, 1035

32. Benson, S. W. 'Thermochemical Kinetics', Wiley, New York, 1976

33. CRC Report No. 559, Coordinating Research Council, 1988, Atlanta GA

Table 1 Properties of Baseline Jet Fuels				
	ASTM* Method	F-2799	F-2747	F-2827
JFTOT≠ Breakpoint (C)	D3241	399	332	266
Sulfur Mass (%)	D4294	0.0	0.0	0.1
Aromatics Vol. (%)	D1319	9	19	19
Existent Gum (mg/100ml)	D381	0.4	0.0	0.0
Flash Point (C)	D93	49	59	50

*American Society for Testing Materials
≠Jet Fuel Thermal Oxidation Tester

Table 2. Results of Thermal Stability Tests on the Three Baseline Fuels			
	F-2799	F-2747	F-2827
Phoenix Rig (µg Deposit)[10]	300	450	2800
Multipass Heat Exchanger (µg/cm^2/hr of Deposit)[17]	56	348	2250
Hot Liquid Process Simulator (mg/cm^2 of Deposit)[12]	3	8	152
Microthermal Precipitation (µg Deposit/50 ml)[12]	2818	4438	7162
JFTOT Breakpoint (C)	399	332	266
Total Insolubles in Gravimetric JFTOT (ppm)[5]	not measured	.2	.8
Microcarbon Residue Test (% Residue)[23]	.11	.10	.46
Flask Test (mg)[18]	0	2	7
Vaporization Deposition (µg)[21]	1183	875	4703

Table 3. Results of Oxidative Stability Tests on the Three Baseline Fuels

	F-2799	F-2747	F-2827
Peroxide Potential (ppm)[9]	not measured	46	2
Onset of Oxidation Exotherm from DSC (C)[12]	189	198	206
Temperature (C) for 1/2 Oxygen Depletion in Phoenix Rig[9]	185	190	215
Total Acid Number[23]	3.54	2.27	0
Sum of Concentration of Alcohol, Ketones, and Acids (moles/l)[11]	.6	1.8	.03

Table 4. Types of Molecules Available in Fuels and BDEs*

Type	Bond	BDE (kcal/mole)
Alkenes	R=R-R—H	87
Substituted Benzene	Φ-C—H	80-85
Thiols	R-S—H	85
Pyrroles	Φ_N-R—H	80-85
Alkanes	R—H	98

*Bond Dissociation Energies (BDEs) are estimated using the methods described by Benson[32].

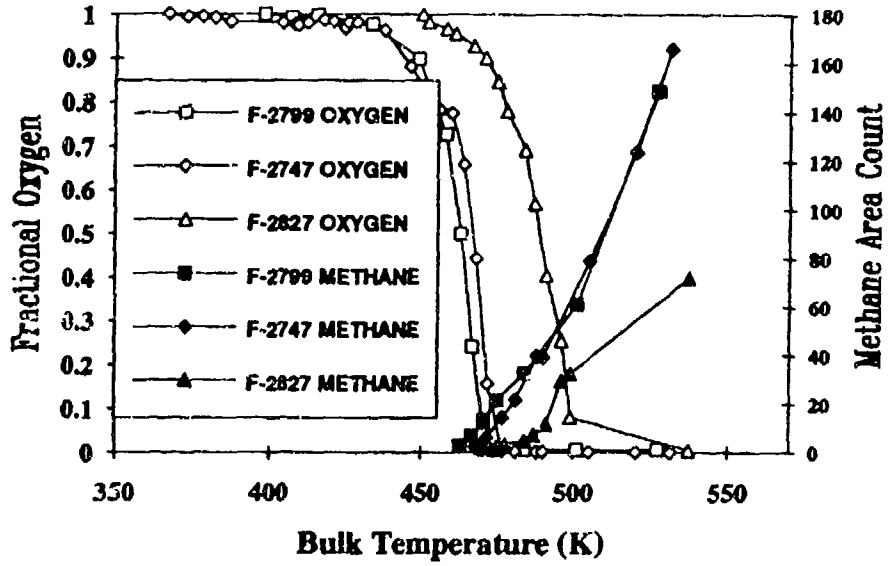

Figure 1. Dissolved oxygen and methane concentrations versus output bulk temperature from a single tube heat exchanger. Input temperature = 30C, Input concentration of Oxygen = 50 ppm. Residence time in heat exchanger = 6.3 seconds (from reference 10).

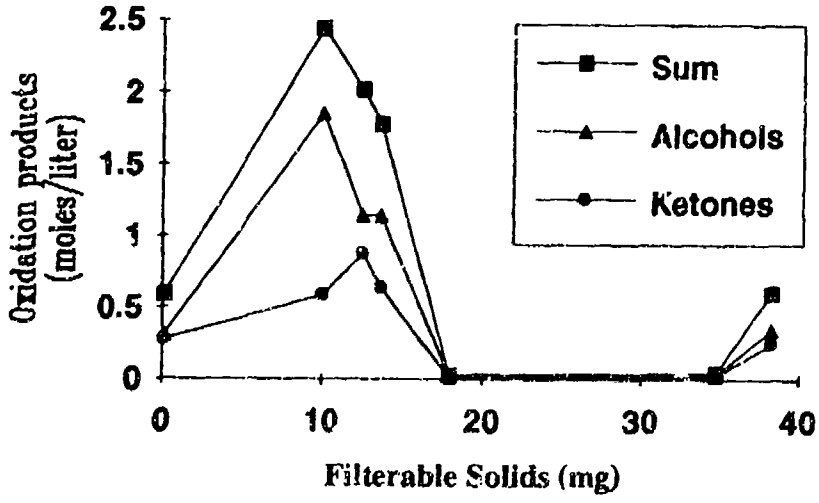

Figure 2. Peroxide potential versus gravimetric JFTOT of 15 fuels. (from Reference 9,22)

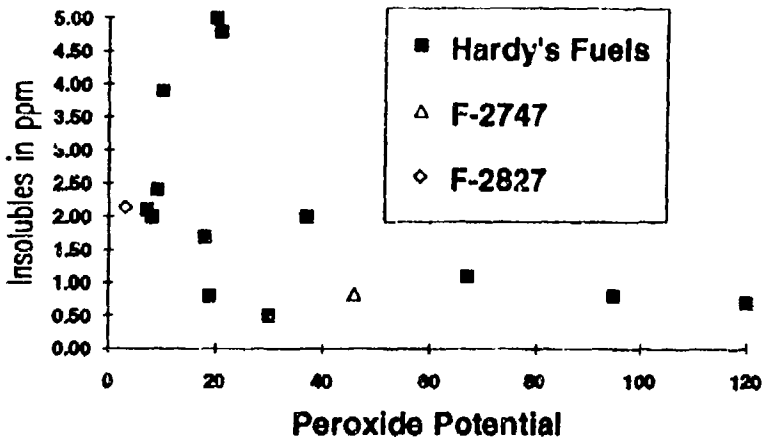

Figure 3. Concentration of alcohols and ketones versus filterable solids (from reference 11).

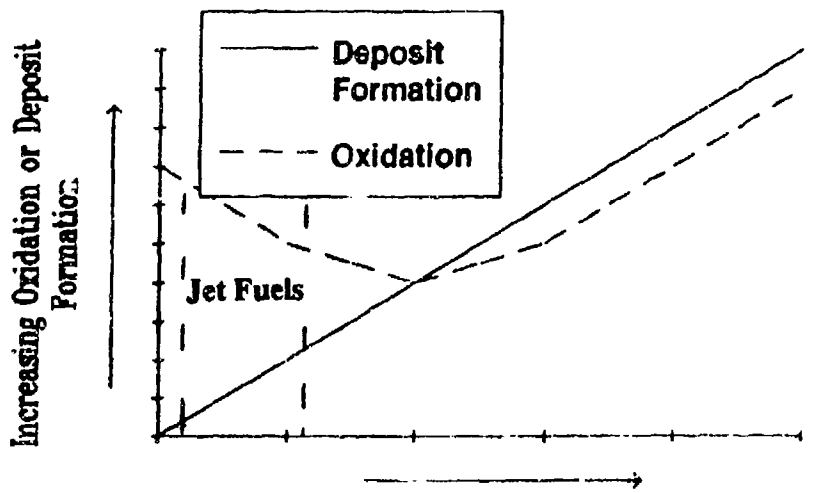

Figure 4. Qualitative behavior of fuel oxidative and thermal stability with increasing concentration of easily oxidized species.

APPENDIX E

A CHEMICAL INVESTIGATION OF THE NATURE OF JET FUEL OXIDATION DEPOSITS AND THE EFFECT OF ADDITIVES ON DEPOSITS.

by

William D. Schulz
Eastern Kentucky University, Richmond, Kentucky

Final Report on UDRI Subcontract No. RI-75851X,
(Prime Contract No. F33615-87-C-2767) as submitted
by Eastern Kentucky University, Richmond, Kentucky

Final Report
Contract F33615-87-C-2767
Subcontract RI-75851X

March 1, 1992

A Chemical Investigation of the Nature of Jet Fuel Oxidation Deposits and the Effect of Additives on Deposits

William D. Schulz
Department of Chemistry
Eastern Kentucky University

1. Summary

We have extensively studied methods for isolation and concentration for the analysis of additives in fuels. A preprint paper for the April, 1992 ACS meeting on this work is included as appendix A. The method described is applicable to nearly all antioxidants, common metal deactivators, deicers and some dispersants. The method development work was done with the previously developed 12 component surrogate fuel (JP-8S).

The surrogate fuel was also used to investigate base parameters (oxygen flow, time vs. oxidized species and insolubles) of the flask test. Quantitative analysis of oxidized species in stressed fuel samples was done by FTIR. This requires no sample preparation, is rapid and reproducible but when applied to real fuels, oxidation product analysis and insoluble material formation give dichotomous results. Fuels including the surrogate, JP-7, JP-TS and POSF 2747 produce increasing amounts of insoluble material with increasing concentrations of oxidized species Fuels such as POSF 2827 produce large amounts of insoluble material with essentially no detectable concentration of oxidation products.

Samples from the stressed surrogate fuel and insoluble deposits were investigated as method development and as a model to better understand the chemistry of deposit formation. Information was extensive. Methanol extraction of the stressed fuel, followed by hexane or petroleum ether back extraction of the methanol solution, concentrated the oxidation products and greatly reduced fuel component interference for analysis by GC-MS. The most abundant oxidation products were those of the substituted aromatic compounds and tetralin.

The fuel insoluble sediment that is formed by the surrogate is essentially all acetone (or methanol) soluble, regardless of the stress time. These deposits contain large amounts of fuel components that are very difficult to remove by washing, but can be eliminated by dissolving, extraction and reprecipitation. Dried samples of treated material can be redissolved in methanol or acetone but gas chromatography

will not separate the components of the solution. The broad, large "hump" that results from attempted GC of the solution suggests a continium of oligomers. However, the dried insoluble material can be thermally desorbed (at 280C) from a "pyroprobe" interface to the GC to give component separation. Mass spectra of the chromatographic peaks from thermal desorption of solids indicate a substantial number of alkenes in addition to acid, alcohols and carbonyls found in fuel soluble oxidation products. The presence of unsaturates, in addition to the apparent decomposition below pyrolysis temperature suggest that the deposits are bonded by peroxide links, similar to those of drying oils, as well as other weaker attractive forces. The preprint paper for the April, 1992 ACS meeting describing the characterization of soluble and residue oxidation products of the surrogate fuel is attached as appendix B.

The marked difference in the oxidative behavior of real fuels POSF 2747 and POSF 2827 and the success in the characterization of oxidation products of the surrogate suggested a comparison of the soluble and insoluble products formed by these fuels under flask test conditions. Stressed POSF 2747 (the "oxidizable fuel") was observed to form a clear, more dense second liquid phase during oxidation, while POSF 2827 did not. POSF 2747 slowly formed a brown adherent viscous gum during oxidation while POSF 2827 formed a flocculant brown precipitate quite rapidly. POSF 2747 is a hydrotreated fuel with a fairly narrow boiling range. POSF 2827 has much wider boiling range and is not hydrotreated. Extraction and G.C. of the identical (19%) aromatic fractions of these fuels indicates that POSF 2827 has aromatics that extend to the di- and tri-substituted napthalene range while POSF 2747 does not contain aromatics of higher molecular weight than methylnapthalenes.

These fuels were stressed with the flask test modified with a Dean-Staerk trap on the stress flask. POSF 2747 produced 2 phases of volatile components, a more dense phase of highly polar compounds and a less dense phase of less polar components. The volatile portion of POSF 2827 that was trapped consisted of a single phase that proved to be non oxidized components of the fuel. Both phases produced by POSF 2747 contained carboxylic acid, alcohol and carbonyl oxidation products. Methanol extracts of the oxidized fuels and the thermally desorbed products of deposits from both fuels have been separated and characterized. The most notable difference is that insoluble residue from POSF 2827 contains much higher concentrations of phenolic compounds.

2. Technical work

The overall objective of this work is a study of the chemistry of fuel deposition. Tasks accomplished in this study are the following:

2.1 Analysis of Additives
2.2 Oxidation Parameters with the Flask Test
2.3 Deposit Chemistry of a Surrogate Fuel
2.4 Deposit Chemistry of POSF 2747 and POSF 2827 Fuels

2.1 Analysis of Additives

The paper attached as appendix A is a presentation of the method development for analysis of additives. Real fuel used to test the effect of additives must be additive free. Anomolous behavior of a fuel during thermal stress may promote suspicion that the fuel contains additives or an additive in addition to those known to be in the fuel. The methanol extraction - heptane back extraction described in the experimental section of appendix A is applicable to concentration and identification of a wide range of additives from fuels. Aliphatic and aromatic amine and hindered phenol antioxidants, amine or imine metal deactivators and alkoxy ethanol deicers can all be isolated and analyzed by gas chromatography-mass spectrometry. We have developed a library of 70eV mass spectra for 30-40 such compounds on disc for use at WL/POSF. Extraction and GC-MS will allow identification of most additives, either by library search or spectral interpretation. Antioxidants including 4,4'-Methylenebis-(2,6-di-tert-butylphenol)a (M.W. 425) have been extracted and identified without interference.

Precise quantitative analysis of an additive should be by the selected ion monitoring (SIM) mode of the mass spectrometer. The compound is extracted and identified by operating the MS in the scan mode, then an appropriate internal standard is selected, added to the fuel and a quantitative extraction is done for SIM analysis.

2.2 Oxidation Parameters with the Flask Test

The flask test is intended as a highly accelerated model for bulk fuel oxidation for the study of oxidation products and processes of fuels. The most serious objection to the use of the flask test for these purposes is that the mechanism of oxidation can be oxygen concentration dependent. The validity of using flowing oxygen for stress of the surrogate fuel was investigated by stressing the surrogate fuel at 175C with and without flowing oxygen. 100 mL. samples were contained in 250 mL. flasks. One sample was saturated with oxygen for thirty minutes prior to heating and the oxygen flow stopped when heating was begun. The second sample was purged with nitrogen until temperature was

attained and then sparged with oxygen at 100 mL/min. for the duration of the experiment. Ten mL. samples of the stressed fuels were collected from the surrogate supplied with oxygen at four and eight hours. Samples of the surrogate not supplied with oxygen were collected at intervals when discoloration indicated about the same extent of degradation as when samples were collected from the oxygenated sample. These intervals were; 22, 46 and 78 hours. The collected samples were extracted with methanol and the methanol extracts were back extracted with hexane, as per the method described in appendix A. The extracts were then analyzed by GC-MS. The results are shown in figures 1a and 1b. Figure 1a is a comparison of a chromatogram of the surrogate fuel stressed for 4 hours with flowing oxygen and a chromatogram of surrogate stressed for 22 hours without flowing oxygen. The chromatograms suggest that different oxidation products are formed under the different conditions. However when chromatograms of the surrogate stressed for 78 hours without oxygen and 8 hours with flowing oxygen (figure 1b) are compared, they are essentially identical.

The flask test, with flowing oxygen, does represent a valid and greatly accelerated method to observe thermal oxidative chemistry and deposit formation for fuel which behave similarly to the surrogate. From other experience, pure organic compounds such as hexadecane, and the fuels JP-TS, JP-7 and POSF 2747 (Sun Super K-1) behave very much like the surrogate fuel. We have begun to apply the term "oxidizable" for this class of fuels. They smoothly form a wide variety of oxidation products and form a dark gum when highly stressed. Essentially all of the gum is acetone soluble. Other fuels, such as POSF 2827 or a blend of hexadecane, methylnapthalene and tetralin, form deposits very rapidly, without a great deal of oxygen uptake. The deposits are crystalline, rather than gummy and substantial amounts of the deposits are acetone insoluble. These observations are discussed in detail in section 2.4 of this report.

Oxidation of the surrogate fuel is dependent on oxygen flow but does not seem to involve an induction period. Figure 2 shows carbonyl and alcohol oxidation products vs. oxygen flow. The sum of the products increases with increased oxygen flow but the rate of increase drops at about 75 mL/minute. The rate decrease is probably due to the physical nature of the 0.54 mM capillary tube oxygen feed and is the result of surface area and rate of diffusion of the oxygen.

2.3 Deposit Chemistry of a Surrogate JP-8 Fuel

Appendix B contains a discussion of the oxidation chemistry of the surrogate fuel, followed by the separation and identification of oxidation products from the surrogate when subjected to thermal-oxidative stress by the flask test. In early stages of oxidation, the predominant products are

predictable. They result from the reaction of strained ring systems (cyclooctane) and hydrogen alpha to an aromatic ring (xylene, butylbenzene, tetramethylbenzene, tetralin and methylnapthalene). As oxidation progresses, the concentration of secondary alkylalcohols and ketones as well as substituted furanones increase. Identification of oxidation products of the surrogate fuel is found in figure 3 of appendix B. The 5-substituted-dihydro-2-furanones must arise from a somewhat complex mechanism of alkane oxidation that should be investigated further.

Figures 3a and 3b of this report represent oxidation products of the surrogate fuel after 22 and 78 hours stress at 75C, without oxygen feed. These, with 46 hour product data that is not shown, depict the changes in soluble oxidation products with time. Product identification is given in Table 1. Some products, such as benzaldehyde and 3-methylbenzaldehyde disappear at longer stress times and no straight forward more oxidized product (benzoic acid, m-toluic acid) is found after longer stress. Other cases show expected sequences: Cyclooctanol and cyclooctanone are formed from cyclooctane; 1,2,3,4-tetrahydro-1-naphthaleneol and 3,4-dihydro-1(2H)-naphthaleneone are formed from 1,2,3,4-tetrahydronaphthalene. (tetralol and alpha-tetralone from tetralin) For both of these sets of compounds, the alcohols (cyclooctanol and tetralol) and the ketones (cyclooctanone and tetralone) are quite evident at 22 hrs. stress but the alcohol concentrations greatly increased at 78 hrs. stress. The same is true for the butylbenzene, 1-phenyl-1-butanol, 1-phenyl-1-butanone series. In none of these cases is there a detectable lower concentration of the parent hydrocarbon, even after 78 hrs. stress. This suggests that the oxidation proceeds rapidly while the fuel is oxygen saturated, but as oxygen is depleted and is not readily replaced, only partially oxidized compounds are subject to more complete oxidation. The study of soluble oxidation products requires isolation and concentration but is fairly straight forward. Conjecture as to the relationship of the soluble oxidation products and insoluble deposits is not so straight forward. Soluble oxidized species can remain soluble and build up in fuel, be incorporated into deposits or be further oxidized. The true nature of deposits can probably only be learned from analysis of the deposits themselves.

Analysis of deposits is complicated by the nature of the deposits. Untreated deposits consist primarily of adsorbed fuel components which interfere with analysis of the deposit matrix. Fuel components can be removed by extensive extractions with hexane or petroleum ether and drying but this leaves the fundamental question of the nature of the deposit being changed by drying, no matter how gentle. We can only assume that the deposit matrix is unchanged and proceed. A large portion of most deposits is acetone soluble. Attempts to separate the components of the deposit

by gas chromatography, with cool, on column injection result in broad humps, with no separation.

Better separation was observed when injecting the acetone solution into a 300C splitless injection port. Because of this observation we experimented with thermal desorbtion of solid deposits from a 2 x 20 mM quartz tube in a "Pyroprobe 1000" pyrolysis accessory. A great deal of the solid deposit is released by thermal desorbtion at 280C and is cromatographically separated to discrete compounds. This indicates that weak forces bond much of the deposit. Deposits are not covalently bonded polymers. This is discussed in Appendix B and figure 4 is an additional chromatogram of thermally desorbed acetone soluble deposit from the surrogate fuel. The chromatogram in figure 4 is very much like figure 5 in appendix B. The difference is that the deposit that produced figure 5, appendix B contained a very large amount of hexadecane. The deposit that produced figure 4 has had more thorough extraction with non-polar solvents. There are nearly two hundred peaks in the chromatogram. Some of these contain co-eluting compounds. The dominant peak (between 57 and 59 minutes R.T.) is 1,3-isobenzofurandione (phthalic anhydride). The second very large peak (at 55.5 minutes R.T.) is 2,3-dihydro-1H-Indene-1-one. The next to last large peak (69.7 minute R.T.) is 5,6-dimethyl-1,3-isobenzofurandione. The phthalic anhydrides are a very substantial portion of the deposit from surrogate fuel. We believe that the anhydrides were present in the deposit and not thermally formed from the acids at the desorbtion temperature. The conditions of thermal desorbtion and chromatography would have indicated water if it had been the co-product of anhydride formation. It is possible that phthalate esters present in the deposit were thermally decomposed but it is expected that representative esters would have survived thermolysis to be detected.

Other components are alkenes, alkanes and dienes from C_4 to C_{16}, alcohols, aldehydes and ketones to about C_{12}, carboxylic acids from acetic to hexanoic, phenols and substituted furanones. At present, the best assumption is that the deposit is simply an aggregate of the observed components in the solid state because pyrolysis of the surrogate deposit at 550C detects essentially the same components, in lesser amounts, as the thermal desorbtion. This is shown in figure 5, with peak identification in Table 3. Final pyrolysis, at 950C, yields C_4 through C_{10} in small amounts, with much larger amounts (declining with molecular weight) of benzene, toluene, xylenes, C_3 and C_4 benzenes, naphthalene, methyl naphthalene, naphthaleneol and methylnaphthalenols. The total ion chromatogram in figure 6 and Table 4 is peak identification. Although aromatic compounds will be formed from normal hydrocarbons by pyrolysis, the much higher abundance of the aromatics in the chromatogram indicates that most of the remaining portion of the deposit is aromatic.

2.4 Deposit Chemistry of POSF 2747 and POSF 2827 Fuels

These two fuels have been extensively used as reference fuels by a number of investigators working with the WPAFB Fuel Laboratory. POSF 2747 is a highly refined, hydrotreated fuel and POSF 2827 is an apparently representative Jet-A fuel. Both fuels are 19% aromatic. POSF 2827 is reported to have 0.1% total weight percent sulfur; POSF 2747 has 0.0% sulfur. Table 5 is a summary of results of standard tests for the two fuels. The behavior of these fuels under thermal stress is very different. POSF 2827 forms dark, crystalline solids very rapidly (under 1 hr.) The solids appear as a "floc" suspended in the fuel, which will settle and is not glass adherent. The term "crystalline", above, is used comparatively to the deposits formed by POSF 2747. This fuel produces deposits only with more extreme stress. After heating at 175C for 4 hrs., with flowing oxygen, POSF 2747 forms visible deposits that are very gummy and glass adherent. The deposits from POSF 2747 are essentially completely soluble in acetone. Over one third of the POSF 2827 is acetone insoluble. This portion of the sample will not melt, but decomposes from the solid while the POSF 2747 deposit melts over a wide range beginning about 90C. Observations of the deposits are summarized in Table 6.

Because of the different nature of the deposits from these fuels, they were subjected to the flask test at 175C, without flowing oxygen. Both fuels were sparged with oxygen for 30 minutes at room temperature, the oxygen flow stopped and then rapidly heated to 175C. The start time was taken as the time temperature was attained. Visible solids were observed in the POSF 2827 after 2 hrs. and the accumulation increased for the 46 hour duration of the test. The POSF 2747 was not visibly discolored for 8 hours and no deposits were observed for the duration of the test. After the test was stopped, the flasks were allowed to cool to room temperature prior to filtering. A gummy deposit then formed in the flask containing 2747. The total insoluble gum plus solids for the fuels was: POSF 2747, 0.060 g., 0.04%; and POSF 2827, 0.190 grams, 0.13%. The conclusion is that POSF 2747 must have oxygen to form significant deposits but POSF 2827 will form significant amounts of deposit with no more than original saturation level of oxygen.

These observations were in line with previous work in which F.T.I.R. was used to determine the extent of oxidation of fuels. (Final Report: Subcontract RI-70791X, prime contract F33615-87-C-2714). In this work we found "good fuels" such as POSF 2747, JP-7 and JP-TS produced a higher concentration of oxidized species (as carbonyl compounds and alcohols) than fuels that produced more deposits. Table 7 is a summary of such results for various fuels. The same observations were made by the UDRI and SWRI groups at about the same time. Although these observations mean that we

cannot use any measure of oxidation as a predictor for deposit formation they suggest that it may be possible to isolate the cause of excessive deposit formation.

Chromatograms of 2747 and 2827 fuels show only that 2827 has a much wider range of components. Figures 7a and b are total ion chromatograms of the unstressed fuels. It can be seen that 2827 has "marker" normal hydrocarbons from octane through hexadecane while the 2747 contains a range only from decane to tetradecane. Methanol extraction of these fuels will concentrate the aromatic hydrocarbon and more polar compounds. Figure 8a and b are total ion chromatograms of methanol extractions of the fuels. The only obvious difference is that 2827 has a much higher concentration of di- and tri-methylnaphthalenes than 2747. All chromatographic peaks that give sufficient mass spectral lines for identification were examined and no known catalysts, inhibitors or sulfur compounds could be identified.

In an effort to understand the course of oxidation and deposit formation, these two fuels were subjected to thermal stress by a modified flask test, with a Dean-Staerk trap between the stress flask and the condenser. The trap will collect volatile products. In 8 hours stress at 175C POSF 2827 produced 4.0 mL of volatile material in a single phase. This phase consisted exclusively of unoxidized fuel components. At the same time, 2747 produced 9.0 mL of volatiles of which 3.5 mL was a lower, separate phase. The upper phase consisted extensively of fuel components but also contained oxidation products. These included alcohols, aldehydes, ketones and carboxylic acids. The lower, very polar phase, contained predominantly carboxylic acids with the same sort of oxidation products as found in the upper phase. The distribution of the oxidation products is simply a function of the distribution coefficient of the compound for the phases. Figure 9 is the total ion chromatogram of a representative polar phase produced by POSF 2747. The large ramp shaped peaks are the carboxylic acids (compounds identified in Table 8) and are at least 100 times as concentrated as the minor components in this phase.

Oxidation products can very efficiently be extracted from stressed fuels with silica gel. Twenty mL. of stressed fuel is passed through a 1.0 gram silica gel solid phase extraction cartridge that has been conditioned with petroleum ether. The cartridge is then washed three times with 2.0 mL of pet ether and excess pet ether expelled with pumping 80-100 mL of air through the cartridge with a syringe. The oxidized products are eluted from the sorbent with methanol. The first 0.3-0.5 mL of methanol is discarded. The following 0.5-1.0 mL of methanol will contain the oxidized species, with very little contamination from aromatic fuel components. Figure 10 and Figure 11 are chromatograms of soluble

oxidation products of POSF 2827 and 2747, respectively, that have been extracted by this procedure. Table 9 is the compound identification for figure 10 and table 10 is the compound identification for figure 11.

The difference in the range and classes of compounds is striking. The soluble oxidation product extract of 2827 is high in phenols and furanone derivatives. The extract of 2747 is high in alkenes and furanone derivatives. The carboxylic acids found in the polar phase from 2747 are not present in the silica gel extract. This may indicate that they have gone into deposits. The obvious question then, is the nature of the relationship of soluble oxidation products to the composition of insoluble gums and solids.

Insoluble gums and solids are isolated from a stressed fuel by filtration with a 0.2 uM. millipore type filter with binder free glass pre-filter or 0.2 uM. metallic silver filter. The silver is expensive but stable to washing and drying. The contents of the stress flask are filtered and the flask is washed 3 times with petroleum ether and the wash filtered. The mass on the filter is then washed another 3 times with 20 mL portion of petroleum ether and dried, with the flask, for 12 hours at 80C and about 6-10 torr in a vacuum oven. The filter and flask are then weighed and the filter repositioned on the holder, the flask washed 3 times with acetone and the washings filtered. The filter is washed with 3 additional 20 mL portions of acetone, redried and reweighed, with the flask. The weighing, with tare weight of flask and filter give total insolubles and solids. Insoluble gum (acetone soluble) is determined by difference. The acetone washings are caught and the insoluble gum is isolated by evaporation under dry nitrogen.

The composition of the deposits can be determined by thermal desorbtion-GC-MS. A small amount of the deposit is loaded into a 2 x 20 mM quartz sample tube and inserted into the platinum coil heater of a pyroprobe 1000™ probe unit. The probe is attached to the interface at room temperature, with the GC oven at room temperature. The oven is then cooled to -50C with liquid nitrogen and the interface heater is turned on to a 280C set point. As soon as the set point is reached, the probe is fired for 100 seconds at the same temperature and the GC-MS turned on. This method gives good resolution of discreet components of the deposits, which are not otherwise chromatographable. Figure 12 is a total ion chromatogram of insoluble gum produced from POSF 2827 and figure 13 is the chromatogram of insoluble gum produced from POSF 2747.

There is probably a degree of thermal rearrangement of deposit compounds involved in this method, but it is the first method that has succeeded in identification of deposit composition. The experiments are difficult and tedious due

to the need for a trial and error approach to determine what amount of different deposits should be loaded to give sufficient spectra for compound identification, but still give good chromatographic resolution. Regardless, more experiments should be done, with lower desorbtion temperatures, to determine what role thermal rearrangement may play in the identity of chromatographed components.

The thermal desorbtion chromatogram of the two fuel deposits are quite consistent with the chromatogram of the soluble oxidation products. The 2827 deposit contains a great many phenols and few alkenes or alcohols. The 2747 deposit contains alcohols and alkenes, with few phenols. Both deposits contain (or yield) furanone derivatives. These must be oxidation products of alkanes (parafins) but it is unclear as to what role they play in deposition if it is not that they are simply polar, fuel insoluble compounds that will aggregate and precipitate.

Thermal desorbtion of deposits can be followed by true pyrolysis of desorbed residue, still in the probe. Pyrolysis of hydrocarbons typically gives alkanes, alkenes, and aromatic compounds. Pyrolysis of the deposits of 2827 and 2747 follows this trend but are very high in aromatics. Pyrolysis at 400 or 500C gives only a very low yield of components after thermal desorbtion. Pyrolysis of the 2827 deposit reflects the composition of the fuel in that there are more high molecular weight aromatic compounds than given by 2747 deposits under the same conditions. In addition many of the substituted phenyls detected by thermal desorbtion of 2827 deposits survive the pyrolysis and are identifiable in the chromatogram.

From the information obtained by GC-MS of soluble oxidation products and deposits the nature of deposits can be speculated upon. The deposits from fuels such as the surrogate and 2747 seem to form deposits that are largely simply mixed, very polar species, with probably some peroxide cross linking that produces a varnish like deposit upon drying. This type of deposit would be vastly alleviated by the use of a proper detergent.

Fuels such as the 2827 have deposits of a different nature. They seem to be more strongly bonded into a solid phase. Neither type of deposit gives the carbon dioxide production in thermal desorbtion or pyrolysis that would indicate that esterification is important to deposition. The compounds produced from deposits of 2827 do indicate that a hemiketal type of bonding [R'OH + RCOR ---> R-O-CH(OR')R]may be responsible for the nature of the deposit. Phenols strongly interacting with carbonyls from aldehydes, ketones (or the furanones) would form a real, reversible, covalent bond to result in an increase in molecular weight and polarity to produce components of deposits. A combination of

experiments with high resolution infra-red spectroscopy on deposits and heated deposits and GC-MS of thermal desorbtion at lower temperature should prove if this hypothesis is correct.

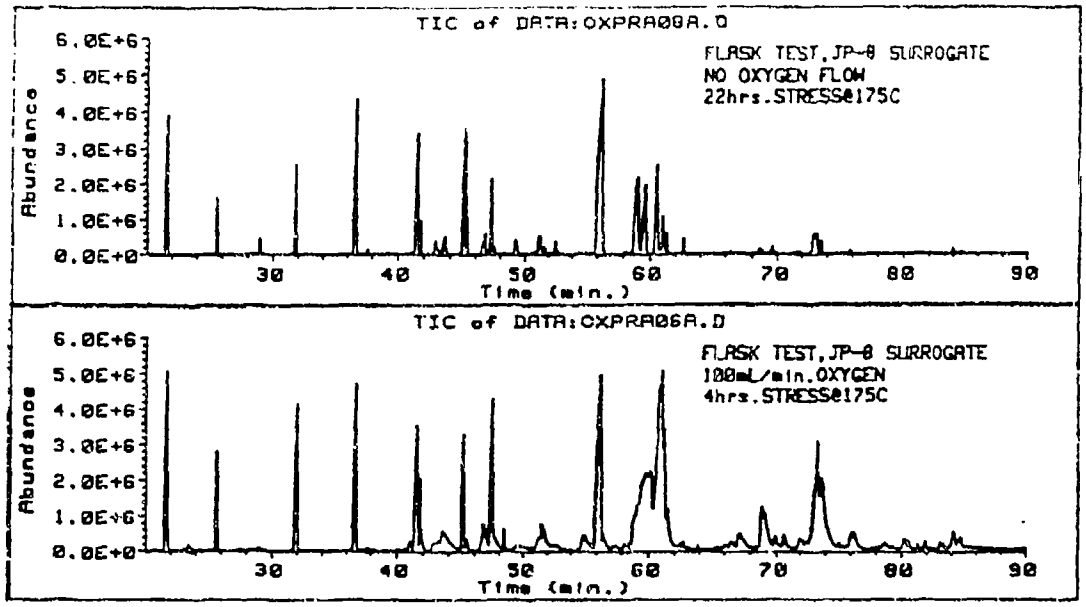

Figure 1a: Comparison of Total Ion Chromatograms of Methanol Extracts of Stressed Surrogate of JP-8 Fuel With and without Flowing Oxygen. Upper Chromatogram; 22 hrs. Stress at 175C without Flowing Oxygen. Lower Chromatogram; 4 hrs. Stress with 100 mL/minute Oxygen Flow.

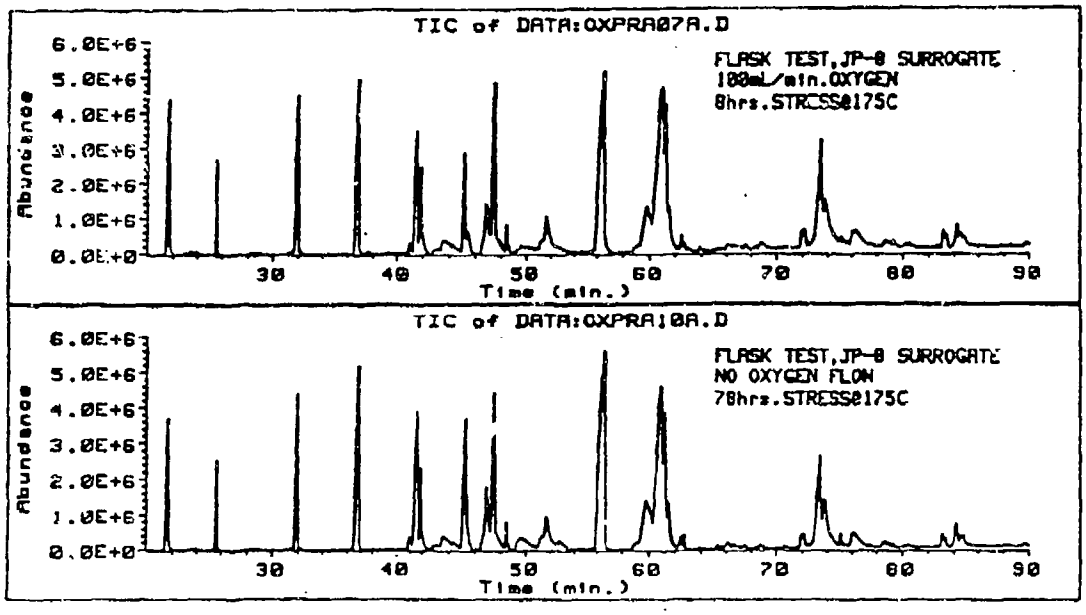

Figure 1b: Comparison of Methanol Extracts of Stressed Surrogate JP-8 Fuel with and without Flowing Oxygen. Upper Chromatogram; 8 hrs. Stress at 175C with 100 mL/min. Oxygen Flow. Lower Chromatogram; 78 hrs. Stress without Flowing Oxygen.

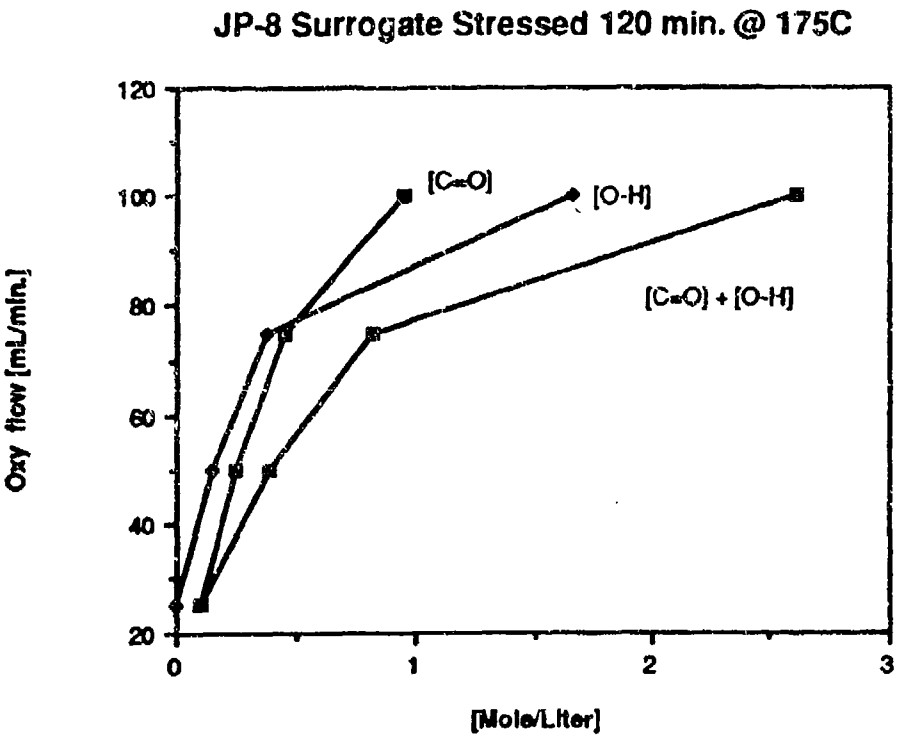

Figure 2: Soluble Oxidation Product Concentration vs. Oxygen Flow for Surrogate JP-8 Fuel. Carbonyl Concentration as 2-Octanone, Alcohol Concentration as 1-Dodecanonol, by FTIR with Horizontal Attenuated Total Reflectance Sampling.

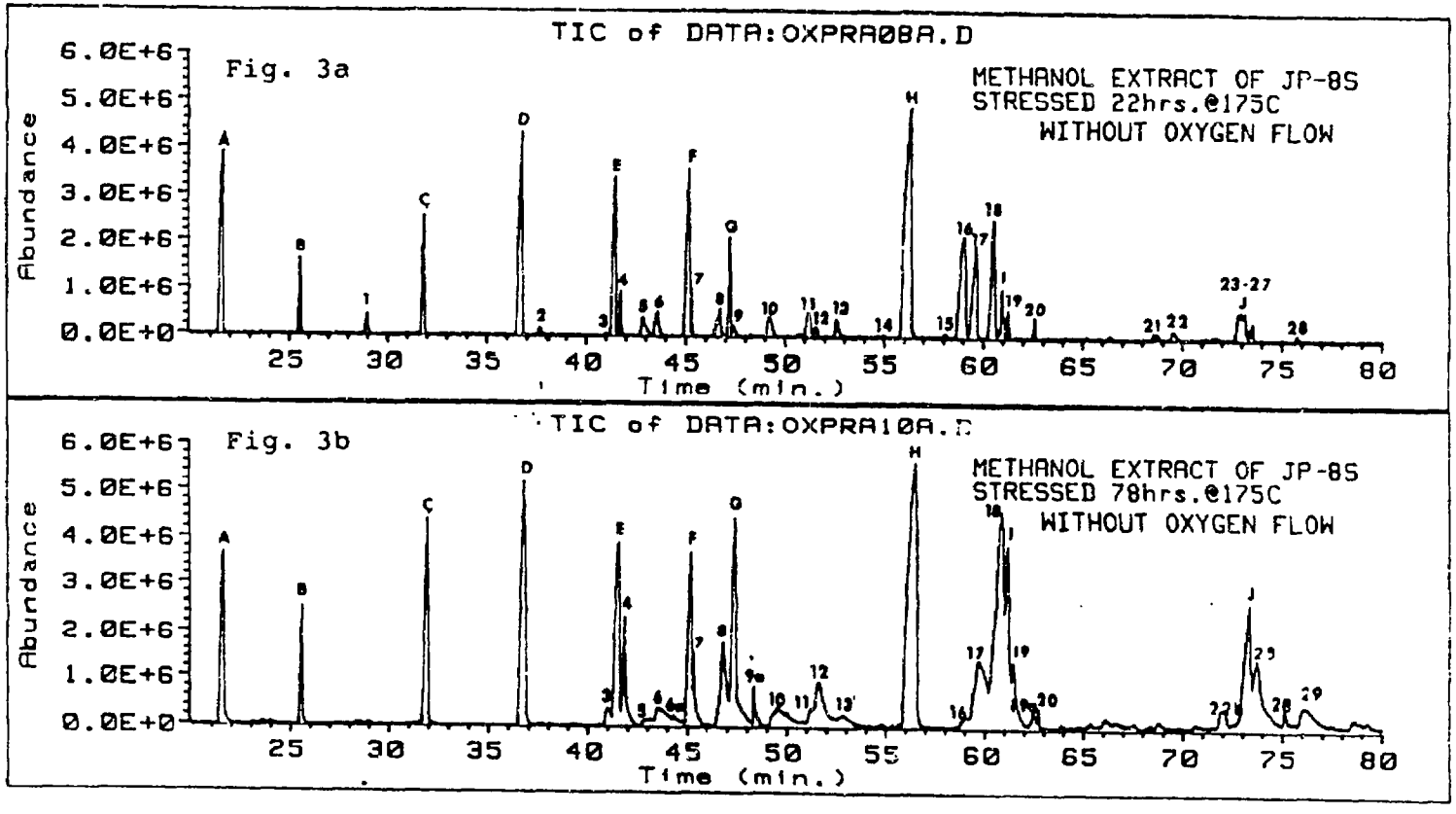

Figure 3a & 3b: Total Ion Chromatograms of Oxidation Products of JP-8 Surrogate Fuel Stressed for 22 and 78 hrs. at 175 C without oxygen sparge. Samples extracted with methanol, back-extracted with hexane.

Table 1: Identification of Chromatographic Peaks for Figure 3a and 3b. (Lettered peaks are surrogate fuel components, numbered peaks are oxidation products; oxidation products in fig. 3b that are not in fig. 3a have suffix "a" after letter.)

Peak #	R.T.(min)	Compound
A	21.61	m-xylene
B	25.55	cyclooctane
1	28.97	benzaldehyde
C	31.86	n-decane
D	36.78	n-butylbenzene
2	37.65	3-methylbenzaldehyde
3	40.95	alpha-methoxy-benzene acetic acid
E	41.51	1,2,4,5-tetramethylbenzene
4	41.75	cyclooctanone
5	42.85	?,?-dimethylphenol
6	43.60	cyclooctanol
F	45.19	1,2,3,4-tetrahydronaphthalene
7	45.29	1,1a,6,6a-tetrahydro-cycloprop[a]indene or 1,2-dihydronaphthalene
8	46.72	1-methylene-1H-Indene or naphthalene
G	47.25	n-dodecane
9	47.42	2-nonanol?
10	49.24	2-propylphenol
11	51.23	alpha-propylbenzenemethanol
12	51.56	1-phenyl-1-butanone
13	52.62	2,4,5-trimethylphenol
14	54.98	sec. alcohol
H	56.39	1-methylnaphthalene
15	58.10	diethylphenol
16	59.08	1,2,3,4-tetrahydro-1-naphthalenol
17	59.66	2,4,5-trimethyl benzenemethanol
18	60.57	3,4-dihydro-1(2H)-naphthalenone
I	60.98	n-tetradecane
19	61.26	2-dodecanol
20	62.61	dimethylphthalate?
21	68.75	1-naphthalencarboxaldehyde?
22	69.56	benzene butanoic acid
23	71.77	1,2,3,4-tetrahydro-1,2-naphthalenediol
24	72.84	1-hydroxymethylnaphthalene
25	72.97	sec. alcohol
J	73.25	hexadecane
26	73.49	1,4-dihydro-1,4-methanonaphthalene-9-ol
27	73.51	sec. tetradecanol
28	75.12	subst. naphthalene
29	75.80	dimethylbenzofuranone
6a	44.31	mixed spectra, a pyran?
9a	48.39	subst. phenol
19a	62.45	subst. 1,2,3,4-tetrahydroquinoline
22a	72.06	C-12 ketone

Table 1 - con't.

27	73.51	sec. tetradecanol
28	75.12	subst. naphthalene
29	75.80	dimethylbenzofuranone
6a	44.31	mixed spectra, a pyran?
9a	48.39	subst. phenol
19a	62.45	subst. 1,2,3,4-tetrahydroquinoline
22a	72.06	C-12 ketone

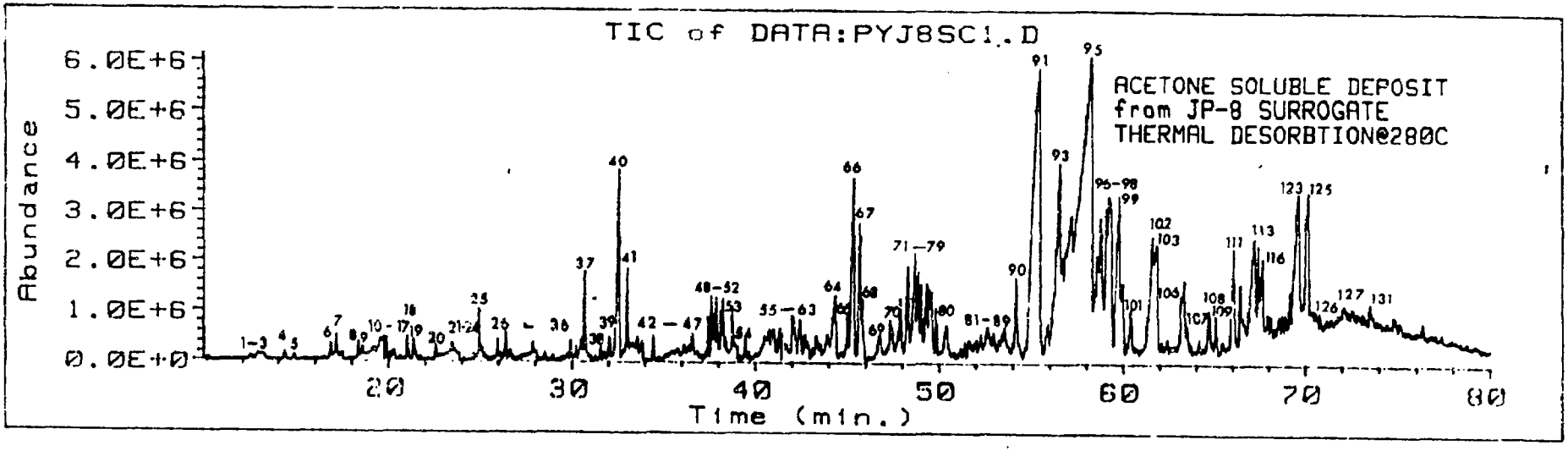

Figure 4: Total Ion Chromatogram from thermal desorbtion of acetone soluble residue from JP-8S stressed 48 hrs. at 175C. 100 second thermal desorbtion at 280C.

Table 2: Peak identification for total ion chromatogram of figure 4. (Thermal desorbtion of acetone soluble deposit from JP-8S at 280C)

Peak #	R.T.	Compound
1.	12.52	1-butene
2.	12.78	butane
3.	13.09	butadiene
4.	14.34	1,3-pentadiene (Z)
5.	14.84	1,3-pentadiene (E)
6.	16.85	1-hexene
7.	17.15	hexane
8.	18.34	1,4-hexadiene
9.	18.57	1,3-hexadiene?
10.	19.19	acetic acid
11.	19.69	acetic acid, mixed with alkene
12.	19.86	benzene
13.	19.87	benzene, mixed alkyls
14.	20.07	methyl pentadiene
15.	20.19	hexatriene
16.	20.31	tetrahydro-2-furanone
17.	20.62	1-propenylcyclopropene
18.	20.99	propycyclopropane
19.	21.35	heptane
20.	22.57	alkyne?
21.	23.33	propanoic acid
22.	23.44	methylcyclohexene?
23.	24.61	C_7 diene
24.	24.74	C_7 diene
25.	24.92	toluene
26.	25.09	dihydrofuranone derivative
27.	25.94	sec. alcohol
28.	26.35	cyclopentanone
29.	26.61	hexanal
30.	27.70	butanoic acid
31.	27.85	diene
32.	28.49	diene
33.	28.92	dihydrofuranone derivative
34.	29.98	sec. alcohol
35.	30.20	xylene
36.	30.52	alkane
37.	30.69	xylene
38.	31.59	heptanol
39.	39.02	styrene
40.	32.57	cyclooctene
41.	33.02	1,4-cyclooctadiene
42.	32.57	hexanoic acid
43.	33.67	dihydrofuranone derivative
44.	34.42	alkene?
45.	35.76	alkene
46.	36.09	methyldihydrofuranone?
47.	36.55	C_{10} alkene
48.	37.43	C_{10} alkene

Table 2 - con't.

49.	37.59	C_{10} alkene
50.	37.63	C_{10} alkene
51.	37.76	phenol
52.	38.22	2-decene
53.	38.75	C_{10} alkene
54.	39.42	alkene?
55.	40.47	alkene?
56.	40.75	alkene?
57.	40.82	alkene?
58.	40.97	propylbenzene
59.	41.30	propynylbenzene
60.	42.02	3,4-dimethyl2,5-furnandione
61.	42.43	1-octanol?
62.	42.69	1-phenylethanone
63.	42.78	?
64.	44.39	4-cycloocteneone
65.	45.04	cyclooctanone?
66.	45.38	tetramethylbenzene
67.	45.63	2-butenylbenzene
68.	45.81	2-ethylcyclohexanone
69.	46.74	5-butyldihydrofuranone
70.	47.34	1-methyl-1H-indene
71.	47.91	bicyclooctanone?
72.	48.31	1,2-dihydronaphthalene
73.	48.62	1-dodecanol
74.	48.89	dodecanol?
75.	49.03	dodecanol?
76.	49.32	dodecanol?
77.	49.46	naphthalene
78.	49.61	naphthalene
79.	49.85	dodecane
80.	50.25	mixed dimethylphenol and alkene
81.	51.16	2,3-dihydro-1,3-dimethyl-1H-indene
82.	51.40	mixed -
83.	51.62	1 ethyl-6-ethylidene cyclohexene
84 to 89.	52.03 to 53.54	mixed spectra, unidentifiable
90.	54.21	2,3,5-trimethylphenol
91.	55.49	2,3-dihydro-1H-indene-1-one
92.	55.90	1,3-isobenzofurandione
93.	56.55	2-methylnaphthalene
94.	57.20	1,3-isobenzofurandione
95.	58.31	1,3-isobenzofurandione
96.	58.58	7-tetradecene
97.	58.80	1H-indene-1,3-2H-dione
98.	59.09	alkane + C_3 benzaldehyde
99.	59.82	methylisobenzofurandione
100.	60.02	3,4-dihydro-1(2H)-naphthaleneone
101.	60.45	3,4-dihydro-2H-1-benzopyrane-2-one
102.	61.63	2H-1-benzyopyran-2-one
103.	61.87	4-methyl-1,3-isobenzofurandione
104.	62.45	1,1'-(1,3-phenelyne) ethanone

Table 2 con't.

105.	63.20	benzopyran-one isomer
106.	63.39	2,2-dimethyl-3,4-dihydro-(2H)-1-benzopyron
107.	64.18	subst. furanone derivative
108.	64.74	subst. benzofuranone
109.	65.10	1,4 naphthalenediol
110.	65.72	?
111.	66.11	1-naphthalenol
112.	66.47	2-naphthalenol
113.	67.251	1,3-benzodioxole 5-(2-propenyl)
114.	67.47	hexadecane
115.	67.59	1-hexadecene
116.	67.69	3,5-methyl-3,4-dihydro-1(2H)-naphthalenone
117.	68.00	alkyl alcohol?
118.	68.13	3,4-dihydro-6-methanolnapthalenone
119.	68.59	?
120.	68.78	5,6-dimethyl isobenzofurandione
121.	69.05	a dimethylisobenzofurandione
122.	69.22	a dimethylisobenzofurandione
123.	69.66	a dimethylisobenzofurandione
124.	70.08	?
125.	70.23	dimethyl-3(2H)-benzofuranone
126.	70.86	
127. to	72.10 to	mixed spectra, unidentifiable
130.	73.16	
131.	73.59	subst. naphthalenol
132.		?

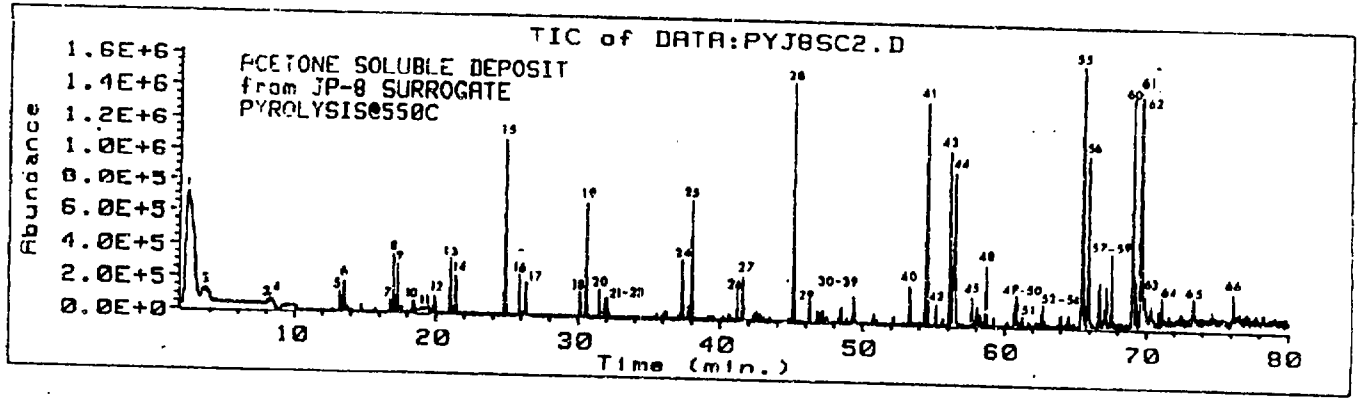

Figure 5: Total Ion Chromatogram from JP-8S fuel stressed 48 hrs. at 175C. 100 second pyrolysis at 550C.

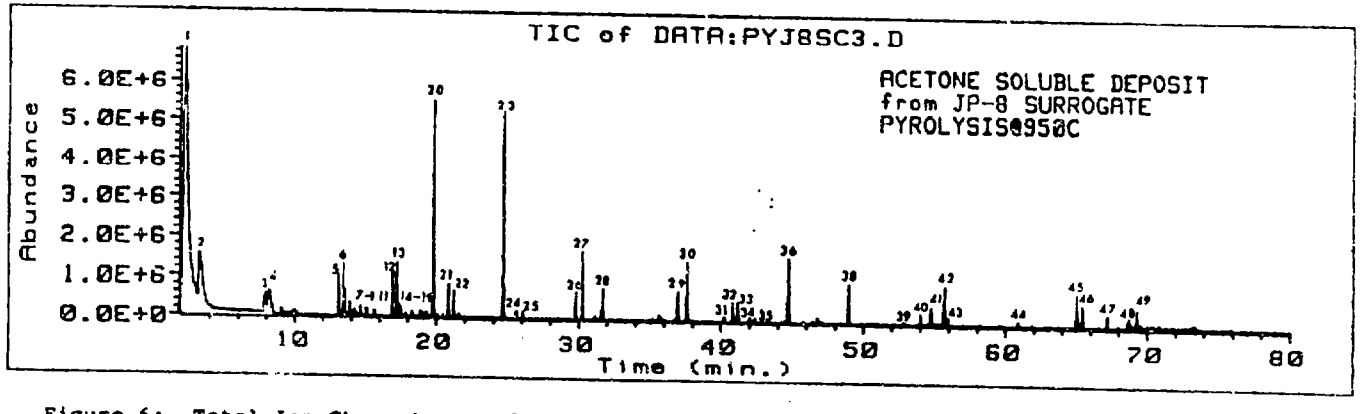

Figure 6: Total Ion Chromatogram from pyrolysis of acetone soluble residue from JP-8S fuel stressed 48 hrs. at 175C. 100 second pyrolysis at 950C.

Table 3: Peak identification for total ion chromatogram of Figure 5. (Pyrolysis of acetone soluble deposit from JP-85 at 550C)

1)	2.85	CO_2 and N_2
2)	3.80	propene
3)	8.36	1-butene
4)	8.51	butane
5)	13.22	pentene
6)	13.53	pentane
7)	16.81	pentadiene
8)	17.02	1-hexene
9)	17.31	hexane
10)	18.45	hexadiene
11)	19.51	nitrogen burp
12)	19.92	benzene
13)	21.03	?
14)	21.39	3-methyl hexane
15)	24.90	toluene
16)	25.90	1-heptene
17)	26.33	heptane
18)	30.15	ethyl benzene
19)	30.60	xylene
20)	31.50	?
21)	31.88	styrene
22)	31.97	C_9-alkane
23)	32.04	xylene
24)	37.34	phenol
25)	38.00	1,2,4-trimethylbenzene
26)	41.23	1-propynyl benzene
27)	41.59	2-methyl phenol
28)	45.15	1,2,3,5 tetramethyl benzene
29)	46.26	?
30)	46.84	
31)	47.19	1-methyl-1H-indene
32)	48.52	?
33)	49.38	
34)	49.38	napthalene
35)	49.52	C_8 benzene
36)	50.78	propyl phenol
37)	51.04	C_5 benyzene
38)	52.20	subst. furanone
39)	52.91	subst. furanone
40)	53.32	2-ethyl-5-methylphenol
41)	54.56	2,3-dihydro-1H-indene-1-one
42)	55.17	2-methyl naphthalene
43)	56.15	2-methyl naphthalene
44)	56.53	1,2-benzenedicarboxylic acid
45)	57.69	1H-indene-1,3(2H)-dione
46)	58.07	1-(3H)-isobenzofuranone
47)	58.31	?
48)	58.72	1-(2,5-dimethylphenyl)-ethanone

Table 3 con't.

49)	60.72	1-(2H)-naphthalenone
50)	60.88	4-methyl-1,2-benzenedicarboxylic acid
51)	61.28	1,2-dimethyl naphthalene
52)	62.71	4-dihydro-2,2-dimethyl 2H-1-benzopypran ?
53)	64.01	
54)	64.53	thyl-1,2,3,4-tetrahydro naphthalene ?
55)	65.56	ththalenol
56)	65.94	-phenyl furan
57)	66.73	5-(2-propenyl)-1,3-benzodioxole ?
58)	67.21	7-methyl, 2H-1-benzopyran-2-one
59)	67.59	2-methyl-1-naphthalenol
60)	69.16	5,6-dimethyl-1,3-isobenzofurandione
61)	69.33	2-methyl-1-naphthalenol
62)	69.66	3-methyl-1-naphthalenol
63)	70.35	?
64)	71.16	5,7-dimethyl-1-naphthalenol
65)	73.40	?
66)	76.21	?

Table 4: Peak identification for total ion chromatogram of Figure 6 (Pyrolysis of acetone soluble deposit from JP-8S at 950C)

Peak	Ret.Time	Compound
1.	2.18	nitrogen, CO_2
2.	3.37	propene
3.	7.92	1-butene
4.	8.21	butane
5.	13.14	1-pentene
6.	13.47	pentane
7.	13.59	2-propanone
8.	14.26	2-methyl-1-butene
9.	14.43	1,1-dimethylcyclopropane
10.	14.69	1,3-pentadiene
11.	15.14	1,3-cyclopentadiene
12.	15.97	1-hexene
13.	17.25	hexane
14.	17.37	2-butanone
15.	17.54	2-hexene
16.	18.34	1,4-hexadiene
17.	18.92	1,3,5-hexatriene
18.	19.11	
19.	19.34	3-methyl-1,3-pentaliene
20.	19.84	benzene
21.	20.89	1-heptene
22.	21.24	heptane
23.	24.76	toluene
24.	25.66	1-octene
25.	26.06	octane
26.	29.84	ethylbenzene
27.	30.31	m & p-xylene
28.	31.74	o-xylene
29.	36.98	phenol
30.	37.65	1,3,5-trimethylbenzene
31.	40.26	benzeneethanol, beta-ethenyl (1-phenyl-2-hydroxy-3-butene)
32.	40.86	1-propynyl benzene or 1 H-Indene
33.	41.19	2-methylphenol
34.	42.02	1-phenylethanone (methylphenyketone)
35.	42.38	3-methylphenol
36.	44.75	1,2,3,5-tetramethylbenzene
37.	46.77	3-methyl-1H-Indene
38.	48.98	naphthalene
39.	52.83	2-ethyl-5-methylphenol
40.	54.01	2,3-dihydro-1H-Inden-1-one
41.	54.75	1-methyl-naphthalene
42.	55.71	2-methyl-naphthalene
43.	55.92	1,3-Isobenzofurandione
44.	60.86	1,4-dimethylnaphthalene
45.	65.02	1-naphthalenol
46.	65.43	3-phenyl furan
47.	67.19	2-methyl-1-naphthalenol
48.	68.70	3-methyl-1-naphthalenol
49.	69.25	4-methyl-1-naphthalenol

Table 5: Comparison of Analysis for POSF 2747 and POSF 2827 Fuels. (Data from SA-ALC/SFTLA, WPAFB, OH 45433-6503)

ASTM#	Test	Results POSF 2747	POSF 2827
D3242	Total Acid Number, mg KOH/g	0.0	0.001
D1319	Aromatics, Vol %	19	19
D3227	Mercaptan Sulfur, Wt %	0.000	0.001
D4294	Sulfur, Total Wt %	0.0	0.1
D 93	Flash Point, Deg C	60.0	50.0
D1298	Specific Gravity, 15.6/15.6 Deg C	0.8076	0.8072
D2386	Freezing Point, Deg C	-60	-43
D 445	Viscosity @ -20 Deg C, cs	4	5
D1322	Smoke Point, mm	22	24
D 130	Copper Strip Corrosion	1	1
D3241	Thermal Stability @ 260 Deg C DELTA P, mm	0	0
D 381	Existent Gum, mg/100 ml	0	1
D1094	Water Reaction Interface	1	0
D2624	Fuel Electrical Conductivity, pS/m	230	183
D5327	Fuel System Icing Inhibitor, Vol %	0.00	0.00

Table 6: Comparison of Deposits Produced by POSF 2747 and 2827 Fuels in Flask Tests at 175C and 100 mL/min Oxygen Flow

	POSF 2747		POSF 2827	
Mass of Deposit	2.849 g		0.904 g	
Wt % of Fuel	1.81%		0.57%	
Time for visible deposit	over 2 hrs.		less than 30 mins	
physical nature	brown, adherent gum		dark brown, non-adherent solid	
Gums and Solids(1)	insoluble gum	solid	insoluble gum	solids
Mass	2.813 g	0.036 g	0.584 g	0.320 g
wt. % of fuel	1.78%	0.023%	0.37%	0.203%
Melting point(C)	90 onset	183 onset	147 onset	doesn't melt

(1) Total deposit given above divided on basis of solubility. Insoluble Gum defined as acetone soluble portion of total deposit; Solids defined as acetone insolbule fraction.

Table 7. Analysis of Oxidation Products of Various Fuels by FT-IR[1]

Fuel	JP-8S	JP-8 (UN 1863)	JP-8 POSF 2813	JP-8 POSF 2814	Super K-1 POSF 2747	JP-7	JP-TS
	Concentrations of Alcohol (As 1-dodecanol) and ketone (As 2-octanone), moles/liter						
Stress time							
30 min	0.018;0.012	0.008;0.021	0.000;0.005	0.998;0.560	1.173;0.355	0.219;0.131	0.021;0.066
60	0.054;0.026	0.009;0.008	0.014;0.007	1.171;0.637	1.267;0.406	0.427;0.219	0.099;0.091
90	0.145;0.056	0.011;0.008	0.018;0.010	1.177;0.783	1.320;0.465	0.492;0.315	0.132;0.177
120	0.352;0.253	0.029;0.020	0.022;0.013	1.142;0.875	1.140;0.636	1.853;0.588	0.312;0.278
Wt. insol @ 120 min.[2]	38.3 mg	34.8 mg	18.0 mg	12.5 mg	13.7 mg	10.0 mg	0.1 mg
Visual	Lt. Brown	Lt. Yellow fine particulates	Lt. Yellow fine particulates	Yellow	Yellow	Lt. Yellow	Lightest Yellow

(1) 100 mL of each fuel stressed at 175°C with 100 mL/min flowing oxygen in flask test.

(2) Sediment from 10 mL sample after hexane wash and drying, 5 torr, 80°C.

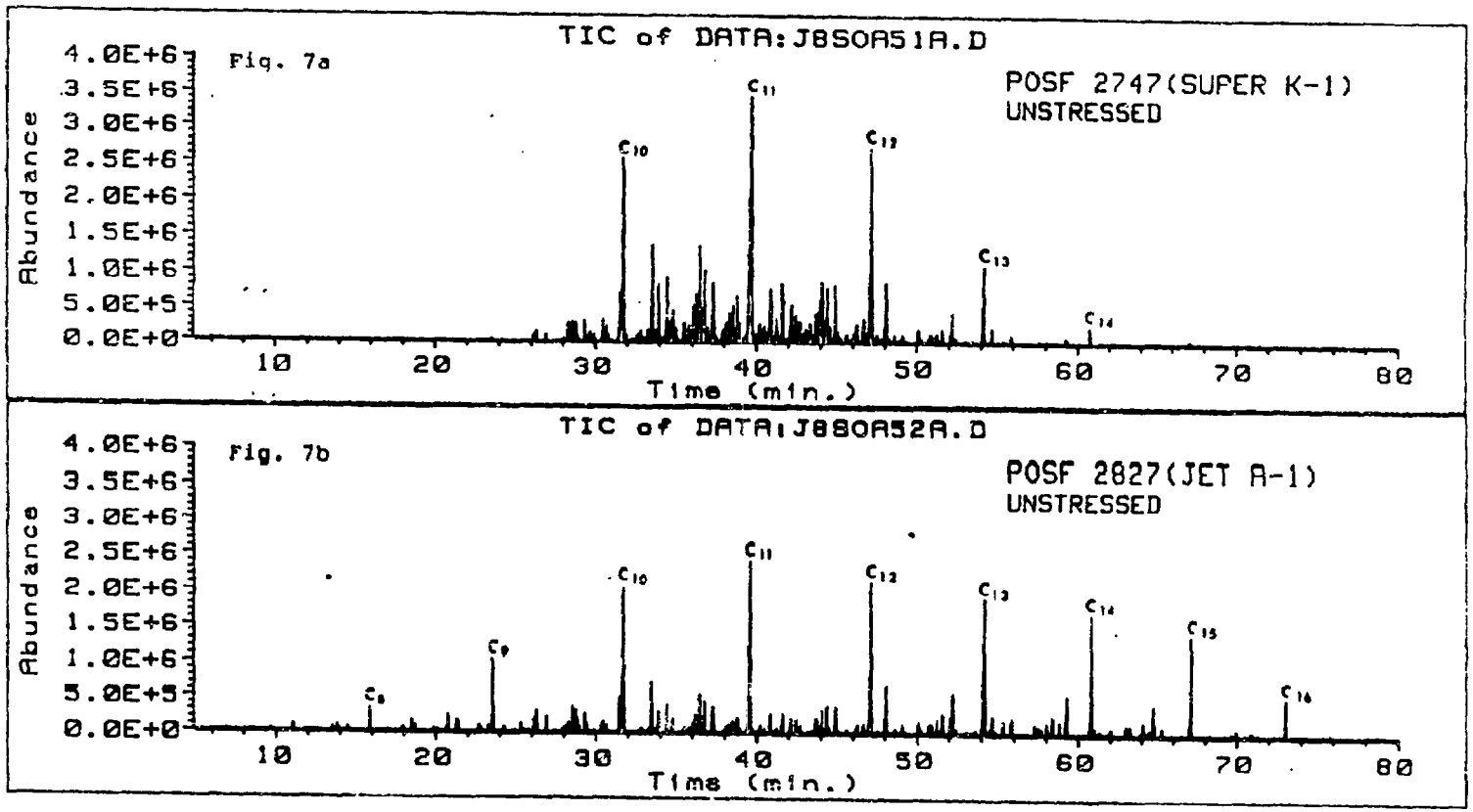

Figure 7a & b: Comparison of Total Ion Chromatograms of POSF 2747 and POSF 2827 Fuels. Normal Alkanes are labeled by carbon number.

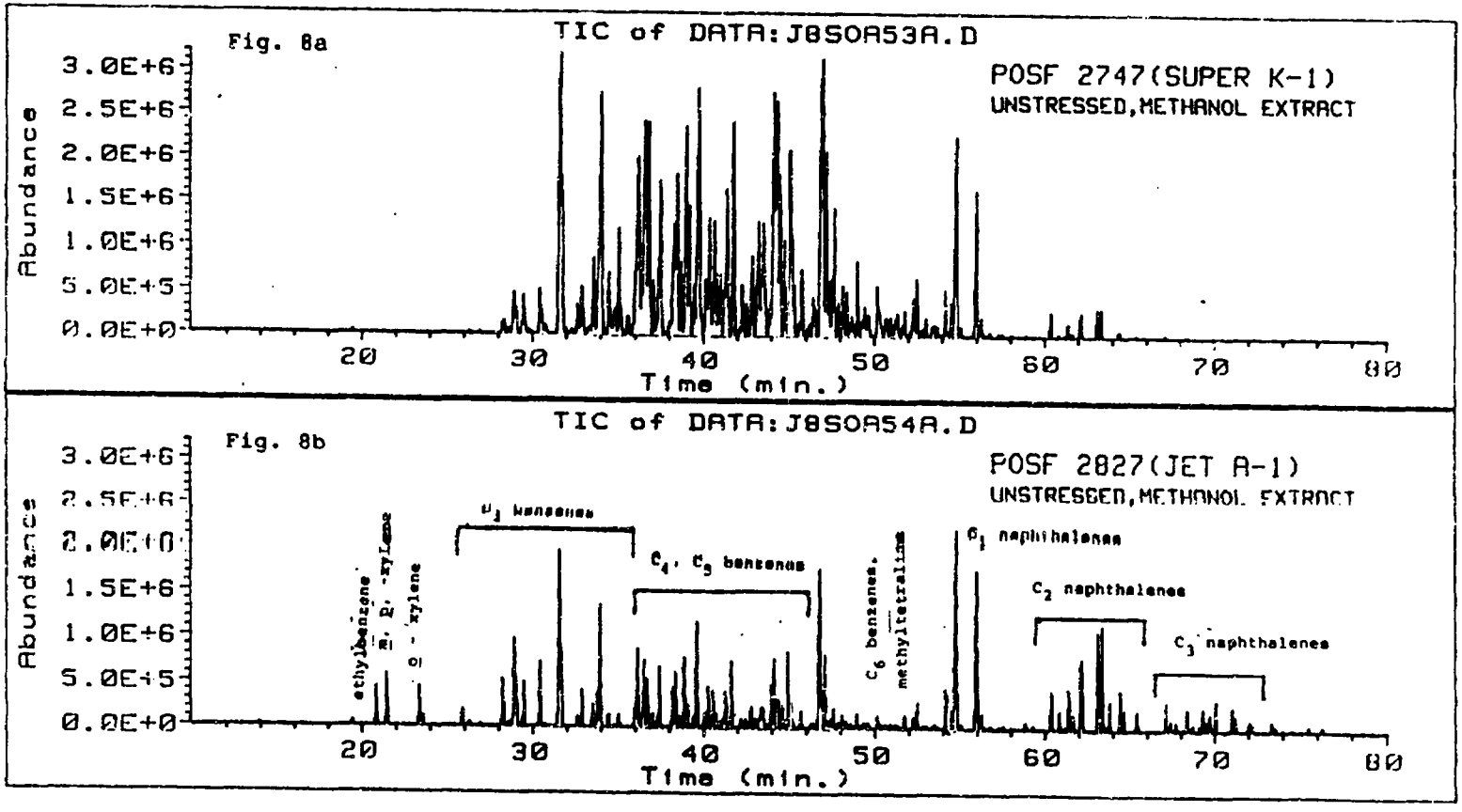

Figure 8a & b: Total Ion Chromatograms of Methanol Extracts of POSF 2747 and POSF 2827 Fuels. Identification of aromatic series given on Fig. 8b pertains to both chromatograms.

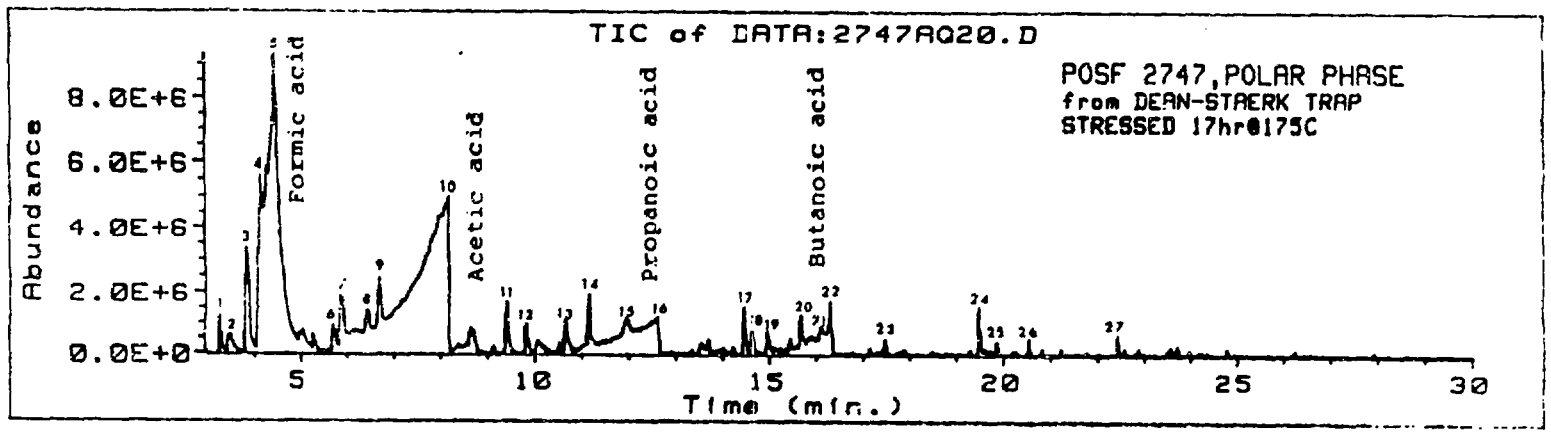

Figure 9: Total Ion Chromatogram of Polar Phase of Oxidation Products formed by Fuel POSF 2747, Stressed 17 hrs. at 175C. Large, ramp shaped peaks are carboxylic acids as identified on chromatogram.

Table 8: Peak Identification of Compounds from Figure 9: (Chromatogram of Polar Phase formed by POSF 2747)

Peak#	R.T. (min)	ID
1.	3.26	methyl formate
2.	3.44	ethanol
3.	3.84	acetone
4.	4.14	ethyl formate
5.	4.45	formic acid
6.	5.71	butanal
7.	5.90	2-butanone
8.	6.42	Incomplete MS, propanol?
9.	6.69	Incomplete MS, propanol?
10.	8.18	acetic acid
11.	9.43	2-pentanone
12.	9.83	pentanal
13.	10.68	propylacetate
14.	11.17	butyl formate
15.	11.97	Incomplete MS, 3-pentane-2-one?
16.	12.64	propionicacid
17.	14.48	2-hexanone
18.	14.66	2-ethyl-1-butanol
19.	14.98	incomplete MS
20.	15.71	butylacetate
21.	16.26	butanoic acid
22.	16.33	1-pentanol
23.	17.47	3-methylcyclopentanone
24.	19.51	2-heptanone
25.	19.86	cyclohexanone
26.	20.56	Incomplete MS, pentyl acetate?
27.	22.43	2-octanone

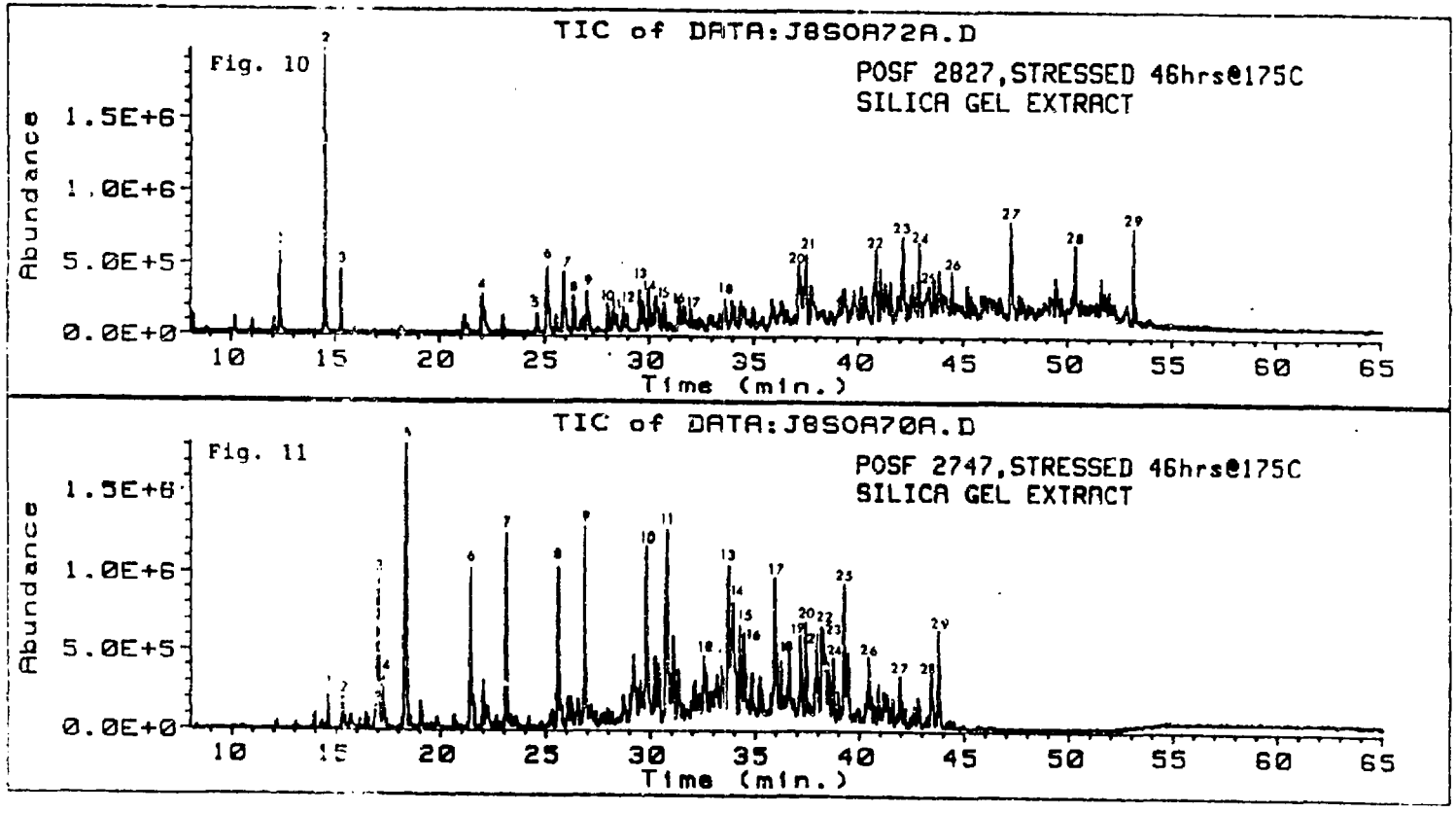

Figure 10 and 11: Total Ion Chromatograms of Oxidation Products Extracted from Fuels Stressed for 46 hrs. with 100 ml/min. Oxygen Sparge. Figure 10 is POSF 2827 extract, peak identification is table 9. Figure 11 is POSF 2747 extract, peak identification in table 10.

Table 9: Peak Identification for Figure 10: Extracted Oxidation Products of POSF 2827.

1.	12.43	1 propoxypentane
2.	14.59	3,3-dimethyl-2-hexanone
3.	15.34	2,2-dimethylpentanol
4.	22.08	4-methylphenol
5.	24.66	ethylphenol
6.	25.18	dimethylphenol
7.	25.98	dimethylphenol
8.	26.43	dimethylphenol
9.	27.09	dimethylphenol
10.	28.07	2?-propylphenol
11.	28.31	propylphenol
12.	28.78	propylphenol
13.	29.58	ethylmethylphenol
14.	30.03	trimethylphenol
15.	30.26	C_3 phenol
16.	31.46	C_4 phenol
17.	31.70	C_4 phenol
18.	33.70	subst. tetrahydrofuranone
19.	34.45	decanol
20.	37.19	methylisobenzofurandione
21.	37.57	undecanol
22.	40.90	mixed spectra, subst. benzoic acid?
23.	42.17	dimethylbenzopyran-2-one
24.	42.95	alkene
25.	43.69	p-cyclohexenylphenol?
26.	44.52	methylnaphthoquinone?
27.	47.31	subst. phenol
28.	50.38	methoxyphenanthrene?
29.	53.20	subst. furandione?

Table 10. Peak Identification for Figure 11: Extracted Oxidation Products for POSF 2747.

1.	14.59	3,3-dimethyl-2-hexanone
2.	15.32	dihydro-2(3H)-furanone
3.	17.06	dihydro-5-methyl-2(3H)-furanone
4.	17.24	tetrohydro-2H-pyran-2-one
5.	18.37	4,4-dimethyl-dihydro-2(3H)-furanone
6.	21.43	subst. furanone
7.	23.10	5-ethyldihydro-5-methyl-2(3H)-furanone
8.	25.59	5-propyl-dihydro-2(3H)-furanone
9.	26.86	3-ethyl-2,5-furandione
10.	29.83	5-butyldihydro-2(3H)-furanone
11.	30.80	2-undecanol
12.	32.55	1,3-isobenzofurandione
13.	33.76	5-pentyldihydro-2(3H)-furanone
14.	33.97	sec-butylethylbenzene
15.	34.28	1-ethyl-3-(1-methylethyl)-benzene
16.	34.49	subst. 2,5-furandione
17.	35.96	4-methylisobutylfurandione
18.	36.62	subst. furanone
19.	37.19	4-methylisobenzofurandione
20.	37.45	5-hexyldihydro-2(3H)-furanone
21.	37.97	methyl-1(3H)-isobenzof randione
22.	38.20	methyl-1(3H)-isobenzofurandione
23.	38.29	methylixobenzofurandione
24.	38.75	2,4,6-trimethylphenzl-1-ethanone
25.	39.29	4-methylphthalic acid
26.	40.42	5,6-dimethyl-3(2H)-benzofuranone
27.	41.95	dimethylbenzofuranone
28.	43.41	ethylmethylbenzofuranone?
29.	43.79	ethylmethylbenzofuranone?

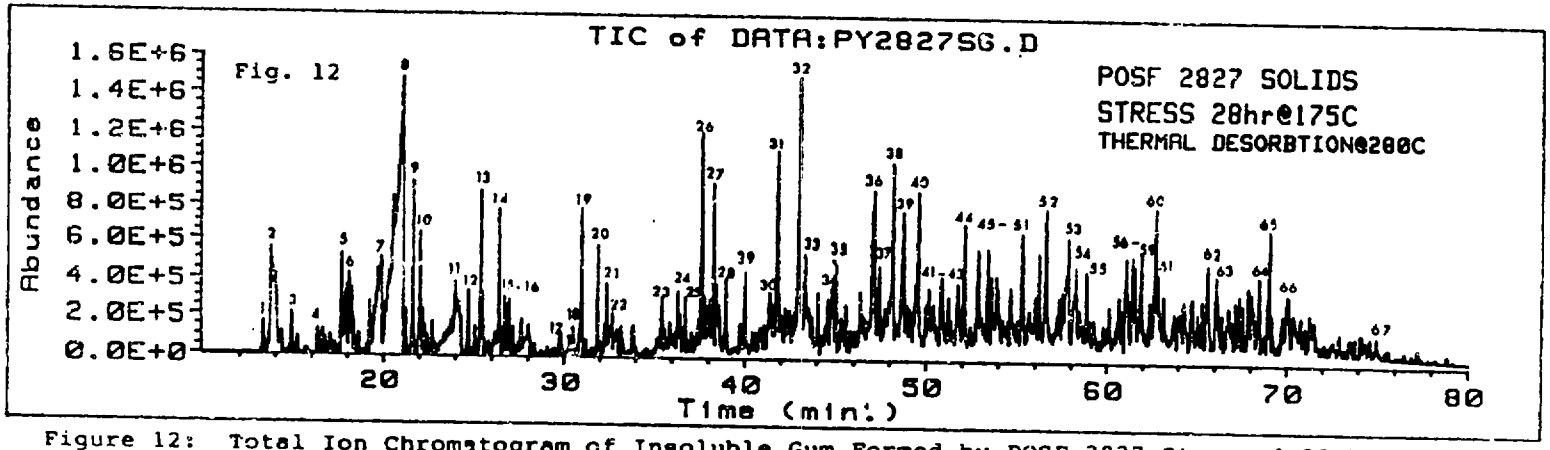

Figure 12: Total Ion Chromatogram of Insoluble Gum Formed by POSF 2827 Stressed 28 hours at 175C with 100 mL/min Oxygen Sparge. Peak identification is table 11.

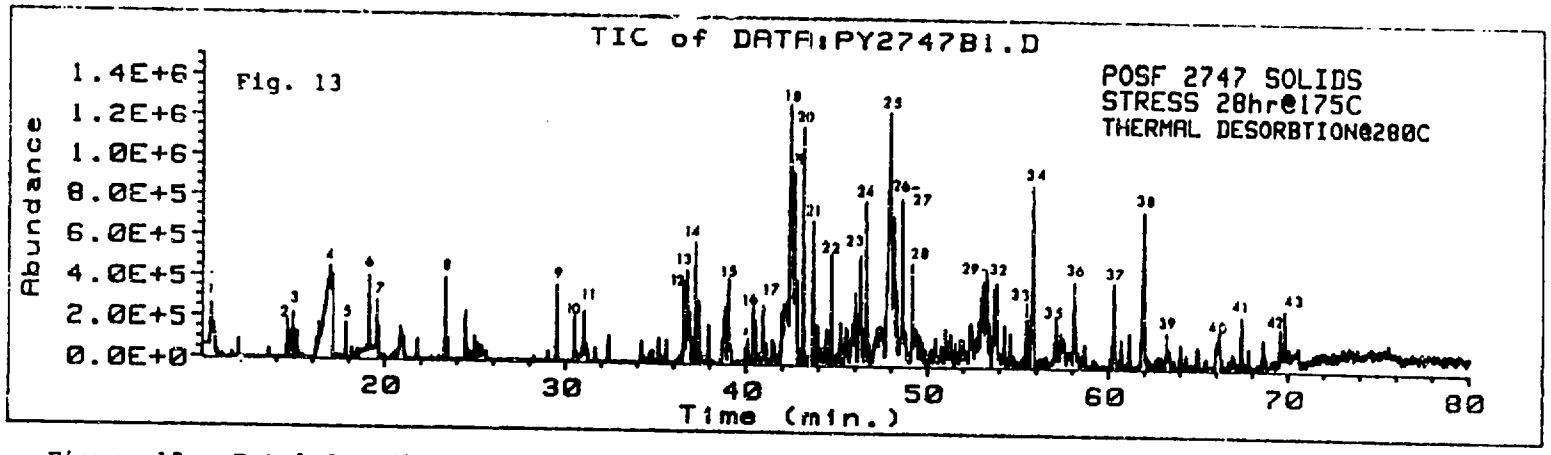

Figure 13: Total Ion Chromatogram of Insoluble Gum Formed by POSF 2747 Stressed 28 hours at 175C with 100 mL/min Oxygen Sparge. Desorbtion at 280C. Peak Identification is table 12.

Table 1i: Peak Identification For Figure12; Thermal Desorbtion Chromatogram of Stressed POSF 2827 Insoluble Gum

1.	13.34	1-butene
2.	13.74	butane
3.	14.88	dimethylcyclopropane
4.	16.34	methylpentene
5.	17.66	1-hexene
6.	18.06	2-butanone
7.	19.88	mixed MS
8.	21.06	acetic acid
9.	21.63	dimethylpentene
10.	22.01	3-methylbutanal
11.	23.99	propanoic acid
12.	24.71	methylpentanol
13.	25.39	toluene
14.	26.38	2-heptenal
15.	26.69	dihydropyran
16.	26.91	sec-alcohol
17.	29.76	methylcyclopentanone
18.	30.52	ethylbenzene
19.	30.97	m & p - xylene
20.	31.89	1-octanol
21.	32.38	o-xylene
22.	32.69	incomplete MS
23.	35.43	ene-ol
24.	36.33	ethylmethylbenzene
25.	36.71	ethylmethylbenzene
26.	37.63	phenol
27.	38.27	trimethylbenzene
28.	38.98	ethylhexanol?
29.	40.02	isopropylbenzene
30.	41.37	2-hydroxybenzaldehyde
31.	41.80	2-methylphenol
32.	43.03	4-methylphenol
33.	43.32	sec-alcohol
34.	44.88	dimethylphenol
35.	45.05	2-methylbenzofuran
36.	47.39	dimethylphenol
37.	47.48	methylindene
38.	48.15	dimethylphenol
39.	48.72	dimethylphenol
40.	49.52	dimethylphenol
41.	50.17	C_3 phenol
42.	50.88	C_3 phenol
43.	51.78	C_3 phenol
44.	52.14	2-hydroxybenzeneacetic acid
45.	52.84	C_3 phenol
46.	53.42	C_3 phenol
47.	53.63	C_3 phenol
48.	53.89	C_3 phenol
49.	54.67	1H-indene-1-one
50.	56.05	ethylmethylphenol

Table 11 con't.

51.	56.24	methylnaphthalene
52.	56.62	isobenzofurandione
53.	57.85	methylbenzofuranone
54.	58.28	ethylbenzoic acid
55.	58.87	dimethylphenyl-1-ethanone
56.	61.10	dimethylbenzofuranone
57.	61.43	dimethylnaphthalene
58.	61.62	dimethylnaphthalene
59.	61.91	dimethylbenzofuranone
60.	62.74	4-methylphthalic acid
61.	62.88	2,2-dimethyl-3,4-dihydro-(2H)-1-benzopyran
62.	65.60	methylnaphthalenol
63.	66.10	3-phenylfuran?
64.	68.47	subst. phenol?
65.	69.04	9H-fluorene
66.	70.06	2-methyl-1-naphthalenol
67.	74.96	dimethylnaphthalenol

Table 12: Peak Identification For Figure 13; Thermal Desorbtion of Stressed POSF 2747 Insoluble Gums

1.	10.34	butane
2.	14.58	dimethylcyclopropane
3.	14.95	2-butanone
4.	16.91	acetic acid
5.	17.83	benzene
6.	19.13	3-butene-2-one
7.	19.56	heptane?
8.	23.38	toluene
9.	29.52	xylene
10.	30.51	octanol?
11.	31.01	xylene
12.	36.56	phenol?
13.	36.72	ene-ol?
14.	37.20	ethylmethylbenzene
15.	39.03	ethylmethylbenzene
16.	40.40	3-methylcyclohexene?
17.	40.94	methylisopropylbenzene
18.	42.42	2-undecene
19.	42.68	4?-undecene
20.	43.16	?-undecene
21.	43.71	?undecene
22.	44.70	C_4 benzene
23.	46.30	hydroxybenzaldehyde?
24.	46.61	ethyldimethylbenzene
25.	47.92	1-dodecene
26.	48.13	?-dodecene
27.	48.61	?-dodecene
28.	49.15	undecanol?
29.	53.10	dodecanol?
30.	53.26	dimethylphenyl-1-ethanone
31.	53.69	alkene
32.	53.81	2,3-dihydro-1H-indene-1-one
33.	55.45	dimethylphenylethanone
34.	55.83	1,3-isobenzofurandione
35.	57.07	1H-indene-1,3(2H)-dione
36.	58.09	methylphenylbutonedione
37.	60.29	dimethylbenzofuran
38.	61.96	methylphthalic acid
39.	63.22	subst. isobenzofurandione
40.	66.14	dimethylbenzofuranone
41.	67.37	dimethylisobenzofurandione
42.	69.53	isobutylmethylbenzene
43.	69.79	alkane

Analysis of Jet Fuel Additives

William D. Schulz

Department of Chemistry
Eastern Kentucky University
Richmond, KY 40475

ABSTRACT

Current U.S.A.F. interest in raising the allowable operating temperature of jet fuels involves experimentation with additives such as antioxidants, metal deactivators, dispersants and detergents. For experiments with additives, it is necessary to know that the test fuel is additive free. A method for isolation and concentration of additives for G.C.-M.S. analysis was developed using a surrogate JP-8 containing twelve components. Various solid phase extraction utilizing commercial cartridges proved less desirable than methanol extraction with heptane back extraction. The liquid-liquid methanol also produced good results for "oxidation products" of fuels such as alcohols, aldehydes, carboxylic acids and ketones.

INTRODUCTION

Because of the extreme complexity of petroleum derived fuels, a twelve component surrogate JP-8 was formulated for the original purpose of investigating the products of autooxidation. The surrogate contains alkanes, cyclanes and aromatics of proportion and boiling range similar to JP-8.

When it seemed necessary to develop an analytical method for the determination of additives, particularly antioxidants in fuels, the surrogate fuel provided an ideal substrate. Because it was also desirable to isolate and concentrate oxidation products from thermally stressed fuels, this was investigated concomitantly with the extraction of additives.

EXPERIMENTAL

Chemicals: Surrogate fuel components (isooctane, 5.0%; wt./wt., methylcyclohexane, 5.0%; m-xylene, 5.0%; cyclooctane 5.0%; decane, 15.0%; butylbenzene, 5.0%; 1,2,3,4-tetramethylbenzene, 5.0%; tetralin, 5.0%; dodecane, 20.0%; 1-methylnapthalene, 5.0%; tetradecane, 15.0% and hexadecane, 10.0%, were 99+% grade purchased from Aldrich. "Oxidation product" probes: Hexanal, hexanoic acid, 1-octene, 2-octanone and dodecanol were Aldrich reagent grade. Solvents: (Acetone, acetonitrile, methanol, toluene and heptane) were

Aldrich reagent or HPLC grade. SPE cartridges were J&W (diol, cyano and C-18) J.T. Baker (silica gel) and Alltech (IC/Ag). All were conditioned and used according to the vendors recommendations.

Solid phase extraction: For normal phase extraction, (silica gel, diol, cyano and tandem IC/Ag and silica gel) 1 gram cartridges were conditioned from water-methanol to heptane. 10 mL spiked fuel samples were passed through the cartridges at ~2 mL/minute and the cartridge was then washed with 3x2 mL portions of heptane. After the last wash excess hexane was purged with 3x10 mL portions of air and the cartridge was eluted with methanol or 50/50 methanol-acetone. Eluent was collected in 1 mL increments for analysis.

Liquid-liquid extraction: 100 mL of spiked fuel was extracted with 3x20 mL portions methanol. The methanol extracts were pooled and back extracted with 3x10 mL portions heptane. The heptane was discarded. For fuel additive analysis the methanol extract was reduced to 2 mL volume by evaporation with a stream of dry nitrogen. For oxidation product analysis the methanol extract was not concentrated or concentrated 50%. 10 mL portions of real stressed fuel samples were extracted with 3x2 mL methanol, the methanol pooled and back extracted with 3x2 mL heptane. The extractions were done in screw cap 12x150 mM culture tubes. The tubes were centrifuged after back extraction and traces of heptane removed with a pastuer pipette.

Analysis: Samples were analyzed on an HP 5890 Series II GC-5970 MS, equipped with an HP 7673 autosampler. Column was a 30 or 50 M.x0.25mMx0.5 M DB-5 type with 2-4 M 0.53mM retention gap. Concentrated samples were injected on column with electronic pressure programming set to maintain 30 cm./sec. flow. Dilute samples were injected splitless, up to 4 mL., with the flow rate adjusted to 30 cm./sec. at 150°C. Initial temperature, time, ramp and hold time depended upon compounds of interest. 40° initial, hold 2 minutes, 4°C/minute to 280°C with a 15 minute hold would adequately resolve and elute all compounds discussed. The MS was scanned 35 to 550 M/z.

RESULTS AND DISCUSSION

The analysis of fuel additives is complicated by the fact that the analyst will not know the identity of the analytes. He must either use several methods or develop a general method that will give acceptable results with a wide range of compounds. GC-MS is rapid, sensitive and can identify components and so is a method of choice for analysis of the hindered phenol, aliphatic and aromatic amine compounds that are usually used as antioxidants. Only one compound, N,N-disalicylidene-1,2- propanediamine seems to commonly be used as a metal deactivator and it is amenable to

GC analysis. Most dispersants and detergents are not volatile enough for even high temperature GC and they have not been included in this work. The additive analysis is further complicated by interference from the very wide range and huge number of fuel components as well as the usual low concentrations of additives.

Solid phase extraction seems an attractive and often effective method of isolation and concentration and would seem ideal for extraction of polar additives from fuel. In several experiments with normal phase extraction, using silica gel, diol and tandem silica gel-silver loaded ion exchange cartridges, recovery of one or more typical antioxidants was unsatisfactory. Table I is a general overview of extraction-concentration methods attempted and gives the problems encountered with various solid phase extractions.

We had previously used methanol extraction for concentration of oxidation products from fuel samples with good success. When we attempted extraction of additives spiked into real fuels with methanol, fuel components presented unacceptable interference for chromatography. Back extraction with heptane removed the interfering fuel components to an acceptable degree. Essentially all remaining fuel components are aromatic hydrocarbons. (This observation is also of some value, since fuels containing more and higher molecular weight aromatics seem to produce the most sediment upon autooxidation.) The liquid-liquid extraction method provides good results for a wide range of additives and oxidation products. Figure I is representative total ion chromatograms of the spiked surrogate fuel before and after extraction, showing recovery of additives and oxidation products. It can be seen that substantial concentration is effected, in fact, showing storage deterioration of the surrogate fuel (tetralinol, tetralinone) and components not known to be in any of the additives (substituted quinoline, others unidentified). Table II is a summary of recovery data from surrogate fuel spiked at 50 ppm. Detection limits have not been established but from Figure I there would still be more than adequate signal to noise for major components at 5 ppm.

Figure II is a comparison of a real fuel known to contain no additives, which is spiked at the 50 ppm level, before and after extraction. In this case some of the "oxidation products" are partially obscured by the coextracting aromatic compounds but all additives are essentially interference free.

The utility of this method was proven when a colleague found evidence of a hindered phenol in a sample of JP-TS fuel by electrochemical analysis. The fuel was known to contain an additive package but should not have contained a hindered

phenol. Methanol extraction, back extraction and G.C.-M.S. analysis proved the presence of 2,5-di-t-butyl-4-methylphenol (BHT) which was later recognized by the supplier as being present due to stocks used in blending of the fuel. The total ion chromatogram for the unspiked fuel is compared to a spiked sample of the same fuel in Figure 3.

ACKNOWLEDGEMENTS

This work was conducted under USAF contract No. F33615-87-C-2714. Thanks to W. M. Roquemore and the POSF staff at POSF/Wl. W.P.A.F.B. as well as Dr. Ballal and the UDRI group.

Table I

Summary of Additive and Oxidation Product Isolation and Concentration

Technique	Disadvantage
1. Silica gel S.P.E. cartridge	Very low recovery of hindered phenols
2. Diol S.P.E. cartridge	General very low recovery hindered phenols and amines
3. Tandem Ag-Ion Exch.	Low recovery in general, very low recovery of hindered phenols
4. Methanol extraction, C-18 "clean-up"	Loss of alkyl-amine compounds
5. Methanol extractions Silica gel "clean-up"	Components of interest spread over a 1-5 mL range of elutions. Dilution, rather than concentration, is effected.
6. Methanol extraction, heptane back extraction	No disadvantage for additives, also can be concentrated by "blow-down". Low recovery only of heptanal noted for "oxidation products."

Table II

Recovery Data for Methanol Extraction-
Heptane Back Extraction at 50 ppm Level

	% Recovery	Std. Deviation (n>4)
Fuel Additives		
JFA-5*		
antioxidant[1]	89	3.56
Metal deactivator	75	3.90
2,6-di-t-butyl-4-methylphenol	87	3.78
N,N'-di-sec-butyl-p-phenylene diamine	92	2.81
4,4'-methylene-bis(2,6-di-t-butylphenol)	94	2.03
Oxidation Products		
heptanal	23[2]	8.20
1-octene	37[2]	5.69
2-octanone	85	3.71
hexanoic acid	97	9.84[3]
1-dodecanol	99	1.51

*Mixed additive: Contains antioxidants, metal deactivator and dispersant.

1. Determined from most abundant of homologous series.
2. Extremely sensitive to back extraction, best to locate by retention time and determine without back extraction.
3. Integrator error: Very poor peak shape from column used.

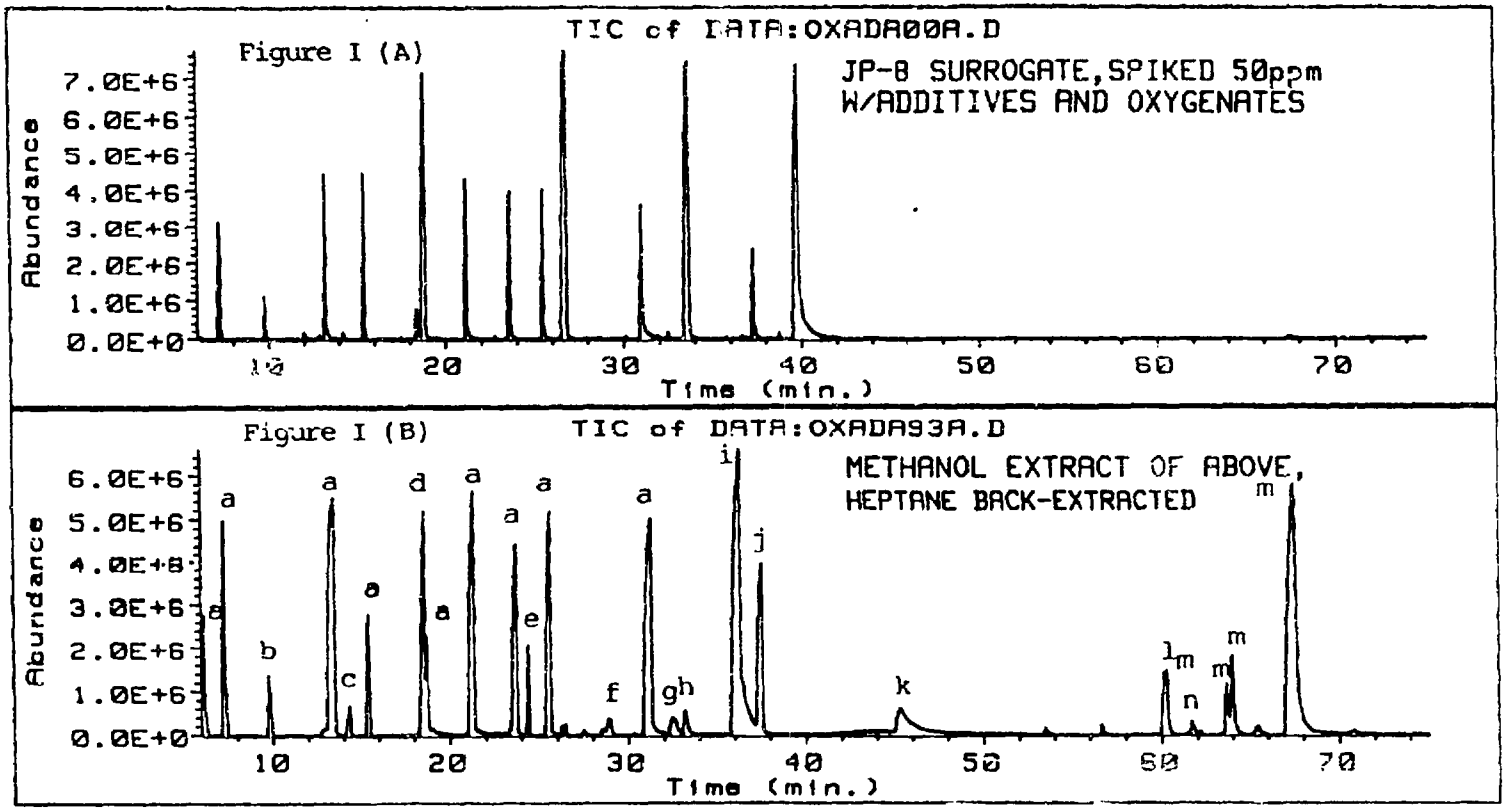

Figure I (A) Total Ion Chomatogram of Surrogate JP-8 Spiked at 50 ppm.
Compounds spiked: JFA-5 fuel additive package, 2,5-di-t-butyl-4-methylphenol ("BHT", "AO-29"), heptanal, 2-octanone and 1-dodecanol

(B) Total Ion Chromatogram of Methanol Extracted, Heptane Back Extracted Mixture of figure I (A). Identity of peaks: a; original fuel, (C) C_2 benzene from JFA-5 solvent, (d) 2-octanone, (e) possible N,N-dialkl-thioacetamide, (f) unknown, (g) tetralinol, (h) tetralinone (i) 1-dodecanol, (j) BHT, (k) substituted quinoline (unknown source), (l) metal deactivator, (m) antioxidants from JFA-5, (n) a hindered phenol

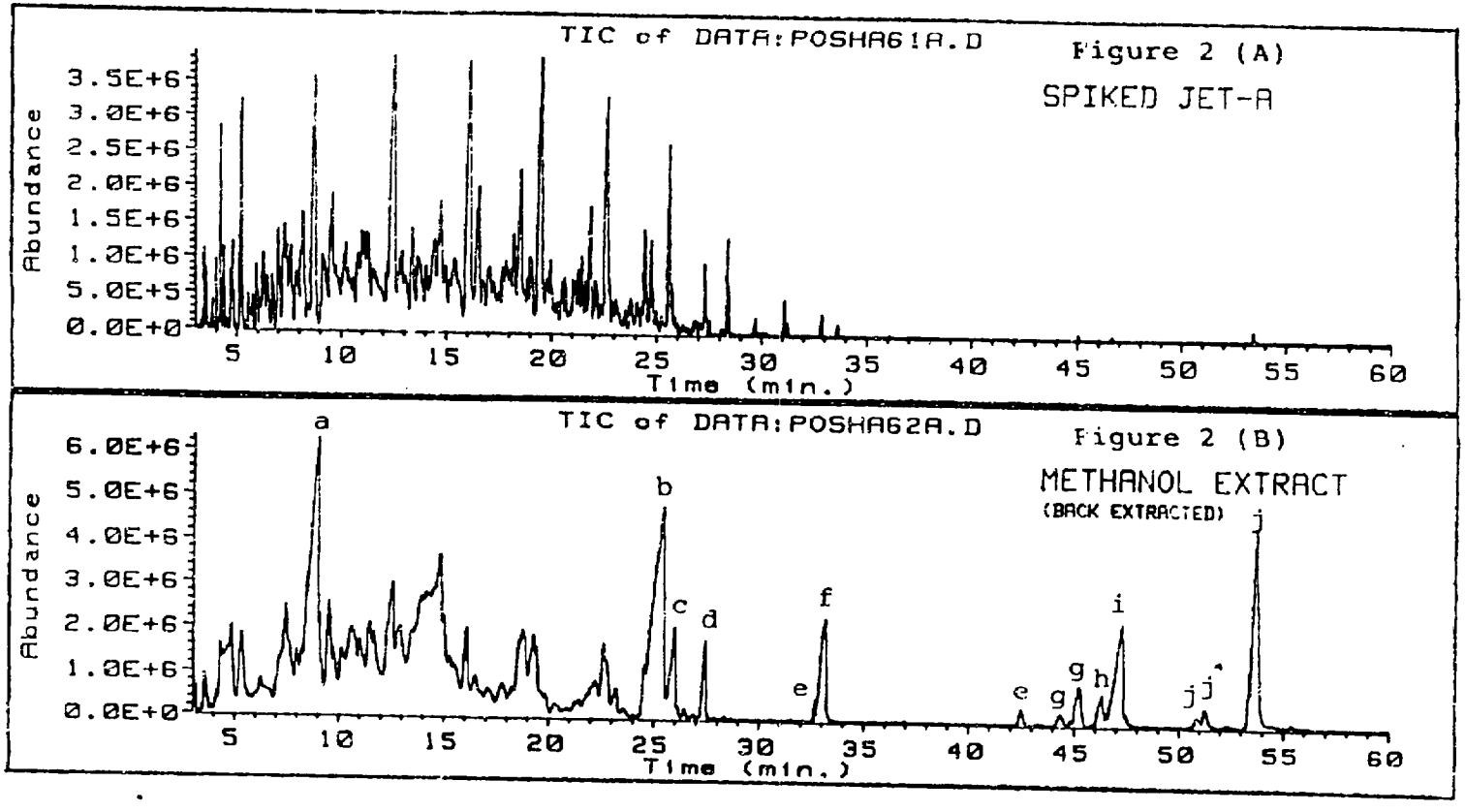

Figure 2 (A) Total Ion Chromatogram of a Jet-A Fuel Spiked at 50 ppm with JFA-5, AO-29, N,N'-di-sec-butyl-p-phenylenediamine, 1-dodecanol and 2-octanol

Figure 2 (B) Total Ion Chromatogram of Methanol Extract, Heptane Back-Extract of Spiked Jet-A Compound Identification: (a) 2-octanone, (b) 1-dodecanol, (c) AO-29 (2-6-di-t-butyl-4-methylphenyl), (d) possible fatty acid, (e) hindered phenols, (f) N,N'-di-sec-butyl-p-phenylenediamine, (g) unknown (h) possible 1,3,8-trihydroxy-6-(1-hydroxypropyl)-9,10-anthracenedione, (i) metal deactivator (N,N'-disalicyidene-1,2-propanediamine), (j) JFA-5 components

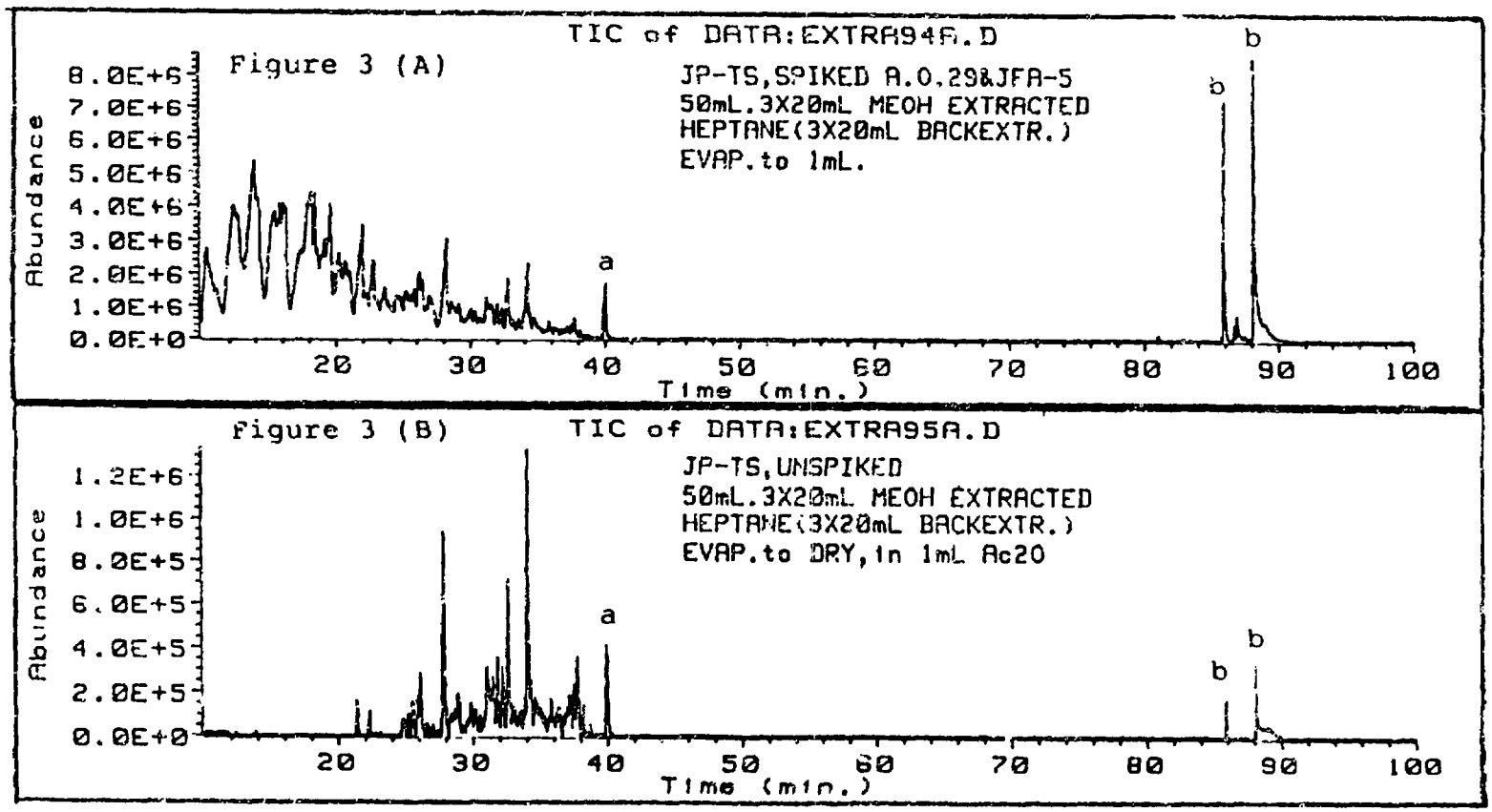

Figure 3 (A) Total Ion Chromatogram of Extract from JP-TS Spiked with AO-29 abd JFA-5
(B) Total Ion Chromatogram of Extract from Unspiked JP-TS
Compound Identification (a) AO-29, (b) JFA-5

APPENDIX B

Oxidation Products of a Surrogate JP-8 Fuel

William D. Schulz

Department of Chemistry
Eastern Kentucky University
Richmond, KY 40475

ABSTRACT

Future high performance aircraft will require fuels with a high operating temperature for use as heat exchange fluids. The determining factor for the maximum operating temperature of a fuel is the formation of gums and solids in the fuel beyond that temperature. A 12 component surrogate JP-8 has been formulated to simplify the study of the chemistry of gum and solid formation by fuels. The surrogate fuel contains chemical class representative compounds that are relatively pure, inexpensive and found in real fuels. Oxidation products of the surrogate fuel, including soluble and insoluble, have been isolated and analyzed by GC-MS and pyrolysis-GC-MS. The analysis of the oxidation products and their fate, with time, is presented.

INTRODUCTION

Fuel stability to storage and thermal oxidation and subsequent gum and solids deposits has probably been of concern since the invention of internal combustion engines. The importance of fuel stability, particularly thermal stability, has increased greatly with the increasing need to use the fuel as a heat exchange fluid in modern aircraft. Literature reviews[1-3] contains hundreds of references, yet Reddy[4] in a February 1989 paper states: "Although considerable effort has been devoted to understanding and solving the fuel degradation problems, knowledge of the detailed chemistry is lacking." Reddy also cites a considerable amount of work for which results "are unclear and at times contradictory." Aircraft malfunction caused by fuel oxidation includes effects ranging from synthetic seal and O-ring failure caused by hydroperoxides[5] to clogged injection nozzles and fouled heat exchange surfaces[4] due to surface deposits of gum and particulates. The fuel deterioration problem is very complex. Although hydroperoxide formation is certainly the first step of the oxidation process, different mechanistic steps can become more important to product formation at different temperatures. As temperatures increase pyrolytic reactions begin to contribute to deterioration and finally predominate at about 500°C.[6] In addition, the physical mechanisms of

depostion or solid formation from insoluble species dispersed in fuel can vary and can probably be rate determining in some cases. The composition of the fuel is, of course, the determining stability factor, and it is also important for solvent properties in gum and particulate formation from oxidized species. The complexity of jet fuels and of the degradation mechanisms, the nature of deposition process and the large number of degradation products implicated in deposit formation combine to make thermal oxidation and fuel deposition studies difficult.

The goal at the outset of this work was to devise a system to simplify and accelerate the study of autooxidation and possibly be of use for additive evaluation. The requirements for a stress apparatus were that it be inert, simple, inexpensive and capable of stressing fuels with rapidity and repeatability. The flask test that we devised is a very simple version of Shell flask test.[9] Standard taper (24/40 and 19/22 glassware is used and oxygen is introduced to the fuel via a 0.53 mM fused silica capillary line that is simply passed through a viton seal alongside of the thermometer. Figure I is a schematic of the flask test apparatus.

To avoid the extreme complexity of real, petroleum derived, fuels, a surrogate JP-8 was prepared. The criteria for the surrogate formulation were that it contain reasonable amounts of compounds representative of the chemical classes found in real fuels, that the physical properties of the surrogate approximate a real JP-8 and that the components be readily available in high purity and reasonably priced. Table I shows the composition of the surrogate and Table II is a comparison of the surrogate and a petroleum derived JP-8.

Gravimetric determination of gums and solids as a measure of thermal stability is difficult, time consuming and imprecise. One goal of this work was to investigate analytical methods for the determination of oxidation products as precursors to gums and solids. If the flask test and surrogate fuel were used to develop a method for determination of alcohol and carbonyl products by FTIR which seemed to promise both as a rapid predictor of fuel stability and as a test method for the efficiency of antioxidants. The method worked well for determining the extent of oxidation but this was, unfortunately, not related to the amount of deposition for different fuels, or with different antioxidants.[10] The flask test and the surrogate (JP-8S) fuel have proven valuable for development of methods for isolation and concentration of oxidation products and fuel additives, and for basic investigation of the chemical composition of oxidized fuels, gums and solids. In this work

we present the results of analysis of the oxidation products of the surrogate fuel, which we hope to compare to results from real fuels in the near future.

EXPERIMENTAL

Chemicals: Surrogate fuel components (isooctane, 5.0%; wt./wt., methylcyclohexane, 5.0%; m-xylene, 5.0%; cyclooctane 5.0%; decane, 15.0%; butylbenzene, 5.0%; 1,2,3,4-tetramethylbenzene, 5.0%; tetralin, 5.0%; dodecane, 20.0%; 1-methylnapthalene, 5.0%; tetradecane, 15.0% and hexadecane, 10.0%, were 99+% grade purchased from Aldrich.

Solvents: (Acetone, acetonitrile, methanol, toluene and heptane) were Aldrich reagent or HPLC grade. High purity nitrogen and oxygen from Central Kentucky Welding Supply were used as purchased.

Flask test apparatus: (Figure I) Temperature control to $\pm$ 1°C was by Therm-o-watch controllers (I^2R Corp.) and mercury thermometers. Resistively heated oil baths and heating mantles were variously employed to heat fuel flasks. 24/40 and 19/22 st. taper pyrex glassware was used throughout. (19/22 joints adapted to 24/40 Friedricks condensor to utilize more available glassware and reduce vapor volume before condensing.) Polyimide coated, deactivated 0.53 mM I.D. fused silica (Restek, H.P.) was used (through viton thermometer seals alongside thermometer) to supply purge nitrogen and oxygen to the bottom of stress flasks. Normal procedure was 50 mL fuel in 100 mL RB. 19/22 flask. Mass flow controller adjusted to 60 mL/min. oxygen flow, than a "T" value switched to purge fuel and system with dry nitrogen for 5 minutes, the heater switched on and purging continued until operating temperature was reached. Stress time was recorded when oxygen flow was begun. When samples were obtained during stressing the thermometer-gas feed adapter was simple lifted up and 5 or 10 mL aliquot withdrawn by pipette. Samples were stored in 12 x 150 mL teflon cap sealed culture tubes at 5°C.

Analysis: Samples were analyzed on an HP 5890 Series II GC-5970 MS, equipped with an HP 7673 autosampler. Column was a 30 or 50M.x0.25mMx0.5uM DB-5 type with 2-4 M 0.53mM retention gap. Concentrated samples were injected on column with electronic pressure programming set to maintain 30 cm./sec. flow. Dilute samples were injected splitless, up to 4 mL., with the flow rate adjusted to 30 cm./sec. at 150°C. Initial temperature, time, ramp and hold time depended upon compounds of interest. 40° initial, hold 2 minutes, 4°C/minute to 280°C with a 15 minute hold would adequately resolve and elute all compounds discussed. The MS was scanned 35 to 550 M/z.

Pyrolysis and thermal desorbtion was done with a CDS model 1000 "Pyroprobe", coil element and 2mM quartz tubes.

For thermal desorbtion: Sample loaded into probe, inserted in interface at GC oven temperature at 30° and interface at room temperature, GC oven then cooled to -40°. The interface temperature then raised to 280° and held 5 minutes without firing probe and GC sequence started; -40° for 6 minutes, purge off 5.5 minutes; 6°/min to 50°, 5°/minute to 150, 8°/min to 280°, final hold 22.75 minutes. Injection port maintained at 280°, column same as that used for liquid samples. For pyrolysis, GC conditions were the same, except probe was fired (550° and 900° - 40 seconds) after the interface tempeature was achieved and GC sequence begun immediately after probe firing.

Filtration and extraction of oxidation products: Stressed fuel samples filtered with Whatman® 47mM GMF 150 grade binder free glass filters. Filtered fuel was saved for extraction. Filters washed with heptane and partially dried by maintaining air flow for 15-20 minutes. Gums were defined as material dissolved from the filter by acetone washing. Material not soluble in acetone was classed as solids. After difficulty in obtaining useful information from acetone soluble gum samples, "gums and solids" were dried in vacuo (20-30 torr, 80°C) 36-48 hours and analyzed by thermal desorbtion and pyrolysis - GC-MS. Oxidation products were extracted from filtered fuel by solid phase and liquid-liquid extraction. Solid phase (S.P.E.) was by 1.0 g silica gel cartridges conditioned from methanol to heptane as per suppliers recommendation. Then, 10 mL filtered fuel dropwise through S.P.E. cartridge, cartridge washed with 3 x 2 mL portions heptane, purged with 100 mL air (syringe) and eluted with 2mL acetone. Alternate extraction was 10 mL fuel extracted with 3 x 2.0 mL methanol, extracts pooled and back extracted with 3 x 2.0 mL heptane. Extraction done in 12 x 150 mL culture tubes, centrifuged and last traces of heptane removed by pastuer pipette after centrifuging.

RESULTS AND DISCUSSION

A. Liquid Stressed Fuels

The affects of individual components of fuels are conveniently investigated with a simple surrogate fuel, so that the component source of isolated oxidation products from stressed fuels can be identified. Concentration of oxidized species is necessary to get sufficient fragment ions for identification without chromatographic interference. Figure 2 shows a comparison of unstressed and stressed surrogate JP-8. It is interesting to note that the alcohol and ketone oxidation products can be identified without concentration in this lightly stressed fuel but that they are frequently not found in more severely stressed samples. The implication is that they are either quickly oxidized further to products not directly related to tetralin or that they are quickly incorporated into deposits of more highly stressed samples.

Figure 3 is a comparison of extracted and unextracted samples of unfiltered stressed surrogate fuel samples. The stressed fuel is brown colored and will form gummy deposits upon standing. (The surrogate will form insoluble solids only with extreme conditions of temperature and time.) The relationship of oxidation products to source is fairly straightforward: cyclooctanol from cyclooctane, hexadecanol from hexadecane, 3-methylbenzylalcohol from m-xylene, etc. Not so straightforward are the furanone derivatives and the source would be questionable if not for a separate experiment in which hexadecane was stressed for 40 hours at 200°C. Analysis of extracted products of this experiment showed high concentrations of the homologous series of carboxylic acids, propanoic through decanoic, and the homologous series of 5-alkyl-2-furanones, with smaller amounts of aliphatic alcohols and alkanes greater than C-16[11].

B. Gums and Solids

Native gums and solids produced from the surrogate fuel (or other fuels) consist mainly of fuel components that are difficult to remove from the oxidation product matrix. The deposits from the surrogate fuel are nearly completely soluble in acetone but gas chromagraphy of such solutions shows a very large envelope of inseparable peaks at long retention time and high oven temperature. Pyrolysis of dried solid produces chromatogram of alkenes, alkanes and aromatics, but little to indicate the true nature of the deposit. A typical pyro-chromatogram is shown in Figure 4. Pyrolysis at 450°C, even for 40 seconds does not yield much information, perhaps because of "glazing" and encapsulation of the sample. Thermal desorbtion for five minutes at 280°C gives a chromatogram of a large number of well resolved peaks. The reason for the separability of deposit components from a thermally desorbed sample versus inseparability of components of a solution sample can only be speculated on at this time: The deposit could be relatively simple compounds bonded only by weak attractive forces or could result from thermally labile covalent bonds such as hemiacetal or ester that are disrupted by decarboxylation. Figure 5 is a chromatogram of JP-8S deposits obtained by thermal desorbtion from the acetone insoluble portion of a sample stressed 20 hours at 175°C. In spite of acetone washing and 48 hours vacuum drying at 80°C, the largest component is hexadecane. A series of carboxylic acids are identifiable by their poor peak shapes. The large "hump" at about 40 minutes R.T. is 2, 5-dihydrofurandione, with several co-eluting components. Phenols are found at 37.15 and 69.57 minutes and substituted dihydrofuranones at 70.21 and 74.56 minutes retention times. The large peaks at about 72 minutes include hexadecanones but have not been positively identified. Other peaks arise from aliphatic aldehydes, alcohols, alkenes, alkanes and ketones. Few aromatic compounds can be identified. Preliminary work with deposits from real fuels indicates that there is a great

deal to be learned from this method of analysis. One fuel produces insoluble, crystal like deposits, while deposits from the other tend to be soluble gums. The difference in the deposits, by thermal desorbtion-GC-MS, is a high concentration of substituted phenols from the crystalline deposit. This fuel also seems oxidation resistant but deposition prone. It is hoped that future work will reveal the nature of deposits and deposition from stressed fuels and contribute to development of more thermally stable fuels.

ACKNOWLEDGMENTS

This work was conducted under USAF contract No, F33615-87-C-2714, subcontract RI-70791X and contract F33615-87-C-2767. Thanks to W. M. Roquemore and the POSF staff at POSF/WL. W.P.A.F.B. as well as Dr. Ballal and the UDRI group.

REFERENCES

(1) Goetzinger, J. W., Thompson, C. J. and Brinkman, D. W., A Review of Storage Stability Characteristics of Hydrocarbon Fuels 1952-1982, "DOE/BETC/IC-83-3, October, 1983.

(2) Brinkman, D. W., Bowden, J. N. and Giles, H. N., (Lube Oil and Finished Fuel Storage Stability: An Annotated Review" DOE/BETC/RI-79-13, February, 1980.

(3) Hazlett, R. N., Ed., "CRC Literature Survey on the Thermal Oxidation Stability of Jet Fuel," CRC Report No. 589, April, 1979.

(4) Reddy, K. T., and Cernansky, N. P., J. Propulsion. Vol 5, No. 1, pp. 6-13, Jan-Feb 1989.

(5) Fodor, G. E., Naegel, D. W. and Kohl, K. B., "Peroxide Formation in Jet Fuels," Energy and Fuels, Vol. 2, pp. 729-734 (1988).

(6) Hazlett, R. N., J. N. and Matson, M., Ind. Eng. Chem. Prod. Res. Dev. Vol. 16, No. 2, pp. 171-177 (1977).

(7) Taylor, W. F., and Frankenfeld, J. W., "Chemistry and Mechanism of Distallate Fuel Stability," Proceeding 2nd International Conference on Long Term Storage Stabilities of Liquid Fuels, S.W.R.I., San Antonio, Texas, Vol, 2, pp. 496-511.

(8) Schulz, W. D., "Oxidative Thermal Degradation Studies of a Surrogate JP-8 with a Modified Thermal Precipitation Apparatus" Final Report; Contract F49620-88-C-0053, WRDC/POSF, W.P.A.F.B., August, 1989.

(9) Kendall, D. R., Clark, R. H. and Stevenson, P. A., "The Influence of Polar Compounds on the Stability of Jet Fuel." Proceeding 2nd International Conference on Long Term Storage Stabilities of Liquid Fuels, S.W.R.I., San Antonio, Texas, Vol. 2, pp. 694-705.

(10) Schulz, W. D., "Development of a Thermal Oxidative Stress Test for Eluciduting Fuel Chemistry and Determining Additive Efficiences" Final Report; Contract F33615-87-C-2714, Subcontract RI-70791X.

(11) Schulz, W. D., "A Chemical Investigation of the Nature of Jet Fuel Deposits and the Effect of Additives on Deposits", Quarterly Report; Contract F33615-87-C-2767.

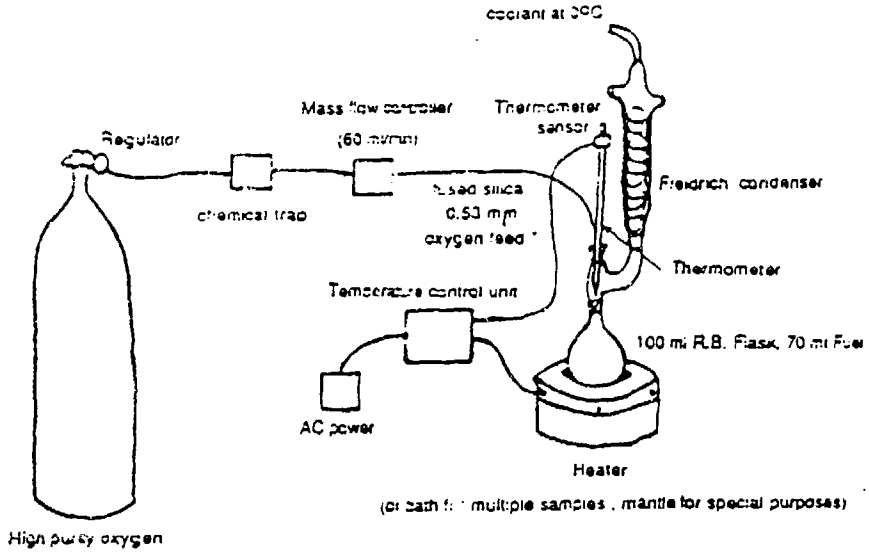

*Deactivated fused silica oxygen tip reaches bottom of fuel in R.B. flask

Schematic diagram modified flask test for thermal oxidation of fuels

Figure 1

Table I. SURROGATE JP-8 COMPOSITION

Peak#	Ret. Time*	COMPOUND	Wt.%	D(g/cc)	bp. (C)
1	9.07	isooctane	5.0	.690	98
2	10.27	methylcyclohexane	5.0	.770	101
3	15.98	m-xylene	5.0	.868	138
4	18.40	cyclooctane	5.0	.834	151(740)
5	21.71	decane	15.0	.730	174
6	23.38	butylbenzene	5.0	.860	183
7	25.58	1,2,4,5-tetramethylbenzene	5.0	.838	197
8	27.06	tetralin	5.0	.973	207
9	28.74	dodecane	20.0	.749	215
10	31.87	1-methylnaphthalene	5.0	1.001	240
11	34.74	tetradecane	15.0	.763	252
12	40.01	hexadecane	10.0	.773	287

*WSFUEL MS-GC Conditions

Table II: COMPARISON OF SURROGATE AND AUTHENTIC JP-8 FUELS

	TEST	SURROGATE JP-8	JP-8 WPAFB TANK S-15
D1319	Aromatics, Vol %	22.0	22.0
D1319	Olefins, Vol %	0.0	2.7
D2887	Distillation Initial Boiling Pt. Deg C	92	124
D2887	Distillation 10% recovered, Deg C	135	160
D2887	Distillation 20% recovered, Deg C	169	173
D2887	Distillation 50% recovered, Deg C	205	212
D2887	Distillation 90% recovered, Deg C	255	259
D2887	Distillation End Point, Deg C	286	296
D1298	Density, kg/l	0.800	0.811
D93	Flash Point, Deg C	26	59
D2386	Freezing Point, Deg C	-14	-54
D445	Viscosity @ -20 Deg C, cs	3.9	3.9
D3338	Net heat of Combustion, MJ/kg	43.1	43.1
D3343	Hydrogen Content, Wt %	13.7	13.6

Figure 2: Comparison of Stressed and Unstressed Surrogate JP-8 Fuel (Peak at 32.69 min. is tetralinol, at 33.22 min., tetralinone)

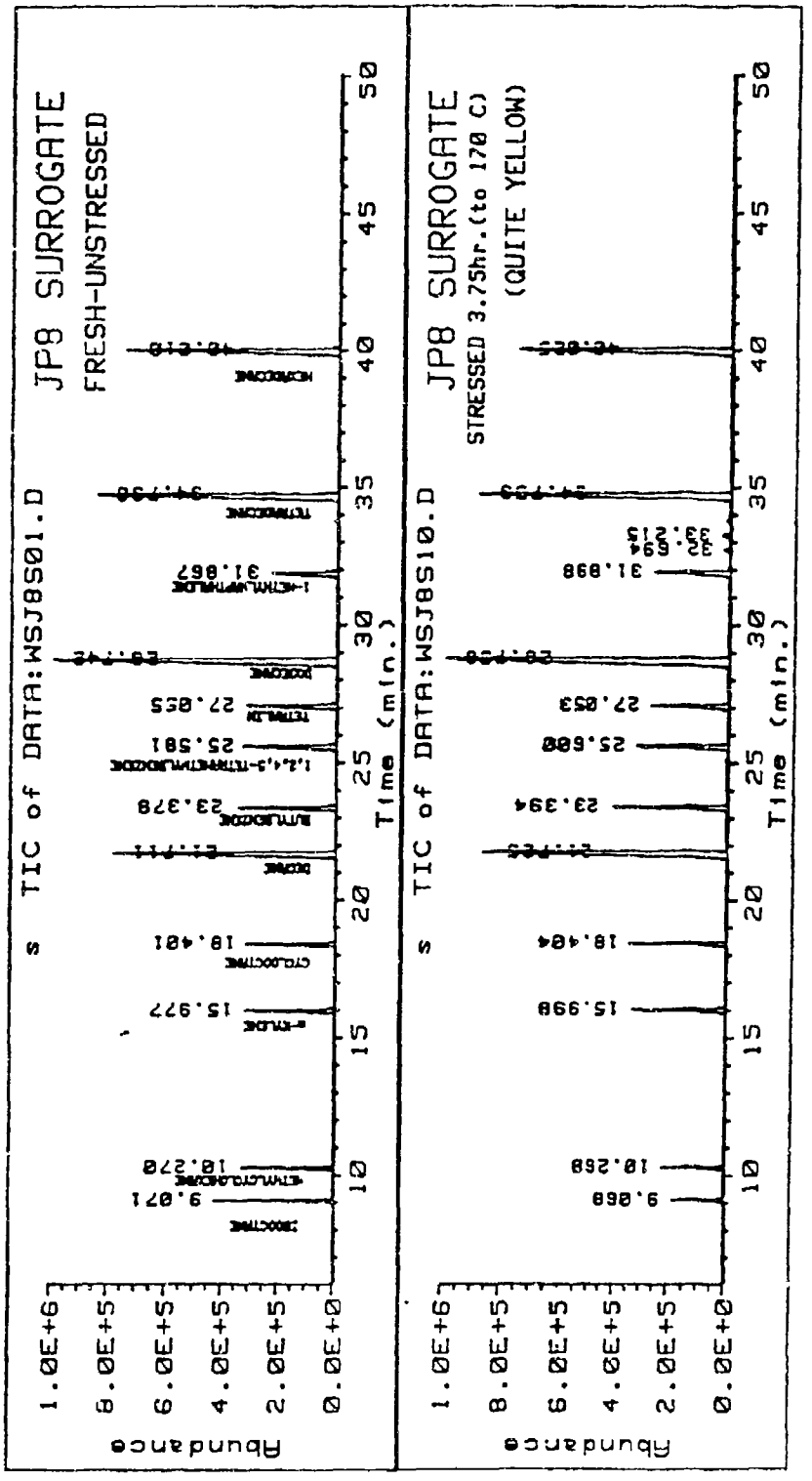

Figure 3 . Isolation and Concentration of Oxidation Products

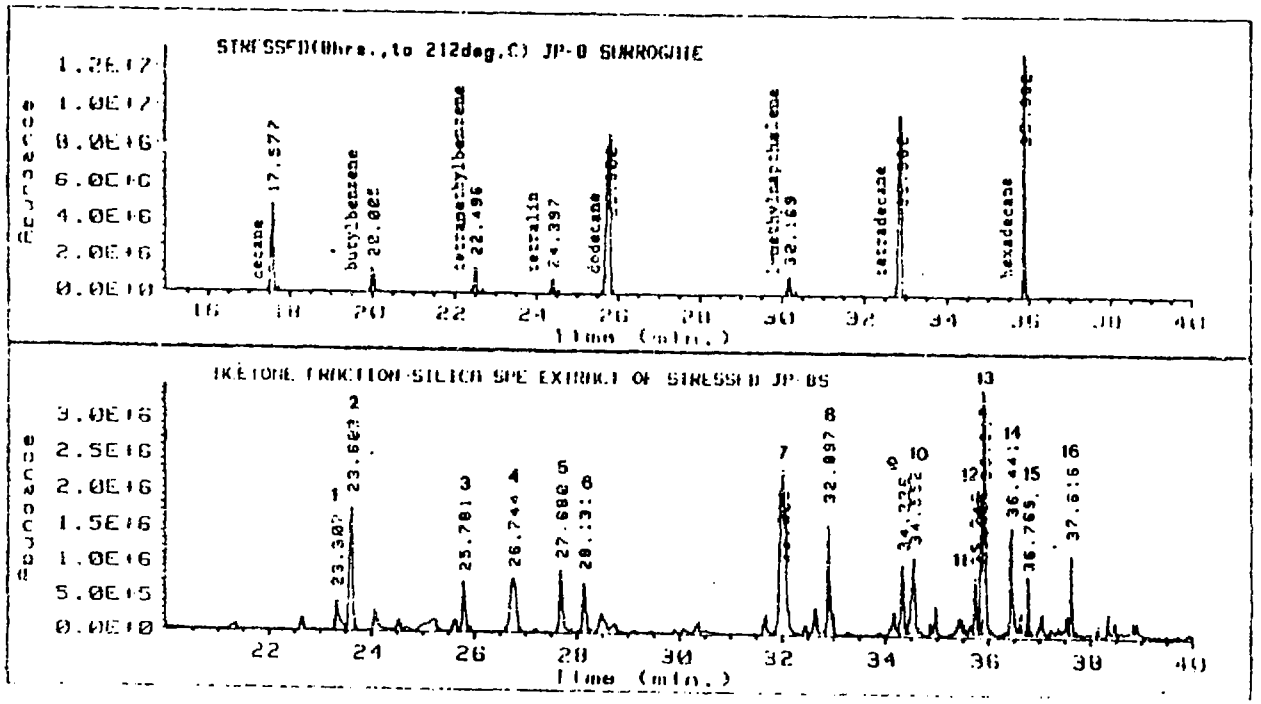

OXIDATION PRODUCT TENTATIVE PEAK IDENTIFICATION:

Peak #	Compound	Peak #	Compound	Peak #	Compound
1	3-methylbenzylalcohol	7	2,4,5-trimethylbenzylalcohol	11	hydroxymethylnaphthalene
2	cyclooctanol	8	2-dodecanol	14	trimethylbenzoylester?
3	2-decanol	9	5-hexyldihydro-2-furanone	15	a dodecylketone?
4	aliphatic aldehyde?	10	2,4,5-trimethylbenzoic acid	16	2-hexadecanol
5	trimethylbenzylalcohol	11	furanone derivative		
6	furanone derivative	12	dimethyl-dimethanolbenzene		

Figure 4: Pyrolysis Products of Solids Produced from Stressed Surrogate JP-8 Fuel

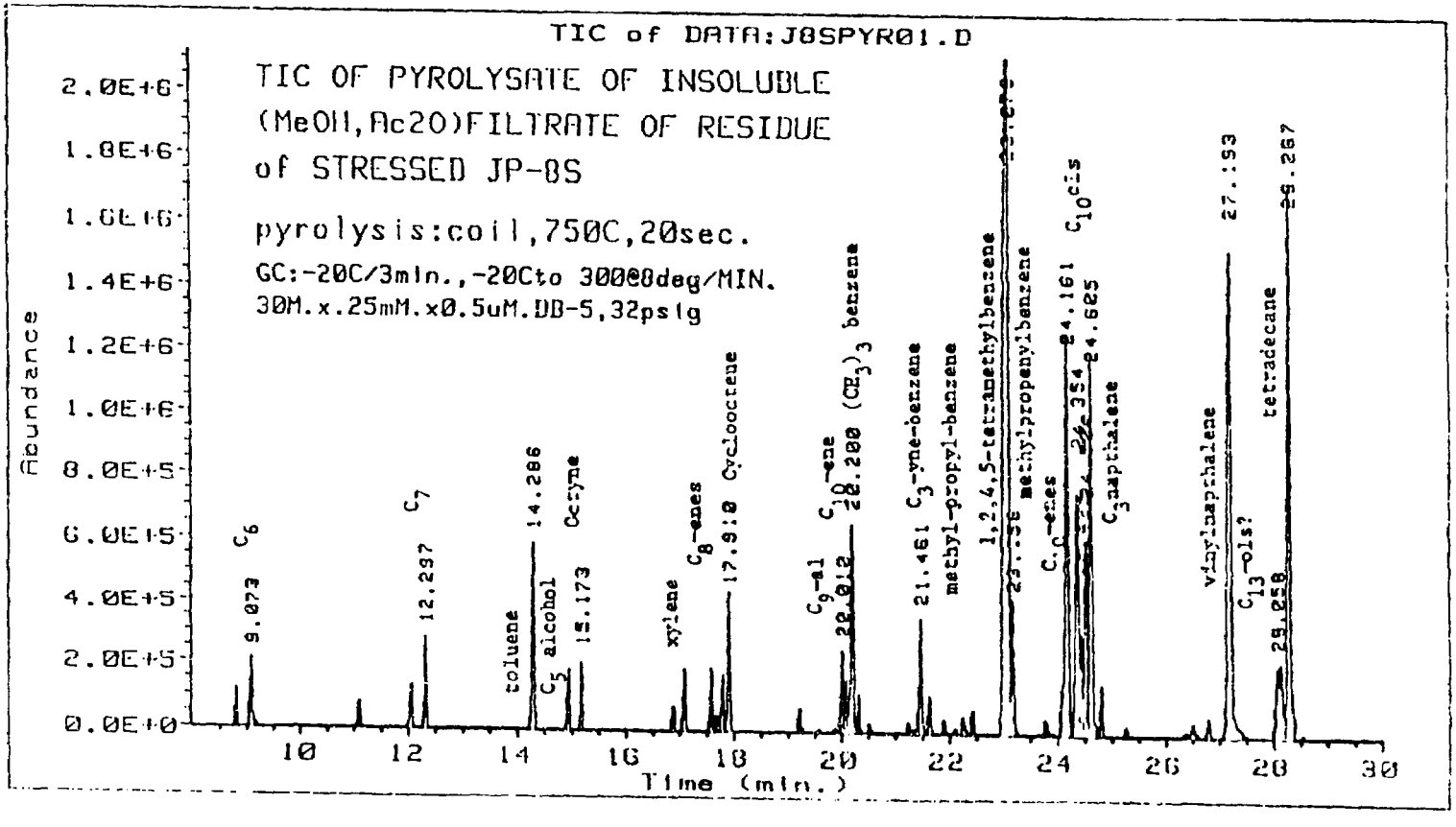

Figure 5: Total Ion Chromatogram of Thermally Desorbed Solid Deposit formed by JP-8 Surrogate Stressed 20 hrs. at 175°C. (Incomplete peak identification discussed in text.)

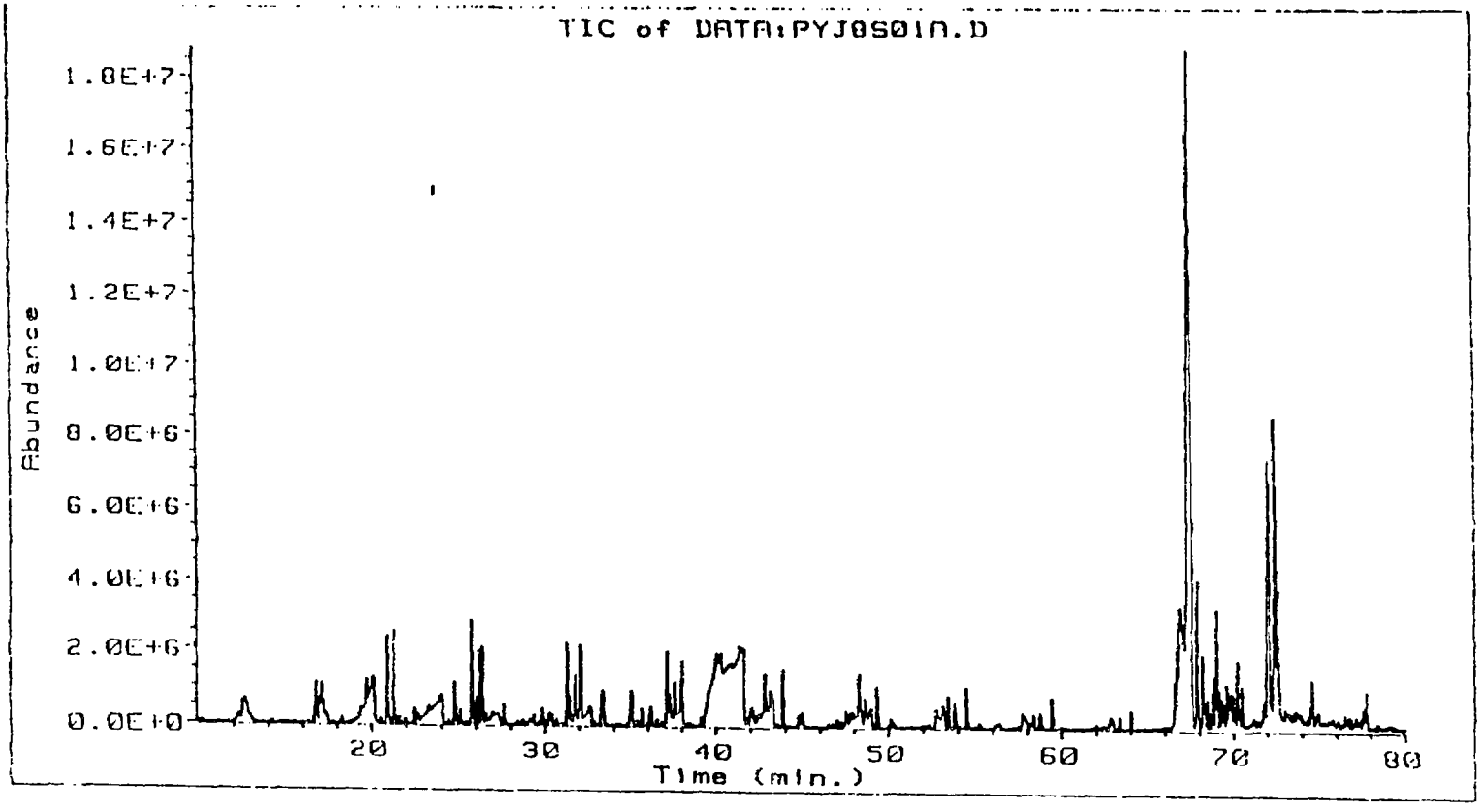

APPENDIX F

EXPERIMENTAL STUDIES ON DEPOSIT FORMATION IN JP FUELS AT HIGH TEMPERATURES

by

Arthur H. Lefebvre
School of Mechanical Engineering
Purdue University, W. Lafayette, Indiana

EXPERIMENTAL TECHNIQUES FOR THE ASSESSMENT OF FUEL THERMAL STABILITY (AIAA Paper No. 92-0685)

by

J. S. Chin and A. H. Lefebvre
Purdue University, W. Lafayette, Indiana

TEMPERATURE EFFECTS ON FUEL THERMAL STABILITY (ASME Paper No. 91-GT-97)

by

J. S. Chin and A. H. Lefebvre
Purdue University, West Lafayette, Indiana

and

F. T. Y. Sun
Gas Turbine Fuel Systems Division Parker Hannifin Corp.
Cleveland, Ohio

INFLUENCE OF FLOW CONDITIONS ON DEPOSITE FROM HEATED HYDROCARBON FUELS (ASME Paper No. 92-GT-114)

by

J. S. Chin and A. H. Lefebvre,
Purdue University, West Lafayette, Indiana

Final Report on UDRI Subcontract No. RI-75852X (Prime Contract No. F33615-87-C-2767) as Submitted by Purdue University, West Lafayette, Indiana.

EXPERIMENTAL STUDIES ON DEPOSIT FORMATION IN JP FUELS AT HIGH TEMPERATURES

OBJECTIVES

The main objective of the Purdue Subcontract was to obtain baseline experimental data on the effects on deposition rates of the following parameters.

Fuel Chemical Properties
Fuel Additives
Surface Composition
Fuel Physical Properties
Flow Conditions

It was known at the outset that none of the existing experimental techniques for the assessment of fuel thermal stability was satisfactory. All were of the "pass/fail" variety or were prone to inaccuracies and inconsistencies in the results obtained. It was imperative, therefore, to develop new and improved laboratory techniques to meet the requirements of the contract. Much time and effort has been spent throughout this investigation in designing suitable techniques to meet the various test requirements, and in the continual development and refinement of those techniques. Consequently, they are described in great detail in the following sections.

EXPERIMENTAL METHODS

The problems arising from the thermal decomposition of aviation fuels are manifested in different ways depending on the temperature-time history of the fuel, the local fuel and wall temperatures, and the flow conditions of pressure, velocity, and turbulence. Thus no single technique for the assessment of fuel thermal stability can hope to achieve universal acceptance.

Much of the experimental data published in recent years in the area of fuel thermal stability was obtained using the "constant heat flux" method as developed at the United Technology Research Center (UTRC) [1,2]. Analysis of this method revealed some drawbacks which provided the incentive for the development of the Purdue "fuel recirculation" and "single-pass" techniques. All of the research carried out at Purdue in the fulfillment of this subcontract employed one of these two techniques.

UTRC CONSTANT-HEAT-FLUX METHOD

In this method, fuel flows through a 2.4 m length of thin-walled tubing (2.37mm internal diameter) that is heated by an electric current passing through it. Since the electrical resistance of the tube material does not vary significantly with temperature, the local heat flux remains sensibly constant along the tube. After completion of the test, the tube is cut into short sections and the mass of carbon in each section is determined. A significant feature of this technique is that, because the local heat flux remains constant, the thermal resistance created by the presence of deposit on the inside wall of the tube causes the outer wall temperature to increase locally. This means that the local wall temperature is always a function of the local deposit thickness; where the deposit is thicker, the wall temperature must be higher to maintain the same heat flux through the tube wall. In some cases, the buildup of deposit during an extended test

run can create wall temperatures as high as 1000K. Such high wall temperatures are unrealistic from a practical standpoint, nor do they have any fundamental significance because, once a substantial thickness of deposit has accumulated, the local wall temperature bears no relationship to either the local fuel temperature or the temperature of the soft carboneous material formed at the interface between the solid deposit and the flowing fuel.

CONSTANT-WALL-TEMPERATURE METHODS

Two different methods for assessing the thermal stability of liquid hydrocarbon fuels have been developed. A key feature of both methods is that the heated tube through which the fuel is passed is maintained at a constant temperature throughout the test. This is in marked contrast to the constant-heat-flux approach whereby the heat flux through the wall is kept constant and the wall temperature is allowed to rise as deposits build up on the inner tube wall.

Research carried out using this method has employed a closed-loop system in which the fuel under test is recirculated continuously through a heated tube for periods ranging from 6 to 22 hours. The other system is a single-pass device whereby the test fuel flows only once through the heated tube and is then discarded. With both methods, the rates of deposition on the tube walls are measured by weighing the tube before and after each test.

Recirculation Method

During the course of this contract, various modifications to the original apparatus were made as part of an ongoing effort to improve the accuracy and consistency of the experimental data, and to provide the best simulation of the deposit formation process in a real aircraft situation. The apparatus in its present form is shown schematically in Fig. 1[3]. [Note: Fig. 1[3] means that the figure in question appears as Fig. 1 in reference 3 which is presented in complete form as an appendix to this report, thus avoiding needless duplication of figures.] It is a closed-loop system, designed to recirculate fuel over wide ranges of temperature, pressure, and flow rate. The major components are the pump, accumulators to contain the test fuel, a fuel heater, a heated test section, a fuel cooler, a flow meter, and another meter for monitoring the pressure drop across the test section. In operation, the test fuel flows from a high-pressure accumulator through the flow meter and fuel heater into the test section; from the test section it flows via a water cooler into the low-pressure accumulator. The function of the pump is to transfer fuel from the low-pressure accumulator to the high-pressure accumulator. The pressures in both accumulators can be set to any desired values, up to a maximum of 4.1MPa (600 psia), by using air from a high-pressure container. The fuel heater is in close proximity to the test section in order to minimize the amount of time the fuel spends at high temperatures outside the test section. The fuel cooler is fitted immediately downstream of the test section for the same reason. Typically, the fuel is returned to the low-pressure accumulator at a temperature of around 340 to 350 K.

The main component of the test section is a thin-walled stainless-steel tube whose principal dimensions are: length, 152mm; outer diameter (O.D.), 3.07mm; and inner diameter (I.D.) 2.15mm. This tube is clamped between two copper segments, as illustrated in Fig. 2[3]. The semicircular grooves cut into the two copper segments are designed to provide good thermal contact between the tube and the copper segments when the latter are clamped together. A number of thermocouples are threaded through one of the copper segments in such a manner that in operation the thermocouple beads are pressed tightly against the stainless-steel tube. These thermocouples are used to measure tube-wall temperatures at inlet and outlet, and at four equispaced stations in-

between. Fuel temperatures are measured only at the tube inlet and outlet. The stainless-steel tube is heated by using between one and four 1,000W electrical rod heaters which are inserted into holes drilled into the copper segments, as shown in Fig. 2[3]. This arrangement ensures that the tube is heated uniformly around its circumference, even when only one electrical heater is operational.

For any given fuel, the fuel pressure and flow rate are set at suitable values and the heaters for the fuel and test section are both switched on. During the fuel heatup period, which is usually less than ten minutes, the flowing fuel bypasses the test section. When the fuel and tube-wall temperatures have both attained the desired values, the bypass valves are operated to divert the hot fuel through the test section. At the same time the water supply to the fuel cooler is turned on.

The main advantage of this procedure is that it allows the start of the test to be clearly defined. Another useful feature is the feedback between the fuel and tube-wall thermocouples, and the fuel and test section heaters, respectively, which allows both fuel and tube-wall temperatures to be maintained at preset values within 1°C for the duration of the test. This flexibility allows tests to be carried out on the influence of fuel temperature on deposition rates while maintaining a constant wall temperature. Alternatively, fuel temperature can be kept constant to permit the separate effects of variations in wall temperature on deposition rates to be studied.

Deposition rates are determined by weighing the tube before and after each test. The fuel supply connections at both ends of the tube are sealed using graphite ferrules. These ferrules are broken off after each test to reduce weight and thereby increase the ratio of deposit mass to tube mass. The weight of the tube is around 4000mg. The deposits usually weigh between 2 and 20mg (depending on the fuel composition and test conditions) but, for very high temperatures, the deposit can weigh as much as 100mg. As the balance employed has an accuracy of within 0.1mg, the weighing procedure is considered capable of giving satisfactory results.

One of the most important aspects of the test procedure is the treatment of the test tube both before and after each test run. Before weighing the tube prior to test, it is exposed to a welding torch flame to remove any oil or grease remaining from the extrusion process used to manufacture the tube. After the tube has been immersed in a solvent (stanisol) for 24 hours, it is "dried" by flowing heated air through it for a few minutes. It is then allowed to dry naturally for another 24 hours before being weighed for the first time. Twenty-four hours later the tube is weighed again; this process is repeated until the tube weight indicates a constant value to within 0.1mg. Tube treatment after the test is even more important and more critical to the repeatability and accuracy of the experimental data. The procedure now being used is based on detailed considerations of all the factors that experience has shown can influence the results obtained. After each test, the fuel is drained from the system and the test section is allowed to cool to a temperature of around 450K. Where necessary, water cooling is applied to the copper segments to accelerate the cooling process. Experience has shown that if the tube-wall temperature is too high (>470K), any residual fuel remaining in the tube will "bake" onto the wall, thereby creating more deposit. On the other hand, if the wall temperature is too low (<430K), the residual fuel does not fully evaporate but is gradually absorbed into the porous structure of the deposit. When the tube-wall temperature has fallen to 450K, heated air is passed through the system for around five minutes. This air bypasses the test section, but the valve at the downstream end of the test section is left open so that air and vapor are drawn continuously out of the tube by the ejector action of the flowing air. The test section is then allowed to cool to normal room temperature, after which the tube is removed from the test section and placed in a vertical position to dry naturally for 24 hours before being weighed for the first time. This weighing procedure is repeated every 24 hours until the difference between two consecutive weights is within 0.1mg. For small deposits, 48 hours of natural drying in a

vertical position is usually adequate but, for larger deposits, up to 144 hours may be needed (as illustrated in Figs. 3[3] and 4[3] for two aviation kerosene fuels). Some typical results obtained using the fuel-recirculation technique are shown in Fig. 5[3].

Single-Pass Method

The main advantages of the fuel-recirculation method described above are that it requires only a small amount of test fuel and it simulates quite closely the deposition process in an aircraft fuel system. However, it is less attractive for basic studies on the effects of fuel composition, fuel temperature, tube-wall temperature, and Reynolds number on deposition rates due to the gradual depletion with time of the oxygen contained in the fuel. To provide more basic information on the effects of fuel properties and flow conditions on deposition rates, a single-pass flow system has been designed and tested. The main features of this new facility are shown in Fig. 6[3]. The main components are feed tanks (which contain the test fuel), a fuel heater, a heated test section, a flow meter, and another meter for monitoring the pressure drop across the section. In operation, the test fuel flows through the flow meter and fuel heater, into the test section, then into a capture tank. The pressure can be set to any desired value, up to a maximum of 4.1MPa (600psia), by using air from a high-pressure container.

The test section, instrumentation, tube preparation, and weighing procedures are virtually identical to those employed in the recirculation method. For any given fuel, the fuel presure and flow rate are set at suitable values and the heaters for the fuel and test section are both switched on. During the fuel heat-up period, the flowing fuel bypasses the test section. When the fuel and tube-wall temperatures have both attained the desired values, the bypass valves are operated to divert the hot fuel through the test section. Deposition rates are again determined by weighing the tube before and after each test. The deposits usually weigh between 2 and 20mg, depending on the fuel composition and test conditions. Generally, it is found that 10 to 15 U.S. gallons of fuel are required for each test, as compared with 1.5 U.S. gallons for the recirculation method.

At an early stage in the development of a suitable test facility for the assessment of fuel thermal stability, it was recognized that the cleanliness of the fuel preheater could influence the amount of deposit formed in the test tube. To minimize this potential problem, the following routine cleaning procedure was devised. After each test run, the fuel preheater is switched off and the test section bypassed; however, fuel is still allowed to flow through the system to absorb the heat remaining in the preheater tube. In this manner, the preheater wall temperature gradually declines until the fuel acquires a temperature which is appreciably lower than its temperature during an actual test. After the fuel temperature at the outlet of the preheater has fallen to between 300 and 340K, cleaning air is directed through the system with the preheater switched on. This air is heated to around 470K in the preheater and flows out at fairly high velocity. The purpose is to remove any deposit formed on the preheater walls during the test run by reheating the preheater tube in the presence of hot flowing air. This procedure usually takes from 20 to 30 minutes, and is repeated several times until the system is considered clean enough to have no influence on the deposit formed in the test tube during the next test run. Essentially, the procedure consists of two steps; a) using fuel to absorb the residual heat in the preheater, and b) using air heated by the preheater to remove the deposit from the preheater wall. This cleaning procedure is checked periodically by dismantling the preheater tube and inspecting its surface for any trace of deposit. No deposit has yet been found, so the cleaning procedure is considered satisfactory.

Some of the data obtained using the single-pass technique are presented in Fig. 5[3]. This figure shows the influence of tube-wall temperature on deposition rates for a kerosene-type fuel flowing at an inlet temperature of 523K, a flow rate of 100 ml/min,

and a pressure of 0.69MPa (100 psia). It should be noted that this pressure would be considered too low for tests on more volatile fuels. To prevent fuel boiling or partial vaporization at high-fuel-temperature conditions, tests are normally carried out at a pressure of 2.52MPa (350psig). Corresponding data obtained by the recirculation method are shown in the same figure for the purpose of comparison. It is clear from Fig. 5[3] that the recirculation method gives the lowest deposit rate, particularly when the wall temperature is high. If the objective were to simulate the situation in an aircraft fuel system involving partial recirculation of fuel back to the wing tank, the single-pass mode would indicate a higher deposit rate than would be obtained in practice.

RELATIVE MERITS OF DIFFERENT METHODS

Although the constant-heat-flux method has been used extensively to determine the thermal stability and heat transfer characteristics of aircraft fuels, it has a drawback in that over most of the tube length the local wall temperature changes markedly during the test period. The constant-temperature method is free from this defect because the wall temperature is controlled to within 1°C of the nominal value throughout the entire test period. This means that the heat transfer from the wall to the fuel diminishes with the buildup of deposit, which is exactly what happens in aircraft fuel systems and engine fuel nozzles. Also, exercising separate control over fuel and wall temperature allows the effects on deposition rates of variations in these two parameters to be clearly distinguished.

The fuel-recirculation method provides the closest simulation to the actual conditions in an aircraft fuel system. Although not shown in Fig. 1[3], the test facility does in fact incorporate provisions to allow the system to operate in a partial recirculation mode, whereby part of the total fuel flow passes through the test section and the remainder is heated but then diverted back into the fuel tank. This mode of operation has the potential for providing an even better simulation of the actual aircraft fuel system, but no systematic measurements of deposit rates have yet been carried out using this approach.

A major asset of the recirculation method is its very low fuel requirement of only 1.5 U.S. gallons per data point. This represents an appreciable savings in cost, and is particularly advantageous when using specially prepared expensive test fuels or other fuels that are in short supply. Its main drawback is the gradual depletion of fuel-dissolved oxygen throughout the test. This deficiency can be alleviated by continuously bubbling small quantities of air into the fuel contained in the low-pressure accumulator. The system employed is shown schematically in Fig. 1[3]. The air injection tube is located near the bottom of the low-pressure accumulator, and air is bubbled into the fuel through 20 holes, each 0.5mm in diameter. However, although this simple system functions efficiently as an oxygen-replenishment device, it introduces another variable into the system. Figure 7[3] shows measured values of deposition rates for a light fuel oil at three different air-bubbling rates. The general tendency is for deposition rates to increase with an increase in air flow rate, the effect becoming less pronounced at the higher air flow rates.

In practice, a few preliminary tests were carried out to determine the air-bubbling flow rate needed to ensure that the recirculation method gives the same deposition rate as the single-pass method for the same fuel and test conditions. This procedure virtually eliminates the problem of oxygen depletion which hitherto has been regarded as a deficiency of the recirculation method.

There are other ways in which the dependence of deposition rate on air-bubbling flow rate can be used to advantage. For example, when carrying out comparative tests on

different test fuels, the fuel which is anticipated to have the highest thermal stability is usually known at the outset. An air-bubbling flow rate is then established for this fuel which is the minimum needed to produce a small but accurately measurable deposit. This same bubbling rate is then used for the remaining test fuels.

The recirculation and single-pass methods both have good potential for providing fairly precise information on the thermal properties of the deposits that govern the rate of heat transfer between the flowing fuel and the adjacent tube wall. Figure 8[3] illustrates the manner in which the temperature rise experienced by the fuel as it flows through the heated tube varies with time. Initially the tube wall is perfectly clean and the fuel temperature rise is relatively high. With the passage of time, the accumulation of deposit on the tube wall creates a thermal barrier between the tube and the flowing fuel which gradually diminishes the heat flux from the tube to the fuel, thereby causing a continuous decline in the temperature rise of the fuel, as illustrated in Fig. 8[3].

If more were known about the physical structure and thermal properties of the deposit, data of the type shown in Fig. 8[3] could be used to develop an elegant and accurate method for the measurement of deposition rates. Even without this information, these data are of interest and value to the designers of fuel/oil heat exchangers. Not only do they illustrate the manner in which the slow but continuous buildup of deposit leads to a gradual reduction in the amount of heat transferred to the fuel, but they also enable this deterioration in heat transfer efficiency to be determined quantitatively.

In summary, the "constant-wall-temperature" recirculation and single-pass methods have significant attributes for both fundamental and practical studies on fuel thermal stability. Both methods were used in this program to study the effects of fuel composition and flow conditions on deposition rates.

INFLUENCE OF FUEL PREHEATER ON DEPOSITION RATES

A series of tests was carried out to examine the effect of the cleanliness of the preheater system on the measured rates of carbon deposition in the test tube. It has been argued that the same mechanisms that are responsible for the deposits formed in the test tube might also cause some deposition to occur on the inner surface of the preheater tube. Any such deposits would pose no problem provided they adhered to the wall; however, the question was raised as to whether some of the deposited material might become detached from the wall and flow out of the preheater and into the test tube, either during a test run or soon after shutdown. Should this occur, some of these preheater deposits might adhere to the test-tube wall, thereby causing an erroneous measurement of the deposits formed solely within the test tube.

To investigate this possibility, the following test runs were made.

1. Measurements of deposition rates were made after a five-hour run, ten-hour run, and fifteen-hour run. Test tubes that were initially clean were used in all three tests.
2. An initially clean tube was run for five hours. After cleaning the preheater, the same tube was run for another five hours.
3. An initially clean tube was run for ten hours. The preheater was cleaned and the same tube was run for another five hours.

All tests were carried out with kerosene fuel at the following conditions.

Fuel temperature	=	473K
Wall temperature	=	473K
Pressure	=	350 psig
Fuel flow rate	=	150 ml/min

The test tubes employed were manufactured from stainless steel (400 series) to the following dimensions

I.D.	=	2.59mm
O.D.	=	3.08mm
Length	=	174mm

The results obtained are shown plotted in Fig. 1. They demonstrate that the mass of deposits formed within the test tube increases linearly with time regardless of the number of times the preheater is cleaned during the total test period. These results suggest that, providing the preheater is cleaned at the end of each test run, the problem of preheater deposits becoming detached and adhering to the test tube should not arise.

INFLUENCE OF FUEL TEMPERATURE HISTORY ON DEPOSITION RATES

Under certain aircraft operating conditions, it is possible for the fuel to be heated and cooled several times before being finally consumed in the engine combustor. Thus, the question arises as to what extent deposition rates are affected by a fuel's preheating history. Tests to examine the influence of previous fuel heating on deposition rates were conducted using the single-pass test facility. The fuel employed was a light hydrocarbon blend with physical and chemical properties that lie between those of kerosene and DF2. The amount of deposition formed was obtained by weighing the test tube before and after each test run. A clean tube was used for each test.

The test-tube-wall temperature was maintained at the same value as the fuel temperature. Throughout the entire test program, the pressure and fuel flow rate were maintained at constant values of 350 psig and 100 cc/min respectively.

The results obtained are shown in Fig. 2. At the lowest fuel temperature examined (413K), the amount of deposit formed was extremely small, even though the test duration was extended from the standard value of five hours to 15 hours. At this low temperature, the average deposition rate was always less than 2 $\mu g/cm^2.hr$, regardless of the amount of fuel preheating. Raising the fuel temperature to 473K and then to 523K produced the results shown in the upper part of Fig. 2. For a fuel temperature of 473K, the average rate of deposition was around 250 $\mu g/cm^2.hr$. Increasing this temperature by 50K to 523K caused a dramatic increase in the amount of deposit formed (as shown in Fig. 2), further highlighting the important effect of fuel temperature on deposition rates. For clean, new fuel, the average deposition rate over a five-hour period was 2000 $\mu g/cm^2.hr$. For fuel which had been subjected to three previous preheatings, the average rate of deposition was 7,500 $\mu g/cm^2.hr$. The general conclusion to be drawn from these tests is that previous preheating history has little or no effect on deposition rates at low fuel temperatures (approximately 413K). With an increase in fuel temperature, the effect of previous fuel heating becomes more significant. For a fuel temperature of 523K, the rate of deposition for a fuel which has been heated to the same temperature on three previous occasions is almost four times higher than for new fuel.

It is believed that two different mechanisms are responsible for the trends shown in Fig. 2. One is the gradual depletion of the oxygen contained in the fuel. During the 12-hour period that the fuel "sits" between each test run, it recovers from the atmosphere some, but not all, of the oxygen consumed in the previous test run. This gradual reduction in fuel oxygen content tends to reduce the rate of deposition. However, at high fuel temperatures this effect is outweighed by the production of intermediate products which remain in the fuel after each test. The concentration of these dehydrogenated products increases with each test run. Thus, when the fuel has been heated more than once, the deposition rate is enhanced by the residual intermediate products from previous test runs.

The presence of these intermediate products is indicated by a discoloration of the fuel. Fuel which has not encountered temperatures higher than 413K retains its original color regardless of the number of test runs. At higher fuel temperatures, the fuel gradually becomes darker as the number of test runs is increased. This is especially true for the fuel heated to 523K. Samples of the fuel, before and after each test run, have been retained should a chemical analysis be considered desirable at some future date.

In a related series of experiments, carried out several months after the tests reported above, the effect of preheater exit fuel temperature on deposition rates was examined. In all runs, the fuel temperature at entry to the test section was maintained constant at 473K and equal to the tube-wall temperature. For the first test, the preheater exit temperature was also 473K. However, for the next two tests, the fuel temperature at the preheater exit was raised to 513K in one case and to 553K in the other. In both cases the fuel was water-cooled to 473K at entry to the test section. The results of these experiments are shown in Fig. 3.

From inspection of this figure, it is clear that a fuel's recent temperature history has a small but noticeable effect on deposition rates. For a preheater outlet temperature of 473K, the deposition rate is around 30 $\mu g/cm^2.hr$. Raising the preheater exit temperature from 473K to 513K and then to 553K caused deposition rates to first increase to 40 $\mu g/cm^2.hr$., then decrease to 20 $\mu g/cm^2.hr$. This result is fully consistent with all other observations on the effect of fuel temperature on deposition rates. An increase in fuel temperature is always accompanied by an increase in deposition rates until a certain critical temperature is reached beyond which any further increase in fuel temperature causes deposition rates to decline. The reason for this occurrence is discussed in a subsequent section which deals specifically with the effect of fuel temperature on deposition rates.

EFFECT OF TUBE-WALL TEMPERATURE

The important role played by temperature in the processes of fuel thermal degradation and deposit formation has been known for some time. In view of the prime importance of temperature to fuel thermal degradation and deposit formation, it is somewhat surprising to find in the literature that in most experimental studies the only temperature recorded is either fuel temperature or wall temperature but not both. In some reported studies on the influence of temperature on thermal stability, it is not clear whether the temperature under consideration is that of the fuel or the wall. Thus, it is easy to understand the considerable scatter that tends to characterize reported experimental data on the effect of temperature on deposition rates.

The influence of wall temperature on deposition rates has been examined by several workers. TeVelde and Glickstein [1] used a heated-tube apparatus to evaluate the thermal stability characteristics of four liquid hydrocarbon fuels: a low aromatic JP 5, a blend of 80 percent JP 5 and 20 percent cracked-gas oil, a blend of 50 percent JP 5 and 50 percent No. 2 heating oil, and a shale-derived JP 5. Deposit formation rates were

obtained for tube-wall temperatures ranging from 480 to 800K. The deposition characteristics of all four fuels were found to be very sensitive to wall temperature, with peak formation rates occurring at surface temperatures around 650 K, as illustrated in Fig. 4[4]. Examination of these data led TeVelde and Glickstein to the conclusion that the effect of tube-wall temperature on deposit temperature was "similar for all four fuels, that is, formation rates increased rapidly with increasing surface temperature up to approximately 700 to 750°F (644 to 672K) and then decreased with further increases in surface temperature."

This result, along with other data in the literature obtained using the constant heat flux method, all suffer from the drawback that they were acquired under conditions for which it is difficult to differentiate between the effects of wall temperature and fuel temperature on deposition rates. In reality, the shape of the curve shown in Fig. 4[4] may more aptly describe the effect on deposition rates of variations in fuel temperature than variations in wall temperature. In fact, for this particular apparatus, after several hours of operation the local wall temperature at any point along the tube length is much more indicative of the local deposit thickness than the local rate of deposition.

The Purdue constant-wall-temperature methods are free from these defects. The fuel temperature at entry to the test tube is governed by a preheater and is accurately controlled to within $\pm$ 0.5°C. The temperature rise experienced by the fuel as it flows through the tube is always quite small and seldom exceeds 10°C. The tube-wall temperature is always maintained at a constant value throughout its entire length. By exercising separate control over fuel and wall temperatures, the effects on deposition rates of variations in these two parameters can be clearly distinguished.

Some of the results obtained with this apparatus on the effect of wall temperature on deposition rates are shown in Fig. 6[4]. They illustrate the effect of wall temperature on deposition rates for a JP 8 fuel at a constant temperature of 523K. The data are consistent with all other data obtained with this apparatus in showing a continuous increase in deposition rate with an increase in wall temperature for a constant fuel temperature.

The effect of wall temperature on deposition rates is further illustrated by the results obtained using a kerosene-type fuel containing 48 percent aromatics, as shown in Fig. 7[4]. These results clearly demonstrate the marked influence of wall temperature on rates of deposition and also show that this influence becomes more pronounced when an increase in wall temperature is accompanied by an increase in fuel temperature. This highlights the need for separate control of fuel temperature in experimental studies on the effect of wall temperature on deposition rates.

EFFECT OF FUEL TEMPERATURE

The considerable body of research carried out on fuel thermal stability has yielded much useful information on the various mechanisms involved in the fuel degradation process, and also on the manner and extent to which thermal oxidation stability is influenced by the physical and chemical properties of the fuel. Thus, it is now known that, for conventional aviation fuels, the degradation process normally stems from oxidation of the fuel by dissolved oxygen in the fuel. This is the primary mechanism in initiating deposit formation. Oxidation products subsequently react with minor fuel constituents and with each other to generate the insoluble materials that deposit on fuel system surfaces. At fuel temperatures higher than around 700K, fuel pyrolysis starts to influence deposition rates and, with further increases in fuel temperature, the reaction mechanism gradually changes from oxidation-controlled to pyrolysis-controlled which causes the rate of deposition to decline. Thus, in discussing the influence of temperature on deposit formation, it is important to bear in mind that the fuel temperature

determines which reaction mechanism is dominant (oxidation or pyrolysis) not the tube-wall temperature.

The pronounced effect of fuel temperature on thermal stability is well illustrated in Fig. 8[4]. The results shown in this figure generally confirm the findings of all previous studies on the influence of fuel temperature on thermal stability. They show, for all three fuels, that deposition rates are relatively low for fuel temperatures below around 400K, but rise steeply with increases in fuel temperature above around 500K. From inspection of Figs. 7[4] and 8[4], it is clear that, over the ranges of fuel and wall temperatures investigated, both of these parameters strongly affect thermal stability although the influence of fuel temperature is more pronounced than that of wall temperature. However, it should be noted that the apparent dominance of fuel temperature over wall temperature may be due in some measure to the fact that the thermal degradation reactions are influenced by fuel temperature throughout the whole test period, whereas wall temperatures can affect these reactions only during the much shorter residence time of the fuel in the test section.

Another explanation for the observed strong influence of fuel temperature is that deposition rates are governed primarily by the temperature of the fuel in the relatively slow-moving boundary layer near the tube wall. This temperature is dictated mainly by the bulk temperature of the fuel (as illustrated in Fig. 8[4]) but is also strongly affected, albeit to a lesser extent, by the adjacent wall temperature which serves to raise or lower the fuel temperature in the boundary layer depending on whether the wall temperature is higher or lower than the fuel temperature.

As discussed earlier, for any given hydrocarbon fuel an increase in temperature always results in increased deposition until a certain critical temperature is reached. Above this critical temperature, whose value depends on several factors including wall temperature and fuel composition, an increase in fuel temperature causes the deposition rate to decline. Due to their relatively high thermal stability and the temperature limitation of the test facility, it was not possible to establish critical temperatures for the aviation fuels employed in this test program. However, the existence of this initial temperature could be demonstrated by switching to a fuel of appreciably lower thermal stability, as shown in Figs. 4 and 5.

Both figures show deposition rate plotted against fuel temperature for a light diesel oil. In one case, the fuel and wall temperatures were maintained at the same values so that an increase in fuel temperature was always accompanied by a corresponding increase in wall temperature; in the other case, wall temperature was kept constant at 623K, regardless of variations in fuel temperature. Although the number of data points in these two figures is insufficient to define the initial temperatures with any degree of certainty, they do suffice to demonstrate the existence of a critical temperature. Below this temperature, deposition rates are oxidation-controlled and, therefore, increase with an increase in temperature; above the critical temperature the deposition rates become increasingly pyrolysis-controlled and, consequently, lower.

INFLUENCE OF FLOW CONDITIONS

The work described in this report, along with many other studies carried out over the past 20 years, have provided a considerable body of information on the effects of fuel temperature, wall-surface temperature, and fuel composition on deposition rates. In contrast, the fluid dynamic aspects of the thermal stability problem have received comparatively little attention. The work described below represents an attempt to remedy this deficiency. It has direct application to the design of fuel injectors for gas turbine engines and, in fact, this phase of the project received some financial support from the Parker Hannifin Corporation of Cleveland, Ohio.

The single-pass test rig shown in Fig. 1[5] was chosen for this study. The relevant properties of the two fuels employed, DF-2 and Jet A, are given in Table 1[5]. The flow variables of principal interest for their influence on deposition rates are the pressure, temperature, and Reynolds number of the flowing fuel. The effect of fuel temperature has already been examined in some detail; therefore, the investigation focused on the effects of pressure and Reynolds number.

PRESSURE

In general, the results contained in the literature show little effect of fuel pressure on deposition rates. Vranos and Marteney [6] found no effect of pressure on deposition rates for No. 2 home heating oil or for Jet A fuel when the pressure was higher than 1.5 MPa (218psia). Marteney and Spadaccini [2] also reported for JP 5 fuel that a wide variation in pressure from 1.72 to 5.5 MPa (250 to 800 psia) had no effect on deposit formation rates. High pressure deposition tests were also conducted and reported by Roback et al. [7]. The fuel pressures generally exceeded 13.8 MPa (2000 psia). The results showed no significant change in wall temperature as a consequence of increasing pressure, suggesting that the rate of deposit formation was relatively independent of pressure over the pressure range from 13.8 to 34 MPa (2000 to 4930 psia). However, Watt et al. [8] reached rather different conclusions. According to these workers, the influence of fuel pressure, while not entirely consistent from fuel to fuel, was to diminish both local and total deposits with increasing pressure.

Some of the results obtained on the effect of pressure using DF 2 as the test fuel are shown in Fig. 2[5]. The data contained in this figure were obtained using a 400 series stainless-steel tube of length 152mm, O.D. 3.08mm, and I.D. 2.59mm. They show the average rate of deposition in $\mu g/cm^2.hr$ plotted against fuel pressure for a fuel flow rate of 250 ml/min and a test duration of six hours.

It is clear from Fig. 2[5] that above a certain minimum pressure the deposition rate is independent of fuel pressure. For the DF2 fuel used in these experiments, this minimum pressure is around 0.8 MPa (115 psia). A limited number of tests carried out on other fuels indicate that the minimum pressure may be higher or lower than 0.8 MPa, depending on the temperature and volatility of the fuel. In general, the minimum pressure above which pressure has no effect on deposition rates decreases with increases in fuel temperature and/or fuel volatility. This suggests that the low deposition rates associated with low fuel pressures may be the result of fuel boiling and the production of fuel vapor. Autooxidation deposit formation rates are lower in the vapor phase than in the liquid phase at the same temperature. Another effect of fuel boiling is to convert the normally smooth flow of fuel through the test section into a two-phase, turbulent flow of relatively high velocity. This produces a vigorous scrubbing action at the tube surface which tends to inhibit deposition and also remove any deposits that might otherwise form on the surface despite the adverse conditions. However, it should be noted that measurements of deposition rates for JP 4 and JP 5 fuels made by Szetela [9] led him to an opposite conclusion. He found deposits to be higher for JP 4; he attributed this to the fact that "boiling increases the deposition tendency." Clearly, the effect of fuel boiling on deposition rates merits further investigation.

Further evidence on the insensitivity of deposition rates to variations in fuel pressure above the critical value is presented in Fig. 3[5]. This figure illustrates the manner in which the temperature rise experienced by the fuel as it flows through the heated tube varies with time. Initially, the tube wall is perfectly clean and the fuel temperature rise is relatively high. With the passage of time, the accumulation of deposit on the tube wall creates a thermal barrier between the tube and the flowing fuel which gradually diminishes the heat flux from the tube to the fuel, thereby causing a continuous decline in the temperature rise of the fuel, as illustrated in Fig. 3[5]. Thus, the temperature rise

of the fuel provides a useful indication of the amount of deposition on the tube wall. Figure 3[5] shows that, for constant conditions of fuel temperature, wall temperature, and fuel flow rate, pressure has no effect on deposition rates for DF 2 over a pressure range from 0.8 to 2.5 MPa (115 to 363 psia).

REYNOLDS NUMBER

On aircraft fuel systems, as the fuel flows from the tank and through various engine components into the fuel nozzle, it experiences a variety of flow conditions corresponding to a wide range of Reynolds numbers. Therefore, it is of some practical interest and importance to examine the impact of variations in this flow parameter on deposition rates. For experimental purposes, Reynolds number can be varied readily by changing one or more of the following:

1. mass flow rate (velocity),
2. tube diameter, and/or
3. fuel temperature.

Unfortunately, variations in fuel temperature not only serve to change the Reynolds number, they also have a pronounced effect on the autooxidation reactions that promote deposition. This leaves mass flow rate and tube diameter as the only two practical options for achieving variations in Reynolds number. For the results presented in Fig. 4[5], the variation in Reynolds number was accomplished by varying the fuel flow rate. The four curves shown in this figure correspond to the following conditions.

(a) Fuel - DF 2
$T_F = 473K$, $T_W = 623K$, $P = 2.5$ MPa
$\dot{m}_{VF} = 100 - 400$ ml/min
Stainless-steel tube, 400 series. I.D. = 2.59mm, O.D. = 3.08mm

(b) Fuel - DF 2
$T_F = 413K$, $T_W = 563K$, $P = 2.5$ MPa
$\dot{m}_{VF} = 150 - 400$ ml/min
Stainless-steel tube, 400 series. I.D. = 2.59mm, O.D. = 3.08mm

(c) Fuel - Kerosene
$T_F = 523K$, $T_W = 673K$, $P = 2.5$ MPa
$\dot{m}_{VF} = 50 - 200$ ml/min
Stainless-steel tube (316) I.D. = 2.10mm, O.D. = 3.08mm

(d) Fuel - DF 2
$T_F = 413K$, $T_W = 413K$, $P = 2.5$ MPa
$\dot{m}_{VF} = 150 - 400$ ml/min
Stainless-steel tube, 400 series. I.D. = 2.59mm, O.D. = 3.08mm

Inspection of the above table shows that in Cases (a), (b), and (c) the wall temperature was 150°C higher than the fuel temperature; in Case (d), the fuel and tube wall were both at the same temperature. In all cases, regardless of fuel type, fuel temperature, or wall temperature, it was found that the effect of variation in Reynolds number on deposition rate (D.R.) could be expressed as:

$$\text{D.R.} = \text{constant} \cdot \text{Re}^{0.65} \ . \qquad (1)$$

The effect on deposition rates of a change in Reynolds number caused by a change in tube diameter is illustrated in Fig. 5[5]. This figure contains the same data shown as (d) in Fig. 4[5], plus additional data obtained for the same fuel at the same conditions of

pressure and temperature, but with the tube I.D. increased from 2.59 to 4.60mm. Figure 5[5] shows that both sets of data tend to fall on the same curve which conforms to the relationship:

$$D.R. = 0.48\ Re^{0.65} . \tag{2}$$

This increase in deposition rate with increase in Reynolds number is attributed to the higher heat transfer between the wall and the fuel and the higher transverse velocity components which are more effective in transporting material from the mainstream fuel flow to the tube walls.

Interest is sometimes expressed in the amount of deposit produced by a given mass of fuel. To examine this situation, a "deposit index" (D.I.) is first defined as:

$$D.I. = \frac{\text{mass of deposit per unit length of tube}}{\text{mass of fuel}} = \frac{\mu g/cm}{kg} . \tag{3}$$

Also, we have:

$$Re = \frac{\rho U d}{\mu} = \frac{4}{\pi} \cdot \frac{\dot{m}_{VF}}{d\nu} . \tag{4}$$

By appropriate combinations of Eqs. (1), (3), and (4), the following relationships between D.R., D.I., and Reynolds number are derived:

$$D.R. \propto Re^{0.65} , \tag{1}$$

$$D.I. \propto Re^{-0.35}\ \mu^{-1}, \text{ and} \tag{5}$$

$$\frac{D.R.}{D.I.} \propto Re\ \mu . \tag{6}$$

Figure 6[5] shows D.I. plotted against Reynolds number for DF 2 fuel flowing through a 400 series stainless-steel tube having an I.D. of 2.59mm and an O.D. of 3.08mm. One practical implication of the results presented in Figs. 5[5] and 6[5] is that for any given fuel flow rate a reduction in tube diameter will cause an increase in deposit thickness. However, it should be noted that in these experiments on the effect of Reynolds number on deposition rates, the flow velocity was always less than a few meters per second. With continual reduction in tube diameter, the scrubbing action along the tube walls could eventually reach a point at which any further increase in flow velocity would cause deposition rates to decline.

INFLUENCE OF THERMAL INSTABILITY ON FILTER DEPOSITS

In September 1981, some interesting results were obtained with the Wright-Patterson Phoenix rig when testing additives of the detergent/dispersant type. When JFA-5 was added to a fuel, it greatly reduced the deposits on the hot test section tube but significantly increased the plugging of the cool filter downstream. To answer some of the questions raised by this result, two fuels were examined: Jet A-1 without additive and

Jet A-1 with additive (JFA-5 11μg/liter) for their rates of deposition on fuel filters.

The test facility employed in this investigation is shown schematically in Fig. 6. Preliminary tests soon revealed that in order to compare fuels for their effect on filter deposits, close attention must be paid to system cleanliness. Only under conditions where it is completely certain that nothing is deposited on the filter from the system upstream can fuels be compared. Thus, a necessary conditions for any comparative test is that there should be no deposits on the filter, nor any change of filter ΔP, when new cold fuel is passed through the system and the filter.

It was also found that the porosity of the filter had a significant effect on the results obtained. For example, when a filter of 230 μm porosity was used, no change in ΔP was observed regardless of the cleaning method employed. Also, no deposit was formed. With a 230–μm filter, the hole sizes are so big that anything in the fuel, no matter what its source, can always pass through the filter without producing any deposit. The fact is that, the finer the filter, the cleaner the system must be to avoid any spurious deposit.

An analysis was conducted to shed light on the relationship between the deposit formed (as shown by the filter weight increase, ΔW) and the change in pressure drop, ΔP. The result of this analysis showed that the deposit formed after time t was related to the maximum deposit formed by the expression:

$$\frac{\Delta W}{\Delta W_{max}} = \frac{(\Delta P_t)^{0.5} - (\Delta P_o)^{0.5}}{(\Delta P_t)^{0.5} - 1} . \qquad (7)$$

For the 60-μm filter, ΔP_o is 1.5 psi for a flow rate of 150 ml/min. For a maximum deposit weight of 90 mg, the curve of predicted deposit weight vs. pressure drop, ΔP_t, is shown in Fig. 7, along with the measured values. These results indicate that quite a large amount of deposit can form in the 60-μm filter without causing a significant increase in filter pressure drop. Comparisons between fuels were made using two different filter porosities of 2 and 60 μm. For the 60-μm filter, the system shown in Fig. 6 was used, with the flow rate kept constant by frequent adjustment of the throttle valve. By measuring both the change of pressure drop across the filter and the final deposit weight (that is the weight increase of the filter element after the test), a comparison between fuels could be made. For a 2-μm filter, the system shown in Fig. 8 was used because it offered several advantages; (1) it reduced system effects to a minimum, and (2) it had no throttle valve. As nothing was changed deliberately during the test run, any change of flow rate was necessarily caused by deposit formation in the filter resulting directly from contaminants in the fuel. These contaminants could only have been generated by the prior heating of the fuel.

Comparison between fuels can also be made by keeping the pressure drop constant ($\Delta P = 350$ psia) and measuring the change of flow rate with time, also the final deposit weight.

The results obtained with a 60-μm filter showed that the additive JFA-5 reduced the deposition rate significantly, in fact, by a factor of three. At the same time it increased the filter deposit by 37 percent. The results obtained with a 2-μm filter showed that for the fuel with additive, the flow rate through the filter decreased more rapidly than for the fuel without additive. It was also found that the minimum flow rate for the fuel with additive was lower than for the fuel without additive. These results suggest that used fuel containing additive (i.e., fuel that has been heated up to 473K with $T_w = 473$K and then cooled to room temperature before passing through a filter) will produce higher deposits in the filter.

From detailed measurements of flow rates, it was found that the variation of fuel flow rate with time usually follows three stages:

1) rapid decrease of flow rate, indicating a rapid build-up of deposit due to the initially high flow rate;

2) the flow rate slows down more gradually; and

3) the flow rate fluctuates around a minimum value, $\dot{m}_{f\,min}$. At this stage the deposit reaches a dynamic balance (i.e., some deposit forms on the filter and some is lost from the filter). Generally speaking, when the system is very clean and the fuel has been subjected to temperatures not exceeding 500K, it is not possible to achieve total blockage of the filter.

Analysis of the results obtained with a 2-μm filter showed that the relationship between fuel flow rate and time during the initial buildup phase could be expressed as

$$\left(\dot{m}_f - \dot{m}_{f\,min}\right)^{-1} = \beta\, t\,. \tag{8}$$

β indicates the tendency of a fuel to form deposits in the filter. Any fuel which has a high deposition tendency will also have a high value of β.

The linear relationship between fuel flow rate and time, as indicated in Eq. (8), is confirmed by the results shown in Fig. 9. The values of β for the fuels with and without additive are given by the slopes of the two straight lines drawn through the origin. For the fuel containing additive, the value of β is 60 percent higher than for the fuel containing no additive.

The results of this test program generally confirmed those obtained with the Phoenix test facility. The addition of JFA-5 to the fuel reduced the deposition in the test tube but increased the deposition on the downstream filter.

SURFACE TREATMENT

Deposition rates depend on the surface pretreatment employed. Relative to the pretreatment, the time, temperature, and pretreatment gas are of importance. The greatest decrease in the amount of coke that collects on metal surfaces results when the surface concentrations of chromium, manganese, and titanium are relatively high, and/or when the surface concentrations of nickel and iron are greatly reduced. It should be emphasized that in the research done in the Purdue School of Chemical Engineering deposit runs at only 850°C and four hours were made. Decreases of about 50 percent were often obtained when pretreated vs. nonpretreated coupons were compared. These results suggest the pretreatment technique may find application in the afterburners of jet aircraft.

A series of tests was carried out to examine the effect of surface treatment of the tube inner wall on rates of deposition. The tests were conducted with the test rig operating in the single-pass mode in order to eliminate any effects of prior fuel heating on the results obtained. The fuel employed was Jet A. The tube material was stainless steel, 300 series. The tube dimensions were measured as:

Length	=	174mm
I.D.	=	2.72mm
O.D.	=	3.23mm

For all tests, the fuel temperature at inlet to the test section was kept constant at 523K and the tube wall temperature was maintained at 673K. The fuel flow rate was 100 ml/min and the test duration was six hours. The test program involved a total of

four tubes. Two tubes received no special treatment apart from the degreasing procers which is carried out on all tubes as part of the normal test procedure. The other two tubes were subjected to special surface treatment. One tube received a H_2/H_2O treatment and the other a CO/H_2O treatment. The results obtained are presented in Table 1.

The results of theses tests are clearly not promising since larger amounts of deposits (tars, coke, etc.) resulted in the tubes. Inspection of the tubes containing deposits suggests that the pretreatments provided in the School of Chemical Engineering were too severe and/or too long. The desired pretreatment should probably result in some enrichment of chromium, manganese, and titanium plus, hopefully, some smoothing of the surface, as experienced for tests with Incoloy 800. Too long or too severe a pretreatment likely causes increased roughness of the surface. Such roughness promotes collection of the precursors that plug the tube.

FUEL COMPOSITION

The air-bubbling technique described in Ref. 3 was used for screening five test fuels supplied by the Air Force. Details of these fuels are provided in Table 2. The test conditions employed for these fuels are listed below.

(a) recirculation test mode

(b) 4.6 liter fuel sample (1.5 gallons)

(c) fuel temperature = 373, 423, 448, and 473K

(d) tube wall temperature = 623K

(e) fuel flow rate = 200 ml/min

(f) P = 350 psig

(g) bubbling air flow rate = 0.13 g/min

(h) test duration hours

The results obtained are listed in Table 2 and shown in graphical form in Fig. 10. As these results are self-explanatory, no detailed discussion is necessary. The main conclusion to be drawn from the experimental data is that the AF-3 JPTS fuel has excellent thermal stability, as evidenced by an exceptionally low deposition rate, while the AF-5 Shell Jet A fuel of low flash point has relatively poor thermal stability and a high deposition rate.

The five fuels ranged from light brown to dark brown after completion of the test. A direct relationship between deposition rate and post-test color was observed-the darker the shade of brown the higher the deposit rate. Samples of post test fuels have been preserved for inspection, if required.

FUEL ADDITIVES

The single-pass technique was used to examine the influence of fuel additives on deposition rates.

All tests were carried out at the following conditions.

Fuel temperature	=	523K
Wall temperature	=	523K
Pressure	=	350 psig
Fuel flow rate	=	100 ml/min
Test duration	=	5 hours

The test tubes employed were manufactured from stainless steel (300 series) to the following dimensions

I.D.	=	2.72mm
O.D.	=	3.23mm
Length	=	174mm

The results obtained are listed in Table 4. For the baseline fuel containing no additives, the mass of deposit was 3.6 mg. For the fuels containing additives, the deposit mass was always appreciably higher, with values ranging from 9.8 to 41.7 mg. After testing all the fuels with additives, a repeat test was carried out on the baseline fuel. The purpose of this test was to verify the low value obtained for the deposit mass in the first test run. This repeat test on the baseline fuel resulted in an even lower deposit of 1.8 mg, thus generally confirming the result obtained in the first test run.

REFERENCES

1. TeVelde, J.A. and Glickstein, M.R., "Heat Transfer and Stability of Alternative Aircraft Fuels," Vol. 1., Report AD A137404, 1983.
2. Marteney, P.J. and Spadaccini, L.J., "Thermal Decomposition of Aircraft Fuel," ASME Journal of Engineering for Gas Turbines and Power, Vol. 108, pp. 648-653, 1986.
3. Chin, J.S. and Lefebvre, A.H., "Experimental Techniques for the Assessment of Fuel Thermal Stability," AIAA Paper No. 92-0685, 30th Aerospace Sciences Meeting, Reno, NV, January 1992.
4. Chin, J.S., Lefebvre, A.H., and Sun, F.T.-Y., "Temperature Effects on Fuel Thermal Stability," ASME Paper No. 91-GT-97, International Gas Turbine and Aeroengine Congress, Orlando, FL, June 1991.
5. Chin, J.S. and Lefebvre, A.H., "Influence of Flow Conditions on Deposits from Heated Hydrocarbon Fuels," ASME Paper No. 92-GT-114, International Gas Turbine and Aeroengine Congress, Cologne, Germany, June 1992.
6. Vranos, A. and Marteney, P.T., "Experimental Study of the Stability of Aircraft Fuels at Elevated Temperatures," NASA CR 165165, 1980.
7. Roback, R., Szetela, E.J., and Spadaccini, L.J., "Deposit Formation in Hydrocarbon Fuels," ASME Journal of Engineering for Gas Turbines and Power, Vol. 105, pp. 55-65, 1983.
8. Watt, J.J., Evans, A., and Hibbard, R.R., "Fouling Characteristics of ASTM Jet A Fuel When Heated to 700°F in a Simulated Heat Exchanger Tube," NASA TN D-4958, 1968.
9. Szetela, E.J., "Deposits from Heated Gas Turbine Fuels," ASME paper N. 76-GT-9, 1976.

Table 1. Influence of surface treatment on deposition rates.

Test Piece	Deposit Mass (mg)	Deposit Rate ($\mu g/cm^2/hr$)
untreated	2.0, 2.2	22.4, 24.7
H_2/H_20 treated	3.8	42.6
CO/H_20 treated	4.5	50.4

Table 2. JP fuels tested using air-bubbling technique.

AF - 1	Jet A kerosene. Middle distillate, no additive SOHIO Code = SOHIO P1825 90-POSF-2747 Flash Point = 33K
AF - 2	Kerosene 1-K. Jet A-1. Hydrodesulferized kerosene. Hydrotreated light distillate containing trace static dissipator additive. Sulfur $< 0.04\%$ 90-PSOF-2814
AF - 3	Jet Petroleum Thermally Stable (JPTS) Exxon Code = 121901-00086 91-POSF-2789 Flash Point = 322K
AF - 4	Shell Jet A Shell Code = 23500 90-POSF-2747 Flash Point = 33K
AF - 5	Shell Jet A 91-POSF-2827 Flash Point = 323K

Table 3. Deposition rates of five JP test fuels, $\mu g/cm^2.hr$.

Fuel Temp. K	AF-1	AF-2	AF-3	AF-4	AF-5
373			0		19.2
423	25.7	45		19.1	159
448			37.2		
473	276	333	31 56	214	1300 1851

Table 4. Influence of fuel additive on deposition rate.

Fuel	Additive 12 mg/liter	Mass of Deposit, mg	Deposition Rate, $\mu g/cm^2.hr$
FSN 91-POSF-2827	No additive. Baseline fuel	3.6,1.8	48.4,24.2
FSN 90-POSF-2827	PL-1605	24.4	328
FSN 90-POSF-2827	PL-1606	9.8	132
FSN 90-POSF-2827	PL-1607	11.6	156
FSN 90-POSF-2827	PL-1608	41.7	560

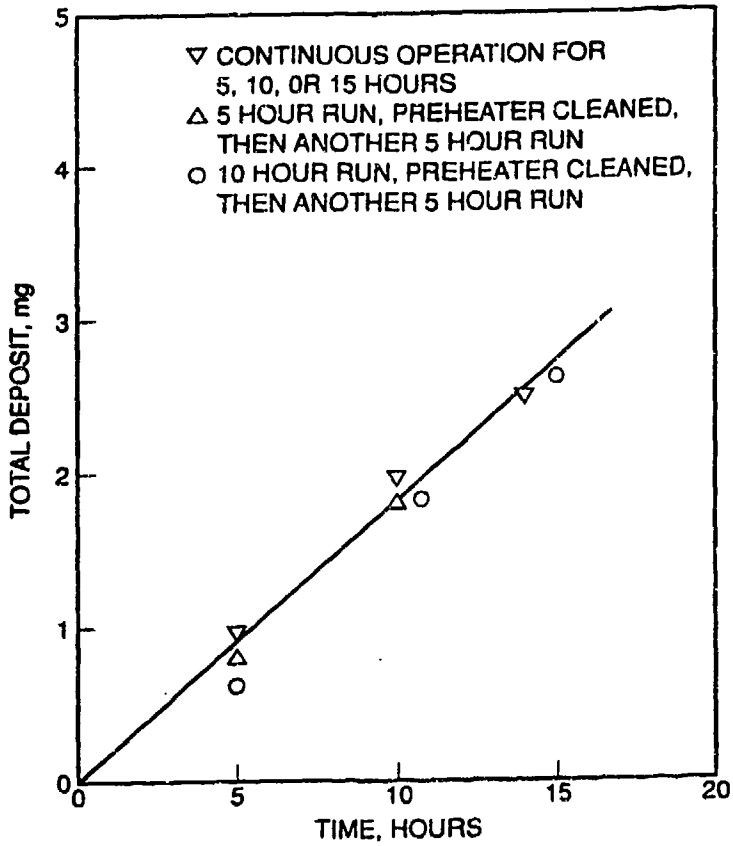

Fig. 1. Influence of fuel preheater on deposits.

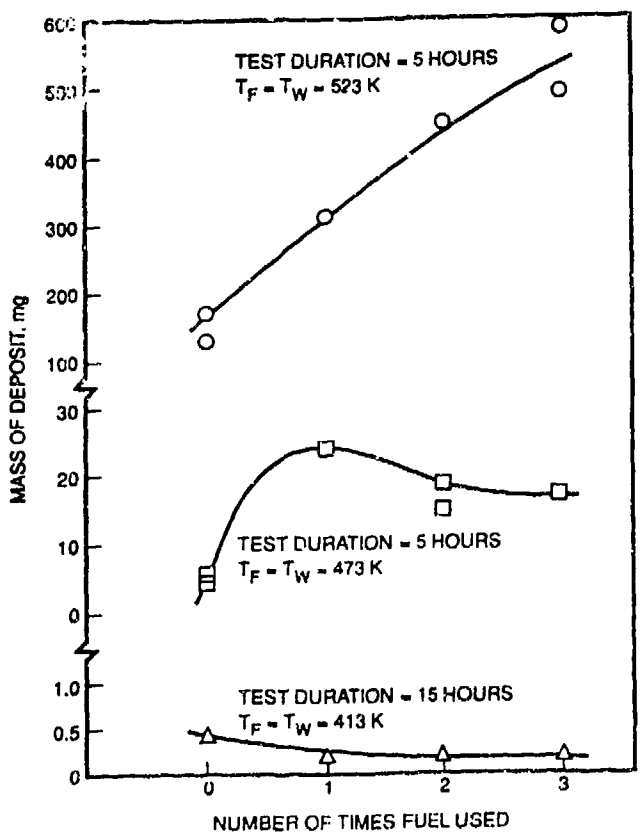

Fig. 2. Influence of previous fuel preheating on deposition. Fuel = DF2: Fuel flow rate = 100ml/min.

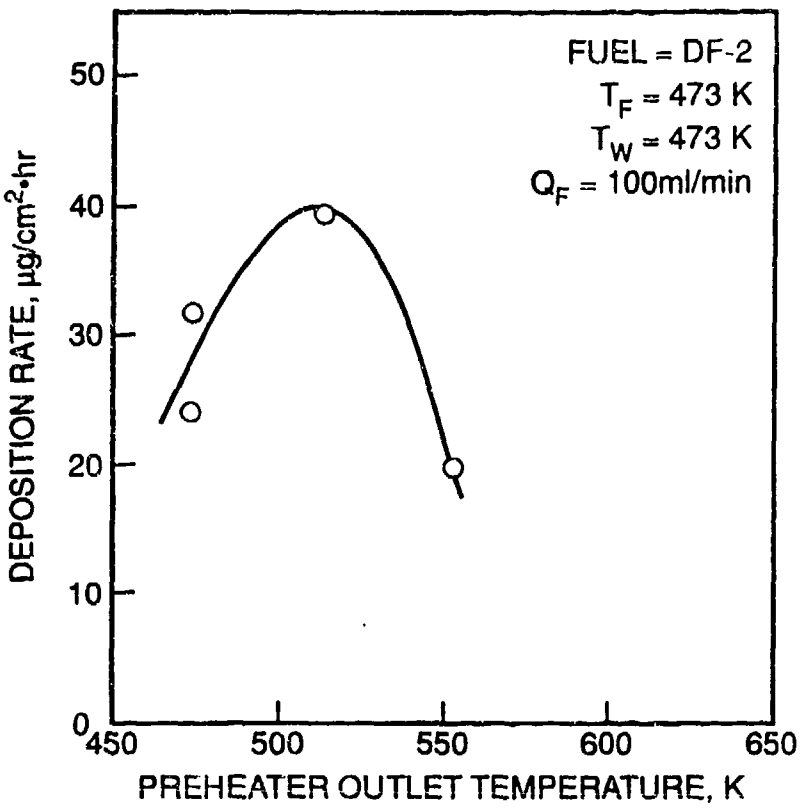

Fig. 3. Influence of preheater outlet temperature on deposition rates.

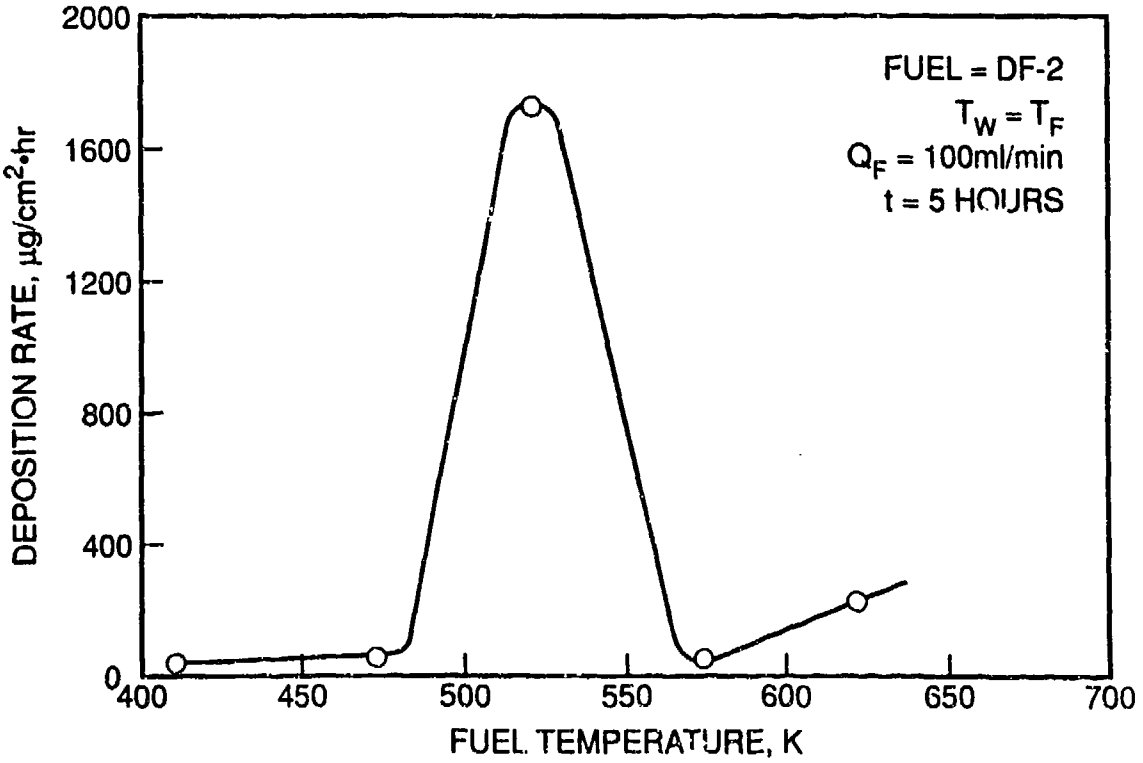

Fig. 4. Influence of fuel temperature on deposition rates.

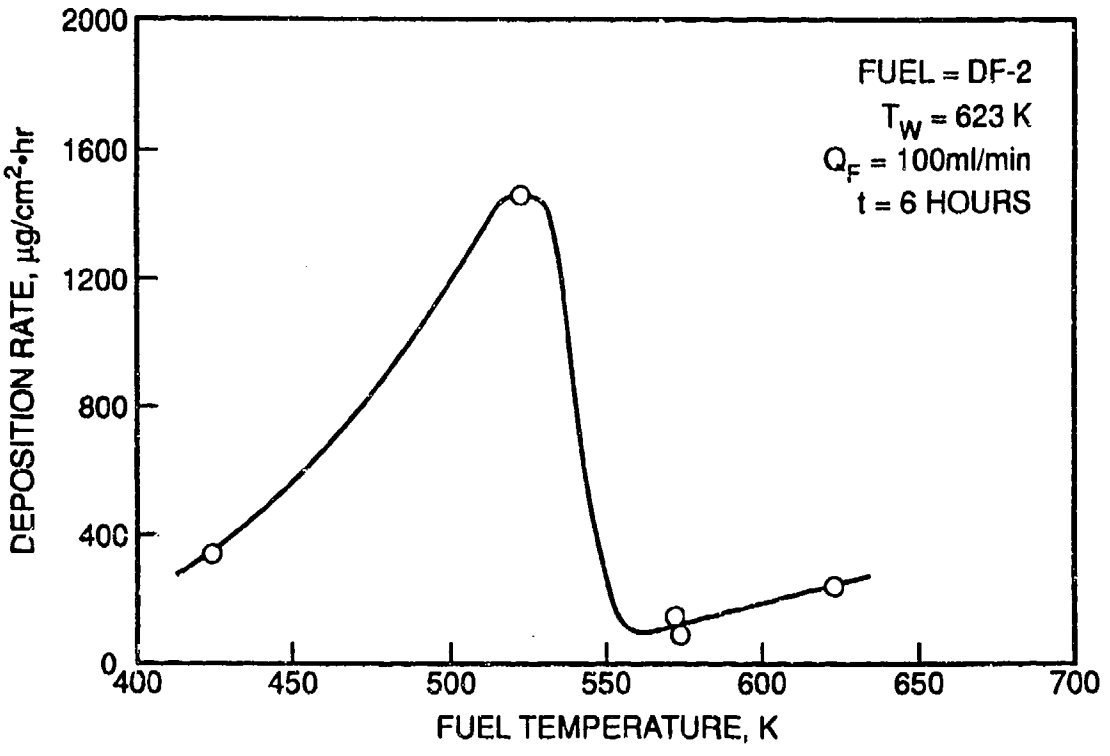

Fig. 5. Influence of wall temperature on deposition rates.

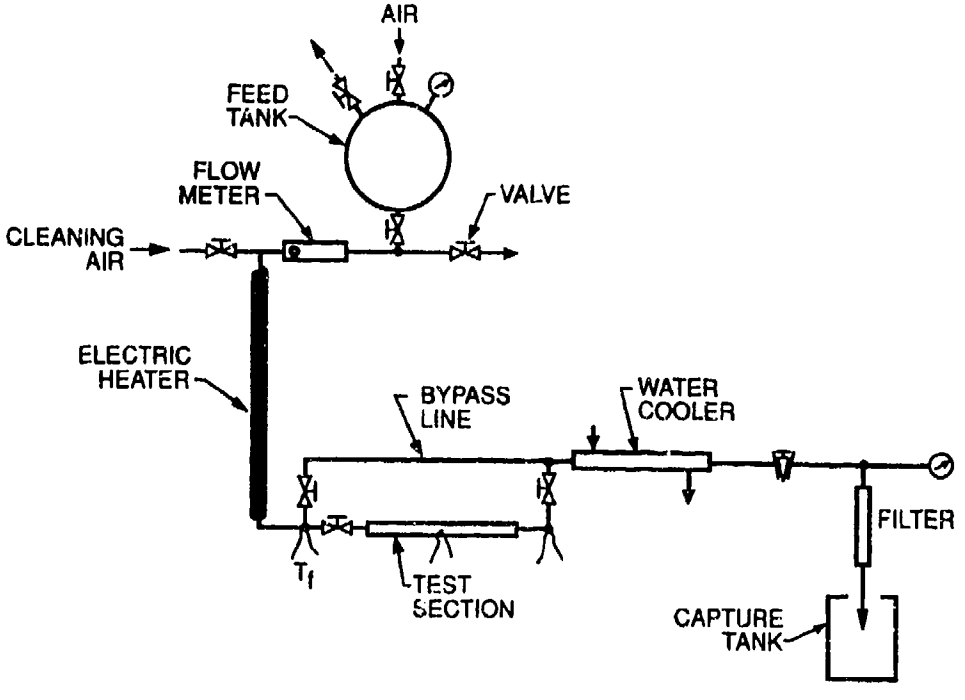

Fig. 6. Fuel thermal stability rig for filter deposit study.

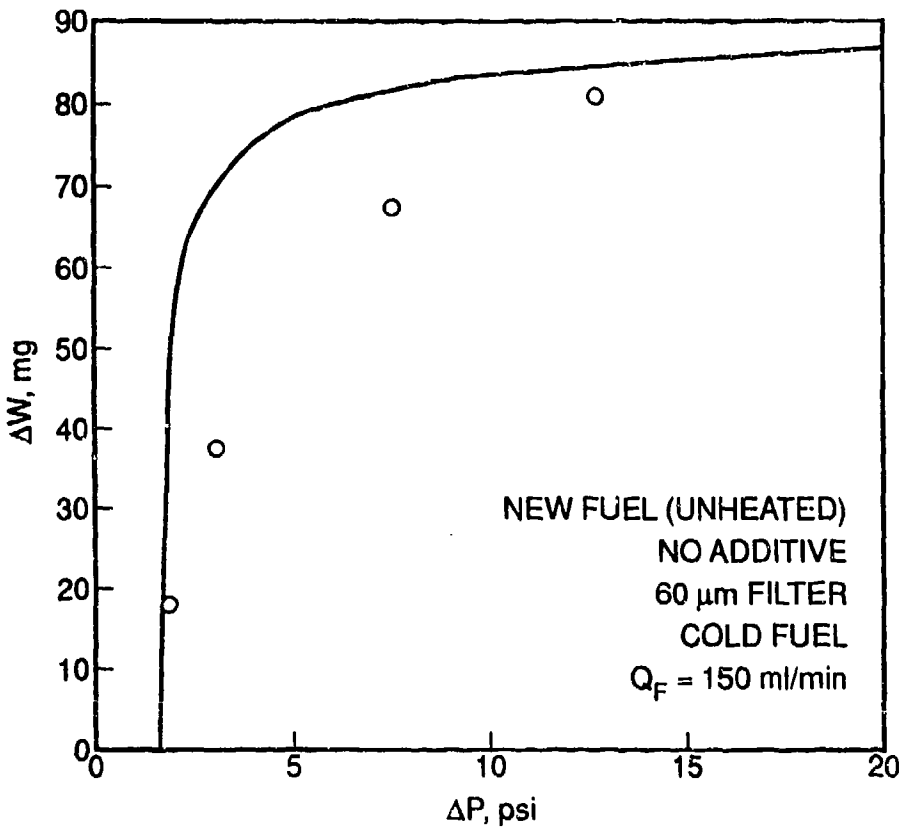

Fig. 7. Comparison between measured and predicted deposits.

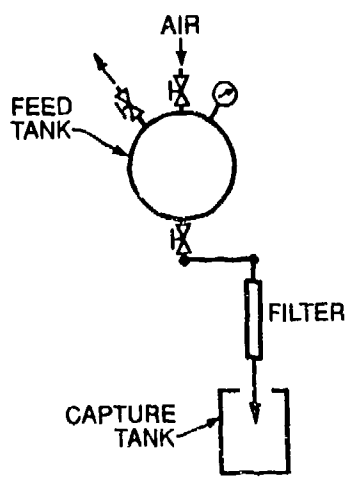

Fig. 8. Simple filter test rig.

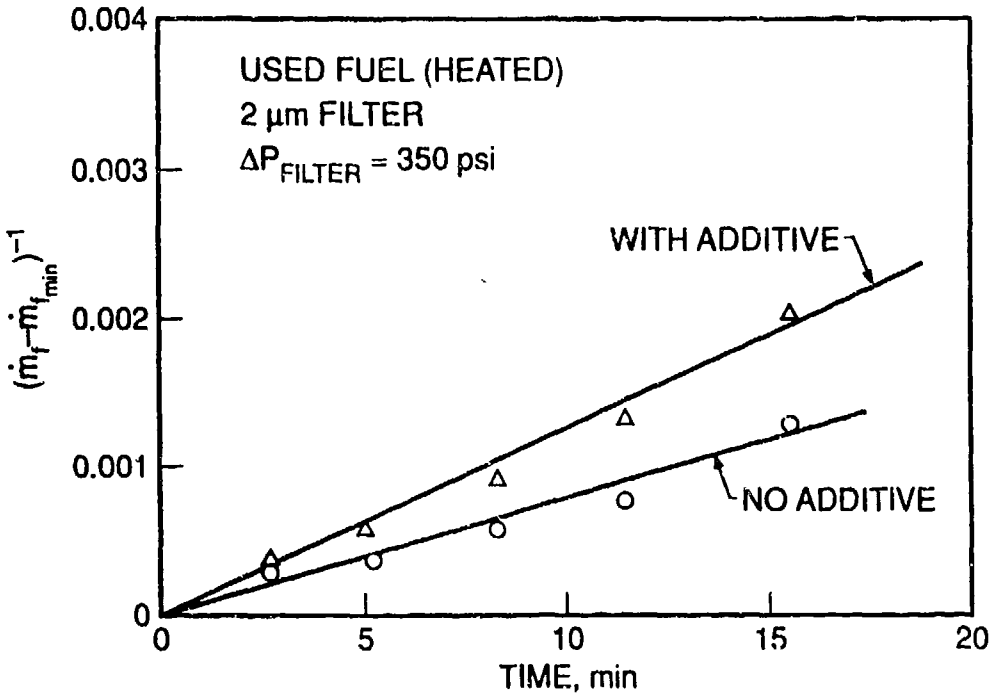

Fig. 9. Graphs illustrating influence of fuel additive on flow rate/time relationship.

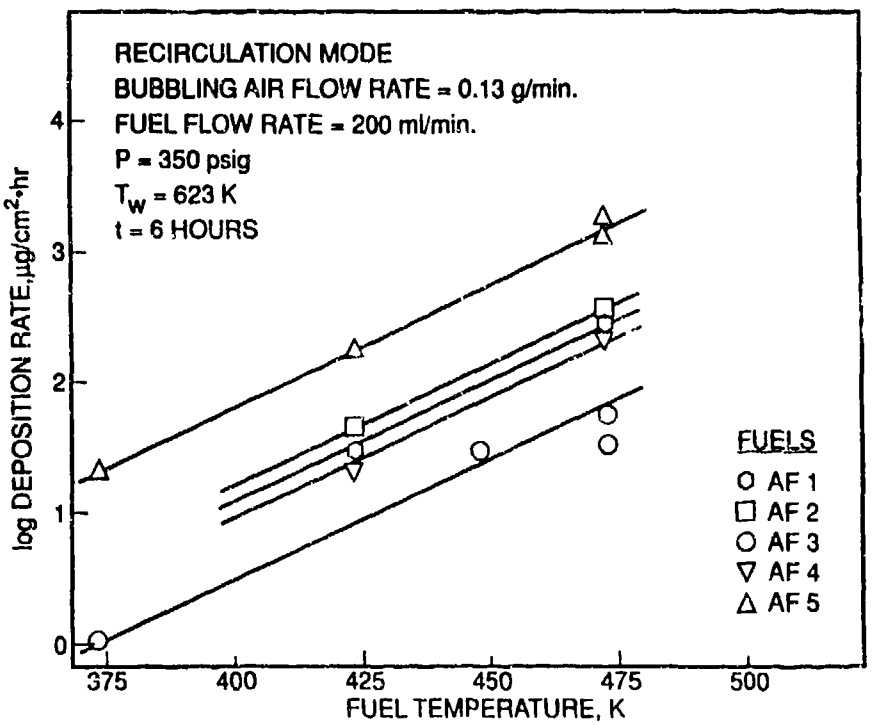

Fig. 10. Influence of fuel temperature on deposition rates for five test fuels.

AIAA-92-0685

EXPERIMENTAL TECHNIQUES FOR THE ASSESSMENT OF FUEL THERMAL STABILITY

by

J.S. Chin* and A.H. Lefebvre†
Purdue University, West Lafayette, Indiana

Abstract

Two different methods for characterizing the thermal oxidative tendencies of aviation fuels have been developed. A common feature of both methods is that the fuel under test is passed through a heated tube which is maintained at constant temperature throughout the test duration. One is a closed-loop system in which the fuel is recirculated continuously for periods up to 22 hours. The other is a single-pass device whereby the test fuel flows only once through the heated tube. These two methods and their relative merits are discussed in some detail, and the extent to which they simulate an actual aircraft fuel system is assessed alongside that of a more established test technique which maintains a constant heat flux through the tube wall and allows the wall temperature to increase continuously throughout the test duration.

Introduction

In an aircraft fuel system, fuel is used to cool the engine lubricant and to absorb waste heat from other aircraft components or systems, such as the hydraulic system. Before the fuel is sprayed into the combustion zone it experiences further heating from the compressor exit air or the afterburner gases. Fuel in contact with hot metal surfaces can attain temperatures that are sufficiently high to stimulate oxidation reactions that lead to the formation of insoluble material which finally deposits on the wall surface. The adverse effects of such deposits on engine operation include: 1) fouling of oil-heat-exchanger surfaces, which reduces the effectiveness of the heat exchanger, 2) malfunction of the fuel system, 3) deposits in the fuel nozzle which tend to block small flow passages and can change the fuel spray pattern to such an extent that it may cause flame tube burn-out and damage to the turbine blading.

Thermal stability problems were first identified by the Pratt and Whitney company in the middle 1950's [1]. In recent years research in this area has been given new impetus by the resurgence of interest in supersonic and hypersonic aircraft. The current state of knowledge may be summarized briefly as follows:

1. The critical engine components have been defined as fuel injector nozzles, fuel/oil heat exchangers, and fuel control systems.
2. The thermal decomposition of hydrocarbon fuels can be classified into three separate regimes, depending on the fuel temperature.
   a. at fuel temperatures lower than 570K, decomposition occurs via an autoxidation reaction. In this regime, which is highly relevant to aircraft fuel systems, deposits increase with increase in fuel temperature.
   b. between 570K and 770K the autoxidation reactions are supplemented by direct pyrolysis of fuel molecules. As the temperature rises within this range the reaction mechanism gradually shifts from oxidation-controlled toward pyrolysis-controlled. Deposit rates tend to peak at temperatures around 700K and then decrease with further increases in fuel temperatures.
   c. at fuel temperatures higher than 770K the autoxidation reaction is no longer significant, and deposits are caused mainly by direct pyrolysis of the fuel. Deposition rates increase with increase in fuel temperature.
3. Removal of oxygen usually improves thermal stability.
4. Compounds containing oxygen, nitrogen, and sulfur atoms are major deposit precursors.
5. Metals, particularly copper, catalyze the formation of deposits.

It is not intended here to review all the experimental techniques employed during the past twenty-five years in the assessment of fuel thermal stability, since full descriptions of these early researches and the experimental techniques used are contained in the CRC Literature Survey on the Thermal Oxidation Stability of Jet Fuel [1], and in publications by Taylor [2], Cohen [3], Peat [4], Roback et al. [5], Baker et al. [6], TeVelde and Glickstein [7], and Marteney and Spadaccini [8]. Instead attention is focused on a comparison between the well-known UTRC method and the techniques now being developed and used in the Gas Turbine Combustion Laboratory at Purdue University. It can be stated at the outset that none of these methods is entirely free from defects. The problems arising from the thermal decomposition of aviation fuels are manifested in different ways depending on the temperature-time history of the fuel, the local fuel and wall temperatures, and the flow conditions of pressure, velocity, and turbulence. Thus no single technique for the assessment of fuel thermal stability can hope to achieve universal acceptance. However, from an engineering standpoint, a satisfactory technique is one that simulates closely the actual aircraft or engine conditions. Any significant deviation from these conditions must detract appreciably from the value of the experimental results for engineering applications.

UTRC Constant Heat Flux Method

In this method, fuel flows through a 2.4m length of thin-walled tubing (2.37mm i.d.) that is heated by an electric current passing through it. Since the electrical resistance of the tube

*Visiting Professor, School of Mechanical Engineering
†Reilly Professor of Combustion Engineering, School of Mechanical Engineering. Member AIAA.

material does not vary significantly with temperature, the local heat flux remains sensibly constant along the tube. After completion of the test, the tube is cut into short sections and the mass of carbon in each section is determined. A significant feature of the UTRC technique is that because the local heat flux remains constant, the thermal resistance created by the presence of deposit on the inside tube wall causes the outer wall temperature to increase locally. This means that the local wall temperature is always a function of the local deposit thickness, because where the deposit is thicker the wall temperature must be higher to maintain the same heat flux through the tube wall. In some cases the buildup of deposit during an extended test run can create wall temperatures as high as 1000K. Such high wall temperatures are quite unrealistic from a practical standpoint, neither do they have any fundamental significance, because once a substantial thickness of deposit has accumulated the local wall temperature bears no relationship to either the local fuel temperature or the temperature of the soft carboneous material formed at the interface between the solid deposit and the flowing fuel.

Purdue Constant-Wall-Temperature Methods

Two methods for assessing the thermal stability of liquid hydrocarbon fuels have been developed. A key feature of both methods is that the heated tube through which the fuel is passed is maintained at a constant temperature throughout the test duration. This is in marked contrast to the UTRC approach whereby the heat flux through the wall is kept constant and the wall temperature is allowed to rise (sometimes to very high values) as deposits build up on the inner tube wall.

Most of the research on fuel thermal stability carried out at Purdue has employed a closed-loop system in which the fuel under test is recirculated continuously through a heated tube for periods ranging from 6 to 22 hours. The other system is a single-pass device whereby the test fuel flows only once through the heated tube and is then discarded. With both methods, the rates of deposition on the tube walls are measured by weighing the tube before and after each test.

Recirculation Method

A general description of the fuel recirculation method has been provided elsewhere [9]. In recent months various modifications to the original apparatus have been made as part of an ongoing effort to improve the accuracy and consistency of the experimental data and to provide the best simulation of the deposit formation process in a real aircraft situation. The apparatus in its present form is shown schematically in Fig. 1. It is a closed-loop system, designed to recirculate fuel over wide ranges of temperature, pressure, and flow rate. The major components are the pump, accumulators to contain the test fuel, a fuel heater, a heated test section, a fuel cooler, a flow meter, and another meter for monitoring the pressure drop across the test section. In operation, the test fuel flows from a high-pressure accumulator through the flow meter and fuel heater into the test section from whence it flows via a water cooler into the low pressure accumulator. The function of the pump is to transfer fuel from the low-pressure accumulator to the high-pressure accumulator. The pressures in both accumulators can be set to any desired values, up to a maximum of 4.1 MPa (600 psi), by using air from a high pressure container. The fuel heater is located in close proximity to the test section in order to minimize the amount of time the fuel spends at high temperature outside the test section. The fuel cooler is fitted immediately downstream of the test section for the same reason. Typically, the fuel is returned to the low pressure accumulator at a temperature of around 340-350K.

The main component of the test section is a thin-walled stainless steel tube whose principal dimensions are - length 152 mm, outer diameter 3.07 mm, and inner diameter 2.15 mm. This tube is clamped between two copper segments, as illustrated in Fig. 2. The semi-circular grooves cut into the two copper segments are designed to provide good thermal contact between the tube and the copper segments when the latter are clamped together. A number of thermocouples are threaded through one of the copper segments in such a manner that in

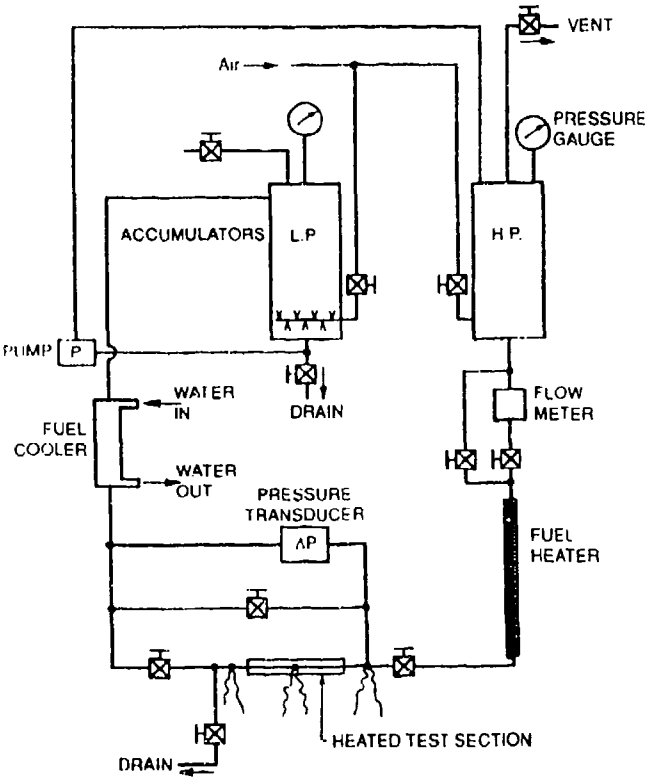

Fig. 1 Schematic diagram of fuel recirculation apparatus

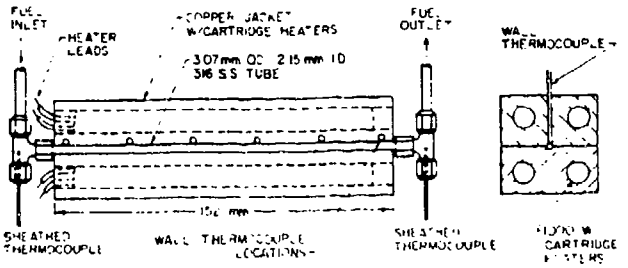

Fig. 2 Details of test section

operation the thermocouple heads are pressed tightly against the stainless-steel tube. These thermocouples are used to measure tube-wall temperatures at inlet and outlet and at four equispaced stations in-between. Fuel temperatures are measured only at the tube inlet and outlet. The stainless steel tube is heated by using between one and four 1,000W electrical rod heaters which are inserted into holes drilled into the copper segments, as shown in Fig. 2. This arrangement ensures that the tube is heated uniformly around its circumference even when only one electrical heater is operational.

For any given fuel, the fuel pressure and flow rate are set at suitable values and the heaters for the fuel and test section are both switched on. During the fuel heatup period, which is usually less than ten minutes, the flowing fuel bypasses the test section. When the fuel and tube-wall temperatures have both attained the desired values, the bypass valves are operated to divert the hot fuel through the test section. At the same time the water supply to the fuel cooler is turned on.

The main advantage of this procedure is that it allows the start of the test to be clearly defined. Another useful feature is the feedback between the fuel and tube-wall thermocouples and

the fuel and test section heaters respectively which allows both fuel and tube-wall temperatures to be maintained at preset values with 1°C throughout the entire duration of the test. This flexibility allows tests to be carried out on the influence of fuel temperature on deposition rates while maintaining a constant wall temperature. Alternatively, fuel temperature can be kept constant to permit the separate effect of variations in wall temperature on deposition rates to be studied.

Deposition rates are determined by weighing the tube before and after each test. The fuel supply connections at both ends of the tube are sealed using graphite ferrules. These ferrules are broken off after each test to reduce weight and thereby increase the ratio of the deposit mass to the tube mass. The weight of the tube is around 4000 mg. The deposits usually weigh between 2 and 20 mg, depending on the fuel composition and test conditions, but for very high temperatures the deposit can weigh as much as 100 mg. As the balance employed has an accuracy of within 0.1 mg, the weighing procedure is considered capable of giving satisfactory results.

One of the most important aspects of the test procedure is the treatment of the test tube both before and after each test run. Before weighing the tube prior to test, it is exposed to a welding torch flame to remove any oil or grease remaining from the extrusion process used to manufacture the tube. After the tube has been immersed in a solvent (stanisol) for 24 hours it is "dried" by flowing heated nitrogen gas through it for a few minutes. It is then allowed to dry naturally for another 24 hours before being weighed for the first time. Twenty-four hours later the tube is weighed again, and this process is repeated until the tube weight indicates a constant value to within 0.1 mg. Tube treatment after the test is even more important and more critical to the repeatability and accuracy of the experimental data. The procedure now being used is based on detailed considerations of all the factors that experience has shown can influence the results obtained. After each test the fuel is drained from the system, and the test section is allowed to cool down to a temperature of around 450K. Where necessary, water cooling is applied to the copper segments to accelerate this cooling process. Experience has shown that if the tube-wall temperature is too high (>470K) any residual fuel remaining in the tube will "bake" onto the wall, thereby creating more deposit. On the other hand, if the wall temperature is too low (< 430K), the residual fuel does not fully evaporate but is gradually absorbed into the porous structure of the deposit. When the tube-wall temperature has fallen to 450K, heated air is passed through the system for around five minutes. This air bypasses the test section, but the valve at the downstream end of the test section is left open so that air and vapor are drawn continuously out of the tube by the ejector action of the flowing air. The test section is then allowed to cool down to normal room temperature, after which the tube is removed from the test section and placed in a vertical position to dry naturally for 24 hours before being weighed for the first time. This weighing procedure is repeated every 24 hours until the difference between two consecutive weights is within 0.1mg. For small deposits, 48 hours of natural drying in a vertical position is usually adequate but, for larger deposits, up to 144 hours may be needed, as illustrated in Figs. 3 and 4 for two aviation kerosine fuels. Some typical results obtained using the fuel recirculation technique are shown in Fig. 5.

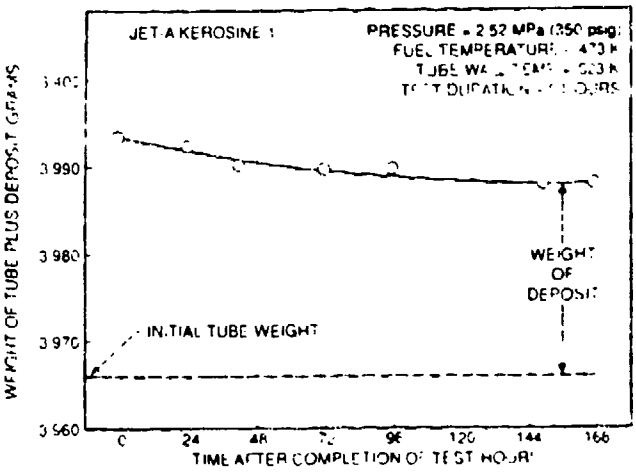

Fig. 3 Influence of drying period on deposit mass

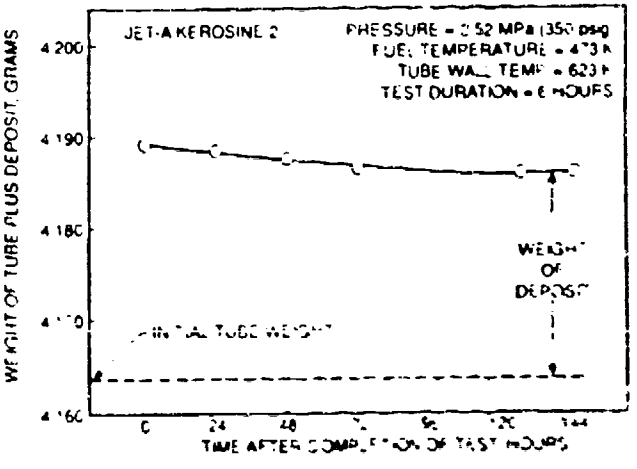

Fig. 4 Influence of drying period on deposit mass

Single-Pass Method

The main advantages of the fuel recirculation method described above are that it requires only a small amount of test fuel and it simulates quite closely the deposition process in an aircraft fuel system. However, it is less attractive for basic studies on the effects of fuel composition, fuel temperature, tube-wall temperature, and Reynolds number on deposition rates, due to the gradual depletion with time of the oxygen contained in the fuel. To provide more basic information on the effects of fuel properties and flow conditions on deposition rates, a single-pass flow system has been designed and tested. The main features of this new facility are shown in Fig. 6. The main components are feed tanks which contain the test fuel, a fuel heater, a heated test section, a flow meter, and another meter for monitoring the pressure drop across the section. In operation, the test fuel flows through the flow meter and fuel heater into the test section from whence it flows into a pressure tank. The pressure can be set to any desired value, up to a maximum of 4.1 MPa (600 psi), by using air from a high-pressure container.

The test section, instrumentation, tube preparation and weighing procedures are virtually identical to those employed in the recirculation method. For any given fuel, the fuel pressure and flow rate are set at suitable values and the heaters for the fuel and test section are both switched on. During the fuel heating period the flowing fuel bypasses the test section. When the fuel and tube-wall temperatures have both attained the desired values, the bypass valves are operated to divert the hot fuel through the test section. Deposition rates are again determined by weighing the tube before and after each test. The deposits usually weigh between 2 and 20 mg depending on the fuel composition and test conditions. Generally, it is found that 10 to 15 U.S. gallons of fuel are required for each test, as compared with 1.5 U.S. gallons for the recirculation method.

Some typical data obtained using the single pass technique are presented in Fig. 5. This figure shows the influence of tube-wall temperature on deposition rates for a kerosine-type fuel flowing at an inlet temperature of 523K, a pressure of 0.69 MPa (100 psi), and a flow rate of 100 cc/min. Corresponding data obtained by the recirculation method are shown in the same figure for purpose of comparison. It is clear

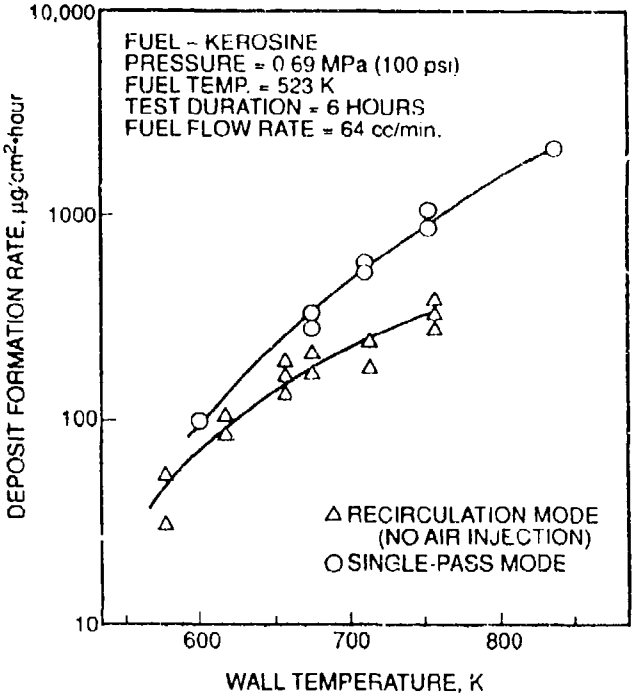

Fig. 5 Comparison of deposition rates obtained by single-pass and recirculation methods

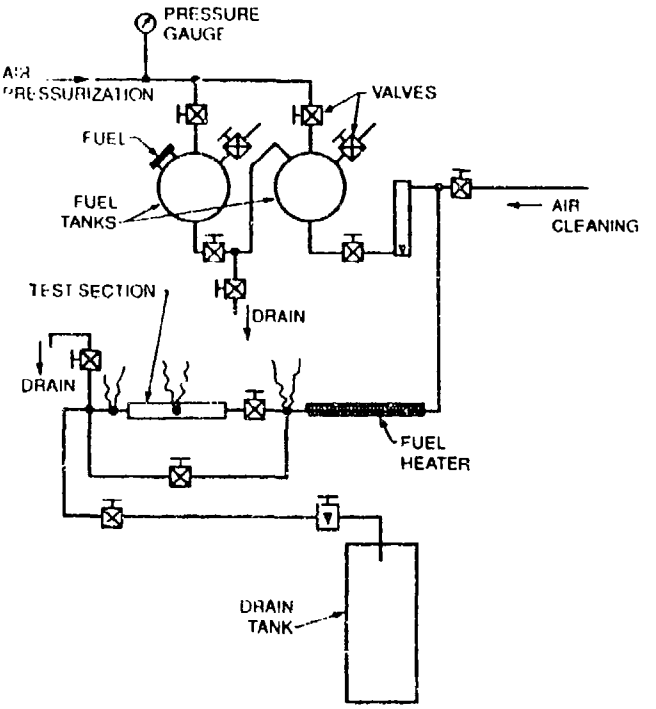

Fig. 6 Schematic diagram of single-pass facility

from Fig. 5 that the recirculation method gives the lowest deposit rate, particularly when the wall temperature is high. If the objective were to simulate the situation in an aircraft fuel system, involving partial recirculation of fuel back to the wing tank, then the single-pass mode would indicate a higher deposit rate than would be obtained in practice.

Discussion

Although the UTRC constant heat flux method has been used extensively to determine the thermal stability and heat transfer characteristics of aircraft fuels, it has a drawback which cast doubts on the relevance of the results obtained to actual aircraft conditions. An inherent deficiency of the method is that over most of the tube length the local wall temperature changes dramatically during the test period. For example, the deposit rate data quoted in [7] for an initial wall temperature of 623K actually represent an average value of the deposit rate over a period of 15 hours, during which time the wall temperature varied from 623K to 953K. The Purdue method is free from this defect because the wall temperature is controlled to within 1°C of the nominal value throughout the entire test period. This means that the heat transfer from the wall to the fuel diminishes with the buildup of deposit, which is exactly what happens in aircraft fuel systems and engine fuel nozzles.

It is sometimes asserted that if the heat flux through the tube wall is kept constant then, regardless of the actual wall temperature, the interface temperature between the deposit and the fuel will remain constant, and this interface temperature might therefore be regarded as an appropriate boundary value. Unfortunately, this concept embodies two key assumptions, neither of which is valid, (1) that at any given cross section the deposit thickness is radially uniform, and (2) the deposit is a solid compact structure, presenting a clearly-defined surface to the adjacent fuel. In practice, it is found that the deposit thickness varies appreciably both radially and axially along the length of the tube. Moreover, during a test run the deposit has a highly complex two-phase structure which cannot be regarded as compact until the liquid fuel has been drained off and the deposit allowed a long time in which to dry. In fact, there is no clear cut interface between the deposit and the fuel. The so-called "interface temperature" is not a physical reality but merely an equivalent "thermal-resistance temperature" which can only be calculated if the deposit is assumed to be distributed uniformly over the tube surface, which it most certainly is not.

In summary, the constant heat flux method suffers from the drawback that the conditions under which the deposits are formed are quite different from actual aircraft and engine conditions. Also, because the local tube-wall temperature varies markedly during the test period, it is very difficult to identify the separate effects of wall temperature and fuel temperature on deposition rates. This drawback is a serious impediment to any quantitative analysis of the experimental data.

An important advantage of the Purdue methods is that the tube-wall temperature is maintained at a constant value throughout its length, regardless of variations in fuel temperature and test duration. By exercising separate control over fuel and wall temperatures, the effects on deposition rates of variations in these two parameters can be clearly distinguished.

The fuel recirculation method provides the closest simulation to the actual conditions in an aircraft fuel system. Although not shown in Fig. 1, the test facility does, in fact, incorporate provisions to allow the system to operate in a partial recirculation mode, whereby part of the total fuel flow passes through the test section and the remainder is heated but then diverted back into the fuel tank. This mode of operation has the potential for providing an even better simulation of the actual aircraft fuel system, but no systematic measurements of deposit rates have yet been carried out using this approach.

A major asset of the recirculation method is its very low fuel requirement of only 1.5 U.S. gallons per data point. This represents an appreciable saving in cost, and is particularly advantageous when using specially-prepared expensive test fuels or other fuels that are in short supply. Its main drawback is the gradual depletion of fuel-dissolved oxygen throughout the duration of the test. At the present time, this problem is being addressed by continuously bubbling small quantities of air into the fuel contained in the low pressure accumulator. The system employed is shown schematically in Fig. 1. The air injection tube is located near the bottom of the low-pressure accumulator,

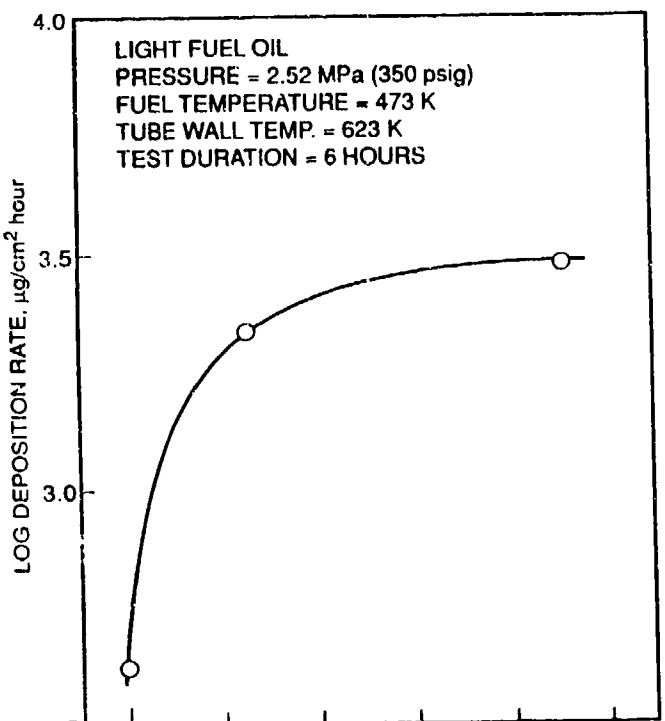

Fig. 7 Influence of injected air on deposition rates

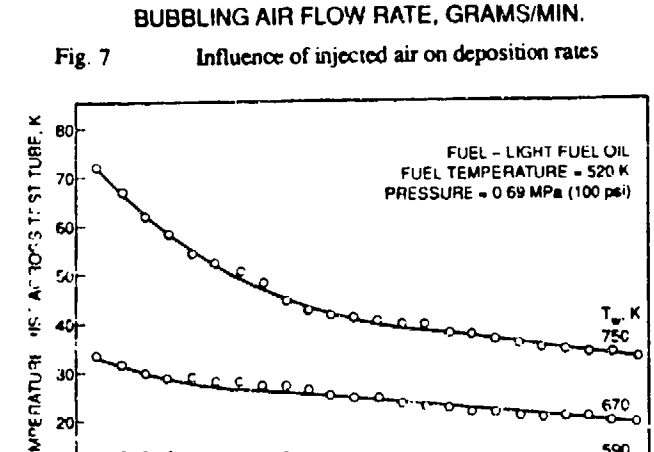

Fig. 8 Influence of deposit thickness on fuel temperature rise

and air is bubbled into the fuel through 20 holes, each of 0.5mm diameter. However, although this simple system functions efficiently as an oxygen-replenishment device, it introduces another variable into the system. Figure 7 shows measured values of deposition rates for a light fuel oil at three different air bubbling rates. The general tendency is for deposition rates to increase with increase in air flow rate, the effect becoming less pronounced at the higher air flow rates.

For any given test fuel, a few preliminary tests are carried out in order to determine the air bubbling flow rate needed to ensure that the recirculation method gives the same deposition rate as the single-pass method for the same fuel and the same test conditions. This procedure virtually eliminates the problem of oxygen depletion which hitherto has been regarded as a deficiency of the recirculation method.

There are other ways in which the dependence of deposition rate on air bubbling rate can be used to advantage. For example, when carrying out comparative tests on different test fuels, the fuel which is anticipated to have the highest thermal stability is usually known at the outset. An air bubbling rate is then established for this fuel which is the minimum needed to produce a small but accurately-measurable deposit. This same bubbling rate is then used for the remaining test fuels.

The single-pass method is ideally suited for basic research on problems of fuel thermal stability such as, for example, the effects of fuel composition and fuel additives on deposition rates. It is also well suited for studies related to deposition problems in aircraft fuel nozzles. However, its fuel requirement is relatively high. Typically, a 6 hour test run requires around 10 to 15 U.S. gallons to obtain a single data point, as compared with 1.5 gallons for the recirculation method.

The recirculation and single-pass methods both have good potential for providing fairly precise information on the thermal properties of the deposit that govern the rate of heat transfer between the flowing fuel and the adjacent tube wall. Figure 8 illustrates the manner in which the temperature rise experienced by the fuel as it flows through the heated tube varies with time. Initially the tube wall is perfectly clean and the fuel temperature rise is relatively high. With the passage of time, the accumulation of deposit on the tube wall creates a thermal barrier between the tube and the flowing fuel which gradually diminishes the heat flux from the tube to the fuel, thereby causing a continuous decline in the temperature rise of the fuel, as illustrated in Fig. 8.

If more were known about the physical structure and thermal properties of the deposit, data of the type shown in Fig. 8 could be used to develop an elegant and accurate method for the measurement of deposition rates. Even without this information, these data could still be of value to the designers of fuel/oil heat exchangers, because not only do they illustrate the manner in which the slow but continuous buildup of deposit leads to a gradual reduction in the amount of heat transferred to the fuel, but they also enable this deterioration in heat transfer efficiency to be determined quantitatively.

In summary, the "constant wall temperature" recirculation and single-pass methods have significant attributes for both fundamental and practical studies on fuel thermal stability. Both methods are now being used at Purdue in two separate research programs on the effects of fuel composition and flow conditions on deposition and heat transfer rates.

References

1. Coordinating Research Council Inc., "Thermal Oxidation Stability of Jet Fuels-A Literature Survey," CRC Report No. 509, April 1979.
2. Taylor, W.F., "Jet Fuel Thermal Stability" NASA TM-79231, 1979.
3. Cohen, S.M., "Fuels Research - Fuel Thermal Stability Overview," *Aircraft Research and Technology for Future Fuels*, NASA CP-2146, 1980, pp. 161-168.
4. Peat, A.E., "Thermal Decomposition of Aviation Fuel," ASME Paper No. 82-GT-27, 1982.
5. Roback, R., Szetela, E.J. and Spadaccini, L.J., "Deposit Formation in Hydrocarbon Fuels," *ASME Journal of Engineering for Gas Turbines and Power*, Vol. 105, 1983, pp. 55-65.
6. Baker, C.E., Bittker, D.A., Cohen, S.M. and Seng, G.T., "Research on Aviation Fuel Instability," AGARD Conference Proceedings No. 353, *Combustion Problems in Turbine Engines*, 1983, pp. 2/1-2/10.
7. TeVelde, J.A. and Glickstein, M.R., "Heat Transfer and Stability of Alternative Aircraft Fuels," Vol. 1. Report AD A137404, 1983.
8. Marteney, P.J. and Spadaccini, L.J., "Thermal Decomposition of Aircraft Fuel," *ASME Journal of Engineering for Gas Turbines and Power*, Vol. 108, 1986, pp. 648-653.
9. Chin, J.S., and Lefebvre, A.H., "Temperature Effects on Fuel Thermal Stability," ASME Paper No. 91-GT-97, 1991.

345 E. 47 St., New York, N.Y. 10017

91-GT-37

Reference 4

Temperature Effects on Fuel Thermal Stability

J. S. CHIN* and A. H. LEFEBVRE**
Thermal Science and Propulsion Center
Purdue University
West Lafayette, Indiana

and

F. T.-Y. SUN
Gas Turbine Fuel Systems Division Parker Hannifin Corp.
Cleveland, Ohio

ABSTRACT

The thermal stability characteristics of four kerosine type fuels are examined using a heated-tube apparatus which allows independent control of fuel pressure, fuel temperature, tube wall temperature, and fuel flow rate. It is a closed loop system, and fuel flows through the heated tube for periods ranging from 6 to 22 hrs. The deposition rates of carbon on the tube walls are measured by weighing the tube before and after each test.

The results obtained show that tube-wall and fuel temperatures both have a marked influence on deposition rates, the impact of fuel temperature being stronger than that of wall temperature. It is also found that deposition rates increase continuously with increases in tube-wall temperature. This finding contradicts the results of previous studies which had led to the conclusion that deposition rates increase with increase in wall temperature up to a certain value beyond which any further increase in wall temperature causes the deposition rate to decline.

INTRODUCTION

Thermal instability is the term used to describe the chemical degradation of hydrocarbon fuels due to the high temperatures encountered in an aircraft's fuel system prior to combustion. The main effect of this increase in fuel temperature is to stimulate oxidation reactions that lead to the formation of insoluble material which has several adverse effects on engine performance. These include fouling of heat exchanger surfaces, which lowers the efficiency of heat transfer, and deposits in fuel nozzles which tend to block small passages and distort the fuel spray.

Several laboratory techniques are available for characterizing the thermal oxidative tendencies of fuels. The current international requirement is that a fuel should perform acceptably in the Jet Fuel Thermal Oxidation Tester (JFTOT). This tester, and its forerunner the ASTM CRC Fuel Coker, both pass the test fuel over a heated tube and then through a filter that traps any degradation products formed during the test. The fuel is rated partly by the extent of filter plugging, as indicated by the pressure drop across it, and also by the visual appearance of the deposit on the heated tube. The drawback to these test methods is that although some fuels are inherently easy to evaluate, since they exhibit a sharp threshold of temperature at which they start to form deposits, other fuels, and especially those having good thermal stability properties, are more difficult to evaluate, and it may be necessary to conduct a series of tests on one fuel at several different temperatures to determine the threshold or "breakpoint" temperature at which the fuel starts to form visible preheater deposits or to plug the filter. They are essentially pass or fail types of tests which are quite inadequate for scientific research. In any case, engineers are basically interested in deposit thickness, as thickness is the major criterion in heat transfer and in the mechanical blockage of small tubes and passages, and thickness is not necessarily related to deposit color.

Research on fuel thermal stability has been actively pursued by the major fuel companies. The Esso Heat Transfer Unit was developed for the U.S. Supersonic Transport Program as a research tool for relating fuel properties with heat exchanger degradation. The Shell Single Tube Heat Transfer Rig was built originally to investigate how turbine fuels would perform in the fuel system of the Concorde, but was used later in a broader role to study aircraft fuel performance in general. Other non-specification fuel testers that have shed useful light on the thermal degradation phenomenon include the NASA Single Tube Heat Exchanger and the UTRC Fuel Deposit Test Apparatus. Fuller descriptions of these and other techniques used for studying the causes and effects of fuel thermal instability are contained in publications by Bachman (1988), Kendall and Mills (1985a, 1985b), Vranos and Marteney (1980), Szetela et al. (1976, 1983a, 1983b, 1985, 1986), Baker et al. (1983), Cohen (1980), and Marteney and Spadaccini (1986).

Some of the techniques now being used for the assessment of fuel thermal stability are criticized [illegible]. Nevertheless, despite their shortcomings, these techniques have yielded useful information on the various mechanisms involved in the fuel degradation process, and also on the manner and extent to which thermal oxidation stability is influenced by the physical and chemical properties of the fuel. Thus it is now known that for conventional fuels the degradation process normally stems from oxidation of the fuel by dissolved oxygen in the fuel. This is the primary mechanism in initiating deposit formation. Oxidation products subsequently react with minor fuel constituents and with each other to generate the insoluble material that deposit on fuel system surfaces. The process is accelerated by the presence in the fuel of heterocompounds containing nitrogen, sulfur, oxygen and trace metals. Copper in particular has been found to be very detrimental to thermal stability. At fuel temperatures higher than around 700 K, fuel pyrolysis starts to influence deposition rates and, with further increases in fuel temperature, the reaction

* Visiting Professor
** Reilly Professor of Combustion Engineering

Presented at the International [illegible] Aeroengine Congress and Exposition [illegible] 3-6, 1991
This paper has been accepted [illegible] in the Transactions of the ASME
Discussion on it will be accepted [illegible] 1991

mechanism gradually changes from oxidation-controlled to pyrolysis-controlled which causes the rate of deposition to decline. Thus, in discussing the influence of temperature on deposit formation, it is important to bear in mind that it is the fuel temperature that determines which reaction mechanism is dominant-oxidation or pyrolysis - not the tube-wall temperature.

The primary role played by temperature in the processes of fuel thermal degradation and deposit formation has been known for some time. A NASA workshop held in 1978 identified wall temperature as the most important parameter affecting deposition rates, fuel temperature being the second most important parameter. Subsequent research has generally confirmed this finding, for example, the results obtained by Giovanetti and Szetela (1986) for Jet A fuel showed that "carbon deposit rates were a strong function of tube wall temperature." In view of the prime importance of temperature to fuel thermal degradation and deposit formation, it is somewhat surprising to find in the literature that in most experimental studies the only temperature recorded is either fuel temperature or wall temperature, but not both. In some reported studies on the influence of temperature on thermal stability, it is not clear whether the temperature under consideration is that of the fuel or the wall. Thus it is easy to understand the considerable scatter that tends to characterize reported experimental data on the effect of temperature on deposit formation rates.

In the present research an attempt is made to study the separate effects of fuel and wall temperatures on deposition rates. This goal is achieved by continuously controlling and regulating the heat inputs to both the fuel and the tube wall to maintain constant fuel and wall temperatures throughout the duration of each test. The test method employed and the results obtained are described below.

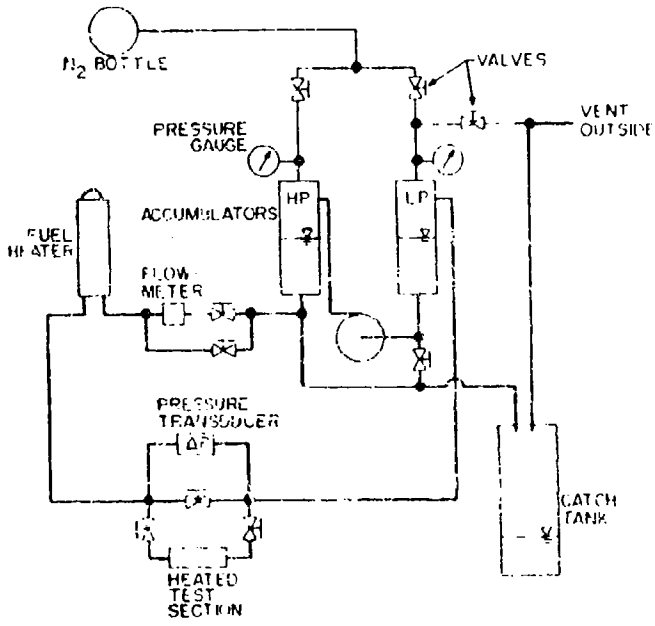

Fig. 1. Schematic diagram of fuel thermal stability rig.

THERMAL STABILITY RIG

The main features of the fuel thermal stability rig are shown in Fig. 1. It is a closed-loop system, designed to recirculate fuel over wide ranges of temperature, flow rate, and pressure. The major components are the pump, accumulators to contain the test fuel, a fuel heater, a heated test section, a flow meter, and another meter for monitoring the pressure drop across the section. In operation, the test fuel flows from a 5 liter high-

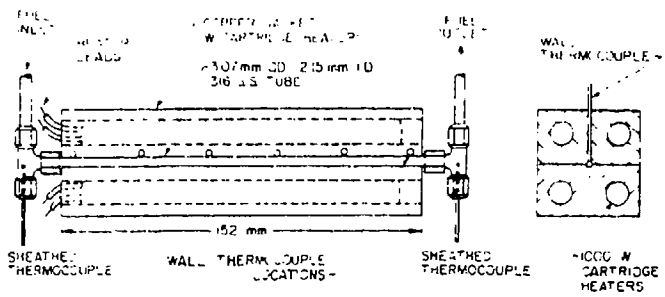

Fig. 2. Details of test section.

pressure accumulator through the flow meter and fuel heater into the test section from whence it flows into the low-pressure accumulator. The function of the pump is to transfer fuel from the low-pressure accumulator to the high-pressure accumulator. The pressures in both accumulators can be set to any desired values, up to a maximum of 4.1 MPa (600 psi), by using nitrogen gas from a high pressure container.

The key component of the test section is a thin-walled stainless steel tube whose principal dimensions are - length 152 mm, outer diameter 3.07 mm, and inner diameter 2.15 mm. This tube is clamped between two copper segments, as illustrated in Fig. 2. The semi-circular grooves cut into the two copper segments form a cylindrical passage when the segments are placed together. The diameter of this passage is designed to be very slightly smaller than the outer diameter of the stainless steel tube to ensure good thermal contact between the tube and the copper segments when the latter are clamped together. A number of thermocouples are threaded through one of the copper segments in such a manner that in operation the thermocouple beads are pressed tightly against the stainless-steel tube. These thermocouples are used to measure tube-wall temperatures at inlet and outlet and at four equispaced stations in-between. Fuel temperatures are measured only at the tube inlet and outlet.

The stainless steel tube is heated by using between one and four 1,000W electrical rod heaters which are inserted into holes drilled into the copper segments, as shown in Fig. 2. This arrangement ensures that the tube is heated uniformly around its circumference and, in fact, calculations show that this circumferential uniformity is maintained even when only one electrical heater is operational.

For any given fuel, the fuel pressure and flow rate are set at suitable values and the heaters for the fuel and test section are both switched on. During the fuel heatup period, which is usually less than ten minutes, the flowing fuel bypasses the test section. When the fuel and tube-wall temperatures have both attained the desired values, the bypass valves are operated to divert the hot fuel through the test section. This is a most useful feature because it allows the start of the test to be clearly defined. Another useful feature of the present test rig is the feedback between the fuel and tube-wall thermocouples and the fuel and test section heaters respectively which allows both fuel and tube wall temperatures to be maintained at preset values within 1°C throughout the entire duration of the test. This flexibility allows tests to be carried out on the influence of fuel temperature on deposition rates while maintaining a constant wall temperature. Alternatively, fuel temperature can be kept constant to permit the separate effect of variations in wall temperature on deposition rates to be studied.

Deposition rates are determined by weighing the tube before and after each test. The fuel supply connections at both ends of the tube are sealed using graphite ferrules. These ferrules are broken off after each test to reduce weight and thereby increase the ratio of the deposit mass to the tube mass. The weight of the tube is around 4000 mg. The deposits usually weigh between 2 and 20 mg depending on the fuel composition and test conditions. As the balance employed has an accuracy of within 0.1 mg, the weighing procedure is considered capable of

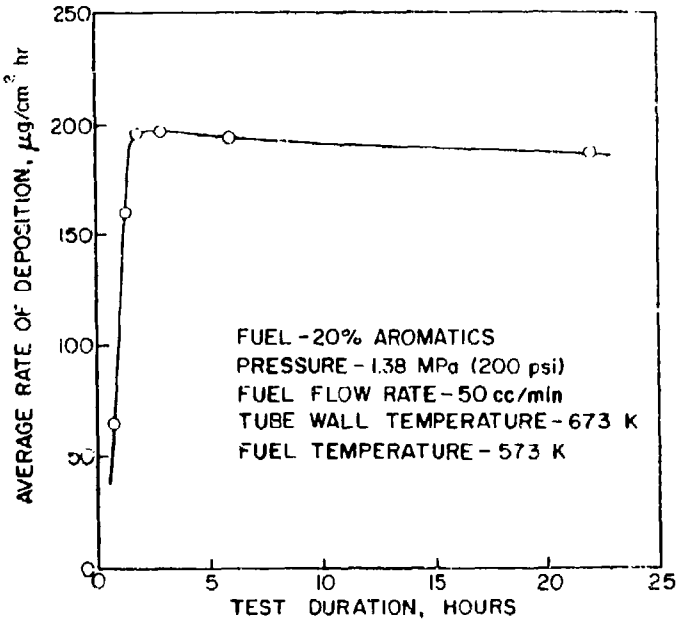

Fig. 3. Influence of test duration on deposition.

giving satisfactory results.

Tube treatment, both before and after each test, was found to affect the results obtained. After some experimentation the following procedure was established. Before weighing the tube prior to test it is exposed to the flame of a welding torch. As the tubes are manufactured by an extrusion process, flame heating is used to remove any remaining oil or grease. The tube is then dried using heated nitrogen gas. After the test the fuel is drained from the test section which is allowed to cool down to normal room temperature. The tube is then removed from the test section and allowed to dry naturally for twelve hours before being weighed. This procedure is found to give consistent and repeatable results.

RESULTS

Some of the results obtained using a light heating oil as the test fuel are shown in Fig. 3. This figure shows the average rate of deposition in $\mu g/cm^2$. hr. plotted against the test duration in hours. The data presented in Fig. 3 were obtained by removing the tube for weighing several times during the total test duration of twenty-two hours. The same fuel was used throughout the test. The purpose of Fig. 3 is to illustrate how the rate of deposition increases initially and then remains fairly constant. It should be noted that the deposition rates shown in Fig. 3 are "average" values, not instantaneous values. For example, the graph shows that during the first six hours the average rate of deposition was 195 $\mu g/cm^2$.hr. Thus the total deposition at the end of six hours was $6 \times 195 = 1170\ \mu g/cm^2$.

Figure 3 is typical of the results obtained at other test conditions and with other fuels. It illustrates that after the first few hours the rate of deposition settles down at a fairly uniform value, which suggests that most of the useful information to be gleaned from a test run can be extracted after five or six hours and there is little to be gained by protracting the test any further. Based on the knowledge and experience gained in a whole series of preliminary tests, it was decided to standardize on a test duration of six hours. This time period has no special significance except that it allows a complete test to be performed within a normal working day.

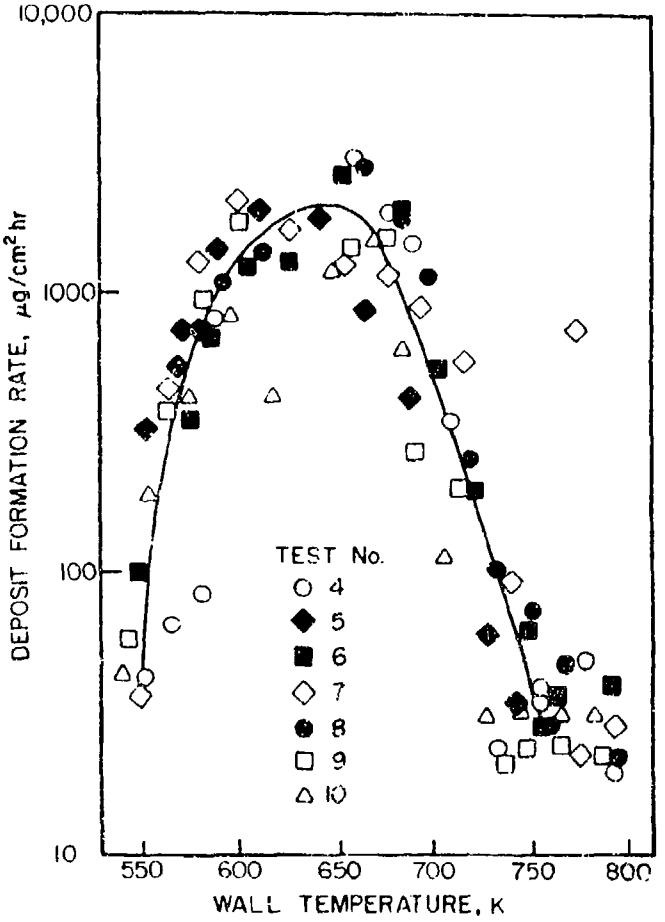

Fig. 4. Influence of tube-wall temperature on deposition rate (TeVelde and Glickstein, 1983).

EFFECT OF TUBE-WALL TEMPERATURE

The influence of wall temperature on deposition rates has been examined by several workers. TeVelde and Glickstein (1983) used a heated tube apparatus to evaluate the thermal stability characteristics of four liquid hydrocarbon fuels - a low aromatic JP 5, a blend of 80% JP 5 and 20% cracked gas oil, a blend of 50% JP 5 and 50% No. 2 heating oil, and a shale-derived JP 5. Deposit formation rates were obtained for tube-wall temperatures ranging from 480 to 800 K. The deposition characteristics of all four fuels were found to be very sensitive to wall temperature, with peak formation rates occurring at surface temperatures around 650 K, as illustrated in Fig. 4. Examination of these data led TeVelde and Glickstein to the conclusion that the effect of tube wall temperature on deposit temperature was "similar for all four fuels, that is, formation rates increased rapidly with increasing surface temperature up to approximately 700 to 750°F (644 to 672 K) and then decreased with further increases in surface temperature." This conclusion appears to have considerable practical significance because it suggests that an effective method of reducing deposition rates would be by increasing the tube-wall temperature, provided the initial wall temperature is in excess of around 650 K. Other workers have reached similar conclusions, but the present work indicates that this conclusion is erroneous and is the result of an inherent defect in the method used to measure deposition rates. With this method the test fuel is arranged to flow through a resistance-heated stainless steel tube. During any given test the local wall temperature does not remaining constant but changes dramatically

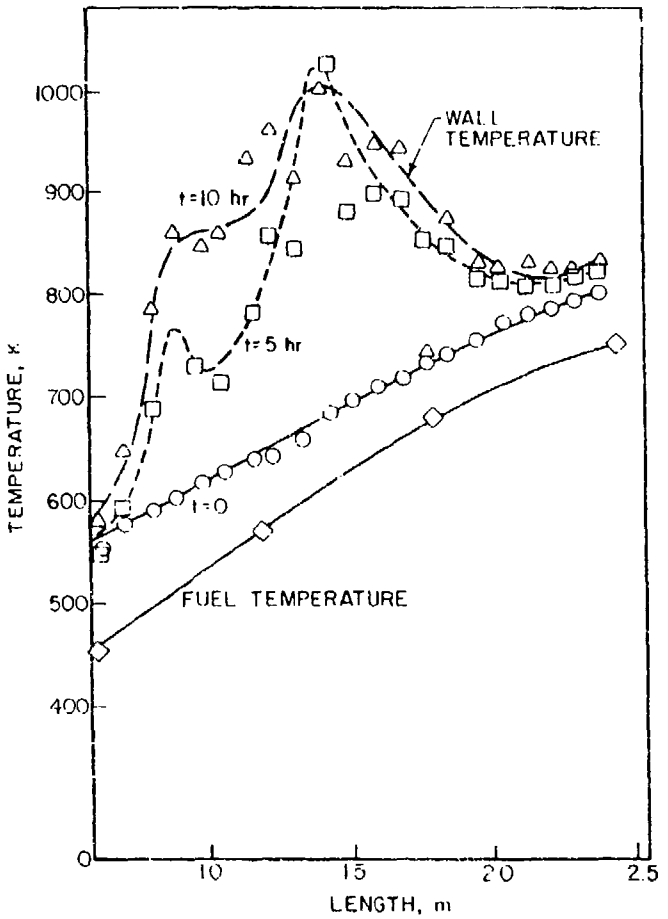

Fig. 5. Distribution of fuel and wall temperatures along tube length (TeVelde and Glickstein, 1983).

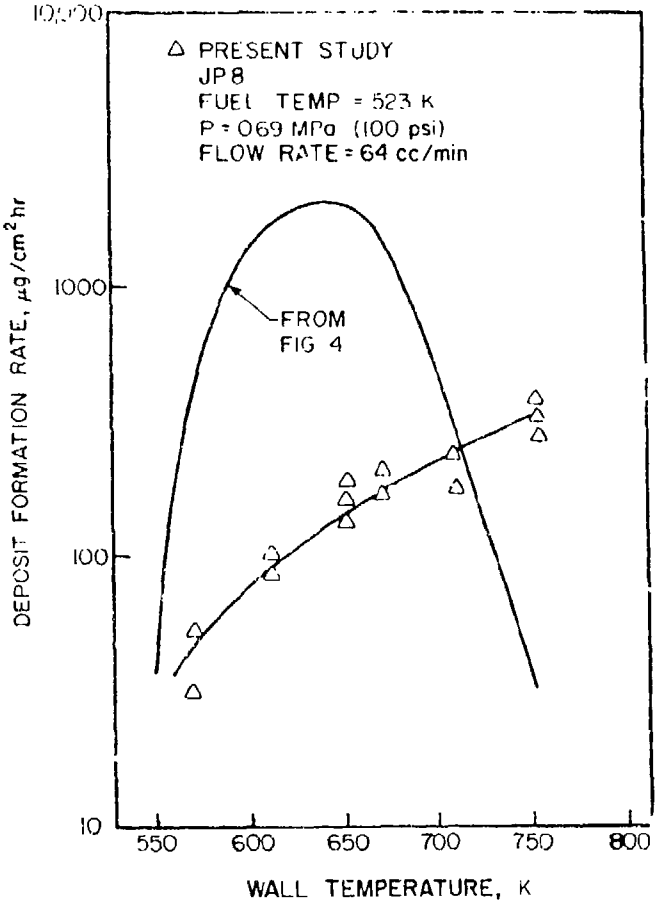

Fig. 6. Comparison of data from Fig. 4 with results of present study.

with time, as shown in Fig. 5 from TeVelde and Glickstein (1983). Moreover, the local wall temperature must always be a function of the local deposit thickness, because where the deposit is thicker the wall temperature must be higher to maintain the same heat flux through the tube wall. Thus, at the entry section to the tube, deposition rates are low because the fuel temperature is low. This, in turn, leads to a low wall temperature, as shown in Fig. 4.

As the fuel flows along the tube its temperature rises and, consequently, so also does the rate of deposition. This increase in deposit thickness leads to an increase in local wall temperature, as illustrated in Fig. 5. This figure shows that, at a point about half way along the tube, the local wall temperature, whose initial value was around 650 K, has risen to around 1,000 K after five hours operation. At this tube location, the combination of high fuel and high wall temperatures produces the high deposition rates shown in Fig. 4 for an initial wall temperature of 650 K. Fuel temperature continues to rise toward the downstream end of the tube, but this does not produce a high deposition rate because the mechanism of formation changes from auto-oxidation to pyrolysis. In fact, the rate of deposition actually declines in this range of high fuel temperatures. This causes a reduction in deposit thickness and hence a lowering of wall temperature during the test duration, as shown in Fig. 5. The combination of a lower wall temperature and the change in reaction mechanisms from auto-oxidation to pyrolysis causes the deposition rate to decline, despite the higher initial wall temperature, as shown in Fig. 4.

Thus, curves of the type shown in Fig. 4, which are intended to demonstrate the effect of tube-wall temperature on deposition rates, are really showing the combined effects of simultaneous variations in both wall and fuel temperatures. Of these, fuel temperature is the most important, and, in reality, the shape of the curve shown in Fig. 4 more aptly describes the effect on deposition rates of variations in fuel temperature than variations in wall temperature. In fact, for this particular apparatus, after several hours of operation the local wall temperature at any point along the tube length is much more indicative of the local deposit thickness than the local rate of deposition.

The results presented in Figs. 4 and 5, along with other data in the literature obtained using the resistance-heated tube method, all suffer from the drawback that they were acquired using an apparatus in which fuel and wall temperatures both increase appreciably along the length of the test tube. Moreover, the local wall temperature changes continuously and markedly during the test period. Under these conditions it is clearly difficult, if not impossible, to differentiate between the effects of wall temperature and fuel temperature on deposition rates.

The apparatus employed in the present research is free from these defects. The fuel temperature at entry to the test tube is governed by a preheater and is accurately controlled to within ± 0.5°C. The temperature rise experienced by the fuel as it flows through the tube is always quite small and seldom exceeds 10°C.

The tube-wall temperature is always maintained at a constant value throughout its entire length. By exercising separate control over fuel and wall temperatures, the effects on deposition rates of variations in these two parameters can be clearly distinguished.

Some of the results obtained with this apparatus on the effect of wall temperature on deposition rates are shown in Fig. 6. They illustrate the effect of wall temperature on deposition rates for a JP 8 fuel at a constant temperature of 523 K. The data are consistent with all other data obtained with this apparatus in showing a continuous increase in deposition rate with increase in wall temperature for a constant fuel temperature. Also shown in Fig. 6, for comparison, is a line drawn to represent the data points plotted in Fig. 4.

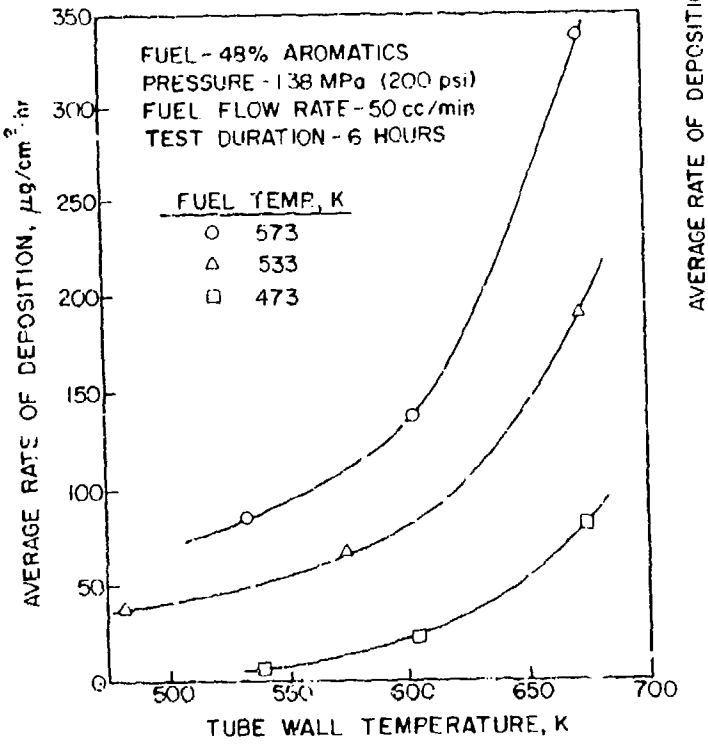

Fig. 7. Influence of tube-wall temperature on deposition rate.

The results for JP 8 fuel shown in Fig. 6 are considered to represent the true effect of wall temperature on deposition rates. Provided the fuel temperature is maintained constant, an increase in wall temperature will always increase the rate of deposition. The observed differences between the two sets of data in Fig. 6 may be explained as follows. At low wall temperatures, fuel temperatures are also low, and both curves are characterized by low deposition rates. At higher temperatures, around 650 K, the UTRC data exhibit much higher deposition rates. This is attributed to (a) a much higher *actual* wall temperature of around 1000 K (see Fig. 5) as opposed to the *initial* wall temperature of 650 K, and (b) a much higher fuel temperature of 600 K in comparison with the JP 8 fuel temperature which remained sensibly constant at 523 K. At the highest levels of wall temperature shown in Fig. 6, the rates of deposition for JP 8 are appreciably higher than for the UTRC fuels. This is attributed to the latter's higher temperatures (755 K versus 523 K) which cause deposit formation to occur by the pyrolysis mechanism as opposed to the more productive auto-oxidation mechanism for the lower temperature, JP 8 fuel. Thus, as noted earlier, the JP 8 data represent the true effect of wall temperature on deposit rates. In contrast, the UTRC data reflect the combined effects of variations in both wall and fuel

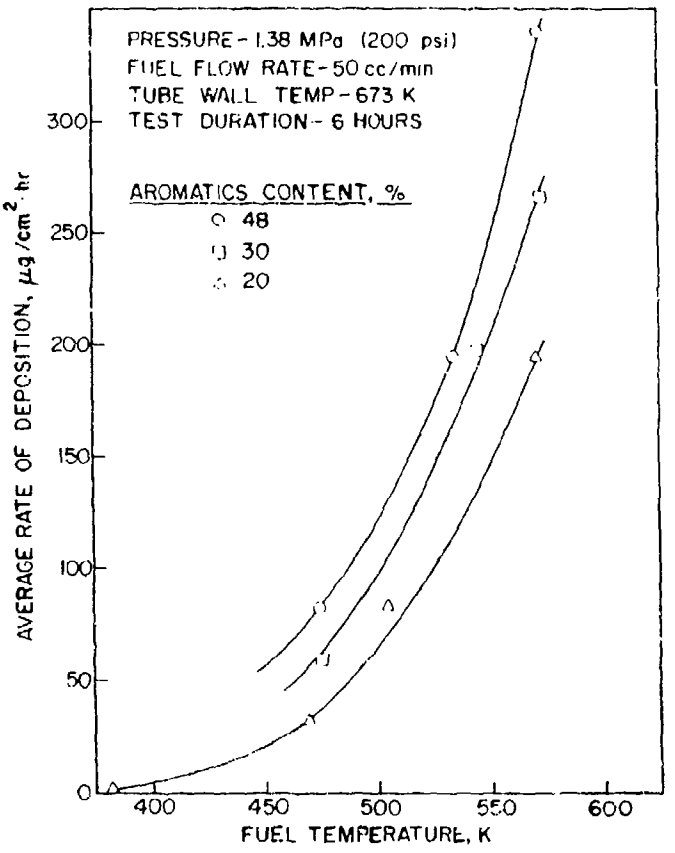

Fig. 8. Influence of fuel temperature on deposition rate.

temperatures, plus the added complication of a change in the mechanisms of deposit formation from auto-oxidation to pyrolysis at the higher levels of fuel temperature.

The effect of wall temperature on deposition rates is further illustrated by the results obtained using a kerosine-type fuel containing 48 percent aromatics, as shown in Fig. 7. These results clearly demonstrate the marked influence of wall temperature on rates of deposition and also show that this influence becomes more pronounced when an increase in wall temperature is accompanied by an increase in fuel temperature. This highlights the need for separate control of fuel temperature in experimental studies on the effect of wall temperature on deposition rates.

EFFECT OF FUEL TEMPERATURE

Fuel temperature has a pronounced effect on thermal stability, as illustrated in Fig. 8. The results shown in this figure generally confirm the findings of all previous studies on the influence of fuel temperature on thermal stability. They show, for all three fuels, that deposition rates are relatively low for fuel temperatures below around 400 K, but rise steeply with increases in fuel temperature above around 500 K.

As mentioned earlier, one of the main assets of the apparatus used in this test program is that it allows separate and independent control of both tube-wall and fuel temperatures. This enables the relative importance of these two parameters to be determined. From inspection of Figs. 7 and 8 it is clear that, over the ranges of fuel and wall temperatures investigated, both of these parameters strongly affect thermal stability. However, these figures also show that the influence of fuel temperature is more pronounced than that of wall temperature. The observed apparent dominance of fuel temperature over wall temperature

may be due in some measure to the fact that the thermal degradation reactions are influenced by fuel temperature throughout the whole test period, whereas wall temperatures can affect these reactions only during the much shorter residence time of the fuel in the test section.

Another explanation for the observed strong influence of fuel temperature is that deposition rates are governed primarily by the temperature of the fuel in the relatively slow-moving boundary layer near the tube wall. This temperature is dictated mainly by the bulk temperature of the fuel, which emphasizes the paramount importance of fuel temperature to deposition rates, as illustrated in Fig. 8. It is also strongly affected, albeit to a lesser extent, by the adjacent wall temperature, which serves to raise or lower the fuel temperature in the boundary layer depending on whether the wall temperature is higher or lower than the fuel temperature.

CONCLUDING REMARKS

Thermal stability characteristics of four kerosine-type fuels have been investigated using a heated-tube apparatus which permits independent control of fuel temperature, wall temperature, pressure, and flow velocity. The results obtained demonstrate the applicability of the apparatus for studying fuel thermal stability and deposition rates over a broad range of test conditions. The measurements indicate that consistent and repeatable results can be obtained to within ±10%.

The results obtained to date shed useful light on the important role played by temperature in fuel thermal stability. They show that tube-wall and fuel temperatures both have a marked influence on deposition rates, the impact of fuel temperature being stronger than that of wall temperature. They also show that deposition rates increase continuously with increase in wall temperature and do not decline at wall temperatures above around 650 K as the results of previous studies would appear to suggest.

Comparisons of the results obtained with light-distillate fuels of different aromatics content indicates that deposition rates are enhanced by an increase in aromatic content the effect becoming less pronounced for fuels of higher aromatic content.

ACKNOWLEDGEMENTS

The authors are pleased to acknowledge the contribution made by Dr. David T. Walker, now at the University of Michigan, Ann Arbor, to the design and construction of the apparatus used in the experiments. They also wish to express their gratitude for the financial support received from the Parker Hannifin Corporation of Cleveland, Ohio.

REFERENCES

Backman, K.C., 1985, "Heat Transfer Unit Evaluates Performance of Jet Fuels for Supersonic Aircraft," SAE Paper 650803.

Baker, C.E., Bittker, D.A., Cohen, S.M. and Seng, G.T., 1983, "Research on Aviation Fuel Instability," AGARD Conference Proceedings No. 353, *Combustion Problems in Turbine Engines*, pp. 2/1-2/10.

Cohen, S.M., 1980, "Fuels Research - Fuel Thermal Stability Overview," *Aircraft Research and Technology for Future Fuels*, NASA CP-2146, pp. 161-168.

Giovanetti, A.J., and Szetela, E.J., 1986, "Long Term Deposit Formation in Aviation Turbine Fuel at Elevated Temperatures," *AIAA J. Propul. Power*, Vol. 2, No. 5, pp. 450-456.

Marteney, P.J. and Spadaccini, L.J., 1986, "Thermal Decomposition of Aircraft Fuel," *ASME Journal of Engineering for Gas Turbines and Power*, Vol. 108, pp. 648-653.

Kendall, D.R. and Mills, J.S., 1985a, "The Influence of JFTOT Operating Parameters on the Assessment of Fuel Thermal Stability," SAE Paper 851871.

Mills, J.S. and Kendall, D.R., 1985b, "The Qualification and Improvement of the Thermal Stability of Aviation Turbine Fuel," ASME Paper 85-GT-33.

Roback, R., Szetela, E.J. and Spadaccini, L.J., 1983a, "Deposit Formation in Hydrocarbon Fuels," *ASME Journal of Engineering for Gas Turbines and Power*, Vol. 105, pp. 55-65.

Szetela, E.J., 1976, "Deposits from Heated Gas Turbine Fuels," ASME Paper 76-GT-9.

Szetela, E.J., Giovanetti, A.J and Cohen, S., 1985, "Fuel Deposit Characteristics at Low Velocity," ASME Paper 85-IGT-130.

TeVelde, J.A. and Glickstein, M.R., 1983, "Heat Transfer and Stability of Alternative Aircraft Fuels," Vol. 1, Report AD A137404.

TeVelde, J.A., Spadaccini, L.J., Szetela, E.J., and Glickstein, M.R., 1983b, "Alternative Fuel Deposit Formation," AGARD Conference Proceedings No. 353 *Combustion Problems in Turbine Engines*, pp. 3/1-3/10.

Vranos, A. and Marteney, P.T., 1980, "Experimental Study of Turbine Fuel Thermal Stability in an Aircraft Fuel System Simulator," Aircraft *Research and Technology for Future Fuels*, NASA CP 2146, pp. 169-176.

THE AMERICAN SOCIETY OF MECHANICAL ENGINEERS
345 E. 47 St., New York, N.Y. 10017

92-GT-114

Influence of Flow Conditions on Deposits From Heated Hydrocarbon Fuels

J. S. CHIN* and A. H. LEFEBVRE**
Thermal Science and Propulsion Center
Purdue University
West Lafayette, Indiana

ABSTRACT

The thermal stability characteristics of two liquid hydrocarbon fuels are examined using a single-pass system whereby the fuel under test flows only once through a heated tube which is maintained at constant temperature throughout a test duration of six hours. Deposition rates on the tube walls are measured by weighing the tube before and after each test.

The experimental data are used to derive empirical equations for predicting the effects on deposition rates of variation in fuel temperature, wall temperature, and Reynolds number. It is found that deposition rates are enhanced by increases in fuel temperature, wall temperature and flow velocity, and by reductions in tube diameter. Pressure has no effect on deposition rates provided it is high enough to prevent fuel boiling.

INTRODUCTION

Right from its inception, the continuing trend in turbojet engine design has been toward higher compression ratios and higher turbine inlet temperatures. These advances have resulted in the fuel becoming subject to a wide range of thermal stresses. Heat must be extracted from lubricating oil, with the fuel providing the heat sink. A further rise in fuel temperature occurs as the fuel flows through the burner feed arm due to the high rate of convective heat transfer from the compressor outlet air. In some fuel nozzles designs, the fuel may experience further additional heating by radiative heat transfer from the combustion gases. The combined effects of these various heat inputs is that by the time the fuel is sprayed into the combustion zone its temperature is appreciably higher than when it left the fuel tank. Unfortunately, this elevation in fuel temperature stimulates oxidation reactions which lead to the formation of gums and other insoluble materials (including carbon) which tend to deposit on heat exchanger walls and control surfaces. Deposition within the fuel nozzle is especially harmful because it can distort the fuel spray pattern to such an extent that it causes overheating of liner walls, turbine blades, and nozzle guide vanes.

The deposits formed in fuel nozzles and on other heated surfaces are a manifestation of thermal degradation of the fuel. Fuels that have a high thermal stability also have a low tendency to form deposits. Current aircraft fuels do not present a major problem in this regard, but the situation could worsen appreciably in the future due to anticipated higher fuel temperatures in heat exchangers and fuel nozzles and to the more widespread use of fuels of broader chemical composition. Several different methods have been developed to evaluate fuel thermal stability and the published literature in this field is quite extensive. Useful descriptions of the various experimental techniques employed are contained in the CRC Literature Survey on the Thermal Oxidation Stability of Jet Fuel (1979), Taylor (1979), Cohen (1980), Peat (1982), Baker et al. (1983), Roback et al. (1983), TeVelde and Glickstein (1983), TeVelde et al. (1983), Mills and Kendall (1985), Marteney and Spadaccini (1986), and Chin and Lefebvre (1992). None of the experimental methods developed so far is entirely free from defects. Even so, they have provided a considerable body of information on the effects of fuel temperature, wall surface temperature, and fuel composition on deposition rates. In contrast, the fluid dynamic aspects of the thermal stability problem have received comparative neglect. The present work represents an attempt to remedy this deficiency. Evidence is presented to show the important effects of fuel and wall temperatures on deposition rates, but consideration is also given to the effect on deposition rates of variations in flow conditions, notably liquid flow rate, velocity, pressure, and Reynolds number. It is hoped that the results obtained will be of interest and value to the designers of aircraft heat exchangers, fuel control systems, and fuel nozzles.

APPARATUS

The apparatus employed in this experimental study on fuel thermal stability is essentially a single-pass system in which the test fuel flows only once through a heated tube which is maintained at constant temperature throughout the test duration. It is basically the same as the apparatus described in a previous publication by Chin and Lefebvre (1992) except that various minor modifications to the original apparatus have been made as part of a continuing effort to upgrade the facility and thereby improve the accuracy and consistency of the experimental data. The apparatus in its present form is shown schematically in Fig. 1. The main components are a feed tank which contains the test fuel, a flow meter, a fuel heater, a heated test section, a water cooler, a back-pressure tank, and a drain tank. In operation, the test fuel flow from the storage tank into the electric heater which raises its temperature to the desired value at entry to the test section. The fuel usually experiences a small increase in temperature as it flows through the test section to an extent which depends on the flow rate and the temperature difference between the fuel and the tube wall.

In some experiments the tube wall is maintained at exactly the same temperature as the fuel flowing through it. This is done to eliminate heat transfer between the tube and the fuel so that as the fuel flows through the tube its temperature remains constant. After

* Visiting Professor
** Reilly Professor of Combustion Engineering

Presented at the International Gas Turbine and Aeroengine Congress and Exposition
Cologne, June 1-4, 1992
This paper has been accepted for publication in the Transactions of the ASME
Discussion of it will be accepted until September 30, 1992

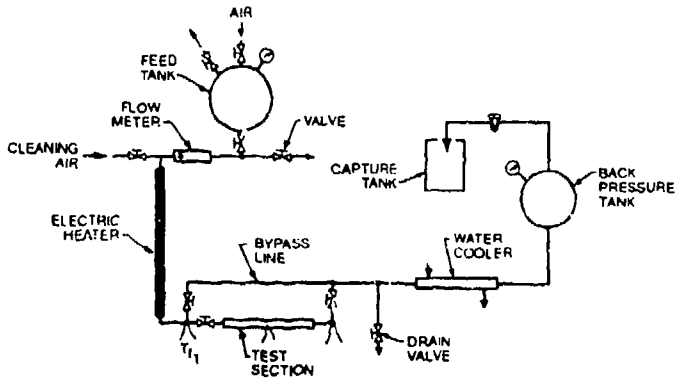

Fig. 1. Schematic diagram of test facility.

emerging from the test section, the fuel flows through a water cooler which reduces it temperature to around 300K before it flows into the back-pressure tank and out of the system. The fuel pressure within the test section can be varied up to around 4 MPa (580 psia), but most tests are carried out at pressures of 2.5 MPa (363 psia) and below.

The back-pressure tank represents a comparatively recent addition to the test facility. Although its presence does not contribute directly to greater accuracy of the experimental data, it makes a useful indirect contribution in that it improves appreciably the flow stability of the system. Before this addition, the throttle valve which controlled the fuel flow rate was located in a hot fuel section. As the pressure drop across this valve was always extremely high [typically 2.5 MPa (363 psia) at inlet and 0.12 MPa (17 psia) at outlet], this meant that the throttle valve was usually barely "cracked open." As the hot fuel flowed through this very small opening it tended to form deposits which caused a continuous decline in flow rate that required frequent adjustment of the valve. Fitting the back pressure tank allowed the throttle valve to be located in a region where fuel temperatures and pressures differentials are both low. The valve now has a much wider opening and deposits no longer form. This improvement in the method of flow control, in conjunction with the large-volume back-pressure tank, has virtually eliminated flow instabilities and flow-rate drift from the system.

The test section, instrumentation, tube preparation, and weighing procedures have been fully described in two previous publications (Chin et al., 1991 and Chin and Lefebvre, 1992). The main component of the test section is a thin-walled stainless steel tube of length 152 mm. This tube is clamped between two electrically-heated copper segments. Semi-circular grooves cut into the two segments provide good thermal contact between the tube and the copper segments when the latter are clamped together. Thermocouples are used to measure tube-wall temperatures at six equispaced intervals along the tube length. Fuel temperatures are measured only at the tube inlet and outlet.

For any given fuel, the fuel pressure and flow rate are set at suitable values and the heaters for the fuel and test section are both switched on. During the fuel heatup period, which is usually less than ten minutes, the flowing fuel bypasses the test section. When the fuel and tube-wall temperature have both attained the desired values, the bypass valves are operated to divert the hot fuel through the test section. At the same time the water supply to the fuel cooler is turned on.

A feedback system between the fuel and tube-wall thermocouples and the fuel and test section heaters respectively, allows both fuel and tube-wall temperatures to be maintained within 1°C of preset values throughout the test duration. Deposition rates are measured by weighting the tube before and after each test. The deposits usually weight between 2 and 100 mg depending on the fuel composition and test conditions.

Experience has shown that for good repeatability of results the fuel preheater should be cleaned after each test run. This is done by supplying electrical power to the preheater so that its inner wall attains a high temperature. At the same time, air is passed through the preheater where it is heated to a temperature of around 500K at outlet.

Table 1 Fuel Properties

(a) Kinematic viscosity

Fuel Temp., °C	Viscosity, $m^2/s \times 10^{-6}$	
	DF 2	Kerosine
100	1.15	0.79
140	0.78	0.58
170	0.62	0.48
200	0.54	0.41
250	0.40	0.29

(b) Density

Fuel Temp., °C	Density, kg/m^3	
	DF 2	Kerosine
20	840	820
140	740	725
250	630	620

(c) Aromatics content

DF 2	30 - 35 percent
Kerosine	20 - 25 percent

This procedure has been found very effective in removing all deposits from the preheater wall.

EXPERIMENTAL

The fuels selected for this study are DF 2 and kerosine. The relevant properties of these two fuels are listed in Table 1. These fuels were chosen partly on the basis of low cost, since long test runs call for large amounts of fuel, and also because they encompass the aromatic contents of present and anticipated future aviation fuels.

The flow variables of principal interest for their influence on deposition rates are the pressure, temperature, velocity, and Reynolds number of the flowing fuel. Also of interest is the influence of tube-wall temperature, since this affects both the temperature and the velocity profile in the boundary layer adjacent to the tube wall. The separate effects of these various parameters are discussed below in turn

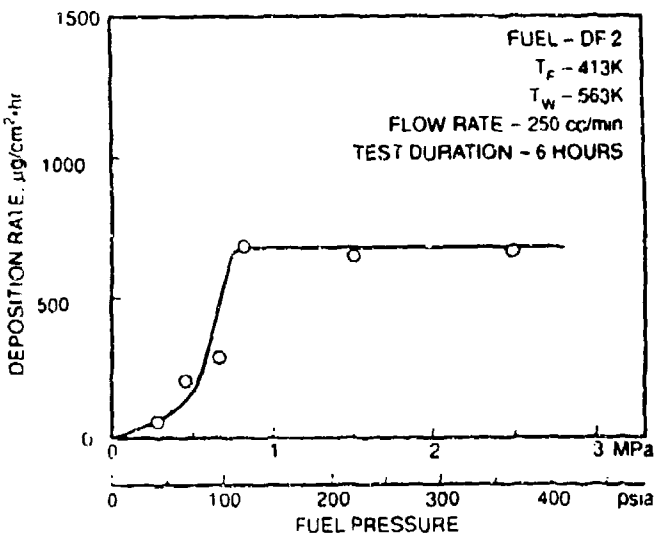

Fig. 2 Influence of pressure on deposition rates.

Pressure

In general, the results contained in the literature show little effect of fuel pressure on deposition rates. Vranos and Marteney (1980) found no effect of pressure on deposition rates for No. 2 home heating oil or for Jet A fuel when the pressure was higher than 1.5 MPa (218 psia). Marteney and Spadaccini(1980) also reported for JP 5 fuel that a wide variation in pressure from 1.72 to 5.5 MPa (250 to 800 psia) had no effect on deposit formation rates. High pressure deposition tests were also conducted and reported by Roback et al. (1968). The fuel pressures generally exceeded 13.8 MPa (2000 psia). The results showed no significant change in wall temperatures as a consequence of increasing pressure, suggesting that the rate of deposit formation was relatively independent of pressure over the pressure range from 13.8 to 34 MPa (2000 to 4930 psia). However, Watt et al. (1968) reached rather different conclusions. According to these workers, the influence of fuel pressure, while not entirely consistent from fuel to fuel, was to diminish both local and total deposits with increasing pressure.

Some of the results obtained on the effect of pressure using DF 2 as the test fuel are shown in Fig. 2. The data contained in this figure were obtained using a 400 series stainless steel tube of length 152mm, outer diameter 3.08mm, and inner diameter 2.59mm. They show the average rate of deposition in $\mu g/cm^2$. hr plotted against fuel pressure for a fuel flow rate of 250 cc/min and a test duration of six hours.

It is clear from Fig. 2 that above a certain minimum pressure the deposition rate is independent of fuel pressure. For the DF 2 fuel used in these experiments, this minimum pressure is around 0.8 MPa (115 psia). A limited number of tests carried out on other fuels indicates that the minimum pressure may be higher or lower than 0.8 MPa, depending on the temperature and volatility of the fuel. In general, the minimum pressure above which pressure has no effect on deposition rates decreases with increases in fuel temperature and/or fuel volatility. This suggests that the low deposition rates associated with low fuel pressures may be the result of fuel boiling and the production of fuel vapor. Autoxidation deposit formation rates are lower in the vapor phase than in the liquid phase at the same temperature. Another effect of fuel boiling is to convert the normally smooth flow of fuel through the test section into a two phase, turbulent flow of relatively high velocity. This produces a vigorous scrubbing action at the tube surface which tends to inhibit deposition and also remove any deposits that might form on the surface despite the adverse conditions. However, it should be noted that measurements of deposition rates for JP 4 and JP 5 fuels made by Szetela (1976) led him to an opposite conclusion. He found deposits to be higher for JP 4 which he attributed to the fact that "boiling increases the deposition tendency." Clearly, the effect of fuel boiling on deposition rates merits further investigation.

Further evidence on the insensitivity of deposition rates to variations in fuel pressure above the critical value is presented in Fig. 3. This figure illustrates the manner in which the temperature rise experienced by the fuel as it flows through the heated tube varies with time. Initially, the tube wall is perfectly clean and the fuel temperature rise is relatively high. With the passage of time, the accumulation of deposit on the tube wall creates a thermal barrier between the tube and the flowing fuel which gradually diminishes the heat flux from the tube to the fuel, thereby causing a continuous decline in the temperature rise of the fuel, as illustrated in Fig. 3. Thus the temperature rise of the fuel provides a useful indication of the amount of deposition on the tube wall. Figure 3 shows that for constant conditions of fuel temperature, wall temperature, and fuel flow rate, pressure has no effect on deposition rates for DF 2 over a pressure range from 0.8 to 2.5 MPa (115 to 363 psia).

Reynolds Number

On aircraft fuel systems, as the fuel flows from the tank and through various engine components into the fuel nozzle, it experiences a variety of flow conditions corresponding to a wide range of Reynolds numbers. It is therefore of some practical interest and importance to examine the impact of variations in this flow parameter on deposition rates. For experimental purposes, Reynolds number can be varied readily by changing one or more of the following:

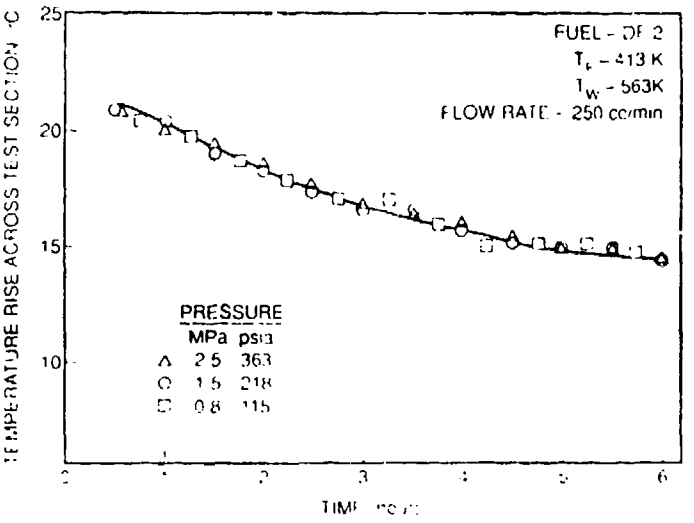

Fig. 3 Influence of deposit thickness on fuel temperature rise

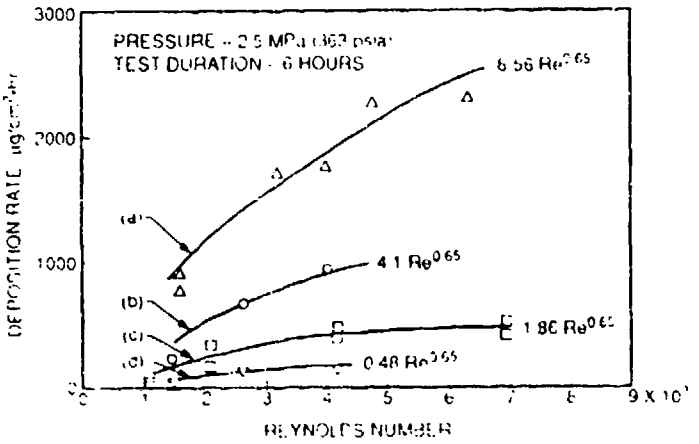

Fig. 4 Influence of Reynolds number on deposition rate

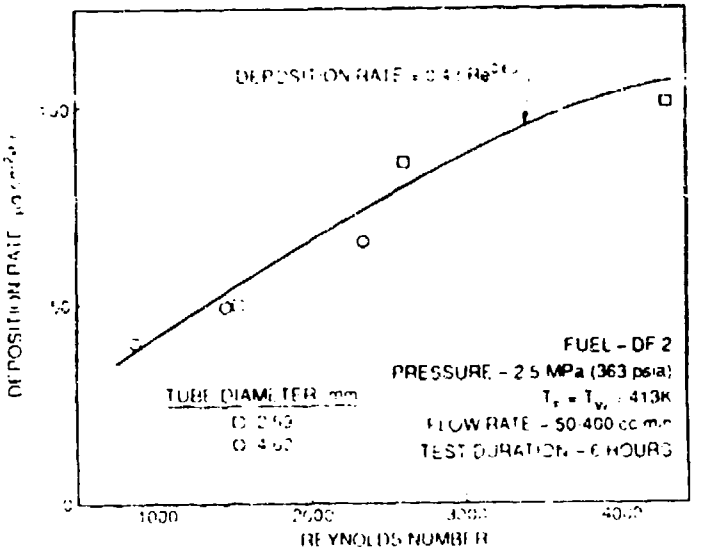

Fig. 5 Influence of tube diameter on deposition rate

1. mass flow rate (velocity)
2. tube diameter
3. fuel temperature

Unfortunately, variations in fuel temperature not only serve to change the Reynolds number, they also have a pronounced effect on the auto-oxidation reactions that promote deposition. This leaves mass flow rate and tube diameter as the only two practical options for achieving variations in Reynolds number.

For the results presented in Fig. 4, the variation in Reynolds number was accomplished by varying the fuel flow rate. The four curves shown in this figure correspond to the following conditions.

(a) Fuel - DF 2
T_F = 473K, T_W = 623K, P = 2.5 MPa
$\dot{m}_{VF}$ = 100 - 400 cc/min
Stainless steel tube, 400 series. I.D. = 2.59 mm, O.D. = 3.08 mm
(b) Fuel - DF 2
T_F = 413K, T_W = 563K, P = 2.5 MPa
$\dot{m}_{VF}$ = 100 - 400 cc/min
Stainless steel tube, 400 series. I.D. = 2.59 mm, O.D. = 3.08 mm
(c) Fuel - kerosine
T_F = 523K, T_W = 673K, P = 2.5 MPa
$\dot{m}_{VF}$ = 50 - 200 cc/min
Stainless steel tube (316) I.D. = 2.10 mm, O.D. = 3.08 mm
(d) Fuel - DF 2
T_F = 413K, T_W = 413K, P = 2.5 MPa
$\dot{m}_{VF}$ = 150 - 400 cc/min
Stainless steel tube, 400 series. I.D. = 2.59 mm, O.D. = 3.08 mm

Inspection of the above table shows that in three cases the wall temperature was 150° C higher than the fuel temperature, while in one case (d) the fuel and tube wall were both at the same temperature. In all cases, regardless of fuel type, fuel temperature, or wall temperature, it is found that the effect of variation in Reynolds number on deposition rate (D.R.) can be expressed as

$$D.R. = \text{constant} \cdot Re^{0.65} \qquad (1)$$

The effect on deposition rates of a change in Reynolds number caused by a change in tube diameter is illustrated in Fig. 5. This figure contains the same data shown as (d) in Fig. 4 plus additional data obtained for the same fuel, at the same conditions of pressure and temperature, but with the tube internal diameter increased from 2.59 to 4.60 mm. Figure 5 shows that both sets of data tend to fall on the same curve which conforms to the relationship

$$D.R. = 0.48\ Re^{0.65} \qquad (2)$$

This increase in deposition rate with increase in Reynolds number is attributed to the higher heat transfer between the wall and the fuel and the higher transverse velocity components which are more effective in transporting material from the mainstream fuel flow to the tube walls.

Interest is sometimes expressed in the amount of deposit produced by a given mass of fuel. To examine this situation a "deposit index", D.I., is first defined as

$$D.I. = \frac{\text{mass of deposit per unit length of tube}}{\text{mass of fuel}} = \frac{\mu g/cm}{kg} \qquad (3)$$

Also, we have

$$Re = \frac{\rho U d}{\mu} = \frac{4}{\pi} \frac{\dot{m}_{VF}}{d\nu} \qquad (4)$$

By appropriate combinations of Eqs (1), (3), and (4), the following relationships between deposition rate, deposit index, and Reynolds number are derived

$$D.R. \propto Re^{0.65} \qquad (1)$$

$$D.I. \propto Re^{-0.35}\,\mu^{-1} \qquad (5)$$

$$\frac{D.R.}{D.I.} \propto Re\,\mu \qquad (6)$$

Figure 6 shows the deposit index plotted against Reynolds number for DF 2 fuel flowing through a 400 series stainless steel tube having an inside diameter of 2.59 mm and an outside diameter of 3.08 mm. One practical implication of the results presented in Figs. 5 and 6 is that for any given fuel flow rate a reduction in tube diameter will cause an increase in deposit thickness. However, it should be noted that in the present experiments on the effect of Reynolds number on deposition rates the flow velocity is always less than a few meters per second. With continual reduction in tube diameter, the scrubbing action along the tube walls could eventually reach a point at which any

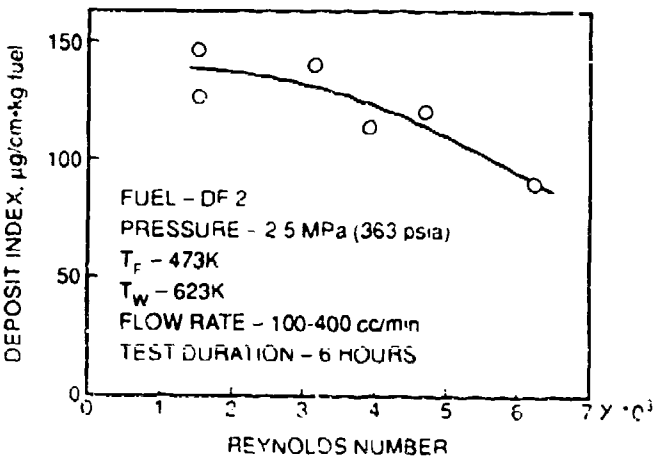

Fig. 6 Influence of Reynolds number on Deposit Index

further increase in flow velocity would cause deposition rates to decline.

Fuel Temperature

As mentioned earlier, the effect of an increase in temperature on deposition rate is twofold, (1) by reducing the fuel viscosity it raises the Reynolds number and hence also the deposition rate, as shown in Fig. 5, (2) it accelerates the auto-oxidation reactions which are responsible for deposit formation. The extent to which deposition rates are enhanced by an increase in fuel temperature depends on whether the fuel flow rate is held constant and the Reynolds number allowed to increase, or whether the flow rate is allowed to decline in order to maintain a constant Reynolds number. These effects are illustrated in Fig. 7.

In many experiments that are performed to show the influence of fuel temperature on deposition rates, the temperature of the tube wall is often appreciably higher than the temperature of the fuel flowing through it. This is done for many reasons, not the least being to simulate the conditions that exist in aircraft fuel systems and fuel injectors. Unfortunately, it produces a steep temperature gradient in the fuel adjacent to the wall which prohibits a precise definition of temperature in the region where the deposition process is actually taking place. To avoid this problem, and to obtain experimental data on the influence of fuel temperature on deposition rates of more fundamental significance, the fuel and tube wall should ideally be at the same temperature. By eliminating heat transfer between the fuel and the tube wall, the effect of wall temperature is removed, so that any observed changes in deposition rates are due solely to variations in fuel temperature.

Some results obtained for kerosine and DF 2 under conditions where $T_W = T_F$ are shown in Fig. 8. Over a range of fuel

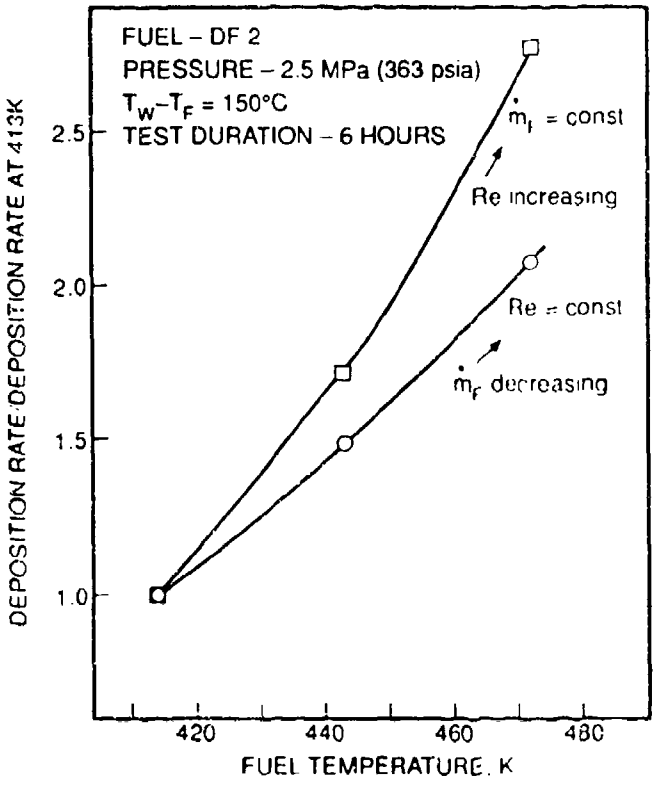

Fig. 7. Influence of fuel temperature on deposition rate

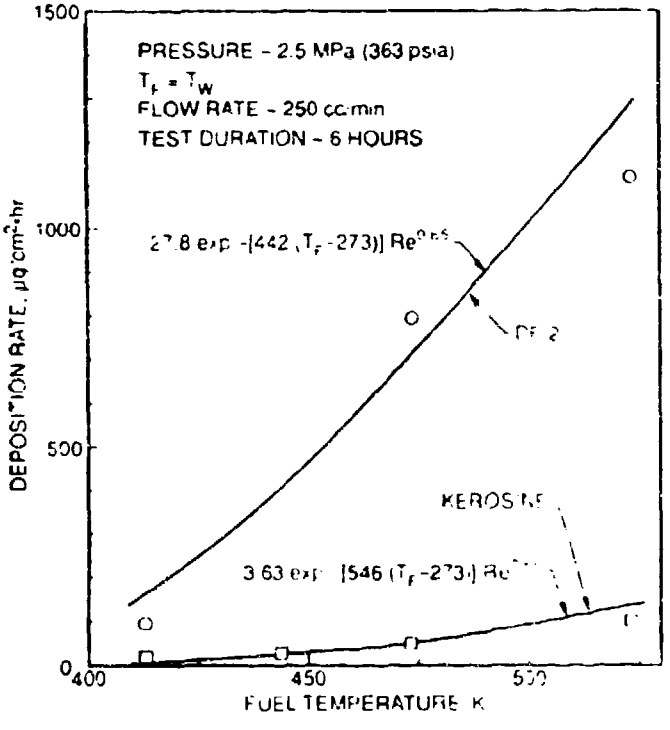

Fig. 8. Correlation of data for various fuel temperatures

temperatures from 413 to 523K, it is found that deposition rates are correlated satisfactorily by an expression of the form

$$D.R. = C1 \exp - [C2/(T_F - 273)] Re^{0.65} \quad (7)$$

where C_1 is a constant whose value depends mainly on fuel composition and the material and condition of the tube wall, and C_2 depends solely on fuel composition (including additives). C_2 represents the activation energy of the auto-oxidation reaction which leads to the formation of deposits.

For kerosine, we have

$$D.R. = 3.63 \exp - [546/(T_F - 273)] Re^{0.65} \quad (8)$$

while for DF 2

$$D.R. = 27.8 \exp - [442/(T_F - 273)] Re^{0.65} \quad (9)$$

In these equations, deposition rate is expressed in terms of $\mu g / cm^2$ hr.

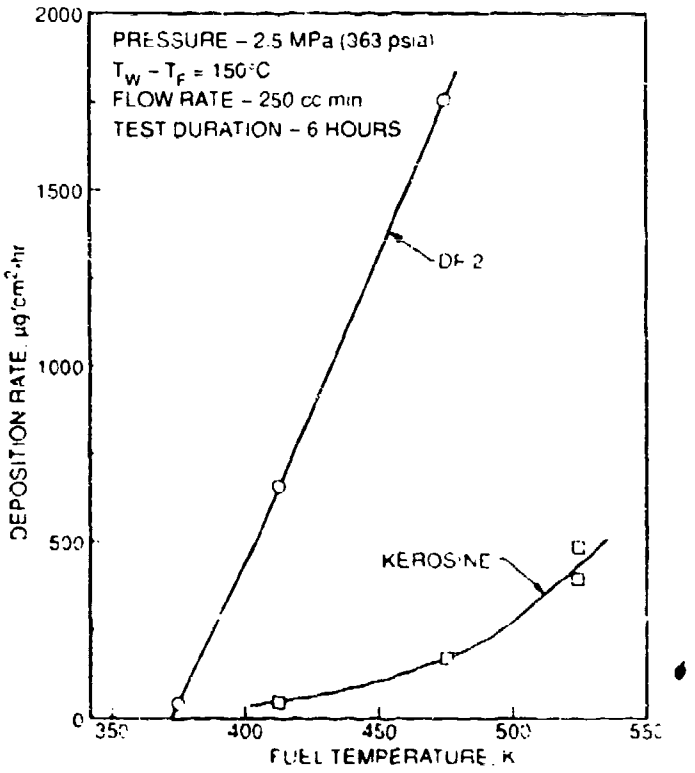

Fig. 9. Influence of fuel temperature on deposition rate

Tube-Wall Temperature

If the tube wall temperature exceeds the fuel temperature, the deposition rate is increased. This is evident from inspection of the data contained in Figs. 8 and 9 which were obtained under identical test conditions except that in one case (Fig. 8) the fuel and wall temperatures were the same, whereas in the second case (Fig. 9) the wall temperature was 150° C higher than the fuel temperature. Comparison of these two figures reveals that an increase in wall temperature leads to a higher rate of deposition. For the two fuels employed in this investigation, kerosine and DF 2, the effect of wall temperature on deposition rates can be accounted for by including the term $\exp [(T_W - T_F) / 166]$ into Eqs. (8) and (9) which then become respectively

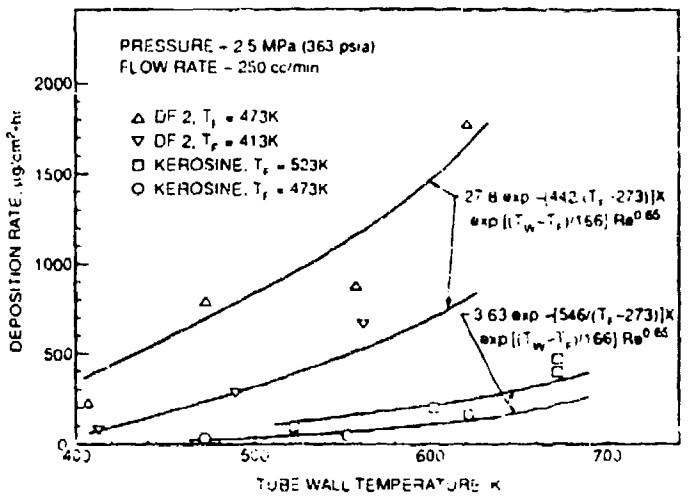

Fig. 10 Influence of tube-wall temperature on deposition rate

For kerosine

$$D.R. = 3.63 \exp - [546/(T_F-273)] \exp [(T_W-T_F)/166] Re^{0.65} \quad (10)$$

For DF 2

$$D.R. = 27.8 \exp - [442/(T_F-273)] \exp [(T_W-T_F)/166] Re^{0.65} \quad (11)$$

These equations are shown plotted in Fig. 10 alongside the corresponding experimental data for DF 2 and kerosine

DISCUSSION

Although Eqs. (10) and (11) have little fundamental significance, they have some practical value because they provide a useful indication of the relative importance of the relevant fuel and flow parameters on deposition rates. For example, they show that the most important factor influencing deposition rates is fuel temperature. Also of importance is the tube wall temperature, specifically the difference in temperature between the wall surface and the adjacent fuel (T_W-T_F). Finally, they show that flow velocity and tube diameter affect deposition rates via their influence on Reynolds number. Over the range of flow velocities covered in these experiments, deposition rates are enhanced by increases in flow velocity and reductions in tube diameter.

Equations (10) and (11) contain no term to account for the influence of fuel pressure on deposition rates. This is because the present study has shown that provided it is high enough to prevent fuel boiling, pressure has no effect on deposition rates.

NOMENCLATURE

d	tube diameter
D.I.	deposit index, μg / cm kg
D.R.	deposition rate, μg / cm² hr
m_f	mass flow rate of fuel
m_{vf}	volumetric flow rate of fuel
Re	Reynolds number, U dρ / μ
T_f	fuel temperature, K
T_w	wall temperature, K
U	flow velocity
μ	fuel viscosity
ρ	fuel density

REFERENCES

Baker, C.L., Bittker, D.A., Cohen, S.M., and Seng, G.T., 1983, "Research on Aviation Fuel Instability," AGARD Conference Proceedings No. 353, *Combustion Problems in Turbine Engines*, pp. 2/1-2/10.

Chin, J.S., Lefebvre, A.H., and Sun, E.T.Y., 1991, "Temperature Effects on Fuel Thermal Stability," ASME Paper 91-GT-97.

Chin, J.S., and Lefebvre, A.H., 1992, "Experimental Techniques for the Assessment of Fuel Thermal Stability," AIAA Paper 92-0685.

Cohen, S.M., 1980, "Fuels Research - Fuel Thermal Stability Overview," *Aircraft Research and Technology for Future Fuels*, NASA CP 2146, pp. 161-168.

Coordinating Research Council Inc., "Thermal Oxidation Stability of Jet Fuels - A Literature Survey," 1979, CRC Report No. 509.

Marteney, P.J., and Spadaccini, L.J., 1986, "Thermal Decomposition of Aircraft Fuel," *ASME Journal of Engineering for Gas Turbines and Power*, Vol. 108, pp. 648-653.

Mills, J.S., and Kendall, D.R., 1985, "The Qualification and Improvement of the Thermal Stability of Aviation Turbine Fuel," ASME Paper 85-GT-33.

Peat, A.E., "Thermal Decomposition of Aviation Fuel," 1982, ASME Paper 82-GT-27.

Roback, R., Szetela, E.J., and Spadaccini, L.J., "Deposit Formation in Hydrocarbon Rocket Fuels," 1981, NASA CR 179579.

Roback, R., Szetela, E.J., and Spadaccini, L.J., "Deposit Formation in Hydrocarbon Fuels," *ASME Journal of Engineering for Gas Turbines and Power*, Vol. 105, pp. 55-65.

Szetela, E.J., 1976, "Deposits from Heated Gas Turbine Fuels," ASME Paper 76-GT-9.

Szetela, E.J., Giovanetti, A.J., and Cohen, S., 1985, "Fuel Deposit Characteristics at Low Velocity," ASME Paper 85-IGT-130.

TeVelde, J.A., and Glickstein, M.R., 1983, "Heat Transfer and Stability of Alternative Aircraft Fuels," Vol. 1, Report AD A137404.

TeVelde, J.A., Spadaccini, L.J., Szetela, E.J., and Glickstein, M.R., 1983, "Alternative Fuel Deposit Formation," AGARD Conference Proceedings No. 353 *Combustion Problems in Turbine Engines*, pp. 3/1-3/10.

Vranos, A., and Marteney, P.J., 1980, "Experimental Study of the Stability of Aircraft Fuels at Elevated Temperatures," NASA CR 165165.

Watt, J.J., Evans, A., and Hibbard, R.R., 1968, "Fouling Characteristics of ASTM Jet A Fuel When Heated to 700°F in a Simulated Heat Exchanger Tube," NASA TN D-4958.

APPENDIX G

LIST OF PUBLICATIONS AND PRESENTATIONS

by

UNIVERSITY OF DAYTON RESEARCH INSTITUTE PERSONNEL

LIST OF PUBLICATIONS AND PRESENTATIONS

Journal Publications

[1] D. R. Ballal, "Joint Laser Raman Spectroscopy and Anemometry," **Combustion Measurements** (Edt. N. A. Chigier), Hemisphere Publishing Company, New York, 1991.

[2] D. R. Ballal, "Turbulence-Kinetics Interaction in Recirculatory Flows," **Major Research Topics in Combustion** (Edts. M. Y. Hussaini, A. Kumar, and R. A. Voigt), Springer Verlag Publishing Inc., New York, pp. 403-423, 1991.

[3] S. P. Heneghan and M. D. Vangsness, "Instrument Noise and Weighting Factors in Data Analysis," *Experiments in Fluids*, Vol. 9, pp. 290-294, 1990.

[4] F. Takahashi and W. J. Schmoll, "Lifting Criteria of Jet Diffusion Flames," *Twenty-Third Symposium (Int.) on Combustion*, The Combustion Institute, Pittsburgh, PA, pp. 677-683, 1991.

[5] G. J. Sturgess, D. G. Sloan, A. L. Lesmerises, D. R. Ballal, and S. P. Heneghan, "Design and Development of a Research Combustor for Lean Blow Out Studies," *ASME, Journal of Engineering for Gas Turbines and Power*, Vol. 114, pp. 13-20, 1992.

[6] J. C. Pan, W. J. Schmoll, and D. R. Ballal, "Turbulent Combustion Properties Behind a Conical Stabilizer," Paper No. 90-GT-51, *ASME, Journal of Engineering for Gas Turbines and Power*, 1991.

[7] S. P. Heneghan, M. D. Vangsness, and J. C. Pan, "Simple Determination of the Width of the Slit Function in Single-Shot CARS Thermometry," *Journal of Applied Physics*, Vol. 69, pp. 2692-2693, 1991.

[8] S. P. Heneghan and M. D. Vangsness, "Analysis of Slit Function Errors in Single-Shot Coherent Anti-Stokes Raman Spectroscopy (CARS)," *Reviews of Scientific Instruments*, Vol. 62, pp. 2093-2099, 1991.

[9] G. J. Sturgess, A. L. Lesmerises, S. P. Heneghan, M. D. Vangsness, and D. R. Ballal, "Isothermal Flowfields in a Research Combustor For Lean Blowout Studies," Paper No. 91-GT-37, *ASME, Journal of Engineering for Gas Turbines and Power*, 1991.

[10] G. J. Sturgess, A. L. Lesmerises, S. P. Heneghan, M. D. Vangsness, and D. R. Ballal, "Lean Blowout in a Research Combustor at Simulated Low Pressures, " Paper No. 91-GT-359, *ASME, Journal of Engineering for Gas Turbines and Power*, 1991.

[11] J. C. Pan, M. D. Vangsness, and D. R. Ballal, " Aerodynamics of Bluff-Body Stabilized Confined Turbulent Premixed Flames," Paper No. 91-GT-218, *ASME, Journal of Engineering for Gas Turbines and Power*, Vol. 114, pp. 783-789, 1992.

[12] J. C. Pan, M. D. Vangsness, S. P. Heneghan, and D. R. Ballal, "Scalar Measurements in Bluff-Body Stabilized Flames Using CARS Diagnostics," Paper No. 91-GT-302, *ASME, Journal of Engineering for Gas Turbines and Power*, 1991.

[13] S. P. Heneghan, M. D. Vangsness, D. R. Ballal, A. L. Lesmerises, and G. J. Sturgess, "Acoustic Characteristics of a Research Step Combustor," Paper No. AIAA 90-1851, *AIAA Journal of Propulsion*, 1991.

[14] G. J. Sturgess, A. L. Lesmerises, S. P. Heneghan, M. D. Vangsness, and D. R. Ballal, "Flame Stability and Lean Blowout in a Research Combustor," *Proceedings of the Tenth International Symposium on Air Breathing Engines*, Nottingham, U. K., pp. 372-384, September 1991.

[15] F. Takahashi, M. D. Vangsness, and W. J. Schmoll, "Near-Field Structure and The Local Extinction of Turbulent Jet Diffusion Flames of Methane in Air," *Proceedings of the 13th (Int.) Colloquium on the Dynamics of Explosions and Reactive Systems,* Nagoya, Japan, July 1991.

[16] S. P. Heneghan, C. R. Martel, T. F. Williams, and D. R. Ballal, "Studies of Jet Fuel Thermal Stability in Flowing Systems," *ASME, Journal of Engineering for Gas Turbines and Power, 1992.*

[17] J. C. Pan and D. R. Ballal, "Chemistry and Turbulence Effects in Bluff-Body Stabilized Flames," AIAA Paper No. 92-0771, Submitted to *AIAA Journal of Propulsion and Power.*

[18] S. P. Heneghan, R. J. Byrd, S. Locklear, S. Anderson, and W. D. Schultz, "Evaluation of Jet Fuel Additives in Static Systems," AIAA Paper No. 92-0686, Submitted to *AIAA Journal of Propulsion and Power.*

[19] G. J. Sturgess, S. P. Heneghan, M. D. Vangsness, D. L. Shouse, A. L. Lesmerises, and D. R. Ballal, "Effects of Back Pressure in a Lean-Blowout Research Combustor," Accepted for *ASME, Journal of Engineering for Gas Turbines and Power, 1992.*

[20] J. S. Chin, A. H. Lefebvre, and F. T. Sun, "Influence of Flow Conditions on Deposits from Heated Hydrocarbon Fuels," Accepted for *ASME, Journal of Engineering for Gas Turbines and Power, 1992.*

[21] F. Takahashi and L. P. Goss, "Near-Field Turbulent Structures and the Local Extinction of Jet Diffusion Flames," *Twenty-Fourth Symposium (Int.) on Combustion*, The Combustion Institute, Pittsburgh, PA, 1992.

[22] S. D. Anderson, J. T. Edwards, R. J. Byrd, T. B. Biddle, W. H. Edwards, S. P. Heneghan, C. R. Martel, T. F. Williams, J. A. Pearce, and W. E. Harrison, "Advanced Thermally Stable Jet Fuel Development," *Aviation Fuels: Thermal Stability Requirements*, ASTM STP 1138, P. W. Kirklin and P. David, Eds. ASTM Philadelphia, 1992.

Papers Under Review

[1] S. P. Heneghan and S. Zabarnick, "Oxidation of Jet Fuels and the Formation of Deposits," Submitted to Fuels, May 1992.

[2] S. P. Heneghan, C. R. Martel, T. F. Williams, and D. R. Ballal, "Effects of Oxygen and Additives on the Thermal Stability of jet Fuels," Submitted to 38th ASME (Int.) Gas Turbine and Aeroengine Conference, Cincinnati, OH, May, 1993.

Presentations

[1] S. P. Heneghan, W. J. Schmoll, and D. R. Ballal, "Studies of CARS-LDA Biasing in Reactive Flows," Fall Technical Meeting, Eastern States Section, The Combustion Institute, Clearwater Beach, FL, December, 1988

[2] S. P. Heneghan and M. D. Vangsness, "Mean Biasing in an LDA-CARS System," 15th AIAA Mini-Symposium, March, 1989, Dayton, Ohio

[3] F. Takahashi, W. J. Schmoll, and M. D. Vangsness, "Effects of Swirl on the Stability and Turbulent Structure of Jet Diffusion Flames," Paper No. AIAA 90-0036, 28th Aerospace Sciences Meeting, January, 1990, Reno, NV.

[4] S. P. Heneghan, "Determination of Bulk A-Factors From Surface Deposition Rates in Jet Fuel Thermal Stability Tests," AIAA, 16th Annual Mini-Symposium on Aerospace Science and Technology, March 29, 1990, Dayton, Ohio

[5] J. C. Pan, "Measurements of Turbulence Properties Behind a Confined Conical Stabilizer," 16th AIAA Mini-Symposium, March, 1990, Dayton, Ohio.

[6] D. R. Ballal, " Gas Turbine Combustion-Contribution of Academia to Research," Central States Section, The Combustion Institute, Cincinnati, OH, May, 1990.

[7] J. C. Pan, M. D. Vangsness, S. P. Heneghan, and D. R. Ballal, "Turbulent Scalar Properties Behind Conical Bluff Bodies Using Laser Diagnostics," Central States Section, The Combustion Institute, Cincinnati, Ohio, May, 1990.

[8] F. Takahashi and W. J. Schmoll, "Mean and Turbulent Velocity Characteristics of Swirling Jet Diffusion Flames," Central States Section, The Combustion Institute, Cincinnati, Ohio, May, 1990.

[9] M. D. Vangsness and S. P. Heneghan, "Probe Volume Effects on the Spatial Distribution of CARS Signal," Presented at Sixth Annual Interdisciplinary Laser Science Conference, Minneapolis, MN, September 16-19, 1990.

[10] S. P. Heneghan and M. D. Vangsness, "Analysis of Slit Function Errors in Single-Shot CARS," Presented at Sixth Annual Interdisciplinary Laser Science Conference, Minneapolis, MN, September 16-19, 1990.

[11] S. P. Heneghan, J. C. Pan, and M. D. Vangsness, "Analysis of The Instrument Slit Function in CARS Thermometry," Presented at The Spring Meeting, Central States Section, The Combustion Institute, Nashville, TN, April 21-24, 1991.

[12] J. C. Pan, M. D. Vangsness, S. P. Heneghan, and D. R. Ballal, "Laser Diagnostic Studies of Bluff-Body Stabilized Confined Turbulent Premixed Flames," Presented at The Spring Meeting, Central States Section, The Combustion Institute, Nashville, TN, April 21-24, 1991.

[13] F. Takahashi, M. D. Vangsness, W. J. Schmoll, and V. M. Belovich, "Turbulent Flow Characteristics of Swirling Jets and Jet Diffusion Flames," Presented at The Spring Meeting, Central States Section, The Combustion Institute, Nashville, TN, April 21-24, 1991.

[14] M. D. Vangsness and F. Takahashi, "LDA/CARS Studies on a Confined Diffusion Flame," 17th AIAA Mini-Symposium, Dayton, OH, March (1991)

[15] F. Takahashi, M. D. Vangsness, and V. M. Belovich, "Conditional LDV Measurements in Swirling and Non-Swirling Coaxial Turbulent Air Jets for Model Validation," Paper No. AIAA-92-0580, AIAA 30th Aerospace Sciences Meeting, Reno, Nevada, Jan. 6-9, 1992.

[16] F. Takahashi, "Intermittency and Conditional Statistics in Reacting and Non-Reacting Turbulent Jets," 18th AIAA Mini-Symposium, Dayton, OH, March 1992.

[17] S. P. Heneghan and W. E. Harrison III, "Anti-Oxidants in Jet Fuels: A New Look," Symposium on Structures of Jet Fuels, American Chemical Society, San Francisco, CA, April 5-10, 1992.

[18] M. D. Vangsness and S. P. Heneghan, "Coherent Anti-Stokes Raman Spectroscopy: System Characterization and Reproducibility," Presented at The Spring Meeting, Central States Section, The Combustion Institute, Columbus, OH, April 26-28, 1992.

[19] F. Takahashi, M. D. Vangsness, and L. P. Goss, "Dynamic Vortex-Flame Interactions in Turbulent Jet Diffusion Flames Near Local Extinction," Presented at The Spring Meeting, Central States Section, The Combustion Institute, Columbus, OH, April 26-28, 1992.

[20] S. P. Heneghan, "Chemistry of Antioxidants and Their Role in the Formation of Solids in Jet Fuels," Coordinating Research Council Meeting, Washington D.C., April 1992.

[21] S. P. Heneghan, D. L. Gieger, and E. Stewart, "Quantitative determination of Sulfur Content in Jet Fuels using Atomic Emission Detection and Gas Chromatography, " Ohio Valley Chromatographic Symposium, June, 1992.

[22] F. Takahashi and M. D. Vangsness, "Structure Measurements in Swirling and Non-Swirling Turbulent Jets and Jet Diffusion Flames," Twenty-Fourth Symposium (Int.) on Combustion, Sydney, Australia, July, 1992.

UDRI Reports

[1] J. C. Pan, "Laser Diagnostic Studies of Confined Turbulent Premixed Flames Stabilized by Conical Bluff Bodies: Vol. I: Theory and Experiments," UDR-TR-91-101, Ph. D. Dissertation, University of Dayton, Dayton, OH, July 1991.

[2] J. C. Pan, M. D. Vangsness, S. P. Heneghan, W. J. Schmoll, and D. R. Ballal, "Laser Diagnostic Studies of Confined Turbulent Premixed Flames Stabilized by Conical Bluff Bodies: Vol. II: Data Set," UDR-TR-91-102, University of Dayton, Dayton, OH, July 1991.

[3] F. Takahashi and M. D. Vangsness, "LDV Measurements in Swirling and Non-Swirling Coaxial Turbulent Air Jets: Report 1: No Swirl, 100 m/s," UDR-TR-91-160, University of Dayton, Dayton, OH, April 1991.

[4] F. Takahashi and M. D. Vangsness, "LDV Measurements in Swirling and Non-Swirling Coaxial Turbulent Air Jets: Report 2: No Swirl, 25 m/s," UDR-TR-91-161, University of Dayton, Dayton, OH, May 1991.

[5] F. Takahashi, M. D. Vangsness, and V. M. Belovich, "LDV Measurements in Swirling and Non-Swirling Coaxial Turbulent Air Jets: Report 3: 30-degree Swirl, 100 m/s," UDR-TR-91-162, University of Dayton, Dayton, OH, July 1991.

[6] F. Takahashi, M. D. Vangsness, and V. M. Belovich, "LDV Measurements in Swirling and Non-Swirling Coaxial Turbulent Air Jets: Report 4: 30-degree Swirl, 100 m/s," UDR-TR-91-163, 30-degree Swirl, 25 m/s," University of Dayton, Dayton, OH, August 1991.

[7] W. D. Schulz, "A Chemical Investigation of the Nature of Jet Fuel Oxidation Deposits and the Effects of additives on Deposits," Subcontractor Final Report, April 1992.

[8] C. R. Martel, T. F. Williams, and H. L. Imwalle, "Studies of Jet Fuel Thermal Stability in a Flowing System-Report I: Analyses," Report No. UDR-TR-92-98, University of Dayton, Dayton, OH, July 1992.

[9] C. R. Martel, T. F. Williams, and H. L. Imwalle, "Studies of Jet Fuel Thermal Stability in a Flowing System-Report II: Data Set," Report No. UDR-TR-92-99, University of Dayton, Dayton, OH, August 1992.